N O T I C E

THIS DOCUMENT HAS BEEN REPRODUCED FROM MICROFICHE. ALTHOUGH IT IS RECOGNIZED THAT CERTAIN PORTIONS ARE ILLEGIBLE, IT IS BEING RELEASED IN THE INTEREST OF MAKING AVAILABLE AS MUCH INFORMATION AS POSSIBLE

TURBULENT BOUNDARY LAYER ON
A CONVEX. CURVED SURFACE

by

J. C. Gillis, J. P. Johnston, W. M. Kays and R. J. Moffat

Report No. HMT-31

Thermosciences Division
Department of Mechanical Engineering
Stanford University
Stanford, California

September 1980

TURBULENT BOUNDARY LAYER ON A CONVEX, CURVED SURFACE

by

J. C. Gillis, J. P. Johnston, R. J. Moffat, and W. M. Kays

Report No. HMT-31

Heat Transfer and Turbulence Mechanics Group
Thermosciences Division
Department of Mechanical Engineering
Stanford University
Stanford, California 94305

September 1980

Acknowledgments

Table of Contents

List of Figures

vi

vii

List of Tables

Nomenclature

a	Structural coefficient, $-\overline{uv}/q^2$.
A^+	Effective sublayer thickness in Van Driest scheme.
$C_f/2$	Skin-friction coefficient, $\tau_o/\rho U_{pw}^2$.
C_p	Static pressure coefficient (see Eqn. 3-1).
e	Fluctuating hot-wire signal.
E	Mean hot-wire signal.
H	Shape factor, δ_1/δ_2.
k	Jørgensen coefficient.
K	Acceleration parameter, $(\nu/U_\infty^2)\,(dU_\infty/dx)$.
ℓ	Mixing length.
ℓ_o	Flat-wall mixing length.
ℓ_τ	Turbulence length scale.
$\dot{m}$	Boundary-layer mass flux per unit spanwise width.
n	Distance normal to surface.
n^+	Non-dimensional distance normal to surface, $n\sqrt{\tau_o/\rho}/\nu$.
	Turbulence production.
P	Static pressure.
p'	Fluctuating pressure.
P_t	Total pressure.
P_s	Static pressure
P_{sw}	Wall static pressure.
P_r	Freestream total pressure.
PL	δ_2.
PR	$\int_o^s (C_f/2)ds$ (see Eq. (3-9)).
$\frac{1}{2}q^2$	Turbulence kinetic energy.
R	Local radius of curvature (Ro + n).

R_{eff} Effective radius of curvature (see Eqn. 4-6).

Re_τ Turbulence Reynolds number (see Eq. (4-9)).

Ri Richardson number.

Ro Wall radius of curvature.

R_{ij} Reynolds stress tensor.

s Streamwise coordinate, measured along <u>surface</u>.

S Stability parameter, $\dfrac{U/R}{\partial U/\partial y}$.

U Mean velocity

U_p Potential flow velocity.

U_{pw} Potential flow velocity at the wall.

U_∞ Flat-plate freestream velocity.

u Fluctuating streamwise velocity.

u_τ Wall shear velocity, $\sqrt{\tau_w/\rho}$.

u^+ U/u_τ.

u' Root-mean-square value of u.

V Velocity normal to surface.

V_p Potential flow velocity normal to surface.

v Fluctuating velocity normal to surface.

v' Root-mean-square value of v.

w Fluctuating velocity parallel to surface in spanwise direction.

w' Root-mean-square value of w.

x Distance along a flat wall.

y Distance normal to flat wall.

y^+ yu_τ/ν.

z Distance from centerline in spanwise direction.

Greek Letters

α Skew angle of flow due to secondary flow.

β Empirical constant in mixing-length correction.

δ Thickness at which velocity is 99% of potential flow velocity.

δ_1 Displacement thickness.

δ_2 Momentum thickness.

δ_{ij} Kroneker delta.

δ_{sl} Width of active shear layer (see Section 4.2).

δ_{sl}^{*} Displacement thickness based on active shear layer (see Section 4.2).

ε Dissipation rate.

κ Karman constant, 0.41.

ν Kinematic viscosity.

ρ Density.

τ Total shear stress.

τ_0 Surface shear stress

Ω Rotational frequency

ω Vorticity.

ABSTRACT

Three experiments were performed to determine how boundary-layer turbulence is affected by strong convex curvature. The data gathered on the behavior of the Reynolds stress suggested the formulation of a simple turbulence model.

Three sets of data were taken on two separate facilities. Both rigs had flow from a flat surface, over a convex surface with 90° of turning, and then onto a flat recovery surface. The geometry was adjusted so that, for both rigs, the pressure gradient along the test surface was zero -- thus avoiding any effects of streamwise acceleration on the wall layers. Two experiments were performed at δ/R approximately 0.10, and one at weaker curvature with $\delta/R \simeq 0.05$.

Results of the experiments show that, after a sudden introduction of curvature, the shear stress in the outer part of the boundary layer is sharply diminished and is even slightly negative near the edge. The wall shear also drops off quickly downstream. In contrast, when the surface suddenly becomes flat again, the wall-shear and shear-stress profiles recover very slowly towards flat-wall conditions. Data suggest that as many as forty boundary layer thicknesses may be needed for significant recovery, whereas the curvature effects are dominating the flow in two layer thicknesses after the beginning of the curved flow region.

It was discovered that, for the shear-stress profiles taken in the curved region, the shear-stress profiles for all three experiments collapse when $-\overline{uv}/u_\tau^2$ was plotted vs. n/R. The strong curvature data of So & Mellor (with different free-stream velocity and radius of curvature) also fell on the same curve. This suggests an asymptotic state for the shear-stress profiles of strongly curved boundary layers. The slope of the curve shows an almost linear dropoff of $-\overline{uv}$ with distance from the wall. The shear stress is approximately zero in the outer part of the boundary layer.

The physical interpretation given to these observations is that the width of the active shear layer has been compressed (by the curvature) close to the wall. Its width is much less than the velocity-gradient boundary layer. In the recovery region, the width of the active shear

layer regrows slowly within the velocity-gradient boundary layer, like a developing boundary layer under a free stream with velocity gradient.

A simple turbulence model, which was based on the theory that the Prandtl mixing length in the outer layer should scale on the width of the active shear-stress layer rather than on the velocity-gradient layer, was shown to account for the slow recovery.

Chapter 1

INTRODUCTION

1.1 Project Background

The primary objective of this program was to extend the understanding of low turbulent-transport processes to control the convection of heat from a solid surface. The work was undertaken as part of an ongoing series of projects at Stanford sponsored by NASA-Lewis Labs. The motivating problem has been the need to accurately predict the heat transfer loading on gas turbine blades.

When the project was begun, NASA used the boundary layer code STAN5 [1], developed at Stanford, to make heat transfer predictions. This code solves the partial differential equations which govern transport of heat and momentum in boundary layers. The crucial step in this procedure is the modeling of the Reynolds stress term which appears in the momentum equation. The code STAN5 has a Reynolds stress model which, compared to some, is mathematically uncomplicated. However, because it contains empirical input from twelve years of careful experimentation, it handles very complicated problems accurately. In particular, empirical input has been used to construct a model which calculates through areas of strong streamwise pressure gradients, transpiration, or combinations of these two effects.

At the time this project was begun, however, any possible effects of longitudinal surface curvature were ignored. Our aim has been to fill this void.

1.2 Previous Research in Curvature Effects

Experimental evidence that the effects of curvature should be included in a good turbulence model has been accumulating for a long time. The first work on the subject was done by Prandtl and his students. Prandtl had apparently convinced himself from mixing-length arguments that curvature effects should be negligible, but the work of his student Wilcken [2] showed large changes in the mixing length of boundary layers on convex and concave surfaces. Further work at

1

Göttingen was done on flows between coaxial rotating cylinders by Wendt [3], in a curved duct by Wattendorf [4], and in convex boundary layers by Schmidbauer [5]. The general conclusion of all this work — that for even small values of δ/R the boundary layer hydrodynamics are greatly affected -- was published but did not inspire further investigation.

In the early 1950s Krieth [6] made use of Wattendorf's result to make a quantitative estimate of the changes in the eddy diffusivity brought about by curvature. His conclusion was that the curvature effects scaled on U/r, which he called the forced vortex parameter. When non-dimensionalized by $\partial U/\partial y$, this forced vortex parameter is now called the curvature Richardson number. At about this same time, Eskinasi and Yeh [7] of Johns Hopkins performed experiments in a curved channel flow. This excellent study is very detailed even by today's standards. Using hot-wire anemometry, a fairly new technique at the time, they took the first measurements of turbulence quantities and drew important conclusions. The ratio of their channel half-width to spanwise dimension was only 15.5, which, based on our experience with boundary layer flows, may not have been enough to ensure two-dimensionality. Indeed, their measured shear stress values did not balance the measured pressure gradients. Their experiments showed a great decline in the u' and v' over the convex surface (and a corresponding increase over the concave surface). Their spectral measurements of u' and v' showed that the decrease was largest in the low-wave-number range. They related this drop qualitatively to the production term in the Reynolds stress transport equations.

Interest in the effects of curvature intensified in the late 1960s, possibly because, by this time, calculational models had been developed to the point where the effects of curvature were not lost in other inaccuracies. The first experiment of this era was performed by V. C. Patel [8] in a wind tunnel with a 90° bend. He measured only mean quantities, and these measurements may have been influenced by secondary flows. Nevertheless, he was able to come to the correct conclusion that curvature affects entrainment by examining the variation of the shape factor δ_1/δ_2.

2

Three years after Patel's work, Thomann [9] published a set of experiments on heat transfer in curved boundary layers. They proved that the Stanton number is affected in much the same way as the skin friction, but no detailed measurements of the hydrodynamic boundary layer were taken. Thomann's measurements were also unusual in that they were the first performed at high Mach number.

In 1972, So & Mellor [10] published results from a very detailed experiment on a curved-wall boundary layer. In this experiment the ratio of boundary layer thickness to radius of curvature was large enough that several gross effects were demonstrated. All the Reynolds stresses were measured, and the flow was acceptably two-dimensional. On the convex wall it was found that the turbulent shear stress was "turned off" (the value of $\overline{uv}$ was approximately zero) in the outer half of the boundary layer. Over the concave wall, they found evidence of a system of streamwise axial vortices, analogous to those formed between rotating cylinders. Wall shear stress was inferred from a Clauser plot, but the turbulent shear stress profile was not measured close enough to the wall to check the wall value by extrapolation.

At about this time, Bradshaw [11] pointed out the analogy between the effects of curvature and the effects of buoyancy. He then proposed that the Monin-Obouhkov formula for the correlation of the apparent mixing length with small buoyancy effects.

$$\frac{\ell}{\ell_o} = 1 + \beta \frac{y}{L} \simeq 1 + \beta \, Ri \quad ,$$

(where β is an empirical constant and Ri is the Richardson number) could be used to model the effects of weak curvature if the "curvature Richardson number" was defined as

$$Ri = \frac{2 \, U/R}{\partial U/\partial y} \quad .$$

This approach met with considerable success. In fact, the value of the constant β could be inferred by analogy from meteorological experiments in stably and unstably stratified boundary layers, where it was found to be of the order of 10. The Bradshaw model was also extended to rotating flows where the "rotation Richardson number" was defined as

3

$$Ri_\Omega = \frac{2\,\Omega}{\partial U/\partial y} \ .$$

Ellis and Joubert [12] of the University of Melbourne measured mean properties in boundary layers of a curved duct. They, too, noticed that the width of the logarithmic zone was curvature-dependent. Convex curvature caused the velocity profile to become wake-like at a lower value of y^+ and the converse for concave. They found some evidence of spanwise irregularities which may have been due to Taylor-Görtler vortices. Much of the rest of their work was concerned with trying to derive a form of the law of the wall which would be applicable over curved surfaces.

In the early 1970s, Bradshaw undertook a series of experiments on the effects of very weak curvature ($\delta/R \simeq .01$), working first with Meroney [13] and later with Hoffmann [14]. The preliminary measurements taken by Meroney and Bradshaw showed again how the effects of convex curvature made the mean velocity profile less steep, following a lower power law -- as had been observed in other experiments. Because the curvature effects in this experiment were approximately one order of magnitude less than for the So & Mellor work, the turbulence profiles were not as dramatically affected. Still, there is a noticeable decline in the shear-stress levels in the outer region of the boundary layer. The extensive measurements taken by Hoffmann and Bradshaw showed that even this weak curvature affected the triple-velocity correlations very strongly. Their measurements of the mixing length displayed an interesting trend. The outer-layer values declined slowly as the flow moved downstream of the start of curvature, eventually the values over the convex surface were approximately one-half of their corresponding flat-wall values. This gave a very strong indication that, for this weak surface curvature, downstream convection of Reynolds stress was a significant factor in determining the shear stress profile at any point.

Simultaneously with the work described above, Bradshaw and Castro [15] were characterizing a highly (convex) curved free mixing layer. This was the first experiment to examine the recovery process, that is, how the effects of curvature die away after a longitudinally curved shear layer encounters a flat downstream wall. In the early stages of

recovery, their data showed an "overshoot" in value of the turbulent kinetic energy relative to its equilibrium flat-wall value. This peculiar behavior was linked to the suppression of the triple products by convex curvature, as previously documented by the boundary layer experiments.

Effects of very mild curvature on boundary layers were also explored by Ramaprian and Shivaprasad [16,17] in an experiment very similar to that of Bradshaw and his co-workers. In general, the results of the two experiments are qualitatively similar.

Mayle et al. [18] performed heat transfer experiments but presented very few data on the hydrodynamics. Nevertheless, their experiment is an advance because it was the first to isolate the effects of curvature by controlling the pressure gradients along the surfaces.

1.3   Objectives of This Program

The experiments described in the previous section provided a good justification for further research into curvature effects. However, it was clear at the time this program started that, if a turbulence model which could predict the effects of convex curvature were to be developed, reliable data from a specially designed experiment were needed.

This experiment was designed to address issues which had been ignored or overlooked by previous experimenters. In particular, although quite a lot of data had been taken over curved surfaces downstream of flat surfaces, there were no data at the time to indicate how the recovery processes would proceed on a flat wall downstream of a curved wall. This situation is of particular importance because it occurs often in practice, for example on airfoils and turbomachine blades.

Another shortcoming of the data available at the start of this project was the possible influence of longitudinal pressure gradients. The experimental layout used by most previous experimenters (the exception is Mayle et al.), as shown in Fig. 1a, is a duct of constant width which is swung through a bend. This configuration leads to a pressure distribution similar to that shown in Fig. 1b. At the start of curvature, there is (over the convex surface) a substantial streamwise acceleration, and, at the end of curvature, there is a substantial

deceleration. A wealth of data shows that such accelerations have a great effect on turbulence structure, and so it is hard to be sure that the effects observed in previous experiments are entirely due to curvature. In this experiment a specially contoured configuration was used which produced a constant static pressure over the entire test surface. Thus, in the turbulent layers near the wall there were substantially no acceleration effects.

Three experiments were performed in two different wind tunnels. The rest of this document will describe the wind tunnels and other equipment used, then present the data and the turbulence model which was developed from the data.
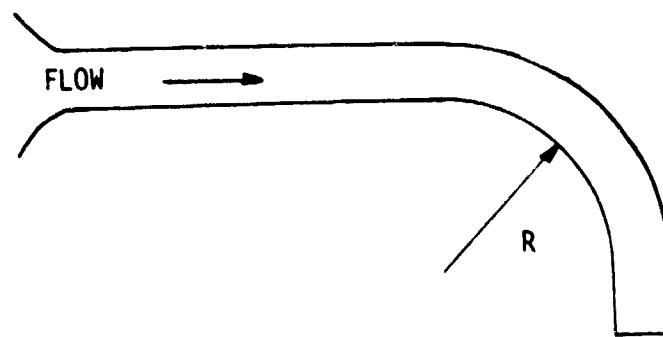
Fig. 1a. Experimental layout used by previous experimenters
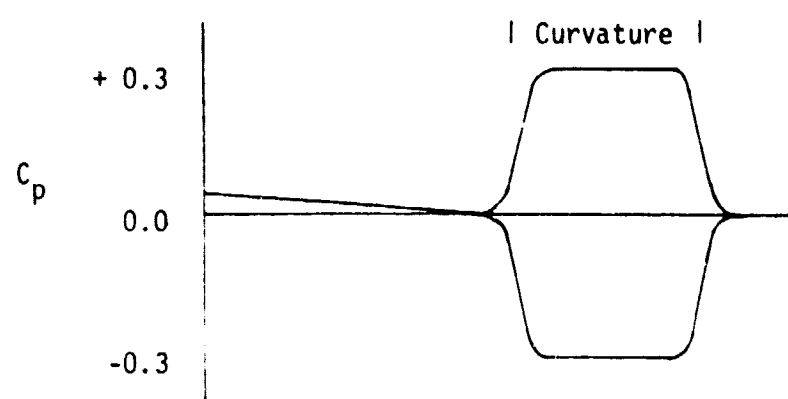
Fig. 1b. Inner and outer wall static pressure distributions
for layout of previous experiments

7

Chapter 2

THE EXPERIMENTAL APPARATUS

2.1 Introduction

A total of three experiments were performed, using two completely
different but geometrically similar wind tunnels. The first experiment
was done on a simple rig which had no facility for heat transfer meas-
urements and which had only a short recovery surface downstream of the
curvature. The last two experiments were conducted on a more elaborate
apparatus, having a longer recovery section and heat-flux instrumen-
tation. In the qualification of both rigs, careful attention was paid
to the control of sidewall secondary flows, in order that the measured
flow be two-dimensional. The secondary-flow control techniques which
were developed for the first experiment (and are described in Appendix
A) were also used on the second and third experiments. The two rigs
will be described in sequence. They are shown in Figs. 4 and 6, and
measurements stations are given in Table 2.1.

2.2 The First Rig

a. Physical Description

The first test section was a 90° curved tunnel of rectangular
cross-section followed by a straight recovery tunnel. This test section
was attached to the end of a long, straight, pretunnel, as shown in Fig.
2a.

The pretunnel is the test section of the two-story Heat and Mass
Transfer Apparatus first described by Moffat [19]. The operating con-
trols and heavy equipment are on the first floor, the wind tunnel (and
curved test section) are on a deck 4.5 meters off the first floor. The
tunnel is open loop; after traveling over the test surface, the air is
exhausted to the room. Incoming air is first filtered through 1.0 micron
retention filter felt. The air then passes through a gate valve, which
is used to regulate the air speed. Once set at a nominal value, the
variation of the freestream speed in experiments performed on the first
rig was about 1%. Downstream of the gate value are two blowers in
series which provide up to 94 cm of H_2O pressure gain at 56 m^3/min

8

flow rate. The flow then passes through a duct from the first to second story, where it empties into a plenum. Downstream of the plenum are a heat exchanger to control temperature, screens to reduce the scale of any unsteady motions, and a two-dimensional nozzle. The side walls of the pretunnel are plexiglass, as is the adjustable top wall. The floor of the pretunnel, over which flows the boundary layer of interest, is a hydraulically smooth surface made of sintered bronze particles. There are 0.063 cm diameter pressure taps in the sidewalls at 15.24 cm intervals in the main flow direction, over the pretunnel's 2.43 meter length. At the start of the experiments the top wall was adjusted so that, for the conditions of the first experiment, the static pressure at all taps was equal within 1% of the freestream dynamic pressure.

As mentioned in the first chapter, one of the aims of this series of experiments was to set up a flow for which the static pressure was constant not only in the pretunnel, but also over the convex test surface and recovery plate. The criterion of constant wall pressure was applied to the design of the curved and recovery sections by use of a theoretical prediction of the static pressure distribution for a tunnel of constant area. An in-house potential flow computer code, RELAX (written by W. C. Reynolds), which uses an irregular star relaxation method, was applied to solve Laplace's equation. Figs. 1a and 1b show the tunnel cross section and predicted pressure distribution for the constant cross-section duct that could have been used without application of the constant-pressure criterion. To maintain the test surface pressure constant, it is clear that the tunnel must be widened at the start of curvature and narrowed near the end of curvature. Figs. 2a and 2b show the tunnel configuration and wall static pressure distributions which were finally obtained after several computer runs. The test surface pressure has been held constant at the price of introducing a severe adverse pressure gradient at the start of curvature and a strong favorable pressure gradient at the end of curvature on the concave wall.

After the tunnel configuration of Fig. 2a had been determined, boundary layer calculations were made for the top (concave) and bottom (convex) walls using STAN5. The results showed that the adverse pressure gradient on the concave side was strong enough to cause a

9

separation which, in turn, was large enough to upset the potential flow pressure distribution. To remedy the situation, a modest amount of suction was applied at the beginning of curvature on the concave wall, and separation was prevented.

To provide the suction at the start of curvature, a restriction was installed at the downstream end of the tunnel. This raised the static pressure in the tunnel to about 1.5 cm--H_2O over atmospheric. At the start of curvature, in the region of adverse pressure gradient, a porous plate was installed as an integral part of the concave wall. On the outside of the porous plate was a plenum box with three sections. The sections spanned the tunnel width and were arranged sequentially in the downstream direction, as shown in Fig. 3. Each of the plenums was connected to the atmosphere by a valve which was adjusted to control the rate of suction. The contours of the final test section and the measuring stations are shown in Fig. 4.

All the static pressure taps were constructed as shown in Fig. 5. First, a .5 cm diameter hole was drilled from the back of the test surface into the spacer, almost all the way through. A .63 mm outside diameter hole was then drilled through from the test surface. Finally, a .5 cm O.D. copper tube, which served as a connector to the tubing transmitting the pressure signal, was inserted and sealed with epoxy.

In the pretunnel, upstream of curvature, there were static pressure taps every 15.24 cm., located in the side walls. From 15 cm upstream of the start of curvature to the end of recovery, the taps were located in the test surface. For 15 cm upstream and downstream of the start of curvature, the spacing of the taps was every 2.5 cm. In the curved region the tap spacing was evey 5 cm. From 15 cm before the end of curvature to 15 cm downstream of the end of curvature, the spacing was again 2.5 cm. In the recovery region, taps were 5 cm apart. There were 128 taps in total, of which 38 were on the tunnel centerline. At 15 stations there were complete spanwise sets of pressure taps at 10 cm spacings in the spanwise direction. About every third centerline tap was part of a spanwise set.

10

b. Qualification of the Flow

The two-dimensionality of the flow was checked as part of the qualification procedure. It was found that, although the flow was very two-dimensional upstream of the curve, the secondary flows generated on the parallel side walls by the pressure gradient normal to the test surface caused significant spanwise non-uniformities in the curved and recovery sections. This problem was solved by skimming off the sidewall boundary layers just upstream of the curvature and also installing boundary layer fences downstream. Details of experiments conducted to study two-dimensionality are given in Appendix A. After installation of the fences, the spanwise variation of the integral properties $(C_f/2, \delta_1, \text{ and } \delta_2)$ across the center 13 cm of the channel was less than $\pm 2.5\%$ at stations 5 (after 40° of curvature) and 9 (in the middle of the recovery plate).

For the test conditions chosen, the free stream speed upstream of curvature was 1600 cm/sec (52.5 ft/sec). Surveys of the boundary layer in the flat pre-tunnel showed it to have normal, zero-pressure-gradient, turbulent boundary layer profiles in the mean velocity and all Reynolds' stresses. The Reynolds number based on momentum thickness was about 5000 at the start of curvature, the point where distance s, measured along the surface, was designated to be zero. The thickness of the boundary layer (based on $U = 0.99 U_p$) varied from 2.95 cm at the first measuring station, Station 1, 71.1 cm upstream of the curvature, to 4.88 cm at the end of the section, Station 10, 44.25 cm downstream of the curvature. In the curved section, the ratio of the 99% boundary layer thickness to radius of curvature varied from 0.085 near the start, Station 3, to 0.097 at the end.

2.3 The Second Rig

a. Physical Description

The second rig was in many ways similar to the first. It, too, had a pretunnel, the test wall of which was a flat preplate, a convex curved test section, and a flat recovery plate downstream. The radius of curvature was 45 cm (17.7 inches), the same as for the first rig, the tunnel height, width, and length of preplate were nearly the same. The

11

major differences were these: the second rig had a recovery plate that was twice as long as that of the first rig; the preplate, the curved, and the recovery test surfaces were copper and fully instrumented for heat transfer measurements; and finally, the second tunnel was a closed-return system.

The physical layout of the tunnel is shown in Fig. 6. A large centrifugal ventilation blower located downstream of the test section delivers pressurized air to a 61 cm diameter duct which connects the blower to a plenum box at the upstream end of the tunnel. Downstream of the plenum is a two-dimensional contraction nozzle with an 11:1 area ratio, a heat exchanger, and six sets of screens. Following the contraction, the potential core has a velocity profile flat within 0.15 percent of the mean and a streamwise turbulence intensity (u'/U_∞) of 0.5 percent. The boundary layer on the test surface is tripped just downstream of the nozzle exit and then flows over the preplate, which is 203 cm long. The tunnel height measured to the wall opposite the test surface, is adjustable to give zero pressure gradient, but in the preplate region, for the experiments to be described, it was always set close to 19 cm.

The convex curved surface was made up of 14 copper plates, each approximately 5 cm in the streamwise direction and 50 cm wide. After assembly, the surface was turned on a large lathe to give a constant radius of curvature of 45 cm. Various types of instrumentation, described by Simon and Moffat [20], was imbedded in the test surface, which allowed very accurate measurement of the surface heat flux. The convex surface also had fourteen .03 mm diameter wall-static pressure taps just off the centerline. On each of three plates -- at the beginning, middle, and end of the curve -- there were five spanwise pressure taps which were used to check for any gross irregularities in the flow. The parallel side walls and the outer (concave) walls of the tunnel were Plexiglas.

As was the case with the first rig, suction had to be applied on the concave wall near the start of curvature. On this rig, however, the suction box design was replaced by a series of seven louvres, as shown in Fig. 7. The skimming of the sidewall boundary layers upstream of

12

curvature was handled in the same was as on the first rig. To replace the air which was exhausted to the atmosphere through these louvers and at various other places, a small blower was used to inject air into a plenum just upstream of the main blower. To assure cleanliness of the injected air, the small blower drew air from a filter box covered with 1 micron retention filter felt. The rate of injection (and hence the tunnel overpressure) was controlled by a slide valve between the blower and the plenum.

b. Qualification of the Flow

As with the first rig, qualification tests were run to see whether the flow was two-dimensional. It was found that the secondary flow techniques developed on the first rig worked well but that the flow upstream of the curve was slightly irregular in the spanwise direction -- integral properties ($C_f/2$, δ_1, and δ_2) varied by about $\pm$ 10 percent relative to the spanwise average of five profiles, each spaced 10 cm apart at the beginning of the curved sector. The problem turned out to be associated with a bend in the return duct, and when this was corrected the flow was everywhere acceptably two-dimensional (spanwise variation les than 5%).

There were two experiments run on the second rig, with different values of δ/R. For the first experiment, the pretunnel freestream speed was 1510 cm/sec (49.5 ft/sec). The inlet boundary layer was, as in the case of the first rig, a normal, zero-pressure gradient turbulent boundary layer as shown by examination of mean velocity and Reynolds' stress profiles at the start of curvature. At the start of curvature, the momentum thickness Reynolds number was 3763, and the ratio of boundary layer thickness to radius of curvature was nominally 0.100.

For the third experiment, one of the two trips used in the second experiment was removed so the boundary layer thickness was less. The freestream speed was 1460 cm/sec (47.9 ft/sec), and the boundary layer momentum thickness Reynolds number was about 2300. In this experiment the ratio of boundary layer thickness to radius of curvature was 0.05.

13

2.4 Measuring Equipment

The most accurate mean flow measurements were taken using wall-static pressures and pitot tubes, which were traversed across the boundary layer (n-direction). The outside diameter of the ends of these tubes was 0.71 mm. The wall-static pressure and total-to-static pressure differences were read from Validyne PM-97 transducers calibrated to assure linearity to ± 0.25% of full-scale output. In the curved region, the static pressure was read at the wall, and the local velocity was then calculated from the formula,

$$ U = \left\{ \sqrt{\frac{2}{\rho}} \ (P_t - P_{sw}) - (P_r - P_{sw}) \left[1 - \frac{1}{(1 + n/R_o)^2} \right] \right\}^{1/2} $$

which is derived and explained in Appendix B.

Mean velocity measurements were also taken using a DISA 55M01 constant-temperature anemometer, a TSI 1076 linearizer, and a DISA 55P01 horizontal wire probe. Because of the limitations of hot wires, these mean-velocity measurements are less accurate than the pitot data. However, they were useful to check the pitot data and, at stations near the start of curvature (where the static pressure distribution was unknown), they provided the only mean measurements.

The horizontal-wire bridge signal was used in conjunction with a TSI 1076 linearizer and a DISA 55D35 True RMS meter to measure turbulence intensities and the dissipation rate.

Measurements of the Reynolds stress tensor were made using two DISA 55M01 bridges, two TSI 1076 linearizers, and a DISA 55P51 x-wire probe. Details are given in Appendix D.

14

Table 2.1

Locations of Measurement Stations for Profiles
of Velocity and Turbulence Properties

First Rig (First Experiment)

Station No.	Location	Streamwise Coordinate, s (cm)
1	Flat wall, pretunnel	−71.75
2	Flat wall, pretunnel	−41.27
3	Flat wall, pretunnel	−6.19
4	Curved region, at 20.6° turn	+16.20
5	Curved region, at 42.8° turn	+33.65
6	Curved region, at 64.7° turn	+50.80
7	Curved region, at 81.6° turn	+64.13
8	Flat recovery zone	+81.91
9	Flat recovery zone	+97.16
10	Flat recovery zone	+112.4

Table 2.1 (cont.)

Second Rig (Second and Third Experiments)

Station Number	Notes	Location	Streamwise Coordinate, s(cm)
1	b,c,d,e	Flat wall, pretunnel	-118.74
2	b,c,d,e	Flat wall, pretunnel	-74.29
3	e	Flat wall, pretunnel	-52.70
4	b,d,e	Flat wall, pretunnel	-41.28
5	b	Flat wall, pretunnel	-29.84
6	a,d,e	Curved region, at 0° turn	0.00
7		Curved region, at 13° turn	+10.39
8	e	Curved region, at 31° turn	+25.19
9		Curved region, at 52° turn	+41.48
10	e	Curved region, at 72° turn	+61.72
11		(This station was never used)	
12		Flat recovery zone	+88.47
13	e	Flat recovery zone	+103.71
14		Flat recovery zone	+118.95
15	e	Flat recovery zone	+124.79
16	e	Flat recovery zone	+149.43
17		Flat recovery zone	+164.78

Notes:

(a)   No pitot mean profiles, second experiment.

(b)   No single hot-wire profiles, second experiment.

(c)   No cross-wire profiles, second experiment.

(d)   No pitot mean profiles, third experiment.

(e)   No turbulence profiles, third experiment.
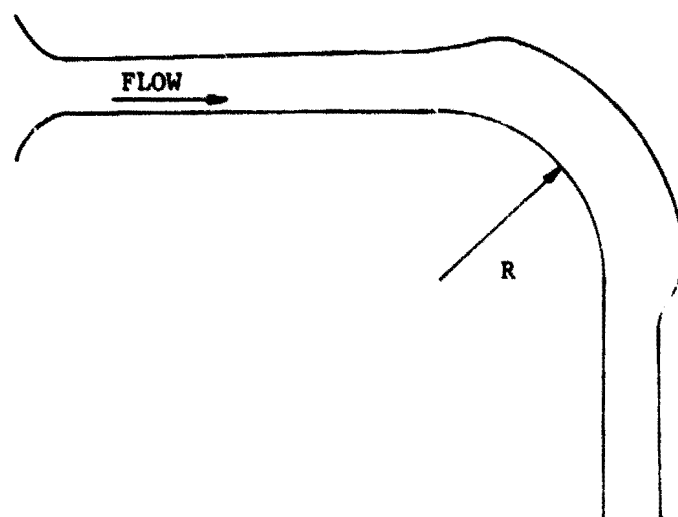
Fig. 2a. Tunnel cross-section for zero pressure wall static
gradient
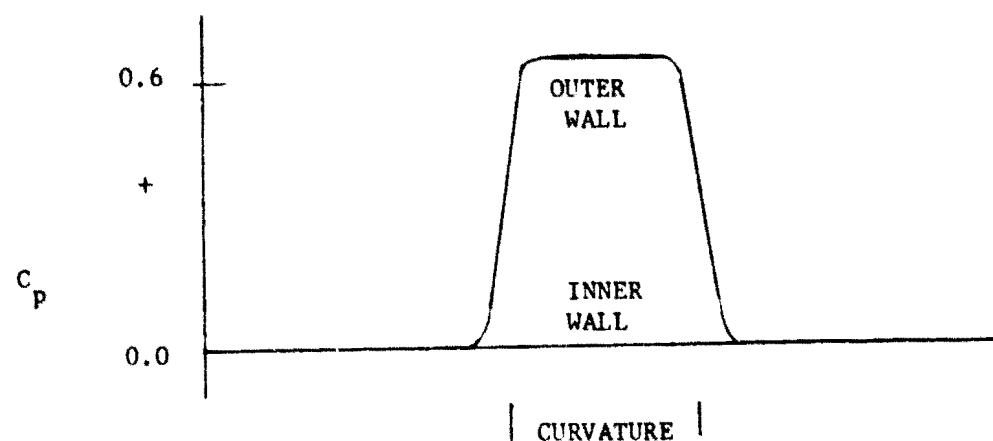
Fig. 2b. Predicted inner and outer wall static pressure
distribution for layout of figure 2a
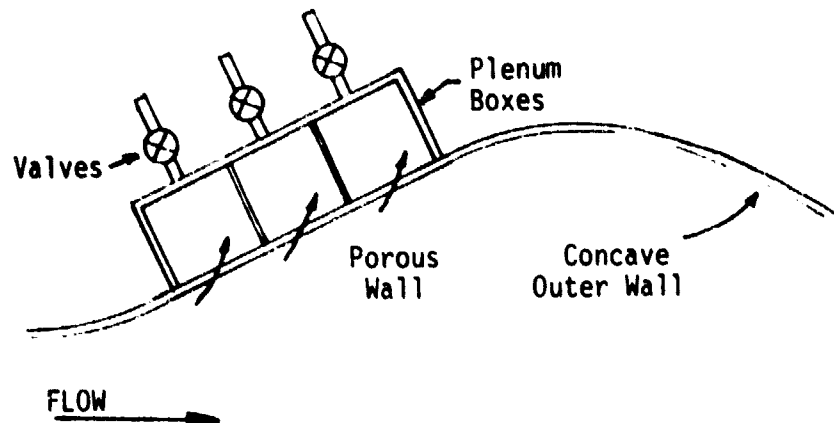
Fig. 3. Suction box located on concave wall (near start of curvature) of first facility
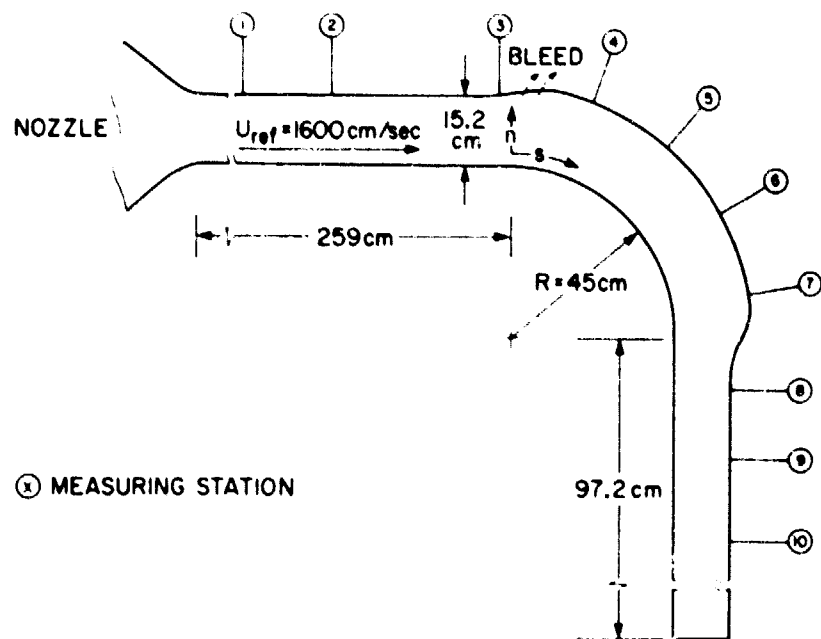
Fig. 4. Schematic of facility for first experiment

FLOW

— 0.63 mm

Test
Surface

Phenolic
Spacer

Epoxy
Sealer

Copper
Tubing
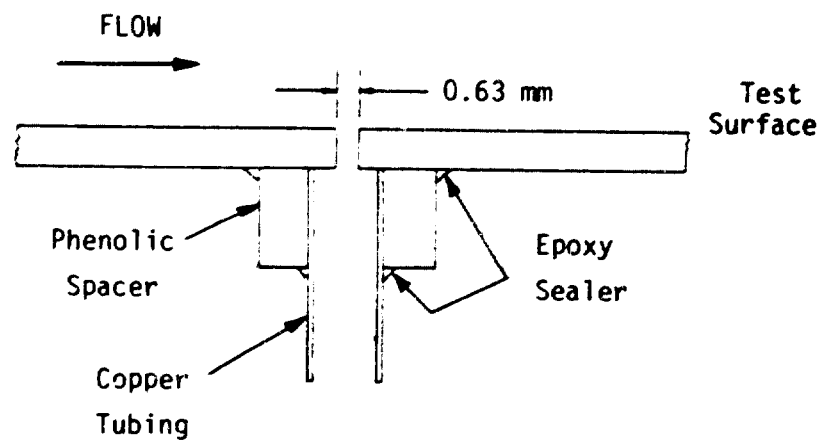
Fig. 5. Typical pressure tap
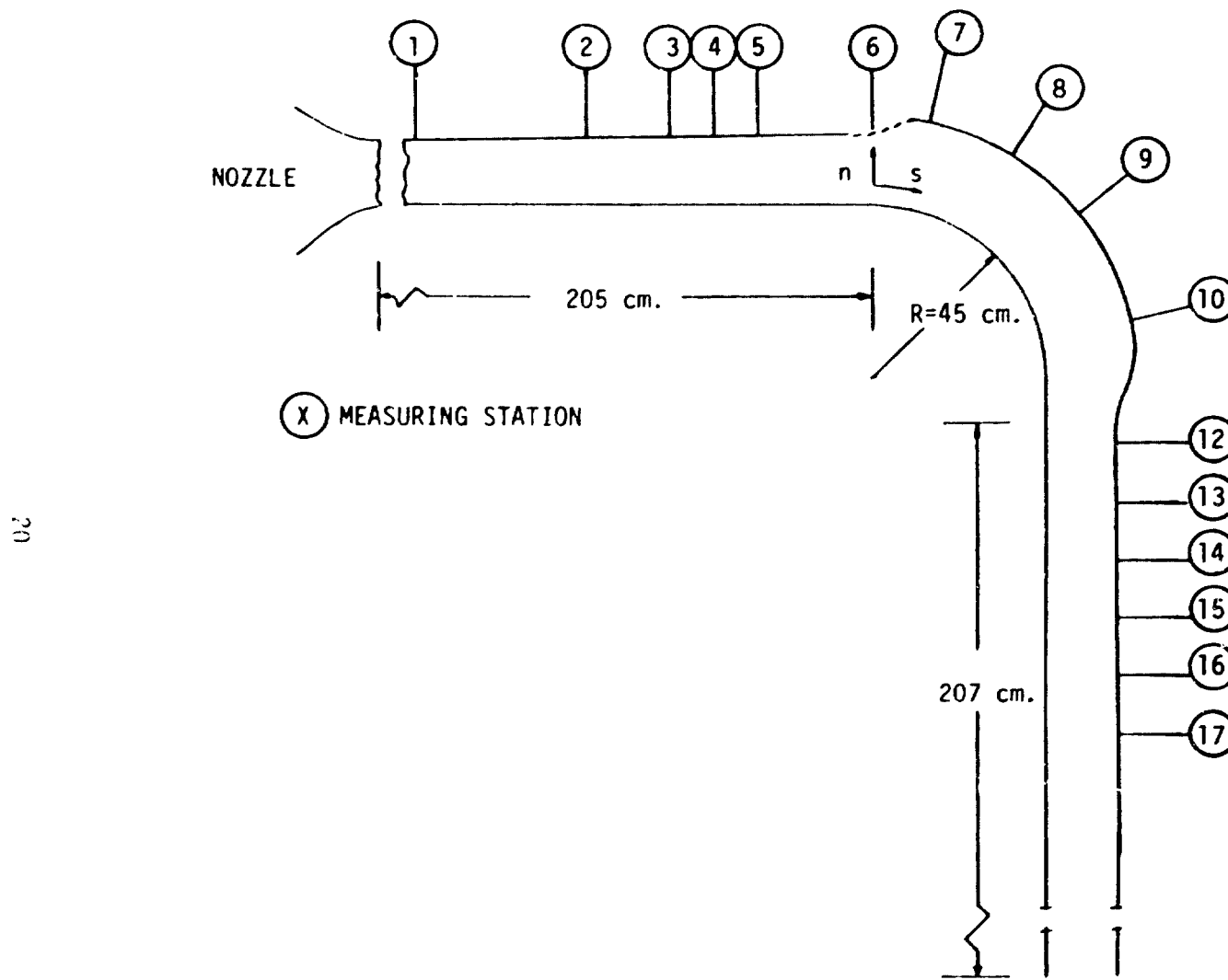
Fig. 1. Schematic of facility for second and third experiment
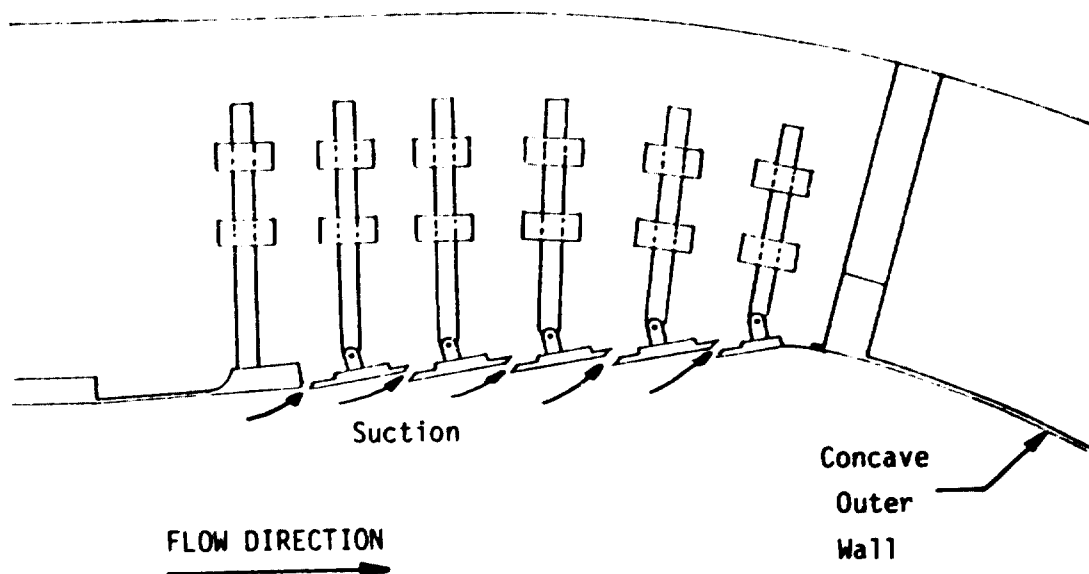
Fig. 7. Louver arrangement located on concave wall (near start of curvature) of second facility

Chapter 3

EXPERIMENTAL RESULTS AND INTERPRETATION

3.1 Introduction

Results from each of the three experiments will be presented in turn, and then general conclusions will be drawn. The first experiment (denoted as Exp. 1) was performed on the cold-flow rig, which had only a short recovery plate. The value of δ/R was close to 0.10. The second and third experiments (Exp. 2 and Exp. 3) were performed on the heat-transfer rig, where more data could be gathered on the recovery process. In the second experiment (Exp. 2) the value of δ/R was again close to 0.10, and so it constitutes a repeat and extension of the first experiment. The third experiment (Exp. 3) was run with a thinner boundary layer; the value of δ/R was 0.05.

3.2 Results of the First Experiment (Exp. 1)

a. Static Pressure Measurements

The distribution of static pressure for the first experiment is shown in Fig. 8. The largest value of the static pressure coefficient, defined as

$$C_p = \frac{P_{sw} - P_{sw,s=0}}{\frac{1}{2} \rho U_{pw}^2} \tag{3-1}$$

is 0.029. This is a small value, however, the pressure coefficient does change from +0.029 to -0.020 in a short distance near the start of curvature. To check whether the resulting pressure gradient was strong enough to affect the turbulence structure, it was necessary to calculate the value of the acceleration parameter K, defined as

$$K = \frac{\nu}{U_\infty^2} \frac{dU_\infty}{dx} = \frac{-\nu}{2U_\infty} \frac{dC_p}{dx} \tag{3-2}$$

To get an approximate value of the pressure gradient, it was assumed that the distribution of C_p near the start of curvature was sinusoidal over a 30 cm length.

$$C_p \approx 0.029 \sin \frac{2\pi x}{30} \qquad\qquad (3-3)$$

$$\frac{dC_p}{dx} \approx 0.029 \frac{\pi}{15} \cos \frac{\pi x}{15} \qquad\qquad (3-4)$$

This pressure field has a maximum value of K of about 2.5×10^{-7}. This value is about an order of magnitude lower than the value needed to significantly change the turbulence structure near the wall. Thus, experimental results should not be affected by any pressure gradients not directly asociated with the curvature.

b. Mean Velocity Measurements

Figure 9 shows mean-velocity profiles taken upstream of curvature, at station 2, at station 5 (after approximately 40° of curve), and at station 10, the last station on the recovery plate for Exp. 1.

It should be explained that the ordinate in Fig. 10 is the local velocity U divided, not by the velocity at the edge of the boundary layer, as is customary on a flat wall, but by the local potential flow velocity U_p. U_p is calculated from an assumed free-vortex distribution:

$$U_p = U_{pw} \frac{R_o}{R_o + n} \qquad\qquad (3-5)$$

where R_o is the wall radius of curvature. After a moment's reflection, it is clear that nondimensionalizing on U_p over the curved wall is the exact analog of nondimensionalizing on the edge velocity over a flat wall. On a flat wall, U_p is effectively the edge velocity at every distance from the wall.

The upstream profile compares well with that expected for a fully turbulent boundary layer; the shape factor, H, is 1.36. The profile at station 5 (after 40° of bend), however, looks more like a transitional or even a laminar boundary layer. The velocity gradient is higher in the wake region and, although it is not readily apparent from Fig. 9, the velocity gradient is lower near the wall. Originally, it was expected that in the recovery region the velocity profiles would relax back toward the upstream profile as the flow moved downstream in

the recovery region. We were very surprised to see the profiles continue to lose their fullness and the shape factors remain high. At the end of the "recovery" section, the recovery of the mean-velocity profile is not apparent at all.

The velocity profiles were then replotted in inner coordinates, as shown in Fig. 10. The method used to calculate u_τ is described in Appendix C. It is clear that the upstream profile from Station 1 follows the law of the wall.

$$\frac{U}{u_\tau} = \frac{1}{.41} \ln\left(\frac{nu_\tau}{\nu}\right) + 5.0 \tag{3-6}$$

It is clear that the profiles in the curved region also follow the law of the wall, although they become non-logarithmic at a lower value of n^+ in the curved region. In the profiles from 60° (station 6) on, it is also possible that there is a second logarithmic zone from $n^+ \approx$ 200 to $n^+ \approx 1500$. The profiles at stations 6, 7, and 8 show the phenomenon most clearly, the second (outer) logarithmic zone seems to be breaking down at Stations 9 and 10, however.

The fact that the curved-wall profiles followed the law of the wall close to the wall but became non-logarithmic at a lower value of n^+ is an indication that the curvature phenomenon is stronger in the outer portion of the flow than in the more highly turbulent layers nearest the wall. This behavior where surface layers are little affected is unusual. In the case of many other phenomena which affect turbulence structure, such as longitudinal pressure gradients, transpiration, or surface roughness, the law of the wall function must be modified to fit the data if accurate fits are needed. With these other phenomena, except for pressure gradients, it is the wall layers which are most affected.

Since the data follow the logarithmic law of the wall, one may calculate the wall skin friction by the Clauser plot method described in Appendix C. The results are shown in Fig. 11, where $C_f/2$ is plotted as a function of distance s along the centerline of the wall. For purposes of comparison, we have included a solid line showing the flat-wall skin friction distribution predicted by the boundary layer code STAN5 [1], using the measured profile at station 1 as an initial

24

condition. The conditions at station 2 are well predicted by the program, but the prediction and the data separate as soon as the flow enters the curve. The effect of the curvature is to reduce the wall-shear stress at Station 7, after 80° of turning, by about 33% -- a large amount, but an amount consistent with that expected from examination of the data of other investigators. The skin-friction data also show the same trend as the mean-velocity profile. Namely, the effects of curvature appear quickly (the dropoff of wall shear is quite apparent at 20° -- only 3.5 boundary-layer thicknesses downstream of the start of curvature), but the disappearance of those effects in the recovery region is clearly an extremely slow process. The last point, at Station 10, is 11.7 boundary-layer thicknesses downstream of the end of curvature, and no recovery is apparent.

In Fig. 12 the displacement and momentum thicknesses have been plotted as a function of s. Over the flat portions of the wall, upstream and recovery, the definition of these quantities is conventional, but for the profiles in the curved region, definitions developed by Honami [21] were used. Honami calculated the integral parameters by imposing the conditions that

$$\int_0^{\delta_1} U_p \, dn = \int_0^\infty (U_p - U) \, dn \qquad (3-7)$$

$$\int_0^{\delta_2} U_p^2 \, dn = \int_0^\infty U(U_p - U) \, dn \qquad (3-8)$$

The physical basis for these definitions, in the case of δ_1, is the idea that the displacement thickness should correspond to the distance the wall must be displaced into the potential flow field to account for the mass-flow deficit caused by the velocity defect in the boundary layer.

Fig. 12 shows a rapid increase in both δ_1 and δ_2 in the recovery section after the dip* at the end of the curved wall. One mechanism which could cause this rapid increase is the action of any residual secondary flow from the channel end walls, which was not removed by the measures described in Appendix A. The secondary flow drives extra-low momentum fluid toward the centerline. If the flow were entirely free of any secondary flow influence, then it is possible to calculate, from the momentum integral equation, the rate of growth of δ_2 in the recovery region. Because the static pressure is constant, the two-dimensional momentum integral equation reduces to

$$\delta_2(x) = \delta_{2_o} + \int_0^x \frac{C_f}{2}\, dx \qquad (3-9)$$

where δ_{2_o} is the momentum thickness at some starting point, here taken at station 8, s = 33 cm. Fig. 13 shows the measured δ_2 (PL) and the calculated δ_2 (PR) in the recovery region. In the recovery region, PL increases faster than PR, indicating that some secondary flows may be present. This idea was checked using a form of the momentum integral equation which allows for secondary flow,

$$\delta_2(x) = \delta_{2_o} + \int_0^x \frac{C_f}{2}\, dx + \int_0^x \delta_2 \frac{\tan \alpha}{z}\, dx \qquad (3-10)$$

where $\alpha = \arctan \overline{W}/\overline{U}$. and $z = 0$ on the centerline. The basic assumptions are that all mean velocity profiles are collateral (not skewed) and that the boundary layer flow is a simple convergent or divergent flow. Using Eqn. (3-10) along with the measured values of δ_2 and $C_f/2$, the effective secondary flow angle for the center 13 cm of the flow was calculated. The results are shown in Table 3-1 below, along with flow angles in the boundary layer measured with the Conrad probe (see Appendices A and E), and the agreement is close enough to sustain the conclusion that the difference between PL and PR is caused by secondary flow.

---

*The "dip" in the first experiment is yet to be explained. The δ_2 at Station 8 was repeatable. The "dip" did not appear in experiments two (Fig. 32) or three (Fig. 47).

Table 3-1

Calculated and Measured Secondary Flow Angles
for the Recovery Section of First Experiment

s (cm)	32.25	38.25	44.25
Eqn. (3-10)	0.7°	3.7°	1.4°
Measured Flow Angle[*]	3°	2°	1.5°

[*]Average value in profile, see tabulated data for details.

From the mean velocity profiles, it was possible to calculate the rate of entrainment. On a flat wall, the boundary layer mass flux is simply

$$\dot{m} = \rho \int_o^\delta U \, dy = \rho \, U_\infty \left[\delta - \delta_1 \right] \tag{3-11}$$

On a curved wall, however, we used the formula

$$\dot{m} = \rho \, U_{pw} R_o \, \ell n \left[\frac{R_o + \delta}{R_o + \delta_1} \right] \tag{3-12}$$

which is derived and explained in Appendix H. Results for upstream and curved regions are shown in Fig. 14. Results are not plotted for the recovery region, because the secondary flow which is present there tends to influence the rate of growth of the integral quantities.

The solid line shown in Fig. 14 has the slope calculated from known correlations for flat-wall turbulent boundary layers without pressure gradients,

$$\delta_2 = 0.037 \, s \left(\frac{\nu}{U_\infty s} \right)^{0.2} \tag{3-13}$$

and

$$\delta = \frac{\delta_2}{0.097} \quad , \quad \delta_1 = \frac{\delta_2}{0.776} \tag{3-14}$$

The fact that the flat-wall data have the same slope as predicted by Eqn. (3-13) is another indication that the boundary layer upstream of curvature is normal. Fig. 14 shows that the entrainment rate, $d\dot{m}/ds$, is greatly reduced by the curvature. Since the mechanism by which free-stream fluid is entrained into the boundary layer has been linked to action of large-scale sweeping motions near the edge of the boundary layer, this result suggests that presence of the pressure gradient normal to the wall $(\partial p_s/\partial n \approx \rho U^2/(R_o+n))$ has inhibited these large-scale motions. Further evidence will be presented to support this hypothesis.

c. Turbulence Intensity Measurements

Turbulence-intensity profiles were taken at all ten stations in Exp. 1. In Fig. 15 is an isometric plot of all ten profiles with distance along the centerline as a parameter. The curvature clearly affects the profile shape. For example, the peak turbulence intensity, which occurs very near the wall, declines quickly after the start of curvature. Fig. 15 also provides some confirmation of the slow recovery trend observed in the mean-velocity profiles. The profile taken at station 10 shows a higher level of turbulence intensity than the profiles taken over the curved surface, but it is not nearly so intense as the profiles upstream of the curve. The recovery that is seen takes place first at the wall and then diffuses slowly outward. At the last recovery station, the "bulge" of increased turbulence, outside of the sharp peak, has reached only about halfway across the layer.

In Fig. 16, the four profiles of u' taken in the curved region have been superimposed. It is interesting that there the profiles at 40, 60, and 80° are very similar. This indicates that, near the end of the curve, the process of accommodation to curvature by the turbulence is nearly complete. By accommodation, we mean that a fair degree of similarity in profile shape is achieved after 40 degrees of curvature. Comparison of curved profiles of Stations 5, 6, and 7 with the upstream profiles shows another interesting fact. In the upstream profile the value of u' falls off sharply at first and then with a steady negative slope from $n/\delta \approx 0.05$ to $n/\delta \approx 0.8$. Beyond 0.80 the rate of dropoff

28

increases, due to the action of intermittency. For the profiles in the curved region, however, after the initial sharp dropoff, there is a region from $n/\delta = 0.40$ to $n/\delta = .80$ where the value of u' is fairly constant. This "shelf" will be discussed in more detail in Section e.

d. Measurement of Dissipation

Approximate measurements were also made of the dissipation rate. In doing so the usual assumption that the small-scale motions which are responsible for the dissipation are isotropic was made. This means the dissipation is approximately [22]

$$\epsilon \simeq 15 \; \nu \; \overline{\left(\frac{\partial u_1}{\partial s}\right)^2} \tag{3-15}$$

Using Taylor's hypothesis, this becomes

$$\epsilon \simeq \frac{15 \; \nu}{U^2} \; \overline{\left(\frac{\partial u}{\partial t}\right)^2} \tag{3-16}$$

Eq. (3-16) was used to determine the dissipation rate from the time-differentiated horizontal wire signal. As pointed out by Klebanoff [23], this method of measuring dissipation is not completely accurate because of assumption of isotropy. However, the measurements are useful for qualitative comparison of the structure of curved and flat boundary layers. Profiles taken at stations 1, 5, and 10 are shown in Fig. 17. The results are nondimensionalized on U_{pw} and δ. The profiles show that the dissipation rate over the curved surface is different from the dissipation rate over the flat surface, especially outside of $u/\delta = 0.1$. The profile at station 10 on the flat recovery surface shows a two-layered structure, not unlike the shear-stress and turbulence-intensity profiles at the same station.

e. Measurements of Reynolds Stresses

Complete Reynolds stress profiles were taken at all ten stations using the rotatable x-wire probe described in Appendix D. Fig. 18 shows the $-\overline{uv}$ profile measured upstream of curvature at station 1, plotted along with a profile taken by Klebanoff. The agreement is reasonable. Further, the value of wall-shear stress obtained by the Clauser method from the mean-velocity profile was used to normalize the data in Fig. 18 to give unity value at $n/\delta = 0.0$, and it is clear that the extrapolated turbulent shear stress line agrees with the wall shear, as it should.

Figure 19 is an isometric plot of all ten shear-stress profiles vs. n/δ. This plot shows the drastic effect of curvature on shear stress. The first three profiles, taken before the onset of curvature, are quite similar and display a high level of turbulent shear stress at the wall and well out into the boundary layer to $n/\delta \approx 0.1$ or 0.2. However, the profile at station 3, which is just upstream of the start of wall curvature, shows a slightly reduced level of turbulent shear stress in the wake, while the near-wall layers seem to be unaffected. Because streamline curvature outside of the wall layers must start a little upstream of $s = 0$, the outer layers are affected by curvature at Station 3. This result gives more evidence that the curvature effects are powerful and that they are felt away from the wall more than in the wall layers. The transformation in profile shape from station 3 to station 4 is dramatic. The shear stress virtually disappears in the outer 70% of the layer and is greatly reduced near the wall. Downstream, the profiles seem to recover a little but have a shape which is much like the profile at $20°$. In the recovery zone, the profile shape changes markedly from the last curved profile, at $80°$ of turn, to the first recovery profile at Station 7. In the recovery profiles there is a layer close to the wall where the gradient of shear stress in the n direction is approximately zero. Nevertheless, the shear-stress profiles also show the "slow recovery" from the effects of curvature already seen in the skin-friction, mean velocity profiles, and the turbulence-intensity profiles. Examination of the last recovery station shows that the value of $-\overline{uv}/U_{pw}^2$ is still very low at all values of n/δ compared to the upstream profiles.

Figure 19 also shows the wall values or shear stress calculated from the mean profiles at each station. At all stations (except station 4), the value of shear stress extrapolated from the $-\overline{uv}/U_{pw}^2$ profiles agrees well with the law-of-the-wall values. Agreement between extrapolated turbulent and mean-velocity wall shear is a good indication that the data presented are reliable. The fact that there is good agreement in the curved region is perhaps a surprise. Many analytical derivations of the law of the wall assume that there is a region in the fully turbulent zones near the wall where the shear stress is nearly independent of distance from the wall and equal to the wall-shear stress. The curved surface profiles do not show such a region.

Figure 20 compares the shear-stress profiles at stations 3 and 4. It is clear that the enormous change takes place in a downstream distance of only about five boundary-layer thicknesses. Such a large change in the Reynolds stress in so short a distance clearly means that the large and medium scale, stress-carrying "eddies" in the boundary layer are far from equilibrium. It is not surprising, then, that the wall shear calculated from the Clauser plot method (which assumes that the boundary layer "eddy" structure is at or near equilibrium) is not in agreement with $-\overline{uv}$ profile extrapolated to give a wall-shear stress. The extrapolated values are believed to be closer to the true values of u_τ.

In Fig. 21 the shear-stress profiles are plotted for the stations nominally at 40, 60, and 80° of the curve. There is a region between $n/\delta = .10$ and $n/\delta = .35$ where all the profiles collapse on a single curve. While this is not a large fraction of δ, it is a significant fraction of the region where $\overline{uv}$ is large. Profile collapse indicates that the boundary layer turbulence structure may have attained an "equilibrium" state, an idea which is supported by the observation that this is the same region where the second log zone appears in the u^+ vs. y^+ data. In the region beyond $n/\delta = .75$, the profile at 40° shows positive values of $\overline{uv}$, as does the 20° profile shown in Fig. 20. The values of positive $\overline{uv}$ are not large but are larger than the uncertainty in the data (see Appendix D). Previous convex-curvature experiments (So and Mellor) at similar conditions also found a region of

31

positive $\overline{uv}$ far from the wall, but attributed it to uncertainty in the data.

As discussed in Appendix D, the design of our cross-wire probe allowed us to measure all the turbulent normal stress $(\overline{u^2}, \overline{v^2},$ and $\overline{w^2})$ at each point. From these we were able to calculate the turbulence kinetic energy $(q^2/2)$. Fig. 22 shows three $q^2/2$ profiles for representative upstream curved-wall and recovery stations. The level of q^2 declines due to curvature, but not as drastically as the shear stress, $-\overline{uv}$.

Plotting profiles of the individual components of q^2 allows a clearer picture to develop. Figs. 23, 24, and 25 show the normal stresses at stations 1, 5, and 7. Upstream of curvature (Fig. 23), the normal stresses are very different in magnitude near the wall but approach the same values near the free stream. Fig. 24, which is a profile typical of the curved region, shows that, near the wall, the three Reynolds stresses are more nearly equal than on a flat wall. The most remarkable thing, however, is the shape of the profiles. All three quantities fall off sharply near the wall, and (at about the same y/δ value where $-\overline{uv}/U^2_{pw}$ has reached a value close to zero) they have approximately the same magnitude (v' is slightly lower than u' and w'). Unlike the upstream profile, the level of each component stays fairly constant from $n/\delta \approx 0.3$ to $n/\delta \approx 0.8$. Beyond $n/\delta \approx 0.8$, the magnitude of the turbulent normal stress drops off due to intermittency of the turbulence at the outer edge of the layer. Thus, there is a region where the values of u', v', and w' are nearly equal and where the gradient of each in the n direction is small. In this same region, the turbulent shear stress is close to zero.

The profiles near 80° of turn, plotted in Fig. 25, show the same behavior, except that the level of the "shelf" is lower.

The explanation for the shape of the normal stress profile is obtained from the turbulence kinetic energy equation. Over a curved wall, it has the form [24]:

32

$$U \frac{\partial(q^2/2)}{\partial s} + \left(1 + \frac{n}{R}\right) \frac{\partial(q^2/2)}{\partial n} = -\overline{u^2}\left[\frac{\partial U}{\partial s} + \frac{V}{R}\right] - \left(1 + \frac{n}{R}\right) \overline{v^2} \frac{\partial V}{\partial n}$$

$$- \overline{uv}\left[\left(1 + \frac{n}{R}\right)\frac{\partial U}{\partial n} + \frac{\partial V}{\partial s} - \frac{U}{R}\right]$$

$$- \frac{\partial}{\partial s}\left[\frac{\overline{p'u}}{\rho} + \overline{q^2 u}\right] - \frac{\partial}{\partial n}\left[\left(1 + \frac{n}{R}\right) \frac{\overline{p'v}}{\rho} + \frac{\overline{q^2 v}}{2}\right]$$

$$- \varepsilon \tag{3-17}$$

where ε is the dissipation rate for conversion of turbulence energy to internal thermal energy. If the gradients of q^2 in the normal direction are small (as the profiles in the outer parts of the curved flow show they are), then the redistribution terms in the line directly above ε can be assumed to be negligible. For this experiment, the three terms $\partial U/\partial s$, V/R, and $\partial V/\partial n$ are also negligible, as they would be in a constant freestream-velocity, plane-wall layer. For the region where $u' \approx v' \approx w'$, we also have seen that $\overline{uv} = 0$. This leaves the dissipation as the only significant term on the RHS of the equation. On the LHS, the second term which depends on $\partial(q^2/2)/\partial n$ will also be small. The TKE equation then reduces to:

$$\frac{d(q^2/2)}{ds} = \frac{\varepsilon}{U} \tag{3-18}$$

This equation predicts that the level of the "shelf" should decline monotonically as the flow moves downstream. Figs. 24 and 25 show this is clearly the case. The turbulence in the outer part of the layer is then "debris" from the preceding flat-wall boundary layer, which simply decays as it is convected downstream.

To test this conjecture, the following calculations were made. First, from the mean-flow data the positions $(n(s))$ of mean-flow streamlines were located. The data were then studied as a function of distance s along the curve. If the turbulence in the outer parts of the boundary layer is indeed quasi-isotropic, then its decay, as it is convected downstream by the flow, should be predictable. We employed a model for the decay of isotropic turbulence given by Reynolds [25] as:

$$q^2 = q_0^2 \left[1 + \frac{5t\varepsilon_0}{3q_0^2}\right]^{-6/5} \tag{3-19}$$

33

where q_o is the initial value of q^2 and ε_o is the initial value of
the rate of turbulence dissipation. ε_0 in our computation was taken
from the dissipation measurements. Using Taylor's hypothesis to replace
t by x/U and with the conditions at station 5 as initial conditions,
the decay of the turbulence was calculated along a streamline. The re-
sults are given in Table 3-2 below.

Table 3-2

Comparison of Calculation and Experiment

Remarks	Turning Angle (degrees)	Station	Distance $s-s_0$ (cm)	Exper. q^2 (cm^2/sec^2)	Calcul. q^2 (cm^2/sec^2)
Curved	40	5	0.0	$6230 = q_o^2$	
Curved	60	6	17.8	4900	4400
Curved	80	7	30.5	4200	3600
Flat Recov.		8	42.2	4900	3100

The model and experiment show fair agreement in the curved region,
although the calculated decay is slightly faster than the experimental
rate up to Station 7. The agreement is bad in the recovery region, Sta-
tion 8, but this is to be expected. The appearance of significant
$-\overline{uv}$ in the outer region during flat-wall recovery produces (generates)
new q^2 which more than balances the decrease due to dissipation. The
agreement is about the same for other streamlines which exist between
the place where the shear stress becomes negligible $(n/\delta \approx 0.4)$ and
where intermittency effects become important $(n/\delta \approx 0.7)$. This cal-
culation is intended only to show that the turbulence decays at roughly
the predicted rate in the curved region; the model employed is too crude
to pursue further, and it is no good in the recovery zone.

The fact that the turbulence in the outer layer decays leads to an
interesting hypothesis; namely, if the curved region were long enough,
the outer part of the layer would eventually become laminar. The "tur-
bulent shear layer" would then fill only the inner 35% of the mean-
velocity-gradient boundary layer, and the outer 65% would affect the

34

wall transport processes only indirectly. If this hypothesis is accepted, then it can be concluded that even close to the start of curvature, the largest scales of the "turbulent shear layer" must be of the order of .35 δ.

Since all the non-zero Reynolds stresses have been measured, the structural coefficient $a = (- \overline{uv}/q^2)$ can be computed. Profiles of a vs. n/δ for three stations are shown in Fig. 26. Upstream of curvature a is nearly constant over almost all of the boundary layer and is about equal to 0.145, a value in good agreement with previous flat-plate measurements [26]. For the curved boundary layer, however, a becomes a strong function of position across the layer. Values of a beyond $n/\delta \approx .4$ are not very reliable, because of the uncertainty in $- \overline{uv}$ on q^2, both of which have low magnitudes. Many calculation methods employ the assumption that $- \overline{uv}/q^2$ is a constant, and so it is clear that some modification will be necessary if these models are ever to handle curvature. In the recovery region, a very surprising trend is noticed. The recovery of the structural coefficient is very quick (compared to the sluggish recovery of the $- \overline{uv}$ and $\overline{u^2}$ profiles).

The idea that the "turbulent shear layer" is concentrated in a narrower zone within the "velocity-gradient layer" could also provide an explanation for the shape of the $- \overline{uv}/q^2$ profiles, if the "turbulent shear layer" has its own intermittency, as sketched in Fig. 27. If the ratio of $- \overline{uv}/q^2$ in the "turbulent shear layer" is about 0.145 as usual (and as it is near the wall), then a probe which time-averages $- \overline{uv}/q^2$ at a point where instantaneous $- \overline{uv}/q^2$ is alternately 0.145 (wall layer) and 0.0 (outer, decaying layer) could easily produce a profile like that at Station 5 in Fig. 26.

3.3 The Second Experiment

Upon the completion of the first experiment, just described, the second rig went into operation. This rig had a recovery section which was about twice as long as that of the first rig and was in addition set up for surface heat-flux measurements. The first experiment run on the new rig was essentially a repeat of the experiment run on the old rig,

as a check on its performance, and to obtain more data on the slow recovery process, which could not be deduced from the first experiment.

a. Static Pressure

Figure 28 is a plot of the measured wall static-pressure distribution; it, too, is flat, as for the first experiment (see Fig. 8), and, as previously noted in Section 3.2A, the effects of pressure gradients on the wall layers are unimportant.

b. Two-Dimensionality and Inlet Boundary Layer

The boundary-layer thickness was adjusted by installing trips in the "transition box" between the nozzle exit and the preplate. For Exp. 1, two 32 mm trips, each 1.25 cm wide, were installed about 25 cm apart. This produced a boundary layer thickness at the start of curvature of 3.75 cm. Figs. 29 and 30 show the turbulence intensity and shear-stress profiles plotted with Klebanoff's data for a constant pressure turbulent boundary layer of different, but fully turbulent, flows (see Re_{δ_2} value denoted in Fig. 29). There is good agreement.

As with the first experiment, careful attention was paid to the two-dimensionality of the flow. In Fig. 31, the momentum thickness measured at five spanwise locations 29.84 cm upstream of curvature are plotted vs. z. The variation is less than ± 5%. Also plotted are five profiles from station 13 in the recovery section. This station corresponds to a place on the first rig where the flow angles reached a maximum. Comparison of results in Fig. 31 to those from Exp. 1 (shown in Fig. A-12) shows that there is less secondary flow interference in this experiment. This observation was confirmed when the skew angles were measured. Finally, a plot of PL and PR, shown in Fig. 32, shows that the two terms grow at the same rate from the middle of the curved region down to the end of the recovery plate. All results indicate that the flow in the longer recovery section of Exp. 2, which was of prime interest here, was very two-dimensional. This point is important because the observations from the first experiment about the slow process of recovery from curved to flat-wall conditions were confirmed in the second experiment. We conclude that the effects noted are

contaminated little if at all by wall pressure gradients or by secondary flow effects.

c. Mean-Velocity Measurements

Figure 33 shows mean-velocity profiles measured upstream (Stn. 5), in the center of the curve (Stn. 9), at the point (Stn. 14) which corresponds to the last recovery station on the first experiment, and the farthest downstream measurement (Stn. 17) in the new experiment. The most important trend noticed in the velocity profiles of the first experiment -- that recovery has not even begun in the outer part of the layer ten boundary-layer thicknesses downstream of the end of curvature -- is clear again. Two new observations can be made from the new profile at station 17, which is 20 boundary layer thicknesses downstream. First, there does seem to be some recovery taking place very close to the wall, below $n/\delta = 0.05$. Second, the profile is smoother beyond $n/\delta = 0.10$, which is interpreted to mean that the effects of the short region of longitudinal pressure gradient in the outer layers, at the end of curvature, have disappeared.

The fact that the values of U/U_p along given streamlines (or approximately at given n/δ) is _increasing_ as the flow moves downstream in the recovery region has certain implications about the shape of the shear-stress profile. As pointed out by Smits et al. [27], the momentum equation, along a streamline in a constant-pressure flow, reduces to

$$\frac{\partial P_t}{\partial x} = \frac{\partial \tau}{\partial y} \tag{3-20}$$

where P_t is the stagnation pressure and τ is the total shear stress. For the recovery points very near the wall, P_t is increasing downstream. Since τ drops to zero at the edge of the boundary layer, one concludes that the gradient of τ must be positive near the wall and that τ must reach a maximum _away from the wall_, even when $\partial P_3/\partial x = 0$.

Figure 34 shows the distribution of wall shear computed from the mean-velocity profiles. Also shown for comparison are the data from the first experiment and the flat-wall predicted values for both data sets. There is obvious agreement. The new data show that the recovery

37

process is still not complete at station 17, about 20 boundary-layer thicknesses downstream of the end of curvature.

Because the flow in the recovery zone of the second experiment was two-dimensional, the growth rate of boundary-layer mass flux could be used to estimate the entrainment rate. The data points plotted in Fig. 35 were obtained using the procedure described in Appendix I. It is clear from the plot that the entrainment rate, which is reduced by the curvature, remains low all the way through the recovery section. In this case as in Exp. 1, Fig. 15, the solid line has the slope entrainment rate) expected for a flat-plate boundary layer, and it fits the data upstream of the start of curvature.

The shape factor computed from the profiles is shown in Fig. 36. The curvature raises H, as might be expected, and, although it drops a bit, H stays high all the way through recovery.

d. Turbulence-Intensity Measurements

Figure 37 shows profiles of turbulence-intensity taken from three spanwise locations downstream of curvature. They indicate clearly that the turbulence field was two-dimensional, when compared to the profiles taken at three streamwise locations (see Fig. 38).

Data from the first experiment showed that the recovery of the turbulence-intensity profiles started as a "bulge" near the wall which migrated across the layer as it moved downstream. In Fig. 38 three turbulence-intensity profiles from the beginning (Stn. 12), the middle (Stn. 14) and the end of recovery (Stn. 17) have been plotted on top of each other. The profiles from Stns. 12 and 14 show the same outward-migrating bulge that was observed in the first data. However, there is not too much change between stations 14 and 17, indicating that the turbulence profiles are nearing completion of their recovery. The "bulge" has all but disappeared by station 17. Figs. 33 and 34, of course, show that the mean-velocity profile is nowhere near completing its recovery.

e. Reynolds Stresses

The turbulent shear-stress profiles for all stations are plotted isometrically in Fig. 39. Again, there is good agreement with the Clauser-plot skin friction everywhere but at the first station in the curved region. In this experiment, the first station in the curved zone is much closer to the start of curvature than in the first experiment, and there is a profile taken exactly at the point where the profile changes from flat to curved. Fig. 40 shows an upstream profile, the profile at the start of curvature, and the first two profiles in the curved region. The results of the first experiment showed that there was a very quick change in the shear-stress profiles after the onset of curvature, but Fig. 39 proves it to be even quicker than the first experiment indicated. Right at the start of curvature, the near-wall value of $-\overline{uv}/U_{pw}^2$ is only slightly less than it is at station 4, which is 28 cm upstream. This indicates that the curvature effects have yet to really begin. At station 6, the change to a typical curved-wall profile is complete -- in only 2.5 boundary-layer thicknesses. In the outer region, the profile at station 7 shows nearly zero shear stress. By station 8, the outer layer shear stress has become negative by a significant amount. A glance at Fig. 39 shows that the negative shear stress disappears as the flow continues downstream. This region of negative shear stress is also apparent in Fig. 19 from the first experiment.

The shear-stress profiles taken over the curved wall in the first experiment collapsed on each other when nondimensionalized on U_{pw}^2. Fig. 41 shows that the last three profiles in the curved region collapse in the second experiment also. It seems clear that there is some sort of simple scaling law waiting to be discovered.

In the recovery region, there is no similarity of profiles when $-\overline{uv}/U_{pw}^2$ is plotted vs. n/δ, as Fig. 42 shows. At the start of recovery, there is a very quick transformation in the shape of the profile. Near the wall, the curved region profiles do not show an obvious region of constant stress, as do the flat-wall profiles upstream. The profile at station 12, however, suggests that there is a constant stress region beyond which the stress level increases to a maximum before

falling off sharply, like the curved-wall profiles. The fact that there is a maximum away from the wall is in accordance with the observations made earlier about the recovery of the mean-velocity profiles. Farther down the recovery plate, the maximum moves away from the wall, and the point at which the shear stress falls off linearly also moves out. Thus, there is a gradual thickening of the width of the active shear-stress layer until it fills the width of the velocity-gradient layer, δ. Examination of the profiles at stations 16 and 17 shows that, at about the time the active shear-stress layer is as wide as the velocity-gradient layer, the shear-stress profiles stop changing, although the maximum is still there.

Figure 43 is an isometric plot of the turbulence kinetic energy (TKE). When compared to the isometric plot of shear stress (Fig. 39), it is interesting to note that the TKE profiles do not change as drastically at the start of curvature. Rather, the decline winds down as it flows downstream. The profile at station 10 has a shape which suggests the two-layer structure discussed before. The TKE drops off almost linearly with distance from the wall out to $n/\delta \approx 0.40$. Beyond $n/\delta \approx 0.40$ is the "shelf" which appears in the normal stress profiles. If the hypothesis that the "shelf" will eventually decay is correct, then a portion of the profile which remains (the part which drops off rapidly near the wall) will have a shape which is similar to the up-stream profiles, except that the width of the layer is about the same as the width of the active shear layer. As with the first experiment, each of the three turbulent normal stresses were measured at each station, allowing the calculation of the structural coefficient "a". "a" changes rapidly from being a function of position in the curved region (as it was in the first experiment) to being about constant (see Fig. 44), as it usually is in flat-plate boundary layers.

3.4 The Third Experiment

The last experiment in this series was run on the long-recovery rig. One of the upstream trips was removed and the remaining trip readjusted in order to give a boundary-layer thickness-to-radius of curvature ratio of 0.05. This procedure enabled us to observe the

effects of curvature at an intermediate value of δ/R. It was also supposed that the recovery process would be more complete, since the number of (velocity-gradient) boundary-layer thicknesses downstream of curvature was greater.

Other than inlet boundary-layer thickness, the only difference in tunnel conditions between the second and third cases was the nominal freestram speed, which was 48.1 ft/sec in Exp. 3. Figure 45 shows the measured distribution of wall static pressure, which is similar to that of the other two cases.

The skin-friction distribution for this case is plotted in Fig. 46, along with the flat-wall prediction. Despite the fact that the original boundary layer is only about one-half as thick as for the previous cases, the $C_f/2$ curve is remarkably similar. The recovery after curvature appears to be no more advanced at the end of the recovery plate than in Exps. 1 or 2.

One of the consequences of thinning the test surface layer was to increase problems with secondary flows generated on the end walls. Since the boundary layers on the side walls and fences were unaffected by the change from thick to thin test- surface boundary layer, the amount of secondary flow fluid coming off the side walls and fences was the same as for Exps. 1 and 2, where $\delta/R = 0.10$. The test-surface boundary layer mass flux, however, was much less, and consequently the skew angles increased. Fig. 47 shows PL-PR calculations for this experiment. The secondary flows are clearly enough to influence the growth rate of integral parameters. The mean skew angle for this case is approximately 4 degs, using the results in Fig. 47. Experience with the first two experiments indicates that measurements of $C_f/2$ and the turbulence quantities should not be greatly affected by small secondary flows and skew angles.

Only six shear-stress profiles were taken in the last experiment. Measurements were made upstream; two were located in the curved region, and three were over the recovery plate. Fig. 48 shows all these profiles.

The trends observed previously are reconfirmed here, except for a couple of peculiarities. First, in the profile taken near the end of curvature (station 9), the region over which there is appreciable shear stress extends over a greater fraction of δ than in the $\delta/R = 0.10$ cases. Second, in the last profile at station 17, the level of $-\overline{uv}/u_\tau^2$ at its maximum is much higher over the entire profile than for the measurements taken upstream. At $n/\delta \approx .50$ the value of $-\overline{uv}/u_\tau^2$ at station 17 is <u>twice</u> what it is at station 5.

As in the $\delta/R = 0.10$ experiments, the structural coefficient, a, became a function of position (y/δ) over the curved surface, as shown in Fig. 49. For this case the steepness of the dropoff at large n/δ is much less than was the case at $\delta/R = 0.1$.

3.5 Comparison of all Experiments

The data from all experiments, both at $\delta/R = 0.10$ and at $\delta/R = 0.05$ show a striking degree of similarity downstream of the start of curvature. It is suggested that, as the width of the active shear layer is decreased, the large eddies which carry the "history" of the turbulence structure are either destroyed or modified in such a way that the "history" is lost. Downstream of the start of curvature, the initial conditions are largely irrelevant. Note that in both flows we have examined the initial boundary layer thickness δ was larger than the thickness of the shear-stress-carrying region. The present suggestion may not be valid for layers that are very thin at the start of curvature.

Support for this interpretation comes mostly from the shear-stress profiles. Fig. 50 shows three plots of $-\overline{uv}/u_\tau^2$ vs. n/R_0. The three plots are from different experiments, but they are all from stations near the end of curvature. It is clear that, for the three experiments presented here, $-\overline{uv}/u_\tau^2$ is a function only of n (R was constant for these three experiments). To check the significance of R, we have also plotted, in Fig. 51, the shear-stress data of So and Mellor, from an experiment in which the radius of curvature and the freestream velocity were somewhat different from those in the present case (R = 32.56 cm, $U_{pw} = 2404$ cm/sec). The data follow the same curve, which again

indicates that the shear stress is a function of n/R rather than n/δ, and that it is, at most, only a weak function of U_{pw}. That U_{pw} is not a strong influence is surprising, since the cross boundary-layer pressure gradient $\rho U^2/R$ is a strong function of U_{pw}.

In Fig. 52, the skin-friction curves for Exps. 2 and 3 have been overlaid. It can be seen from these curves that the curvature exerts an "organizing influence" -- the values of skin friction after the start of curvature are much closer in value than they were over the preplate. Measurements of Stanton number for the same two experiments, taken by T. W. Simon and shown in Fig. 53, show the similarity of conditions after curvature even more clearly.

The main effect of strong curvature, then, is to impose a limit on the size of the largest eddies. If the initial large-eddy size is larger than this limit, eddies larger than the limit must either shrink or be destroyed. In the recovery region, the large-scale eddies grow back slowly, just as large eddies grow slowly in a developing boundary layer.

Apparently our experiments at $\delta/R = 0.05$ and $\delta/R = 0.10$ simply approach the same "asymptotic convex boundary layer" from two slightly different initial conditions. Whether an initially thin layer such as that of Hoffman and Bradshaw ($\delta/R \simeq 0.01$) approaches this limit from below is an open question. If our results do indeed show an asymptotic state, the results of Bradshaw & Hoffmann, as plotted on Fig. 51, must be well below that asymptotic state.
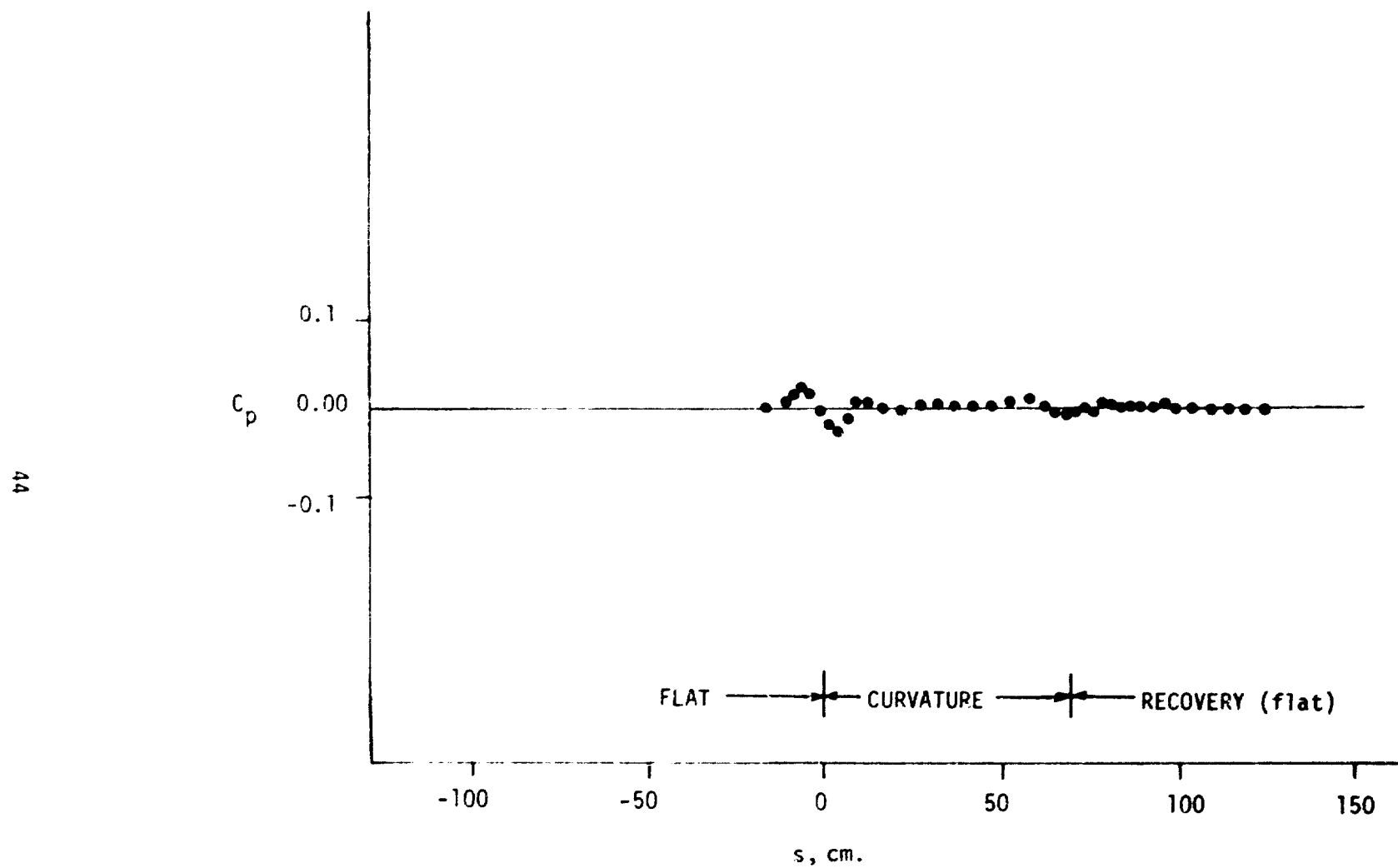
Fig. 8. Measured convex-wall static pressure distribution for first
experiment

44
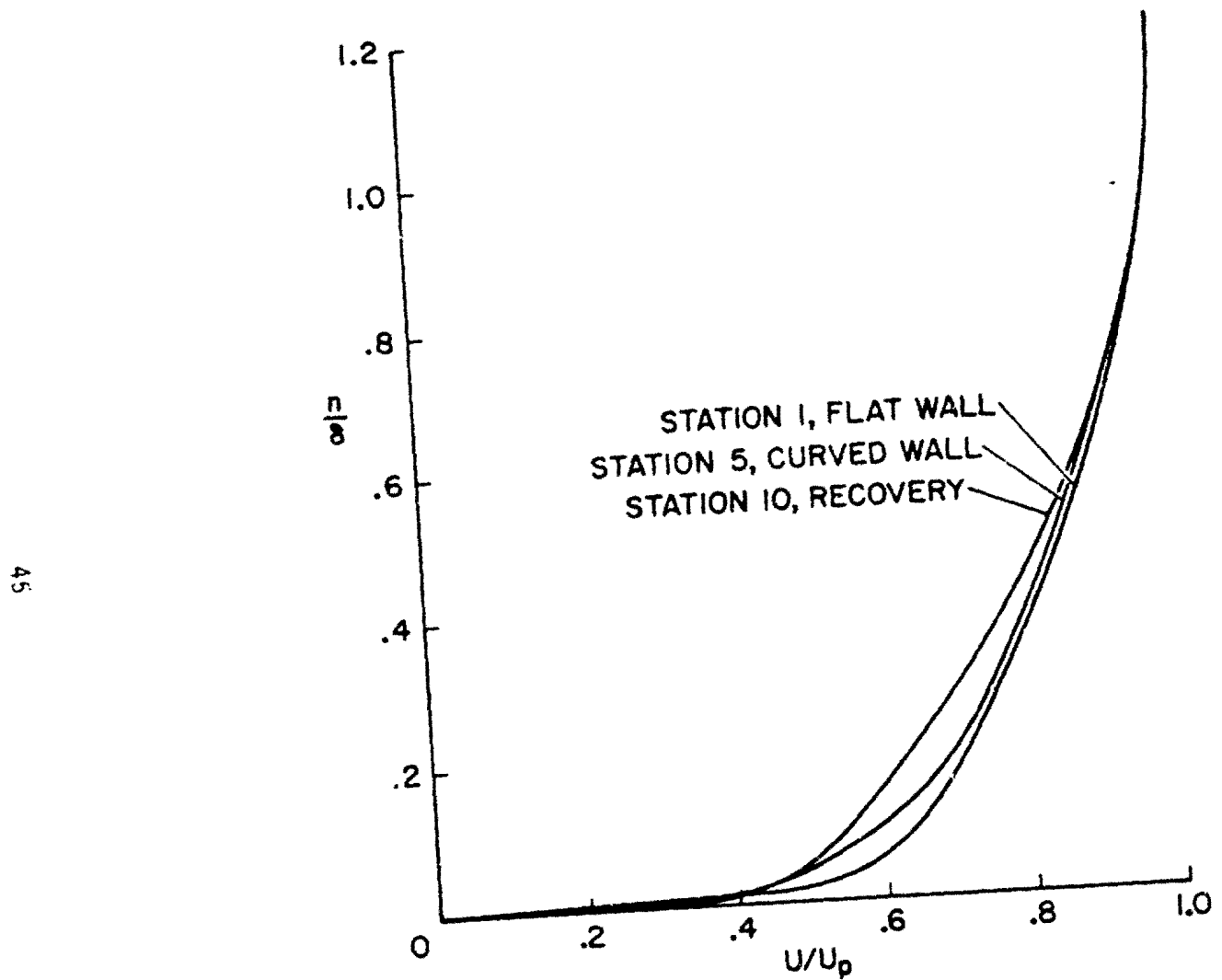
Fig. 9. Mean-velocity profiles at representative stations for first experiment
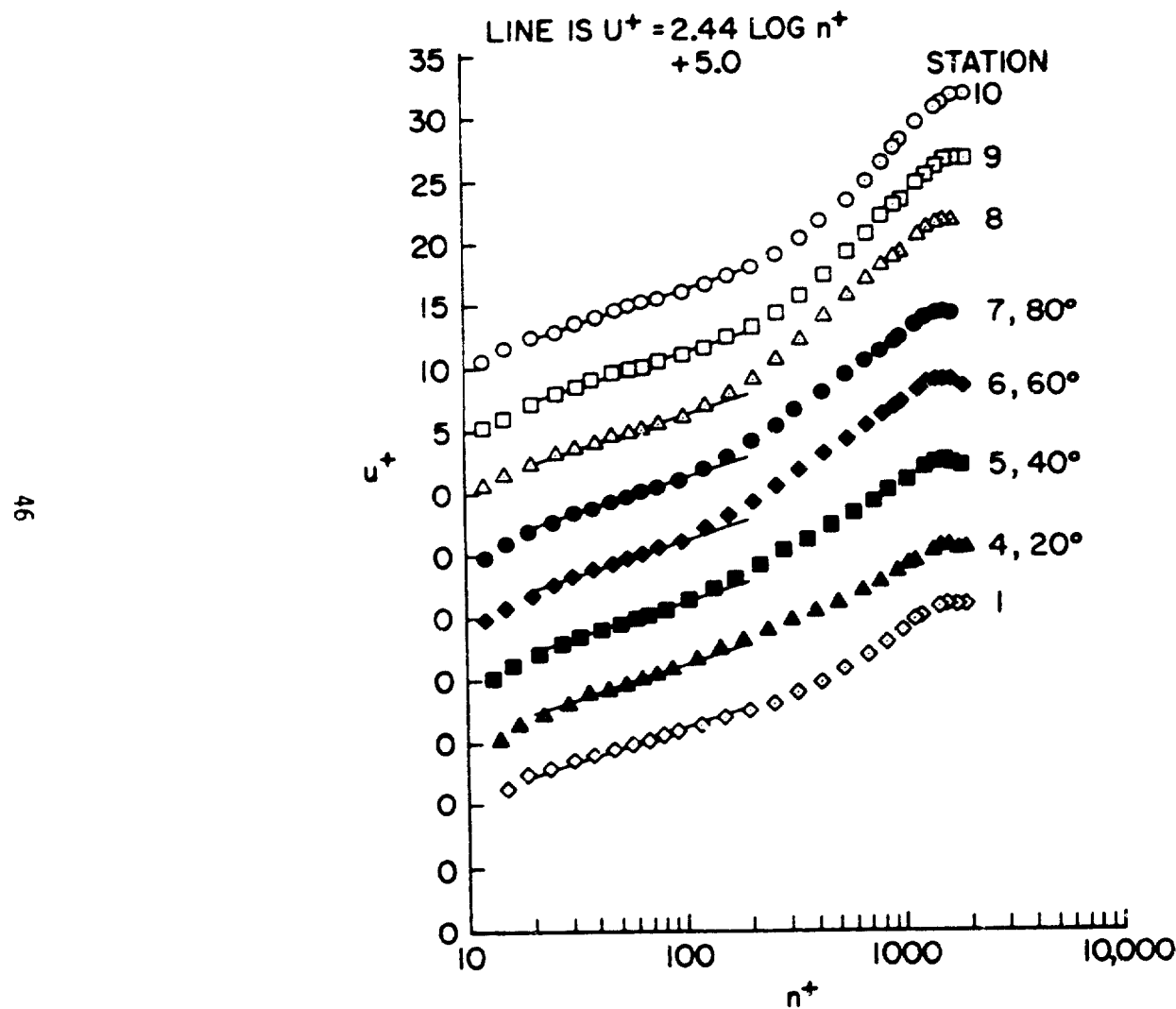
Fig. 10. Mean-velocity profiles plotted in wall coordinates for first experiment
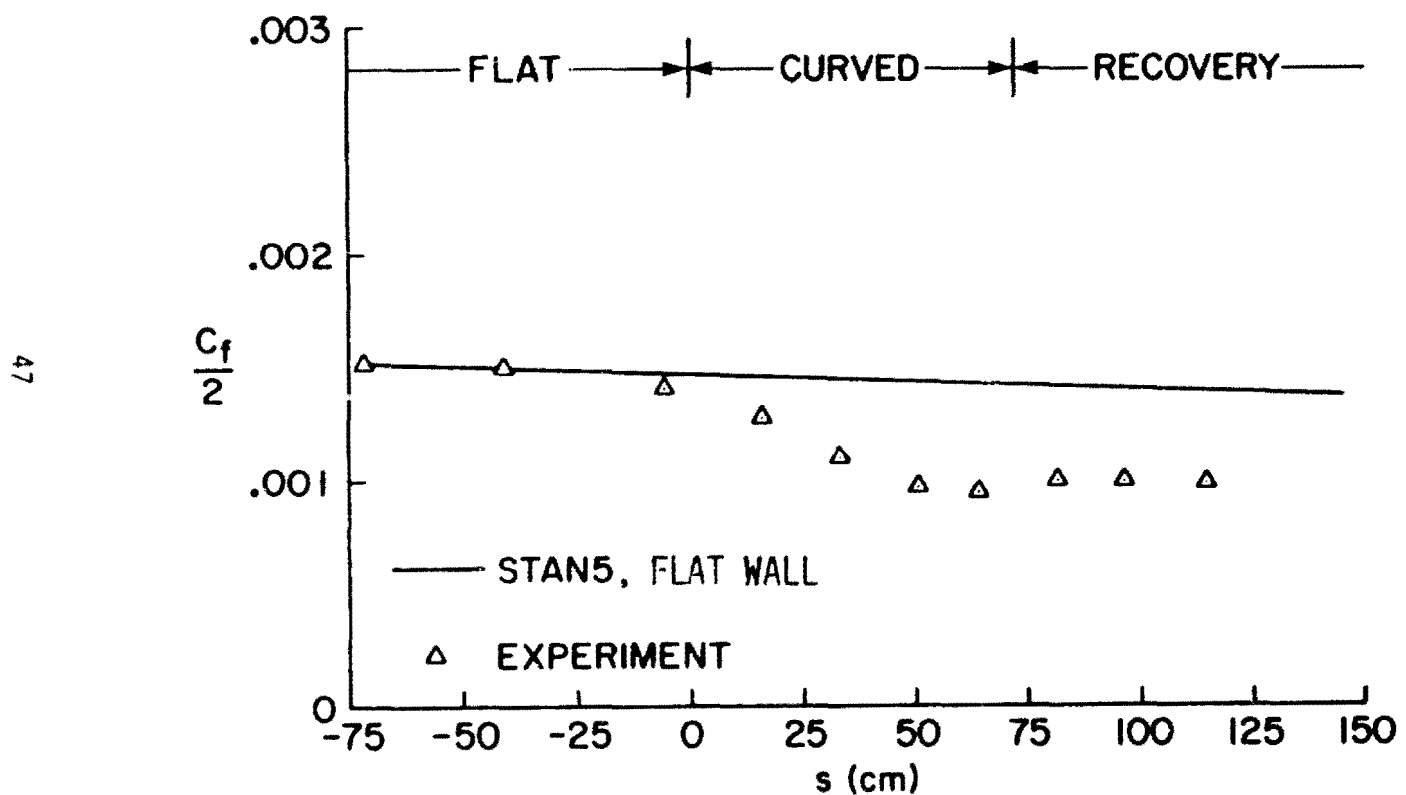
Fig. 11. Skin friction (from Clauser plot) vs. distance in flow
direction for first experiment
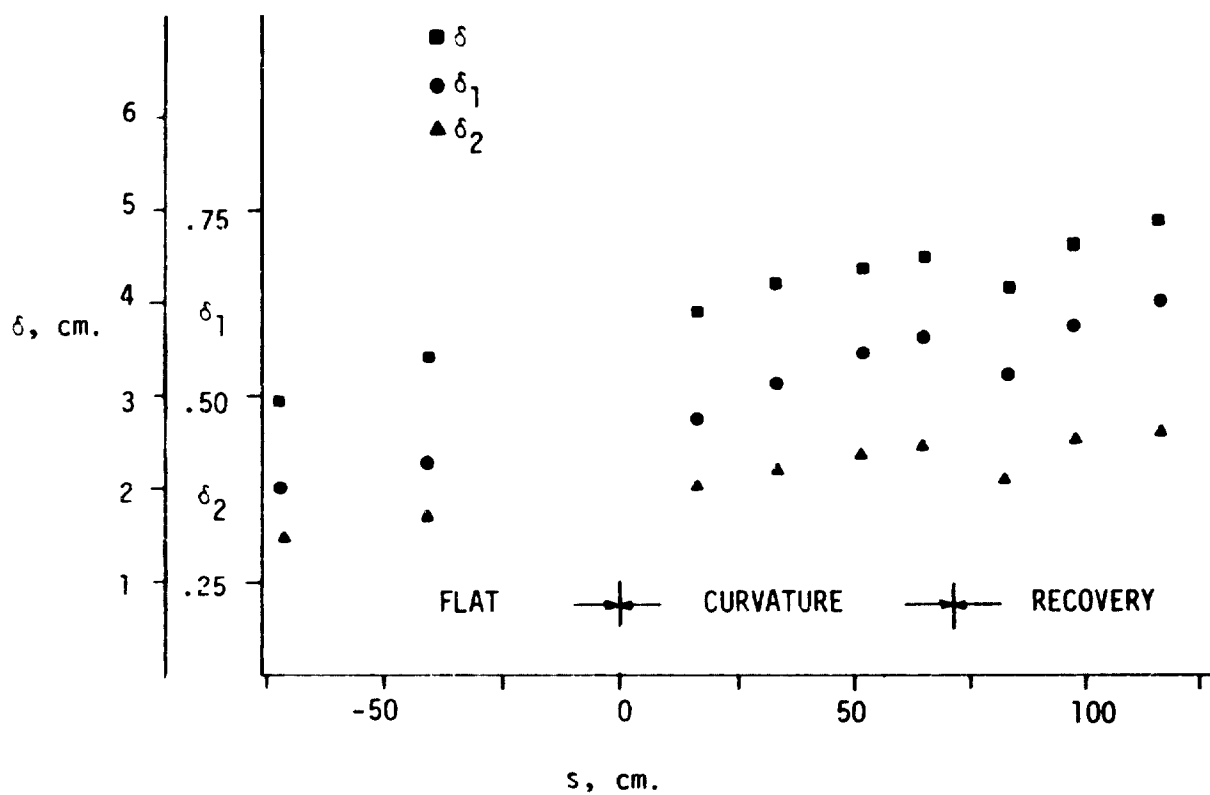
Fig. 12. Plot of integral properties vs. streamwise distance for
first experiment
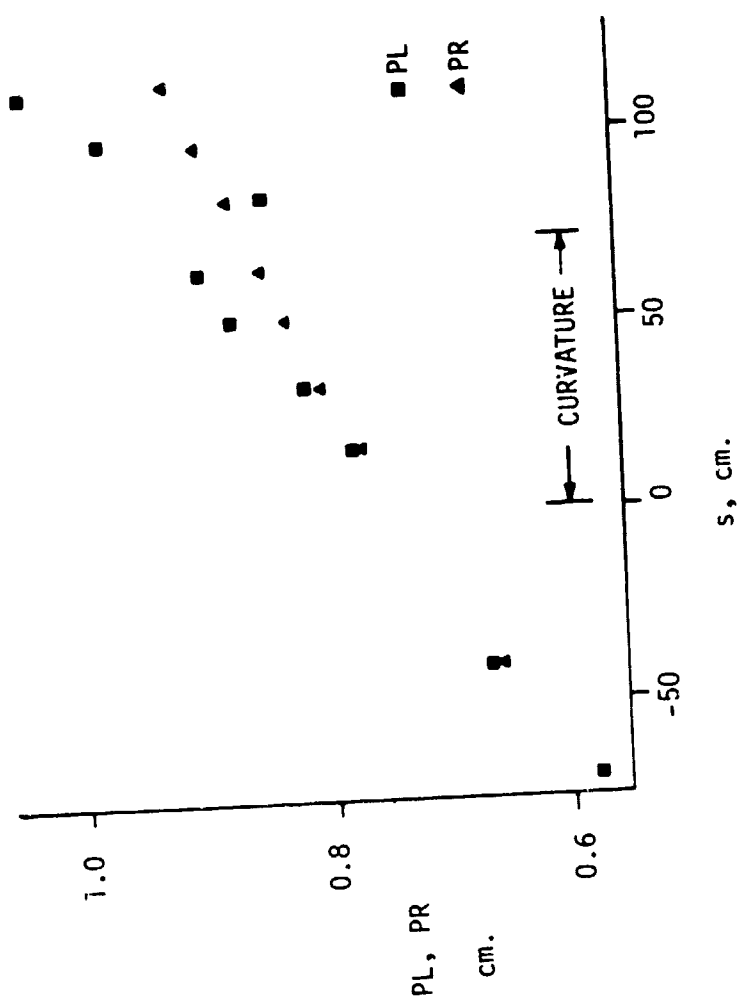
Fig. 13. PL and PR for first experiment
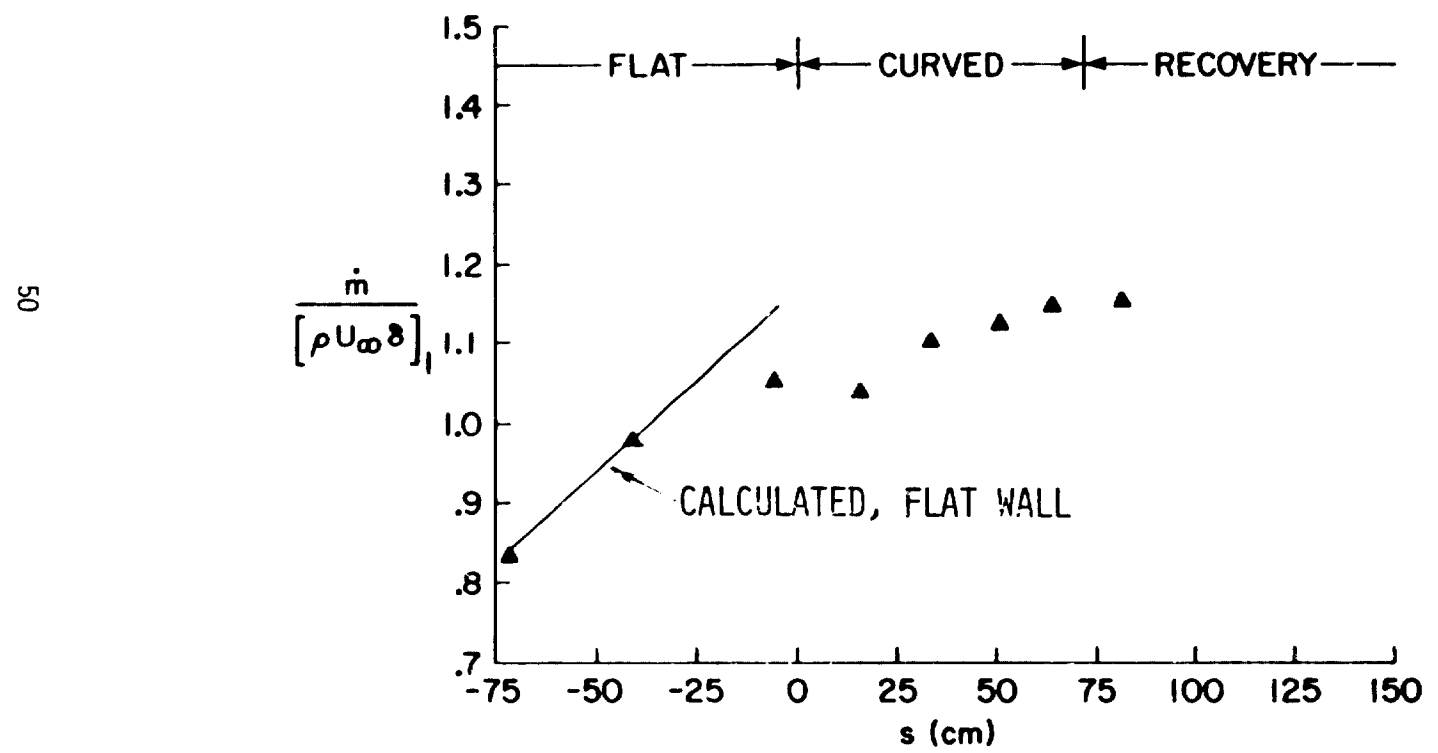
Fig. 14.   Boundary-layer mass flux vs.   s   for first experiment
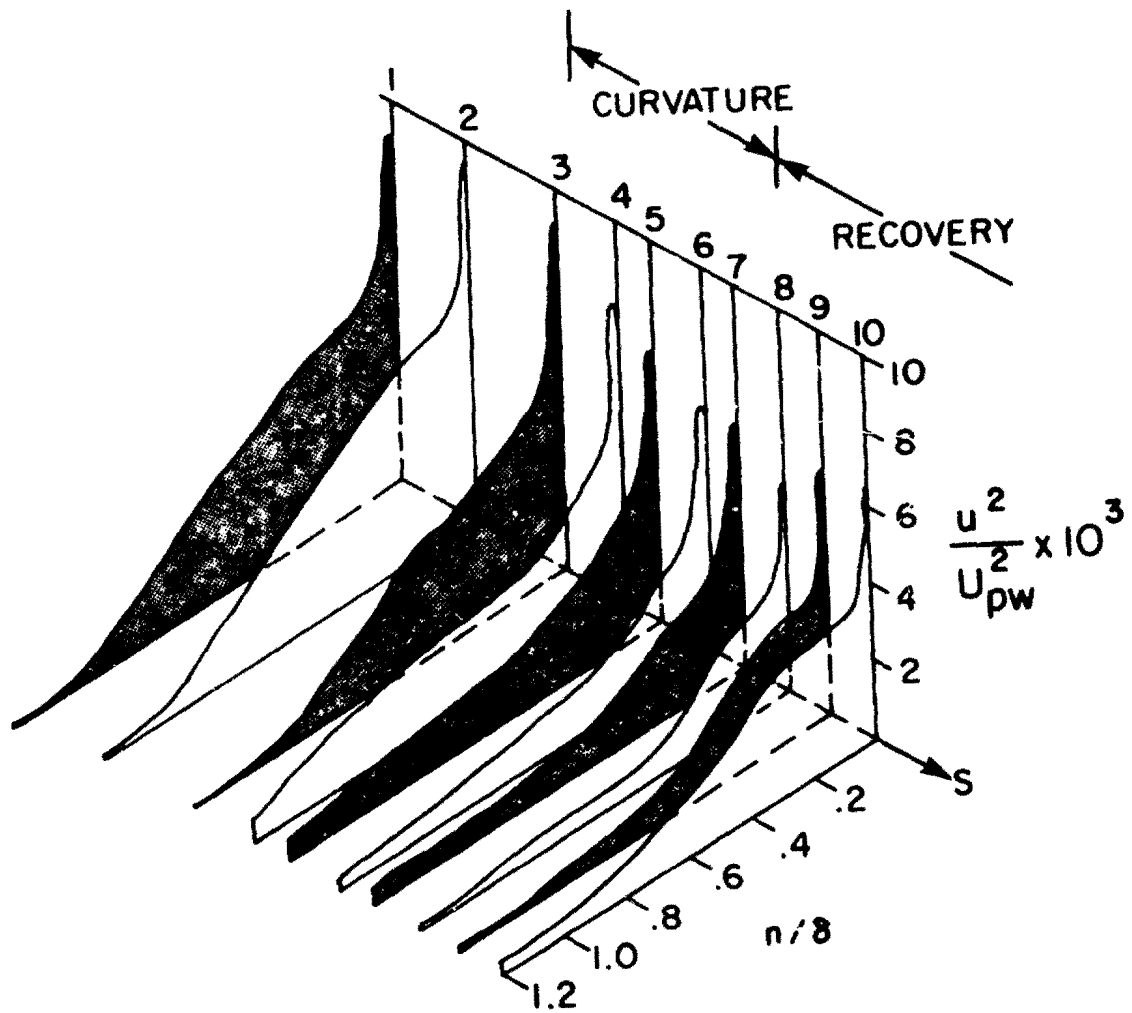
Fig. 15. Isometric plot of turbulence intensity vs. distance in streamwise direction for first experiment
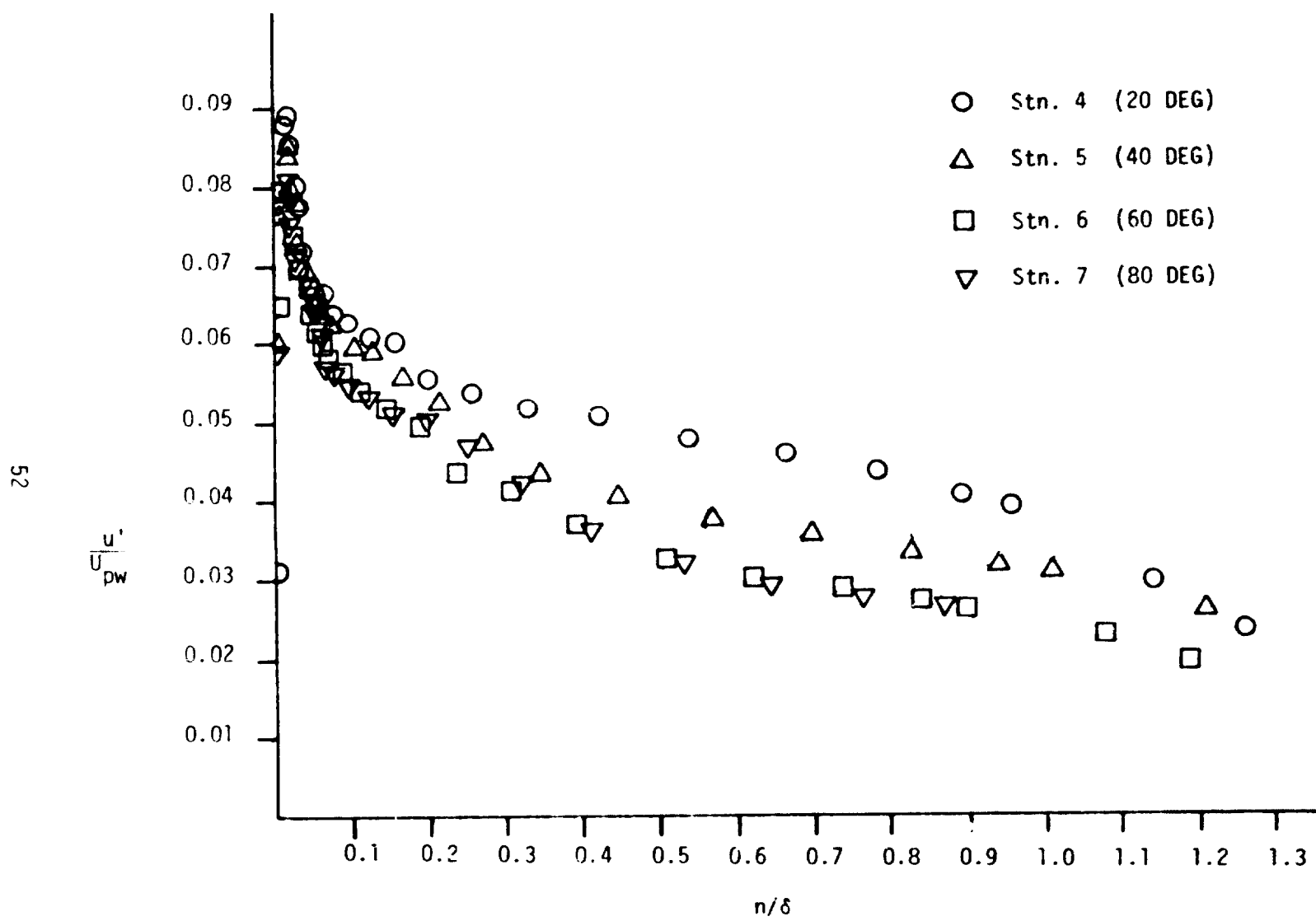
Fig. 16. Turbulence-intensity profiles in curved region for first experiment
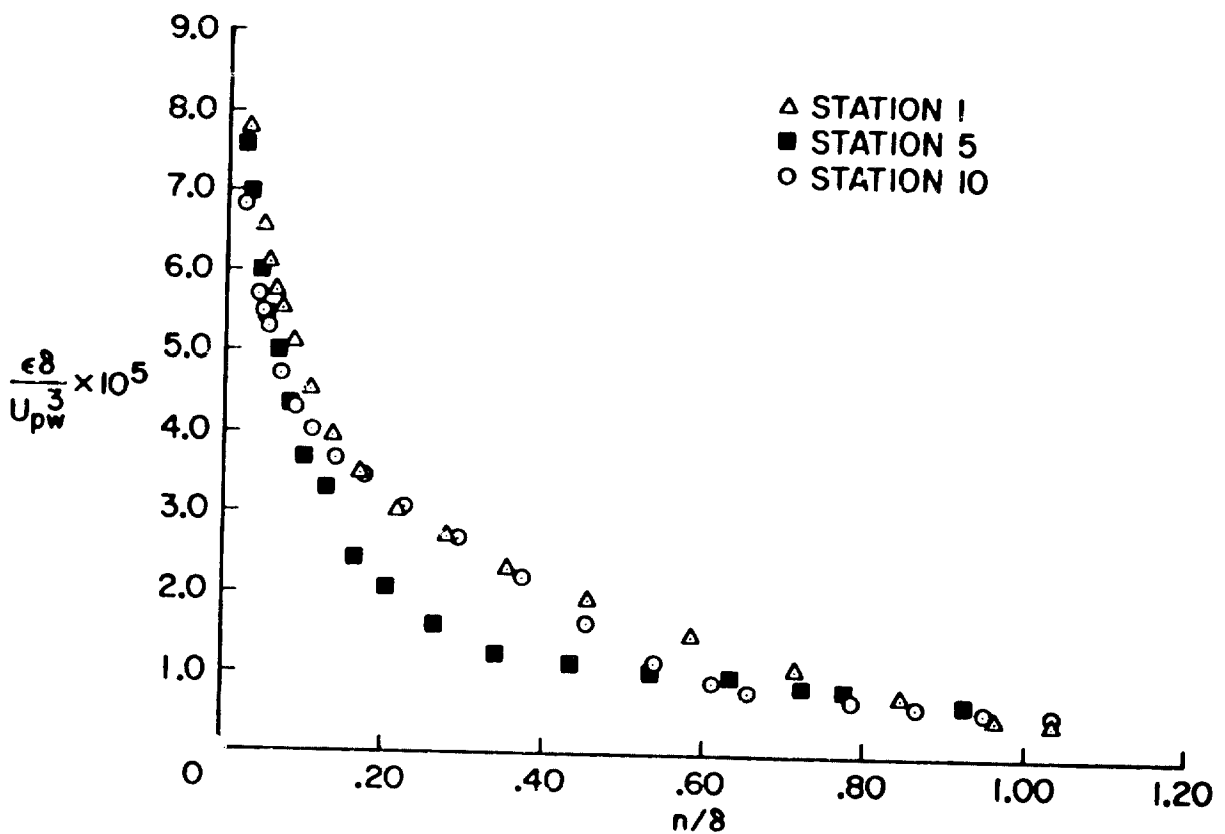
Fig. 17. Dissipation profiles for representative stations from first experiment

53
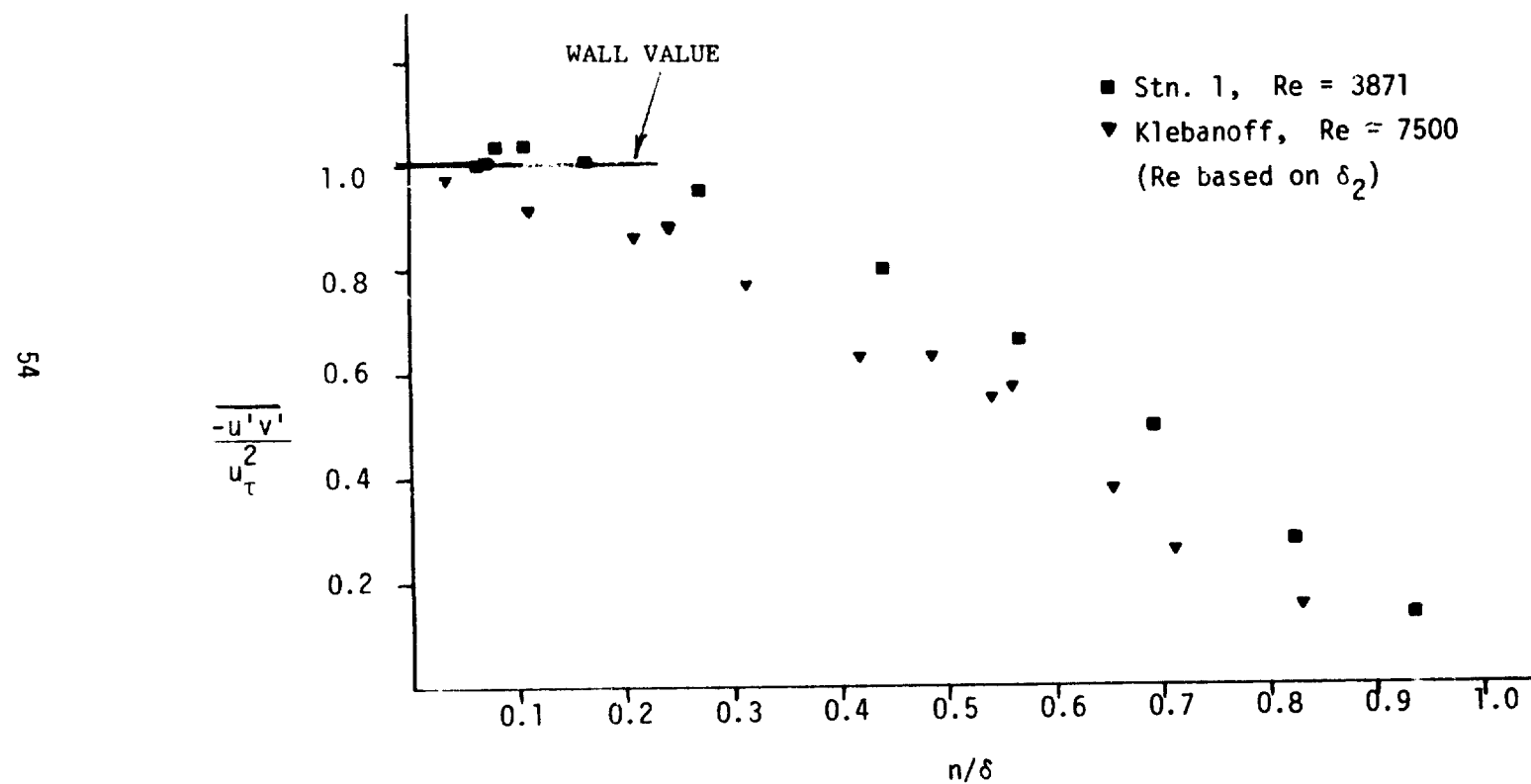
Fig. 18. Comparison of shear-stress profile at Station 1 with data of Klebanoff
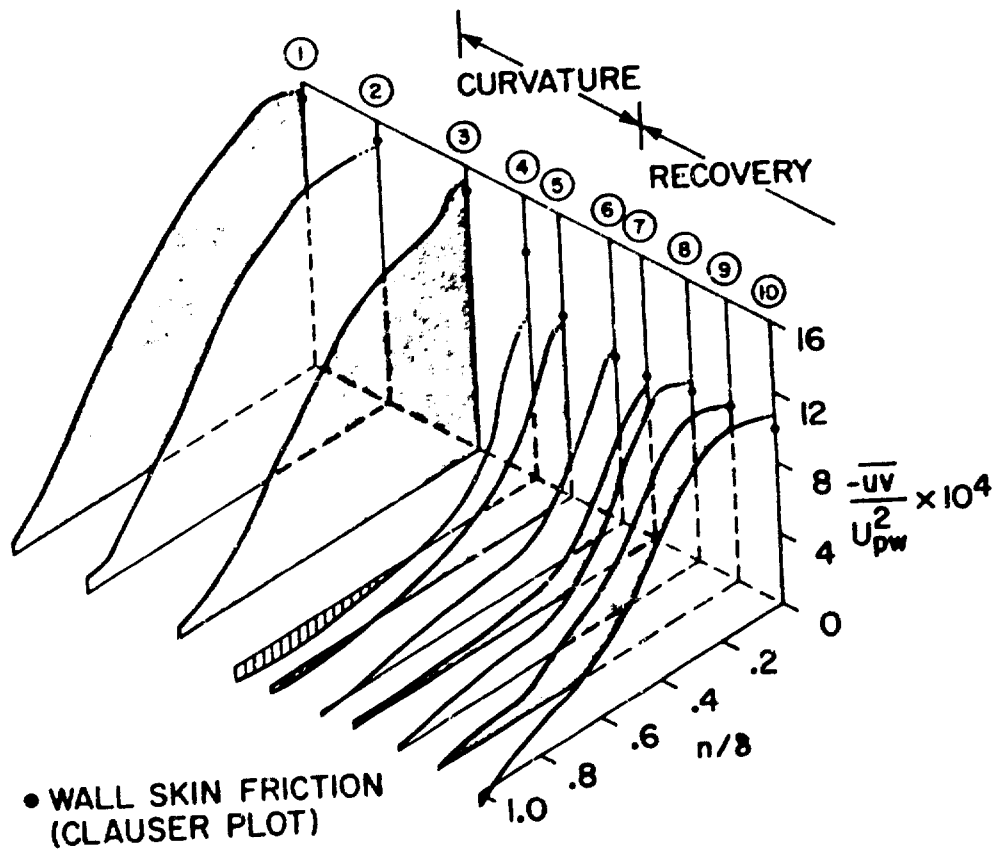
Fig. 19. Isometric plot of first experiment shear-stress profiles vs. distance in flow direction

55
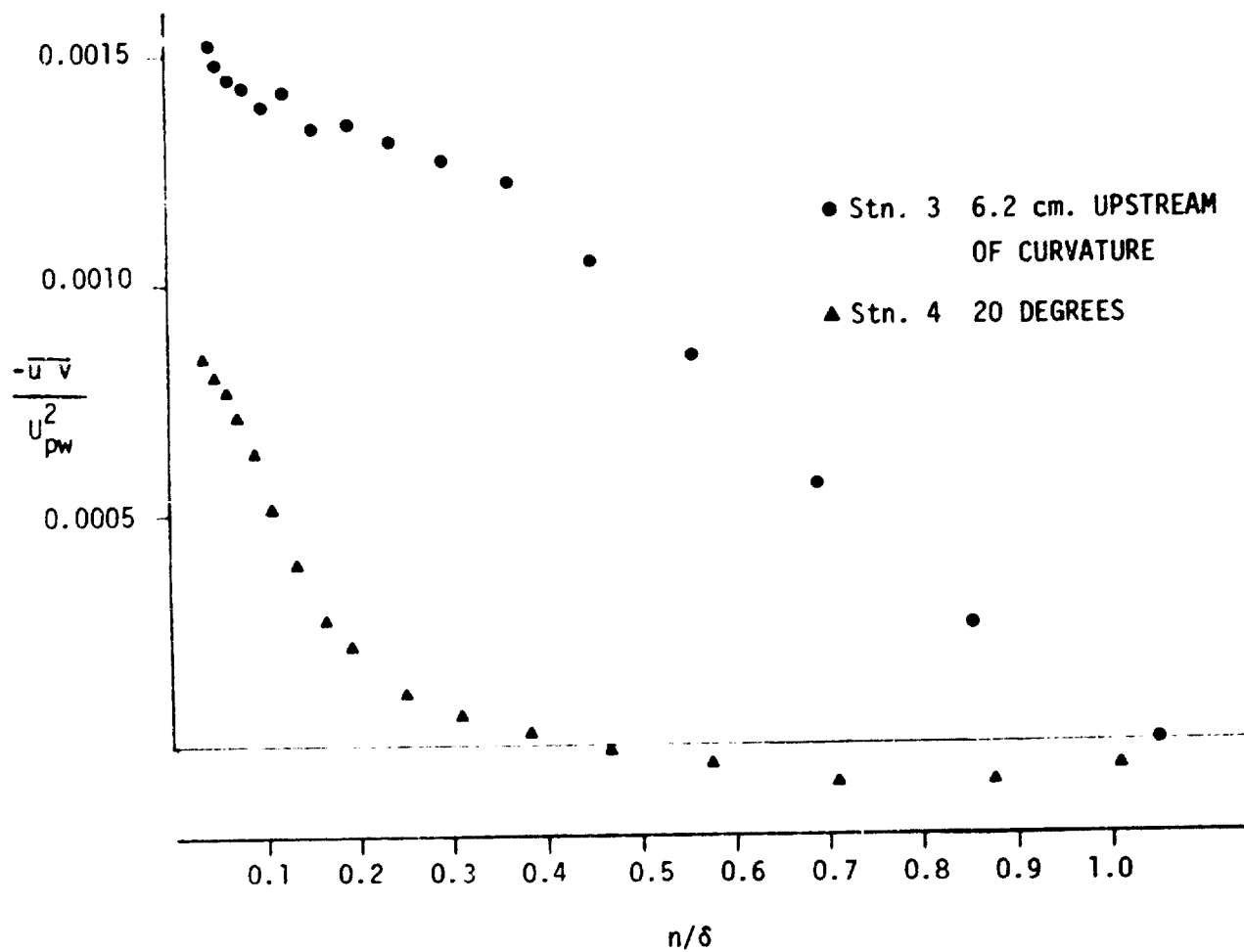
Fig. 20. Shear-stress profiles near the start of curvature for first
experiment
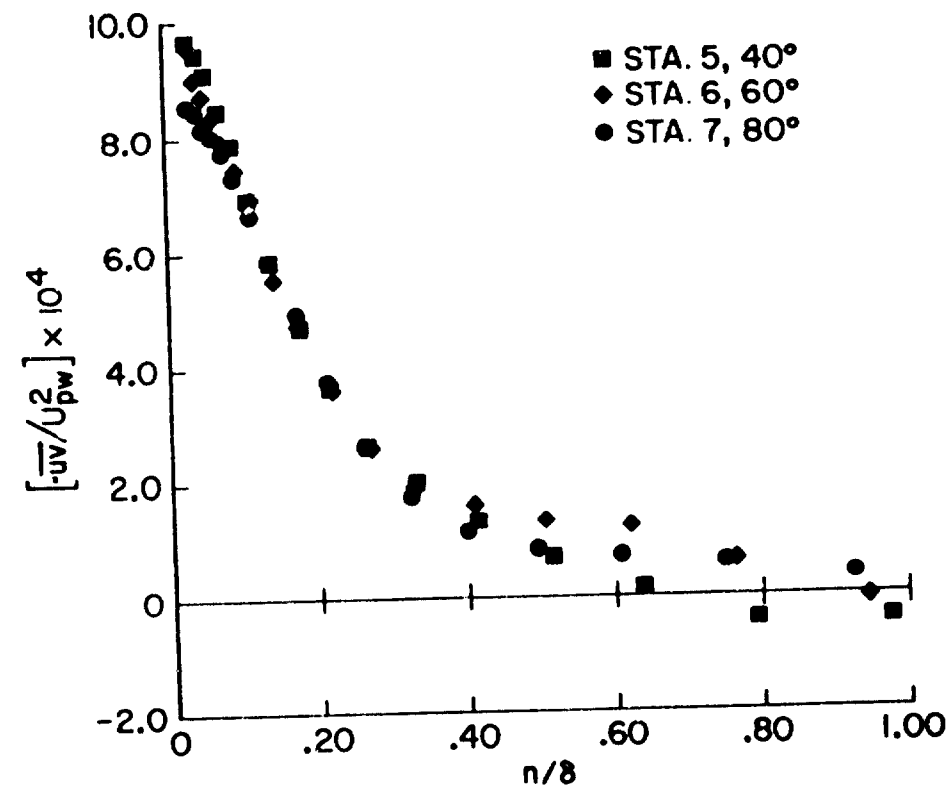
Fig. 21.   Partial collapse of curved-region shear-stress profiles
         for first experiment
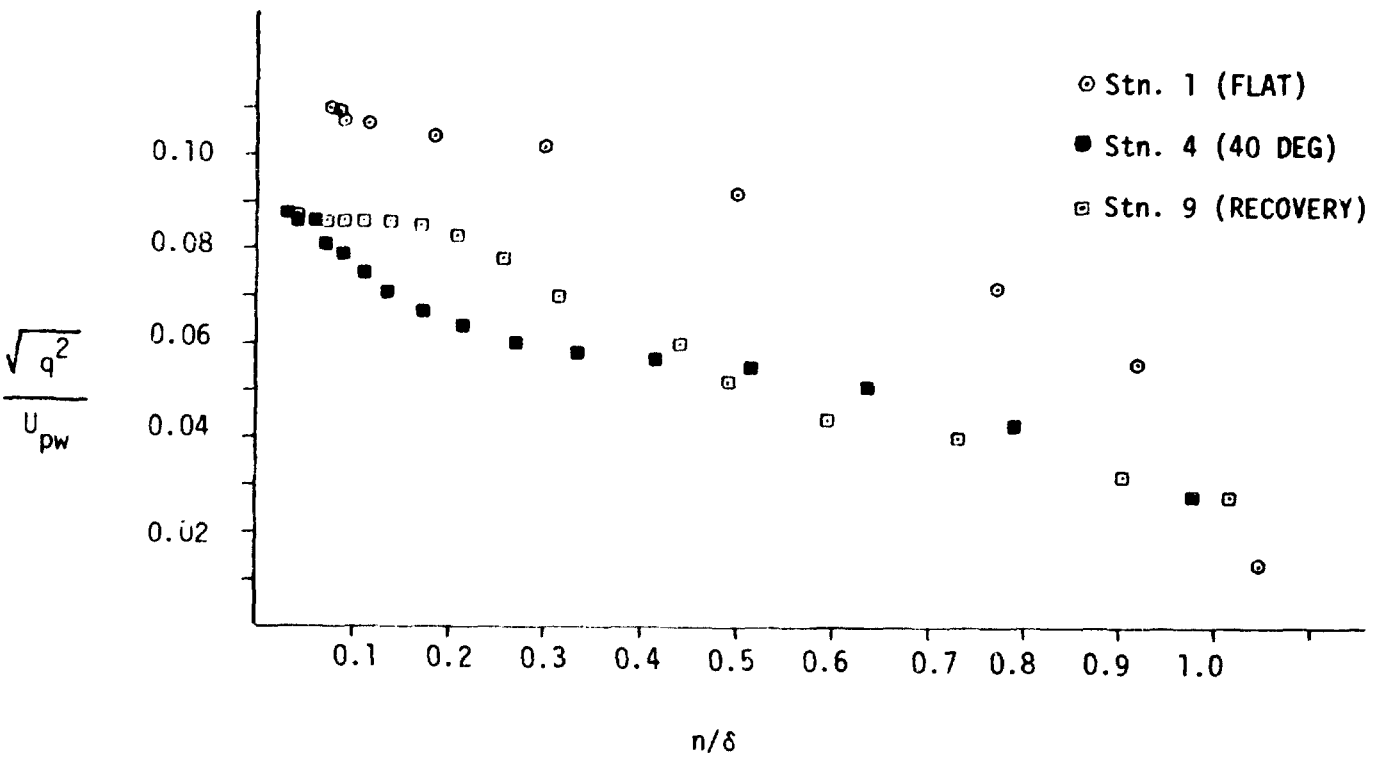
Fig. 22.   Turbulence kinetic energy profiles at three representative
          stations for the first experiment
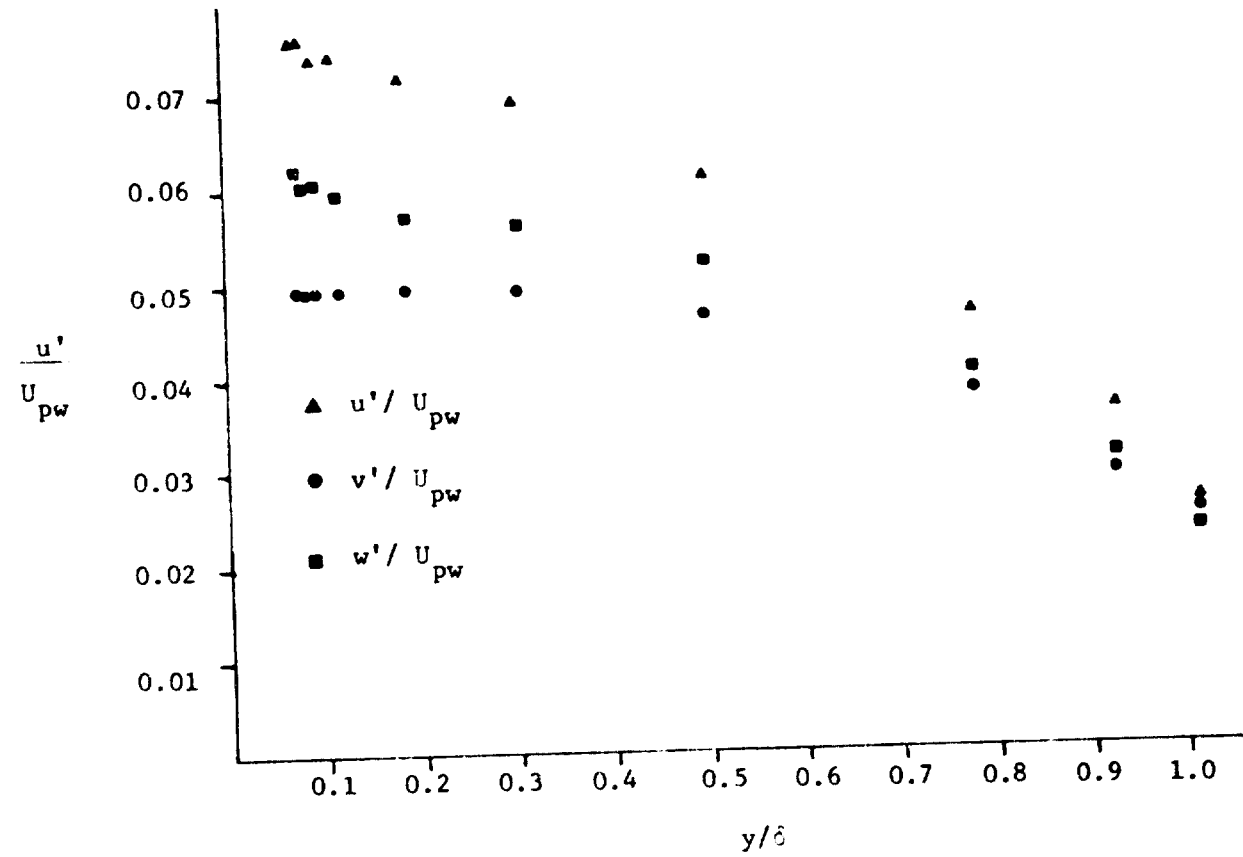
Fig. 23. Turbulent normal stress profiles at Station 1 (upstream of curvature) of first experiment
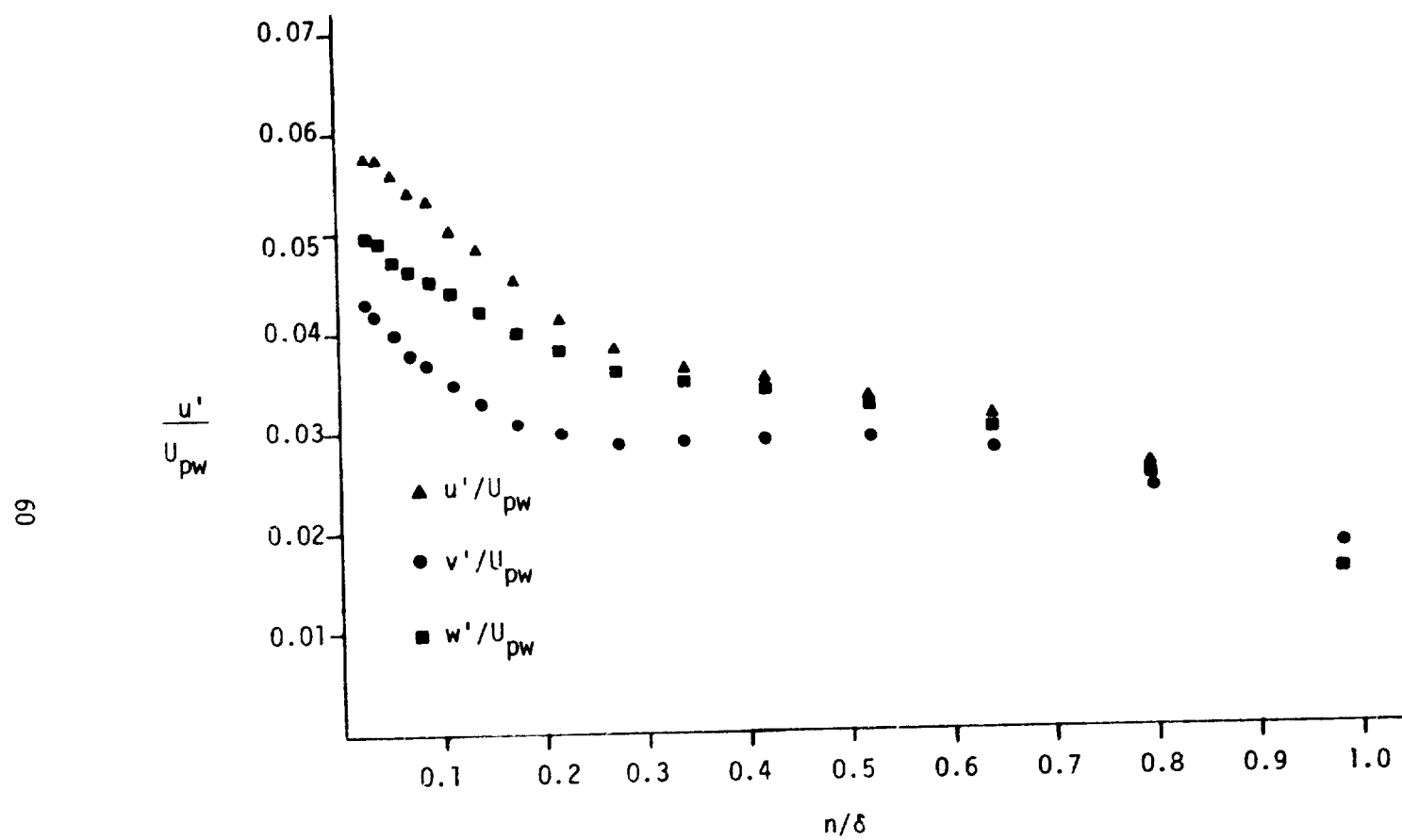
Fig. 24. Turbulent normal stress profiles at Station 5 (after 40° of curve) of first experiment
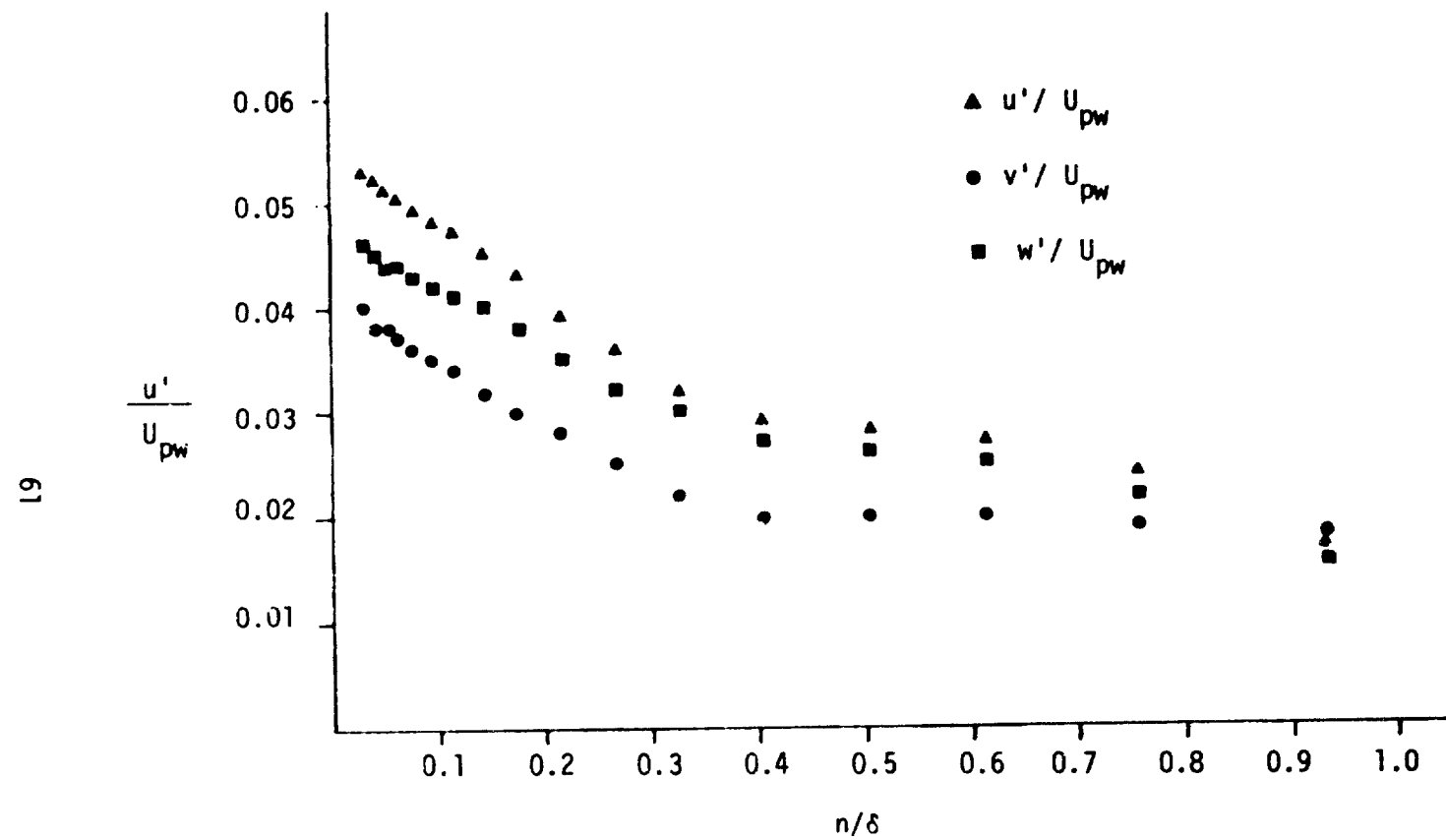
Fig. 25. Turbulent normal stress profiles at Station 7 (after 80° of curvature) of first experiment
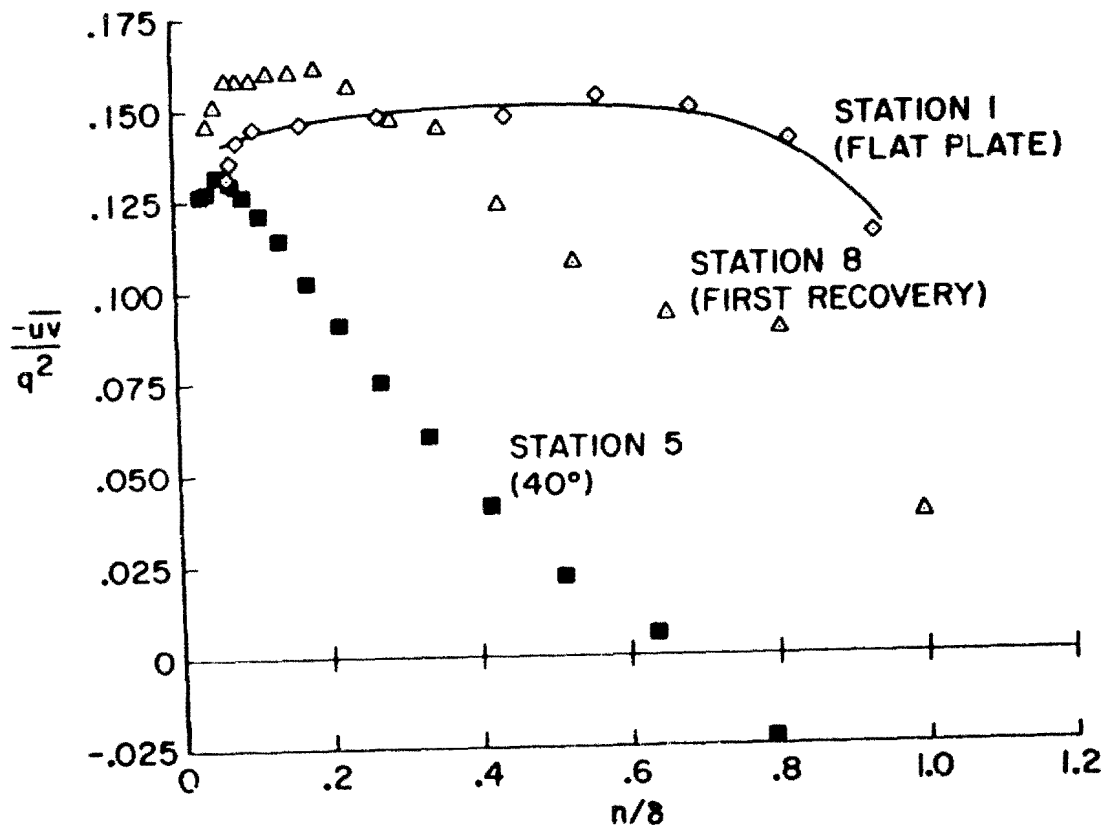
Fig. 26. Plot of structural coefficient, $-\overline{uv}/q^2$, vs. distance from the wall for representative stations of first experiment

PROBE

$$\overline{UV} = 0$$
$$q^2 \neq 0$$

$$\overline{UV} \neq 0$$
$$q^2 \neq 0$$
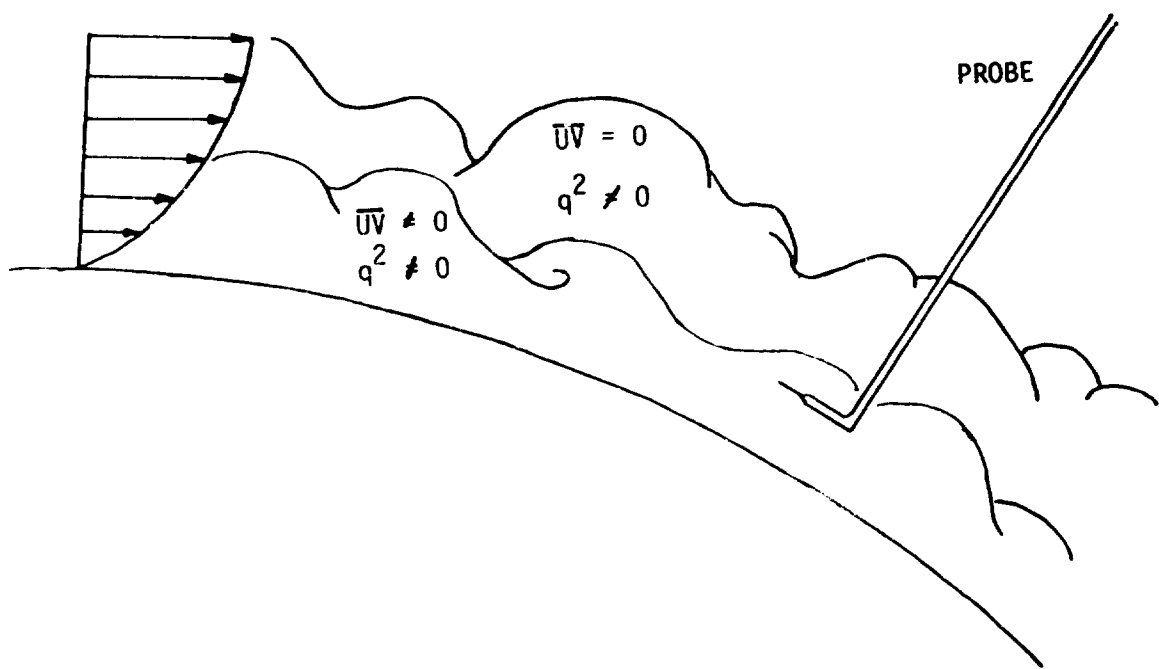
Fig. 27. Two-layer conceptualization of outer part of curved boundary layer

$$C_p = \frac{P_s - P_{s,\,(s=0)}}{1/_2\ \rho U_{pw}^{\ 2}}$$

FLAT ———————————— CURVATURE ——————————— RECOVERY (flat)

s,cm.
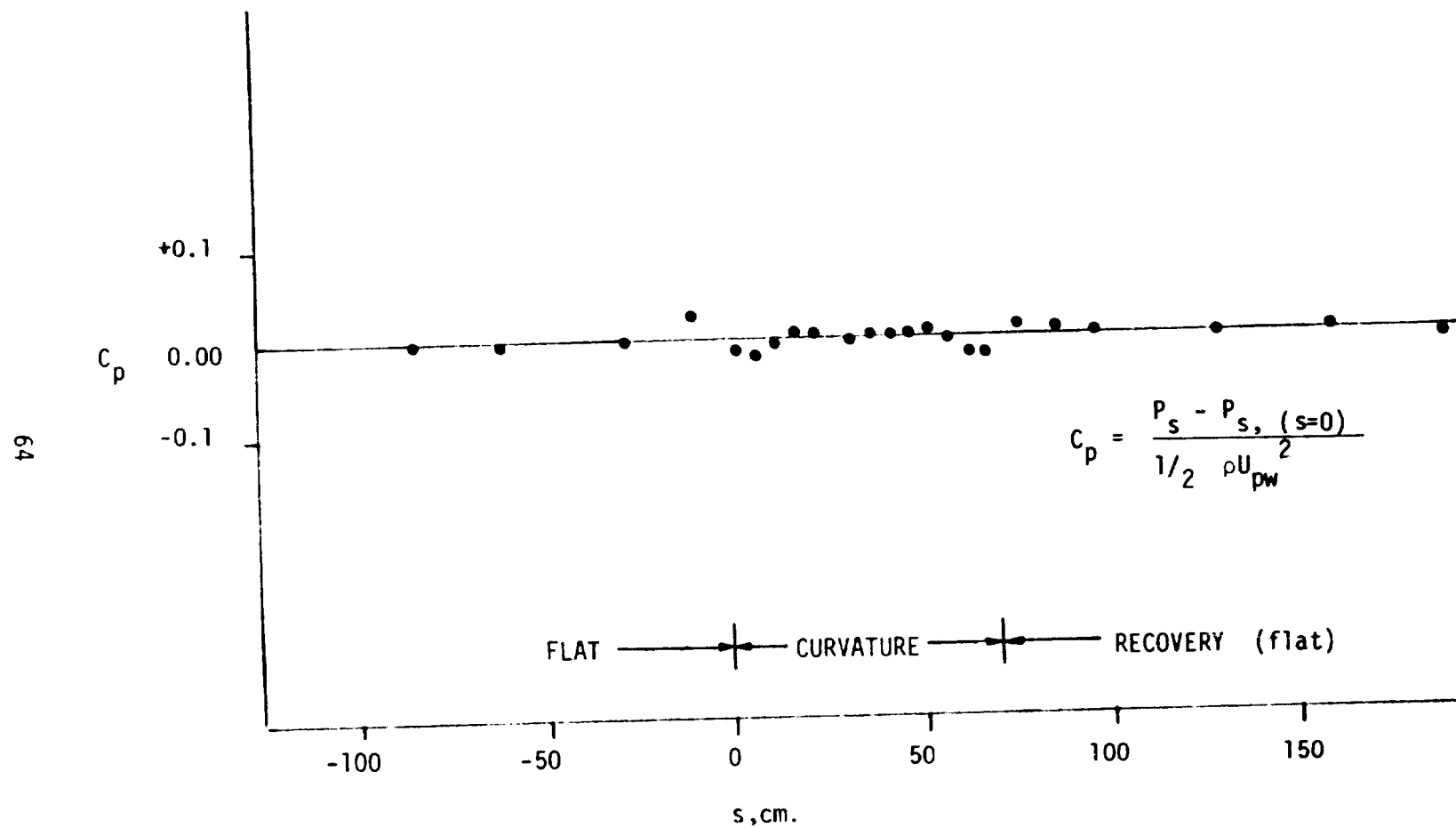
Fig. 28.   Measured convex-wall, static-pressure distribution for second
experiment

64
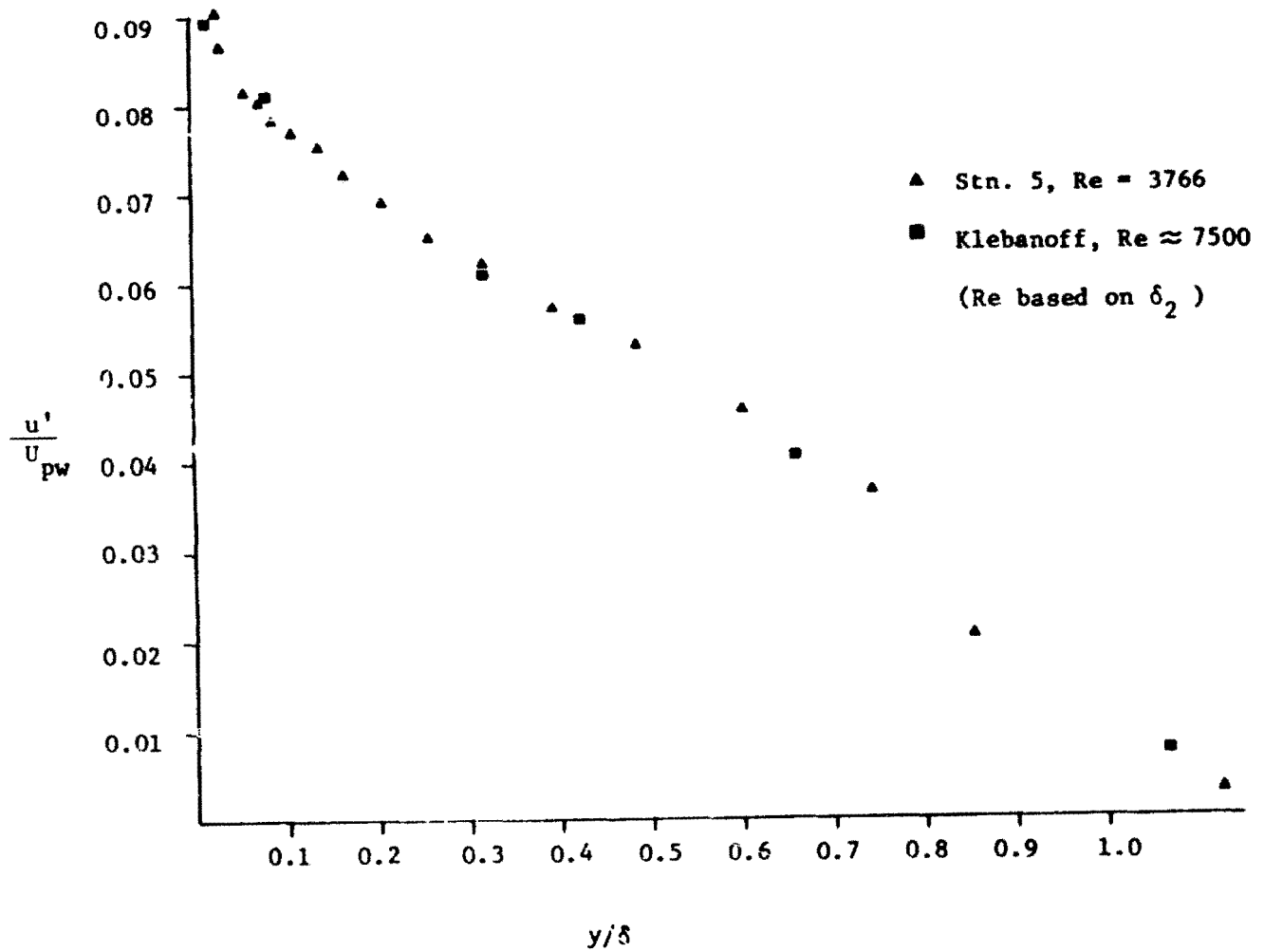
Fig. 29.   Comparison of upstream turbulence-intensity profiles from second experiment with data of Klebanoff
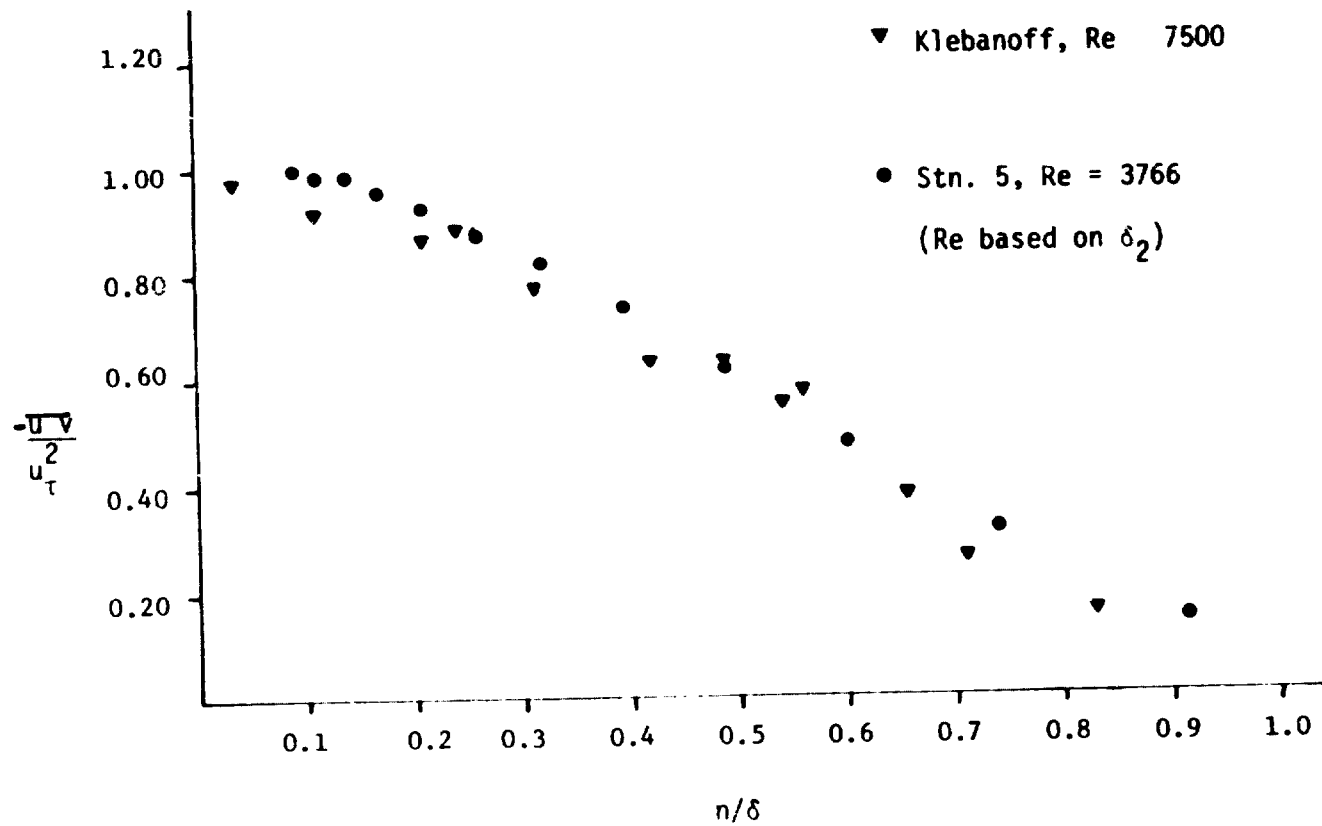
Fig. 30. Comparison of shear-stress profile upstream of curvature with data of Klebanoff
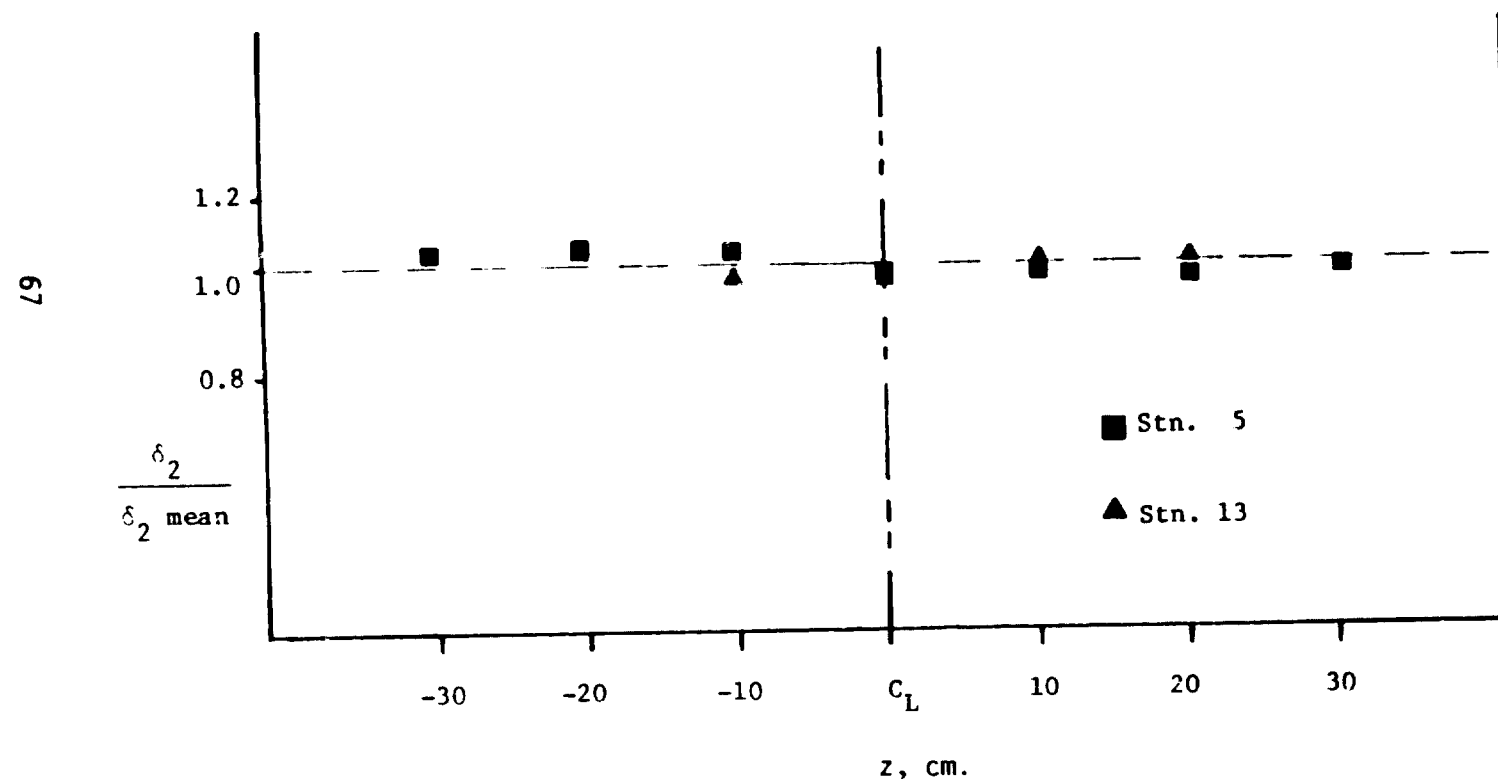
Fig. 31. Spanwise distribution of momentum thickness at stations on preplate and afterplate of second experiment
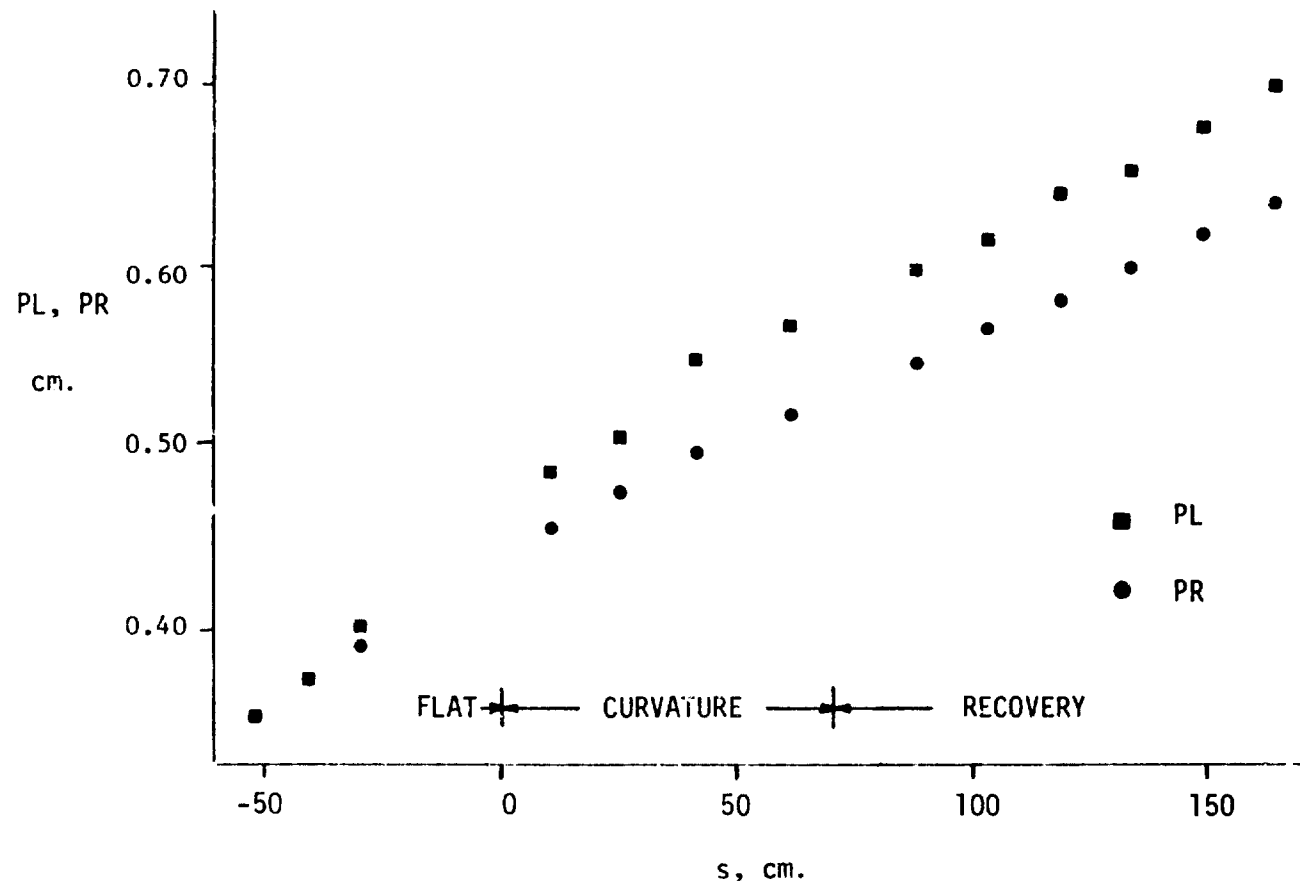
Fig. 32. PL and PR for second experiment
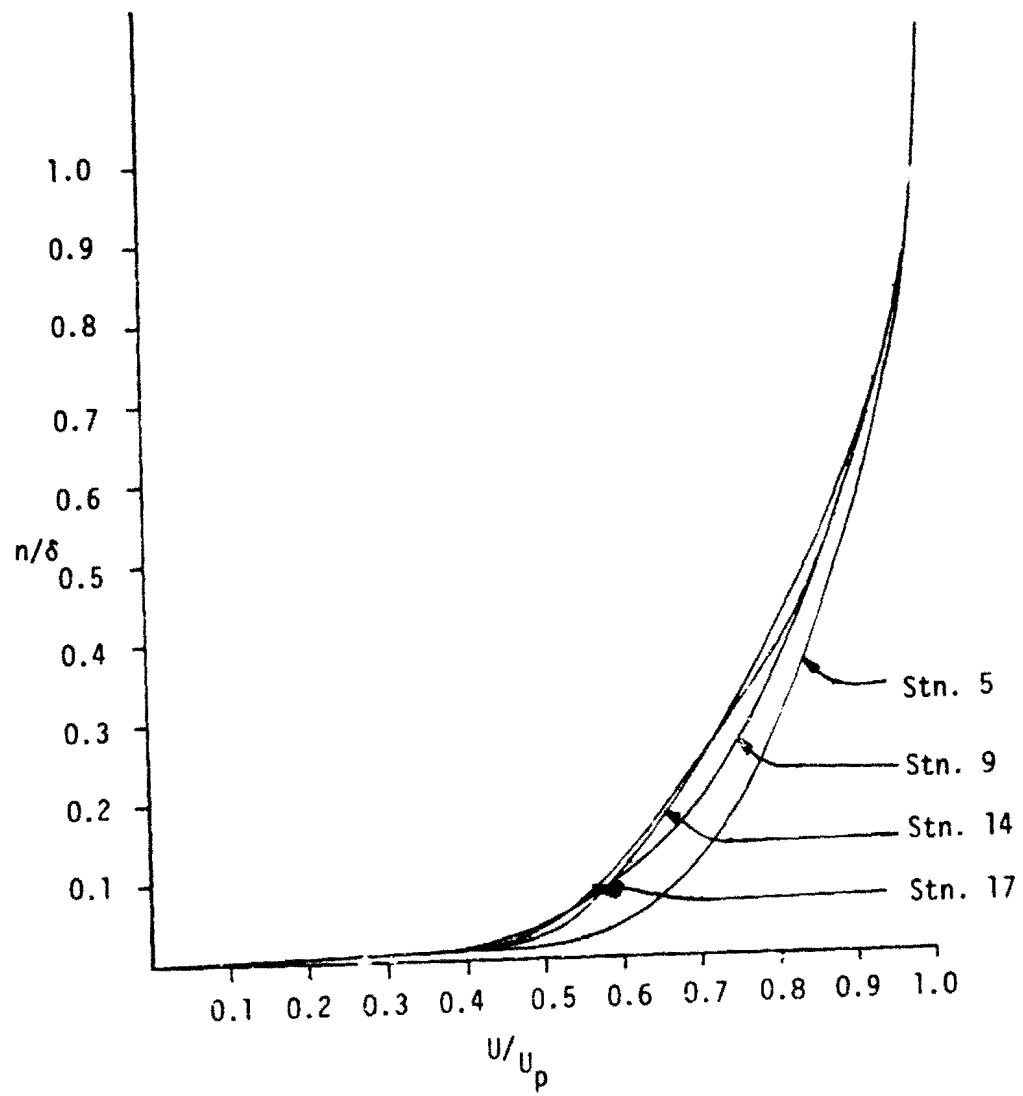
Fig. 33. Mean-velocity profiles for four representative stations of the second experiment

69
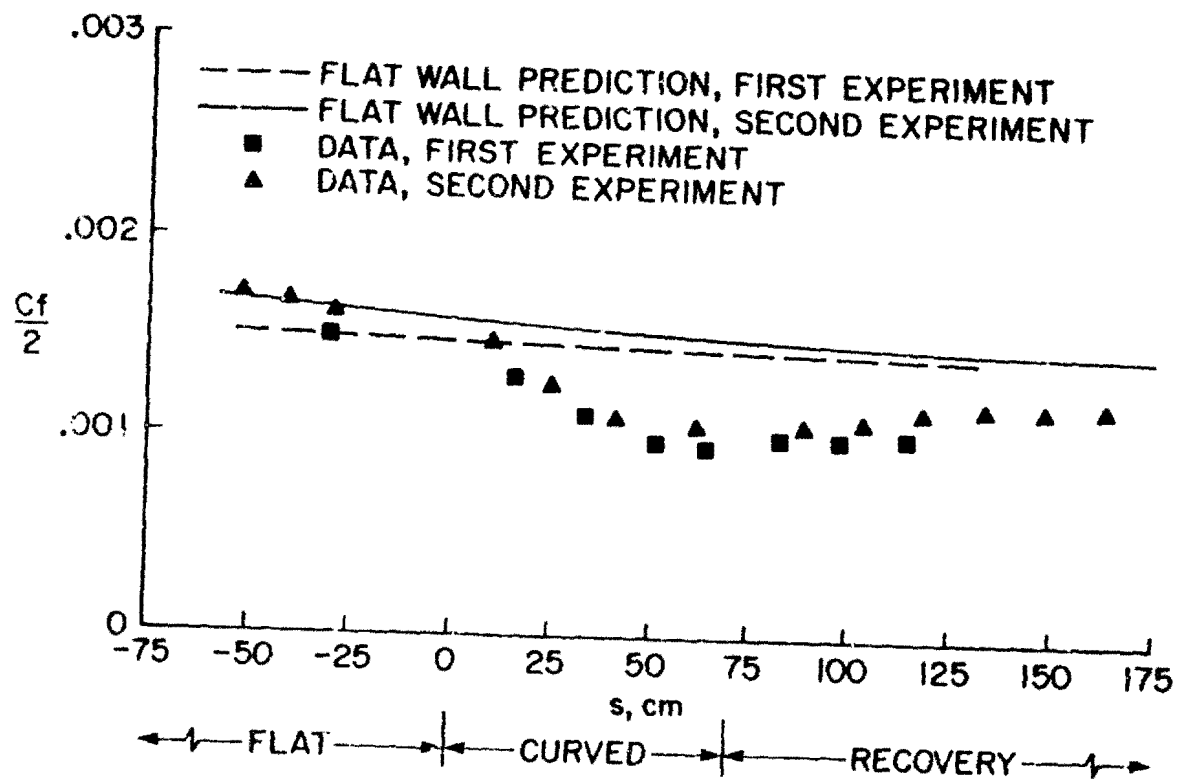
Fig. 34. Skin friction (from Clauser plot) vs. distance in flow direction for first and second experiments
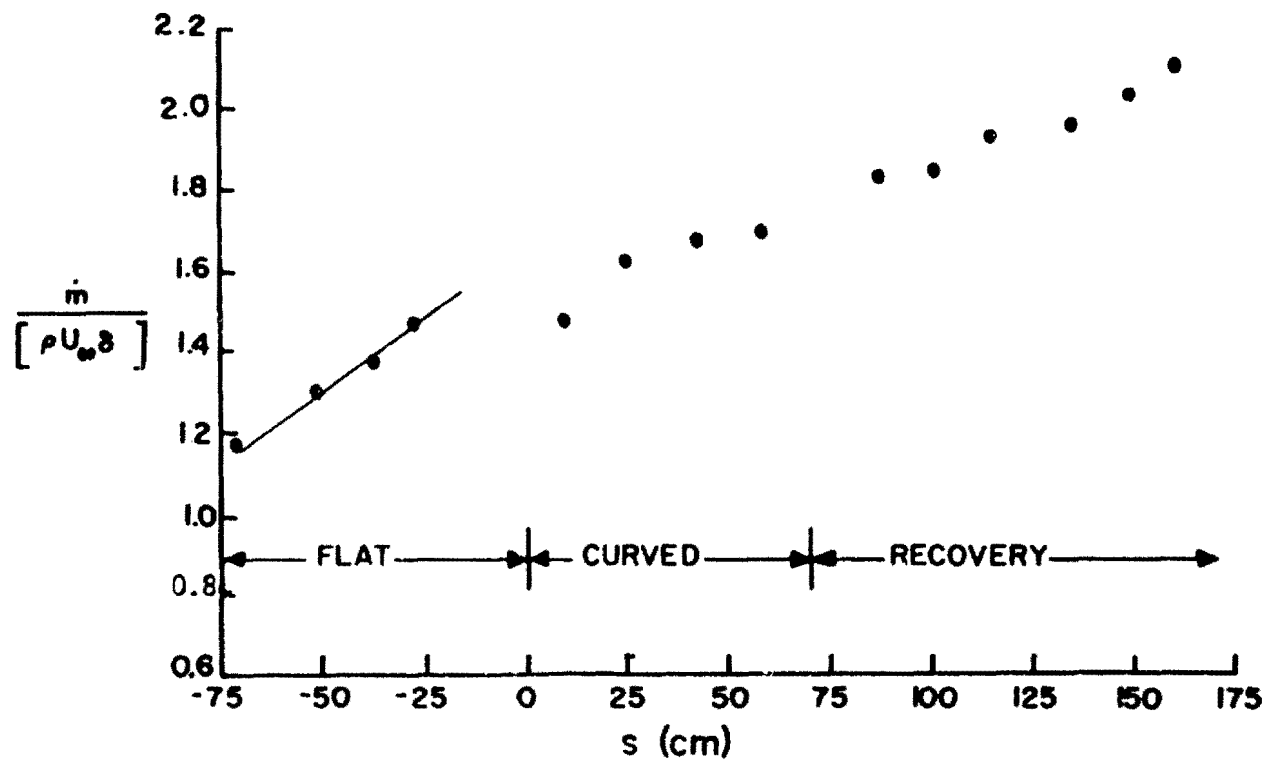
Fig. 35. Growth of boundary-layer mass flux for second experiment
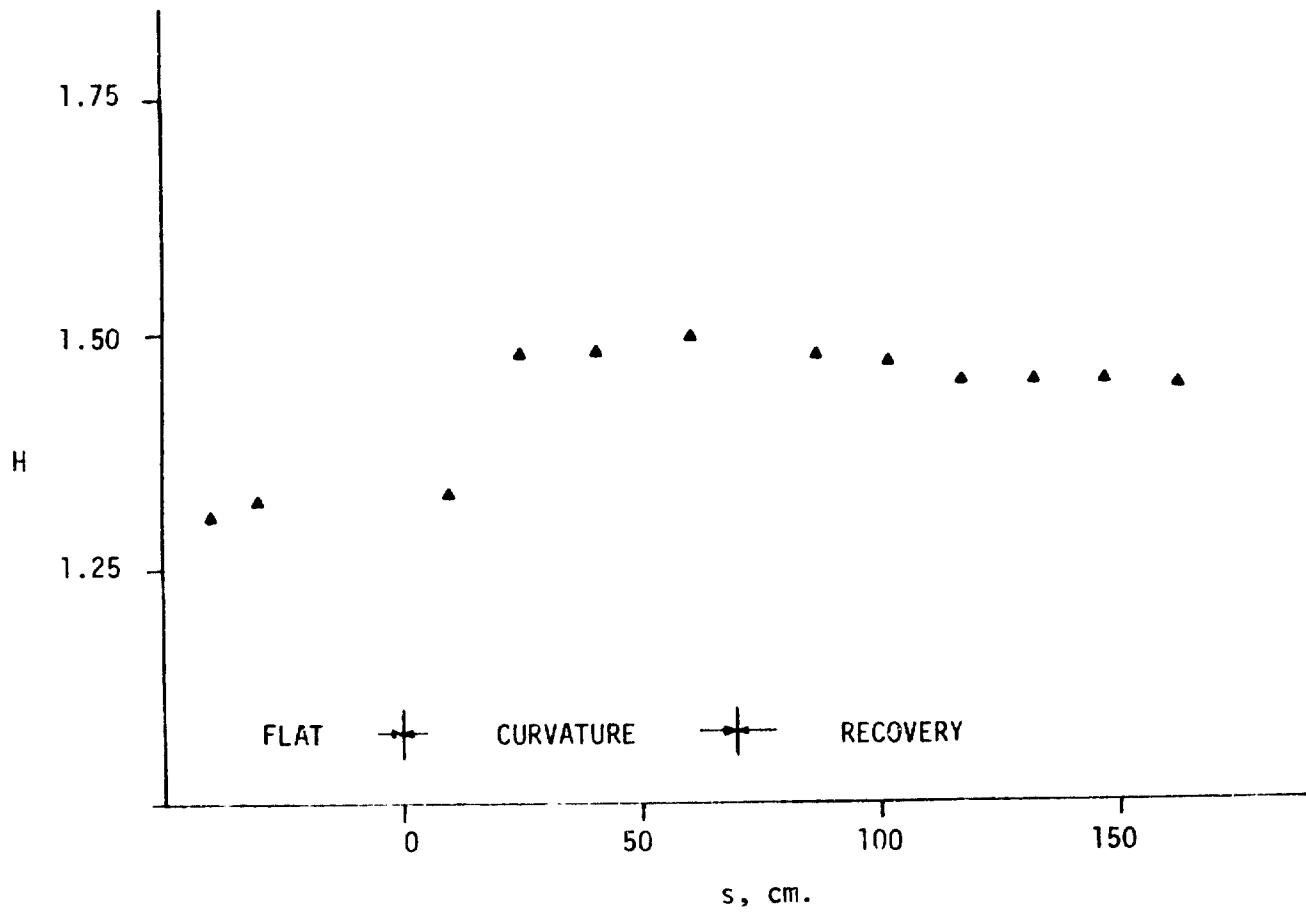
Fig. 36. Shape factor (δ_1/δ_2) vs. distance in streamwise direction
for second experiment
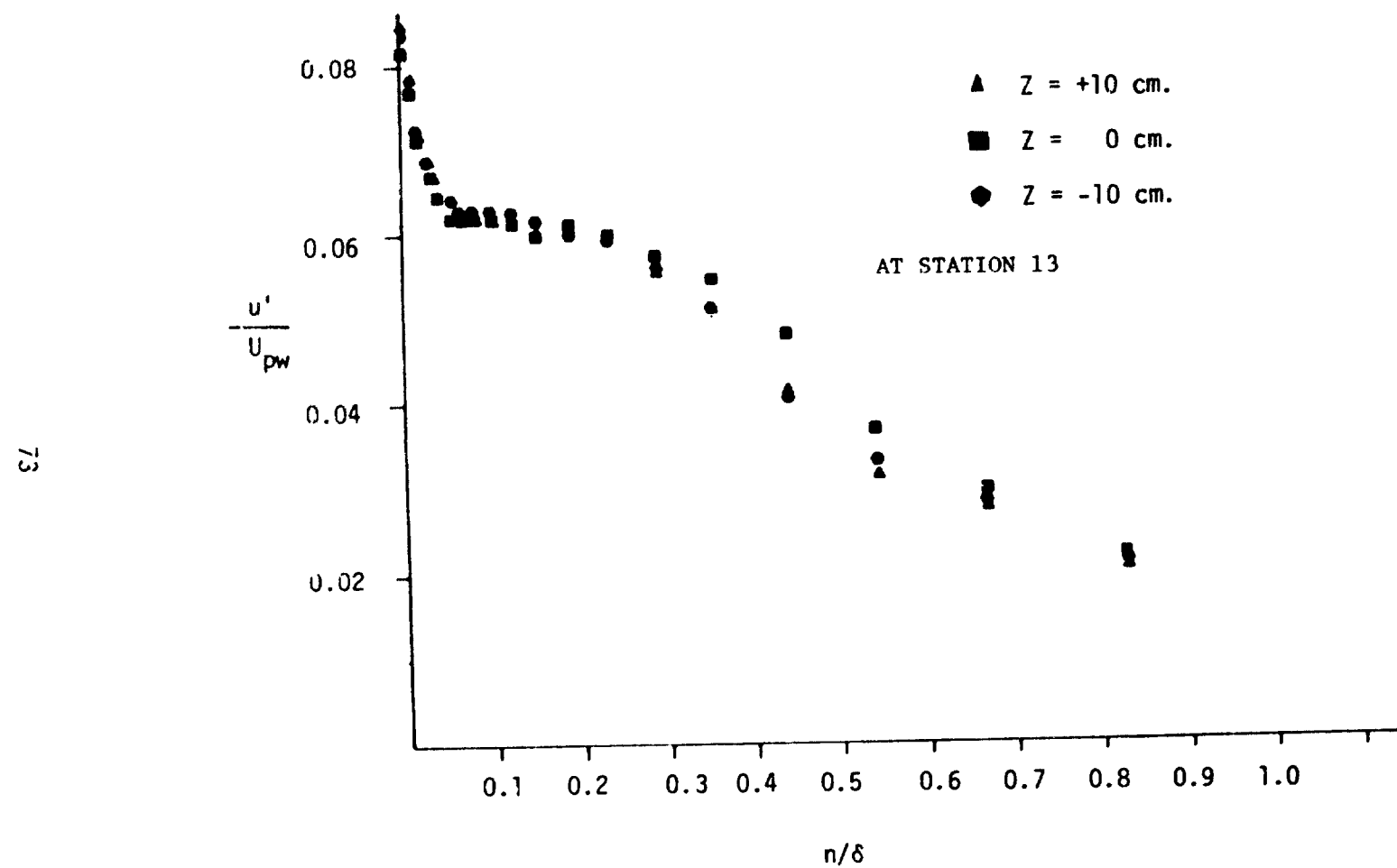
Fig. 37. Spanwise turbulence-intensity profiles in recovery region
of second experiment
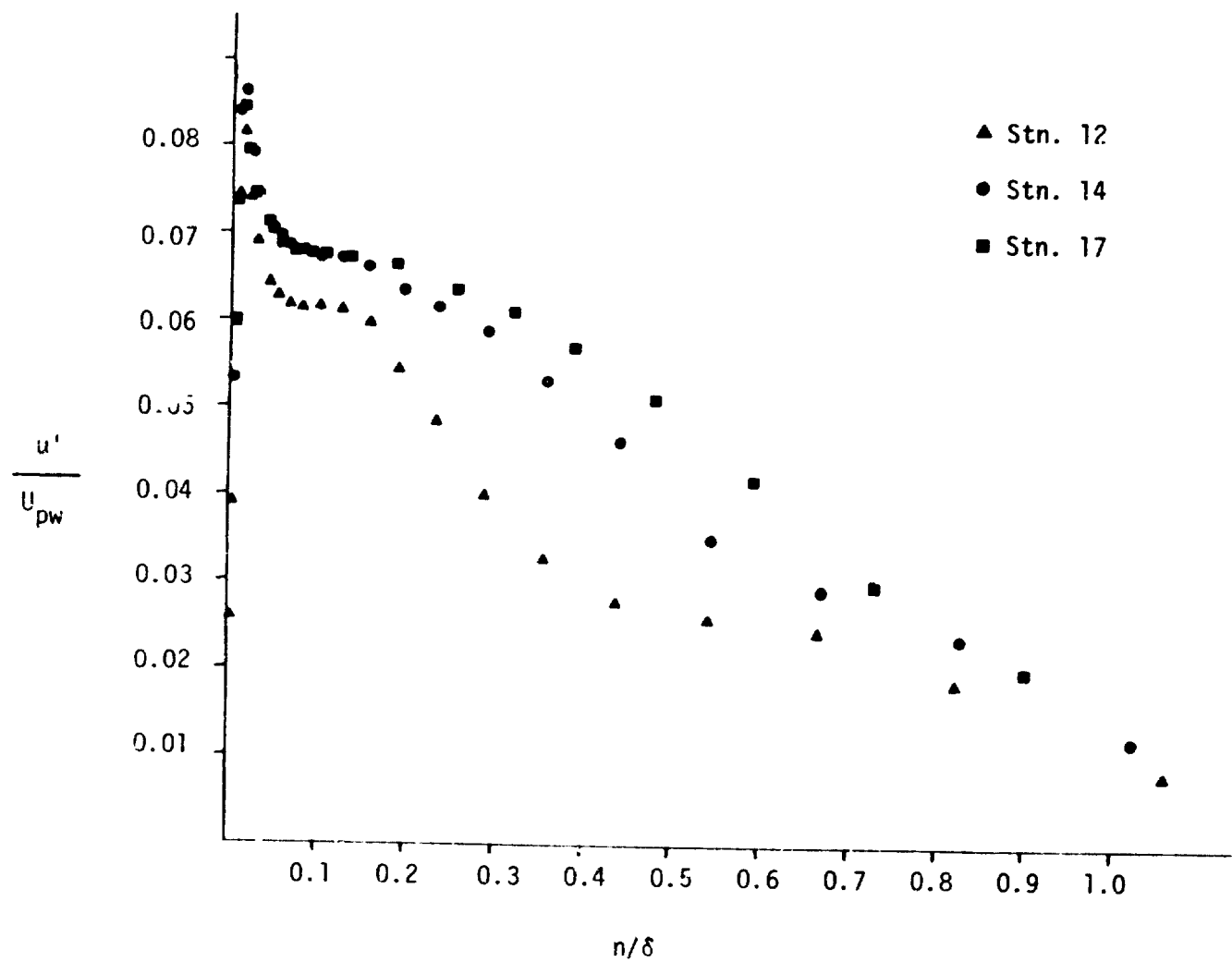
Fig. 38. Turbulence intensity profiles in recovery region of second experiment

74
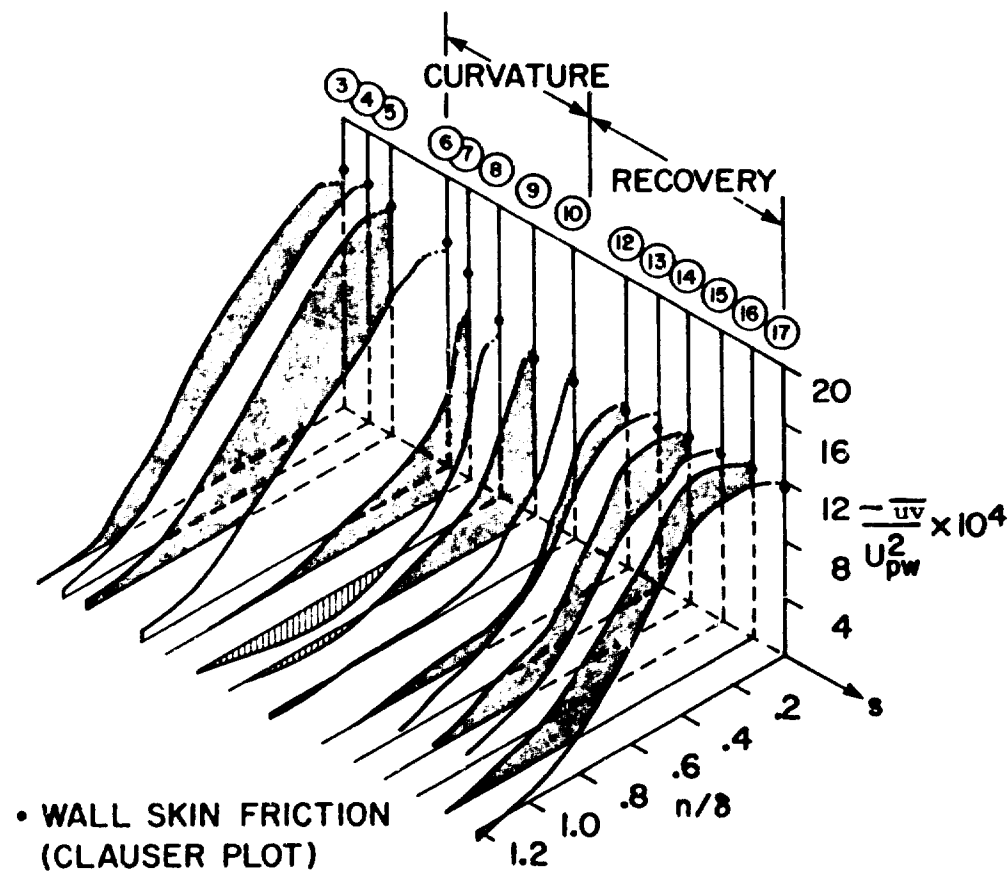
Fig. 39. Isometric plot of shear-stress profiles vs. distance in flow
direction for second experiment
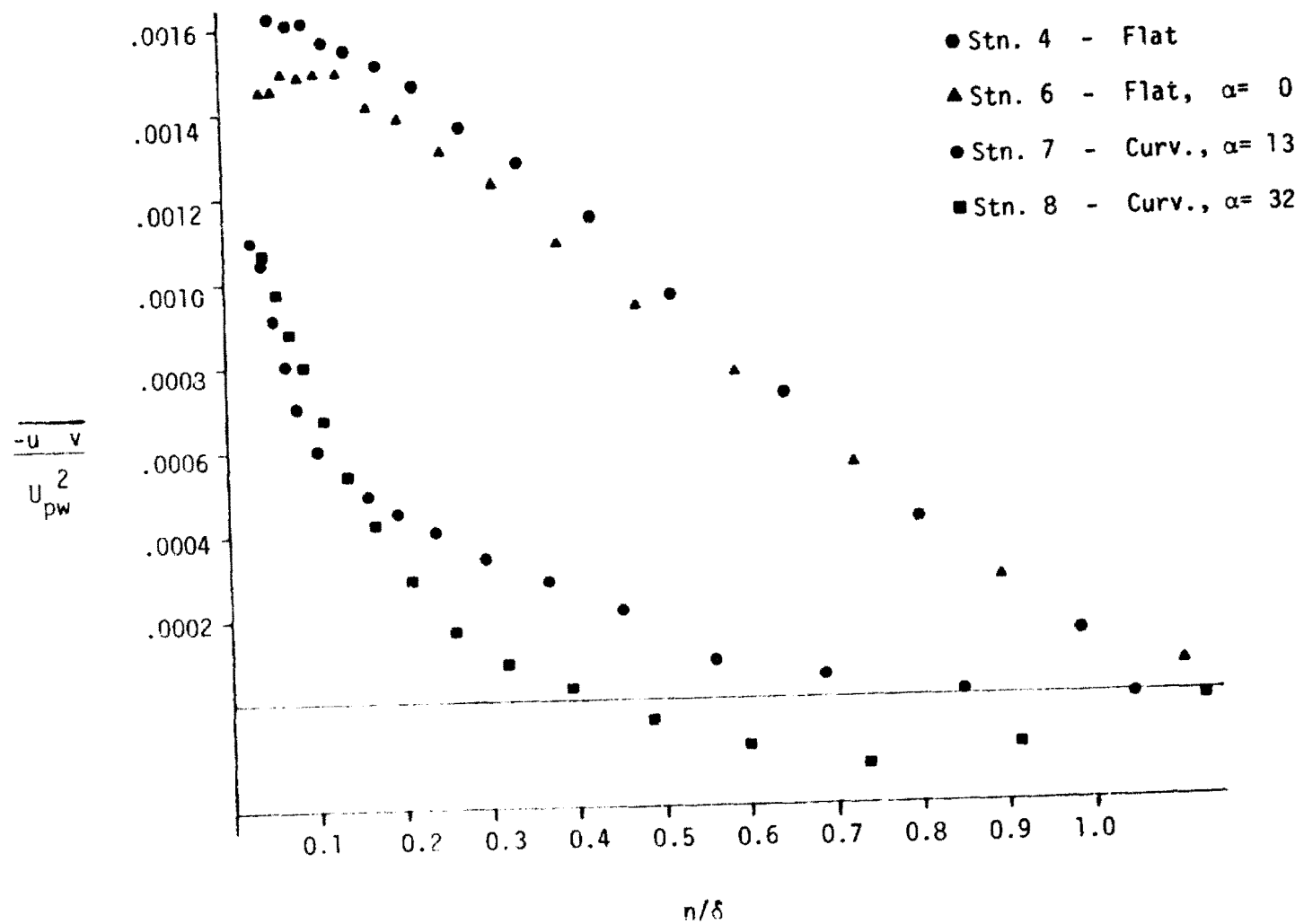
Fig. 40. Shear-stress profiles near start of curvature or second experiment

$$\frac{-\overline{u}\,\overline{v}}{U_{pw}^2}$$

- ● Stn. 8
- ■ Stn. 9
- ▲ Stn. 10

0.0012

0.0010

0.0008

0.0006

0.0004

0.0002

0.1　0.2　0.3　0.4　0.5　0.6　0.7　0.8　0.9　1.0

n/δ
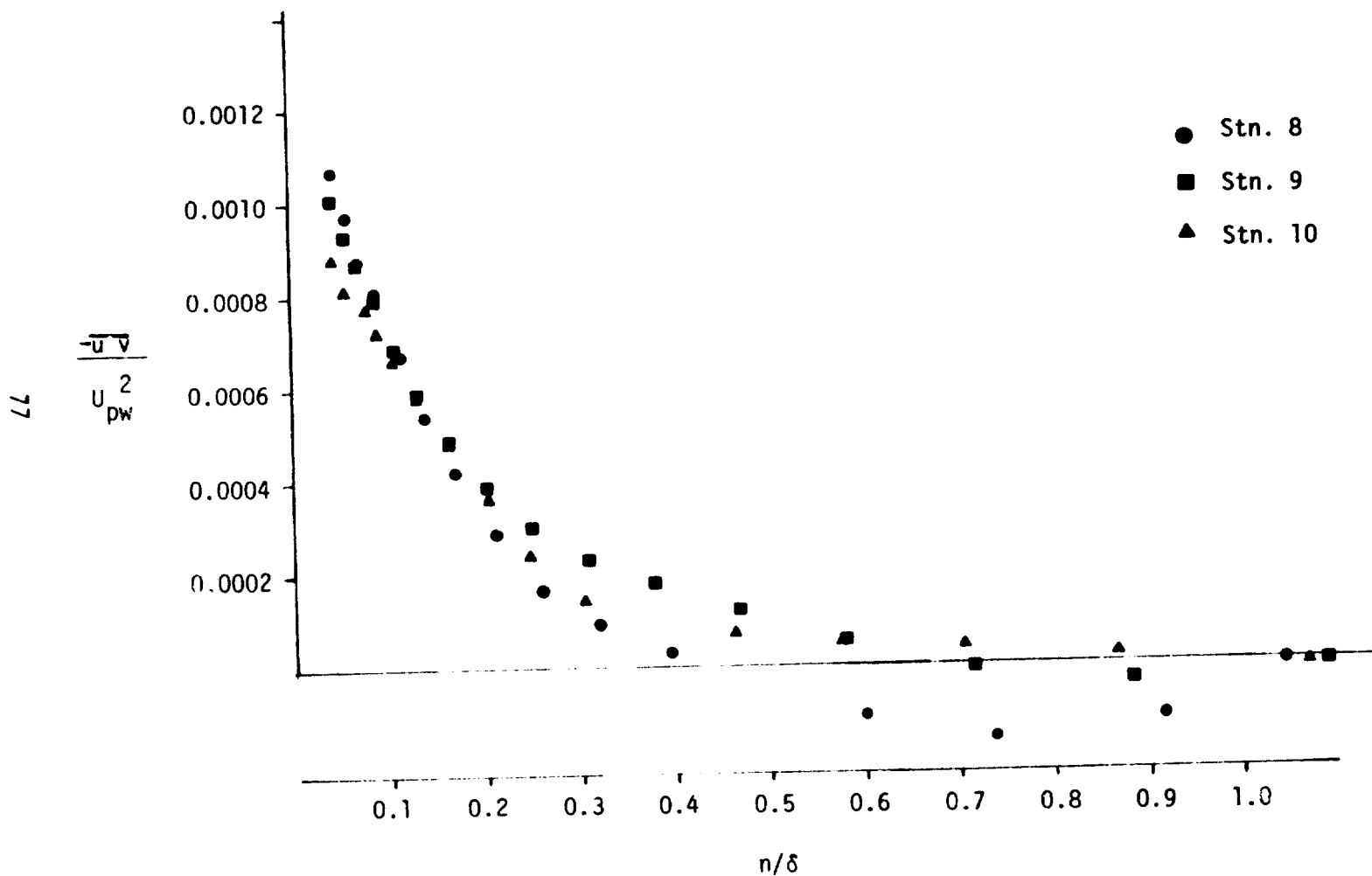
Fig. 41.　Partial collapse of shear-stress profiles in curved region
for second experiment
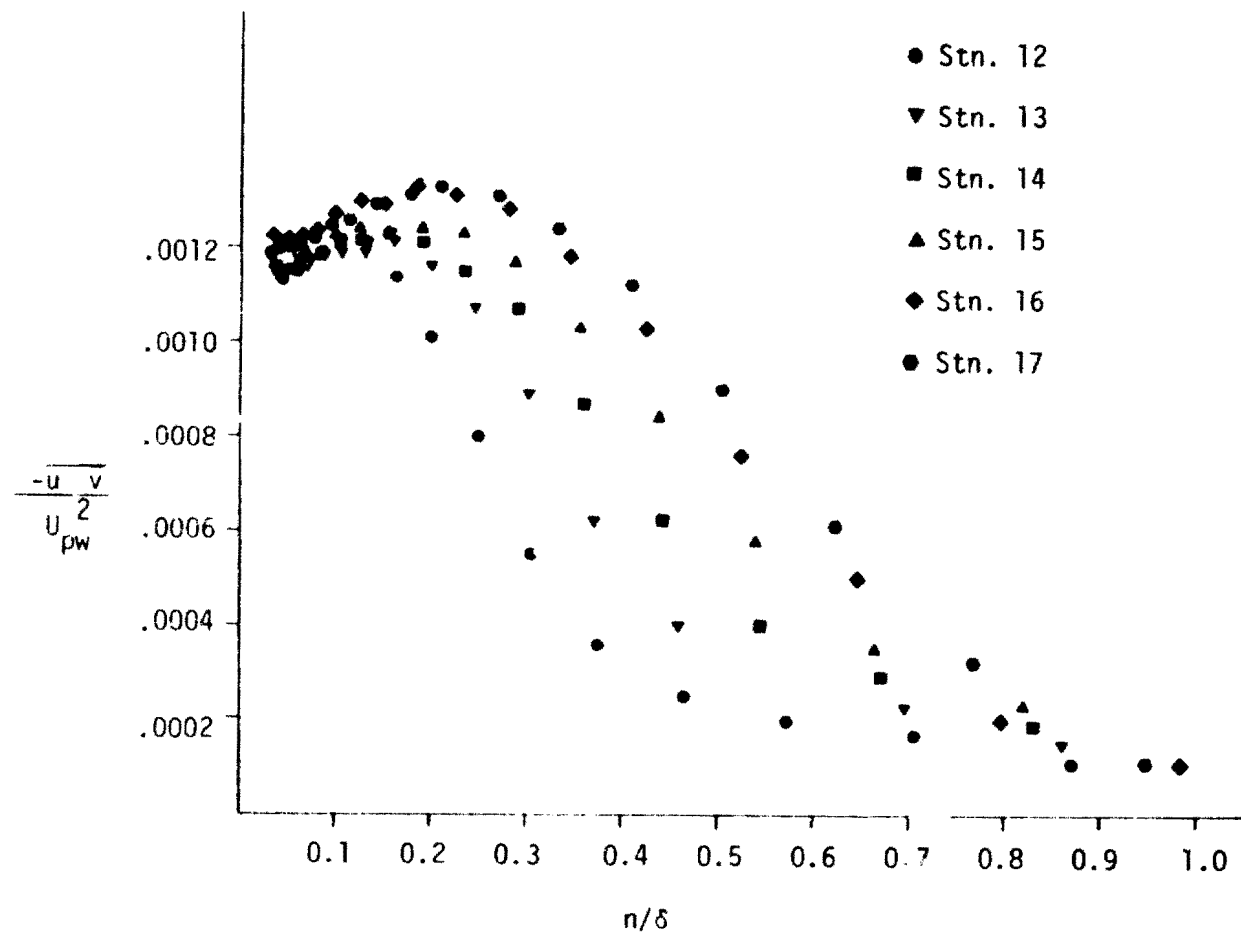
Fig. 42. Shear-stress profiles in recovery region of second experiment
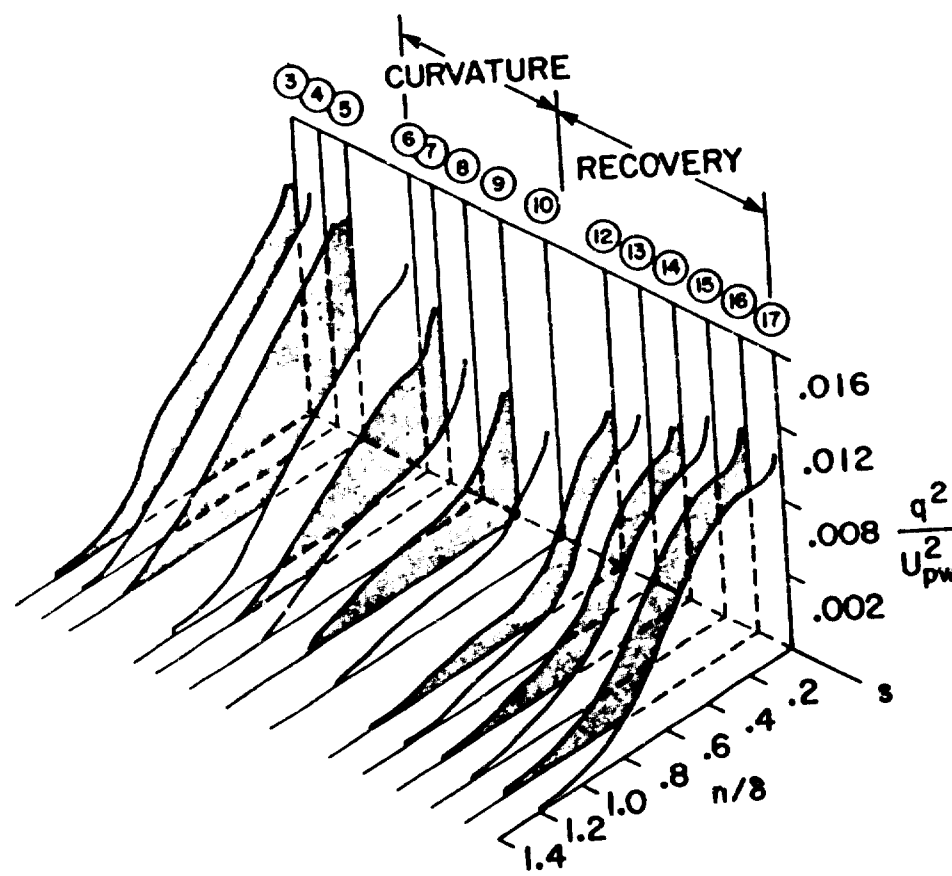
Fig. 43. Isometric plot of TKE profiles vs. distance in flow direction
for second experiment
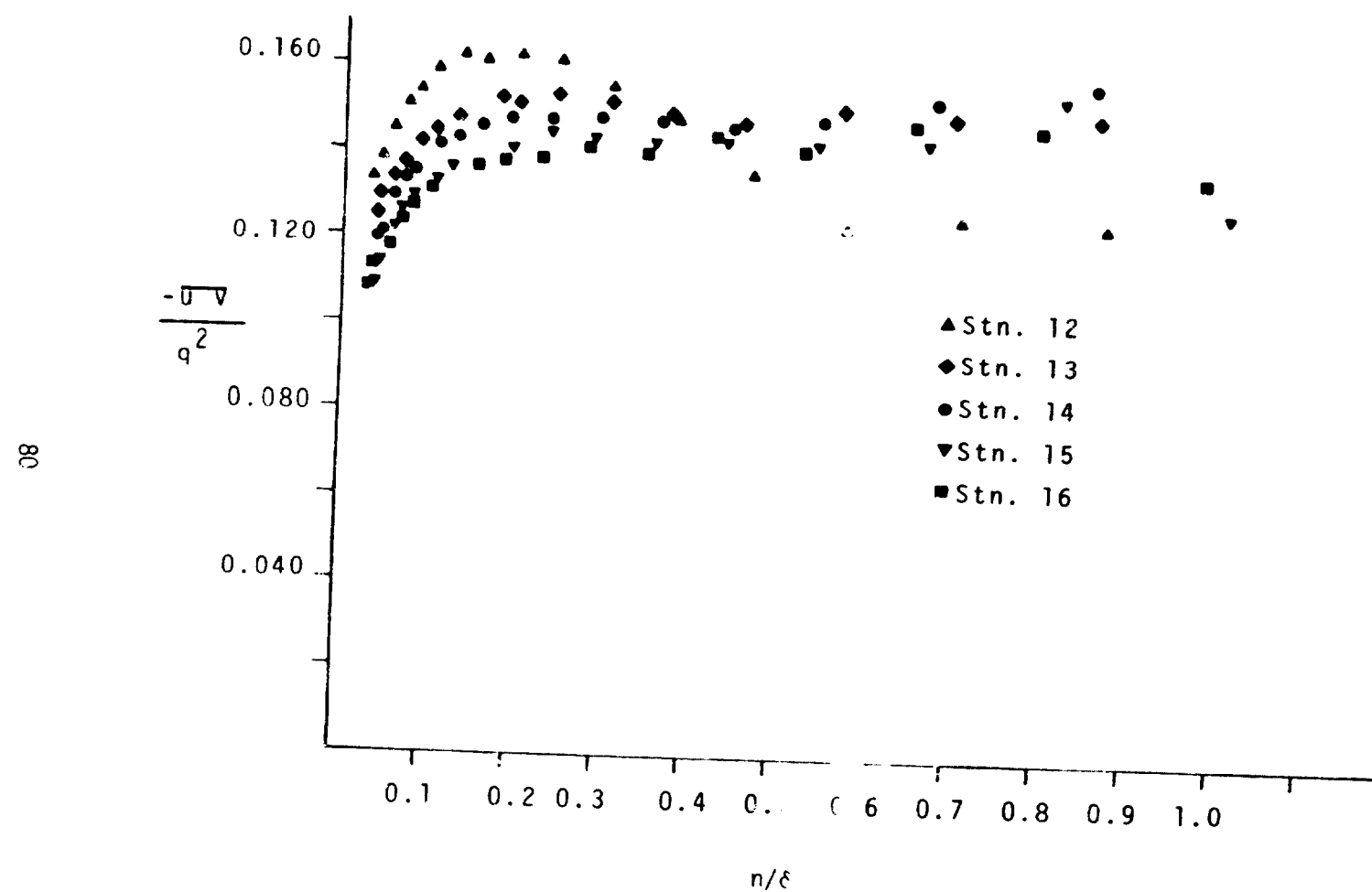
Fig. 44. Structural coefficient $(-\overline{uv}/q^2)$ profiles in recovery region of second experiment

$$C_p = \frac{P_s - P_{s,\ (s=0)}}{1/2 \ \rho \ U_{pw}^2}$$

FLAT ——+—— CURVATURE ——+—— RECOVERY (flat)
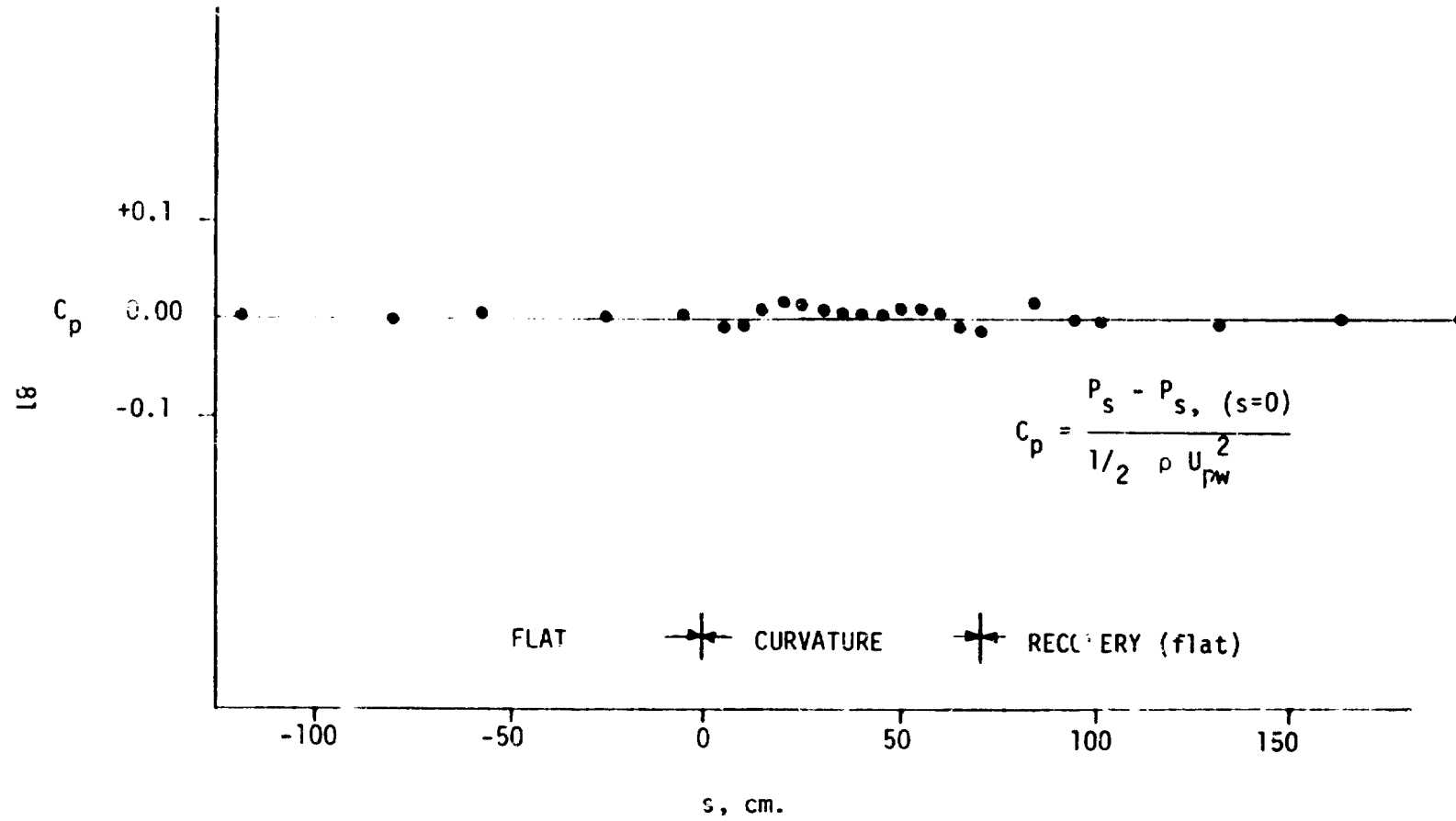
Fig. 45. Measured wall-static-pressure distribution for third experiment
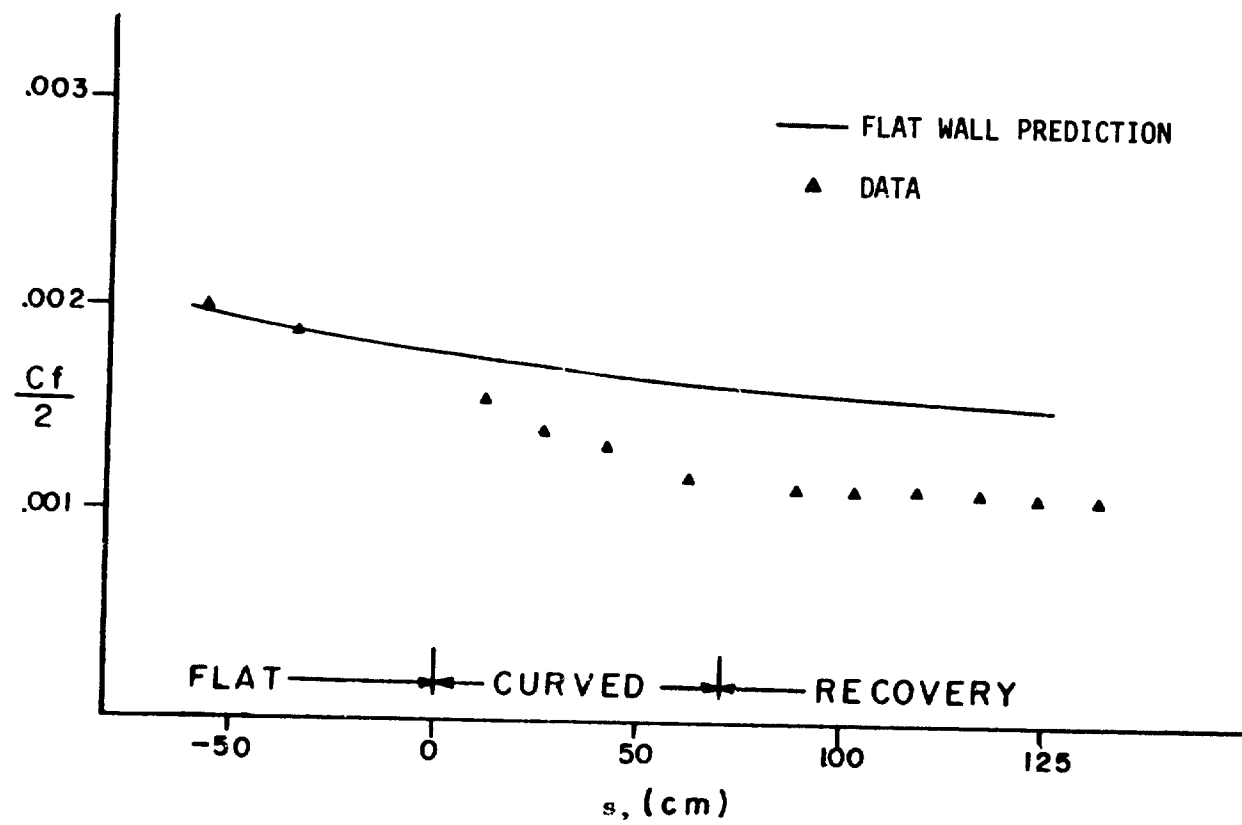
Fig. 46. Skin friction (from Clauser plot) vs. distance in flow
direction for third experiment
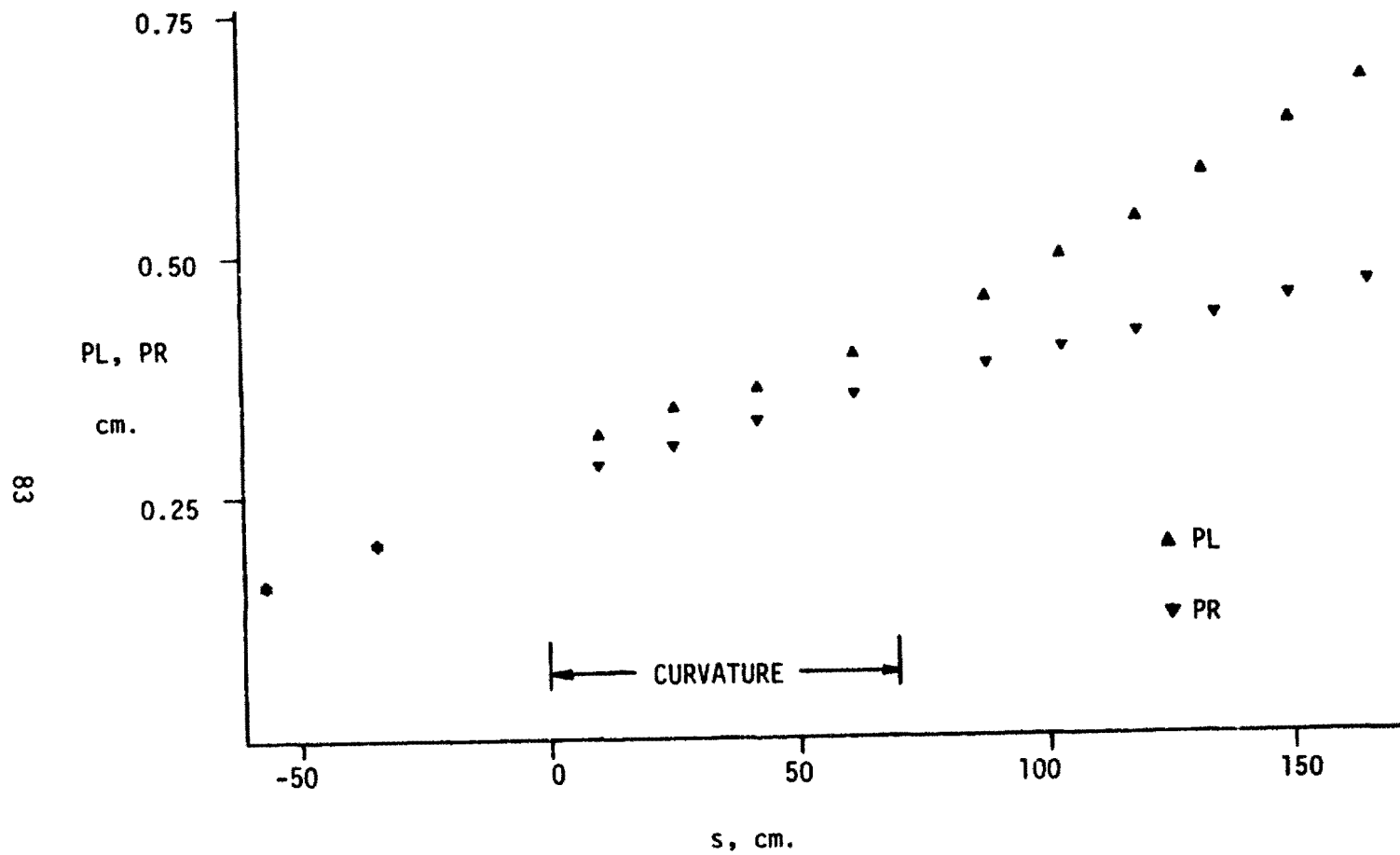
Fig. 47. PL and PR for the third experiment
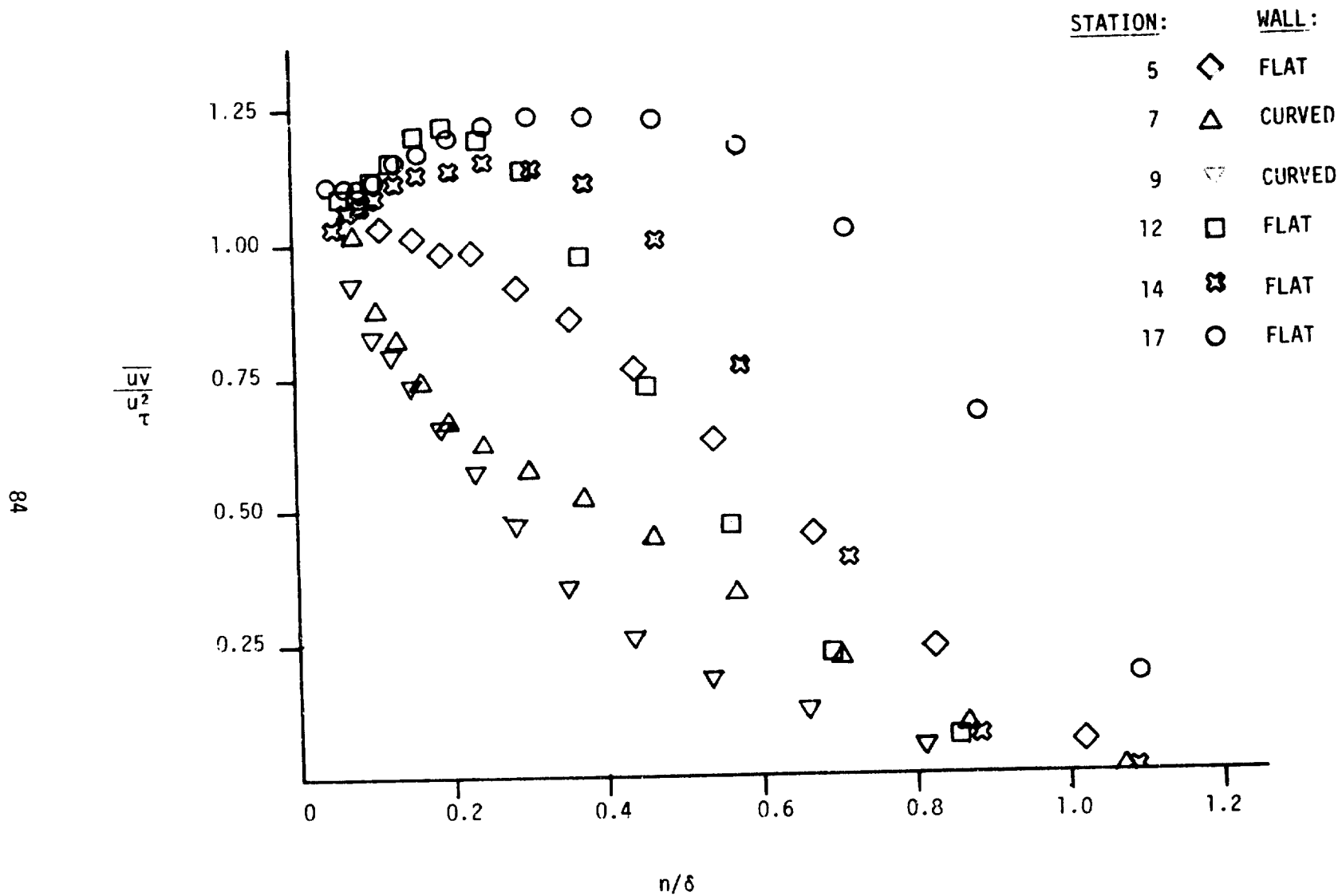
Fig. 48. Shear-stress profiles for third experiment
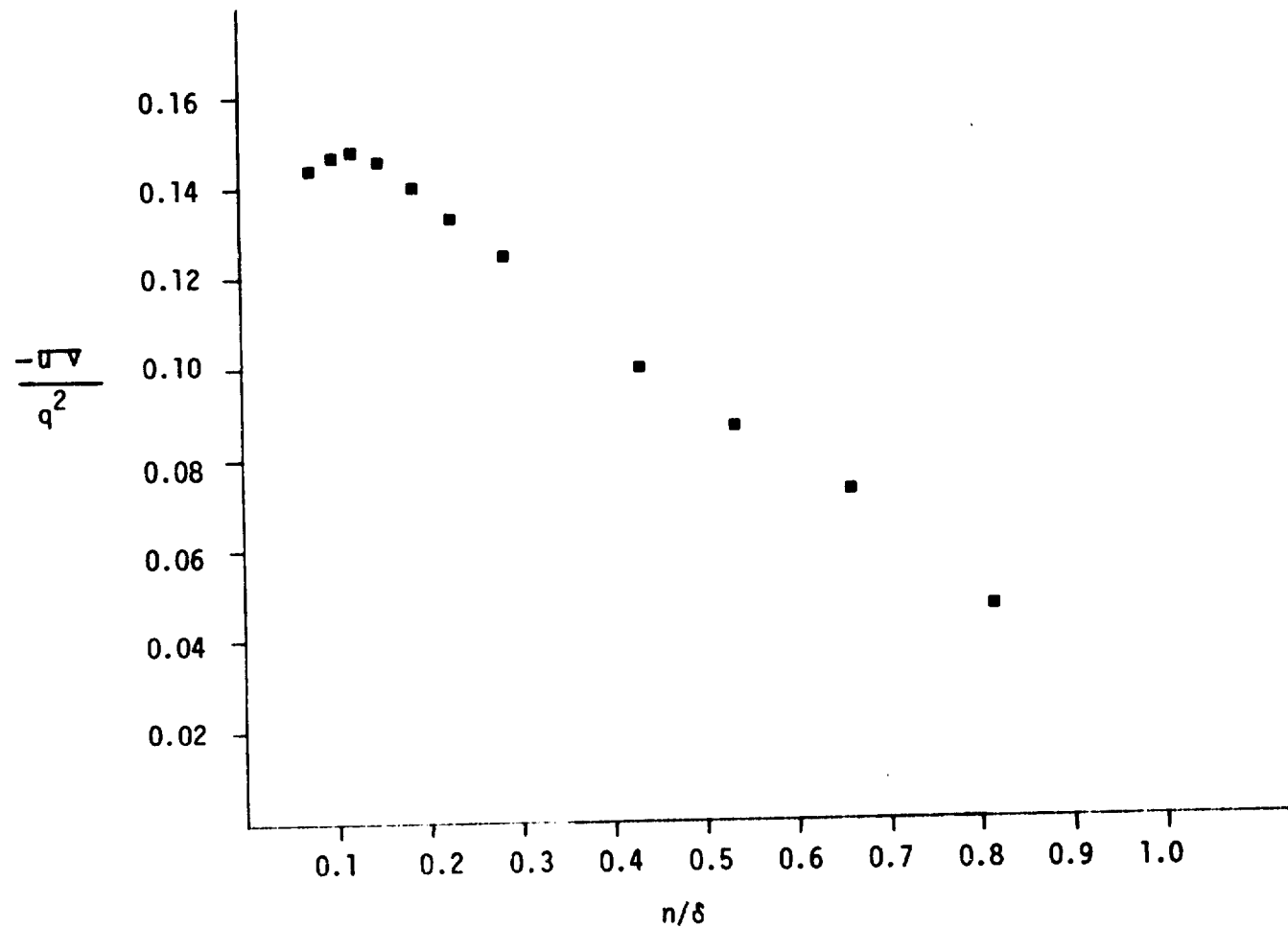
Fig. 49. Plot of structural coefficient for Station 9 (after 78° of curvature)
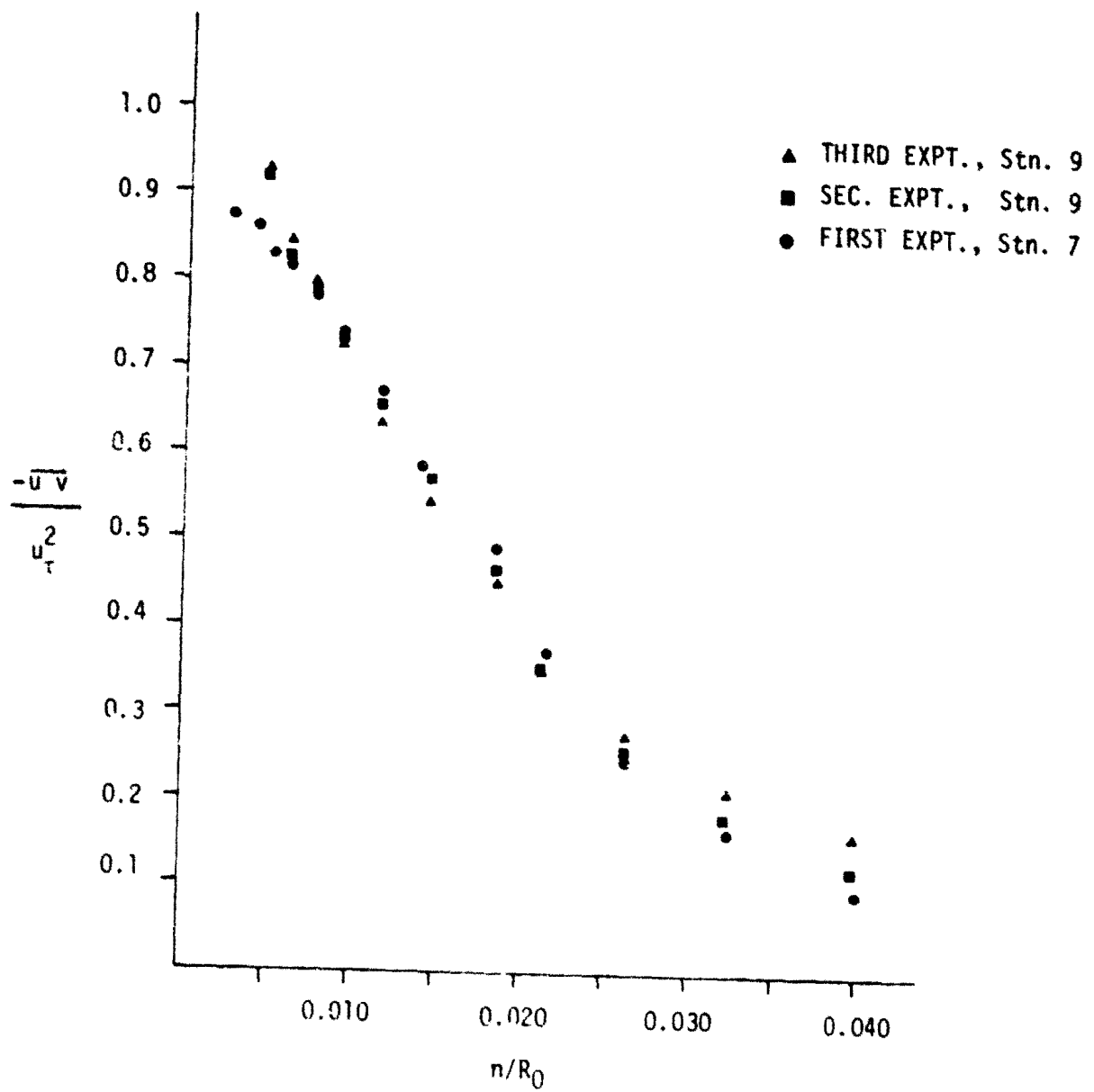
Fig. 50.   Collapse of curved region shear-stress profiles
for three experiments
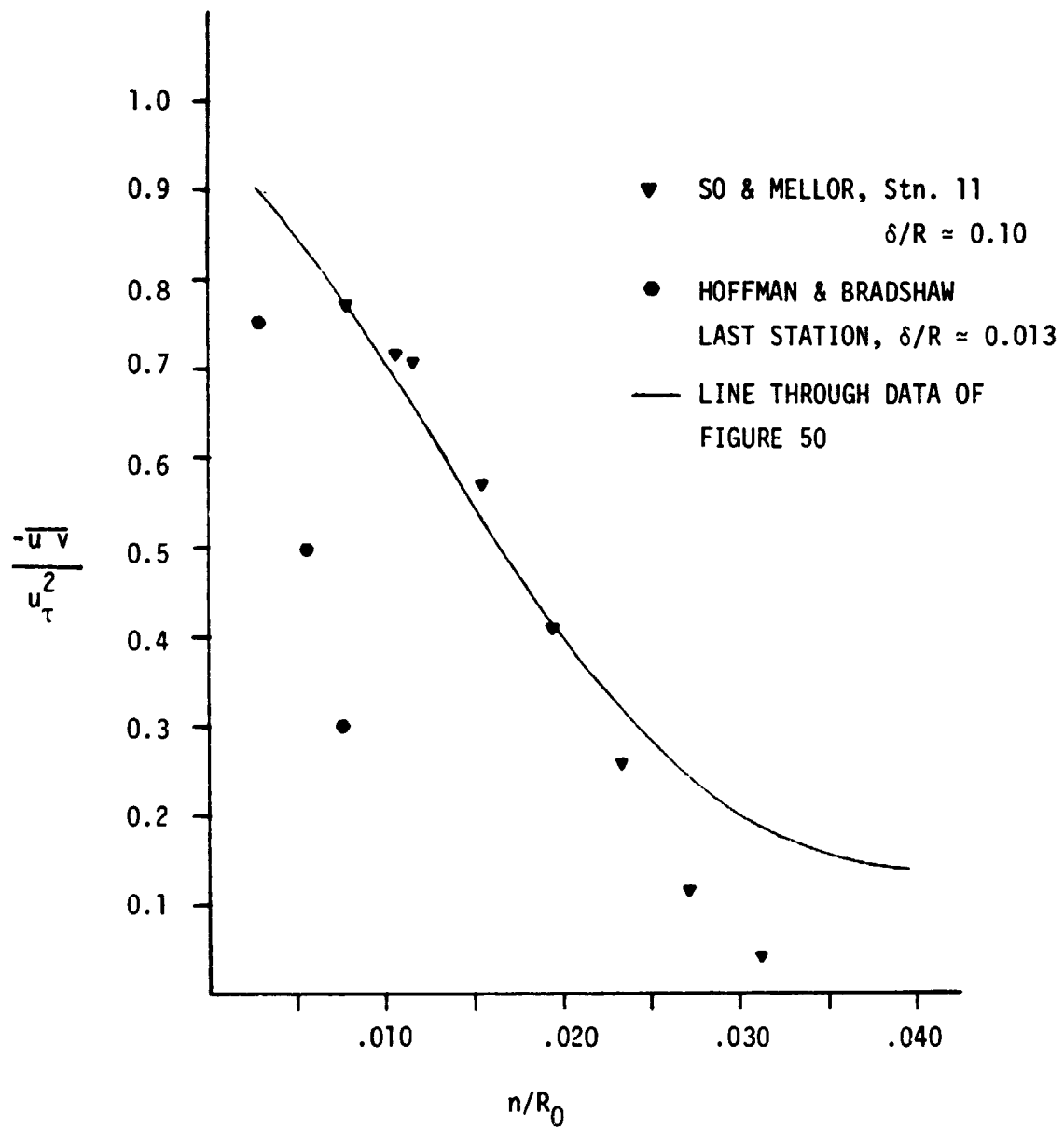
Fig. 51. Comparison of shear-stress profile from present program with data of previous experiments
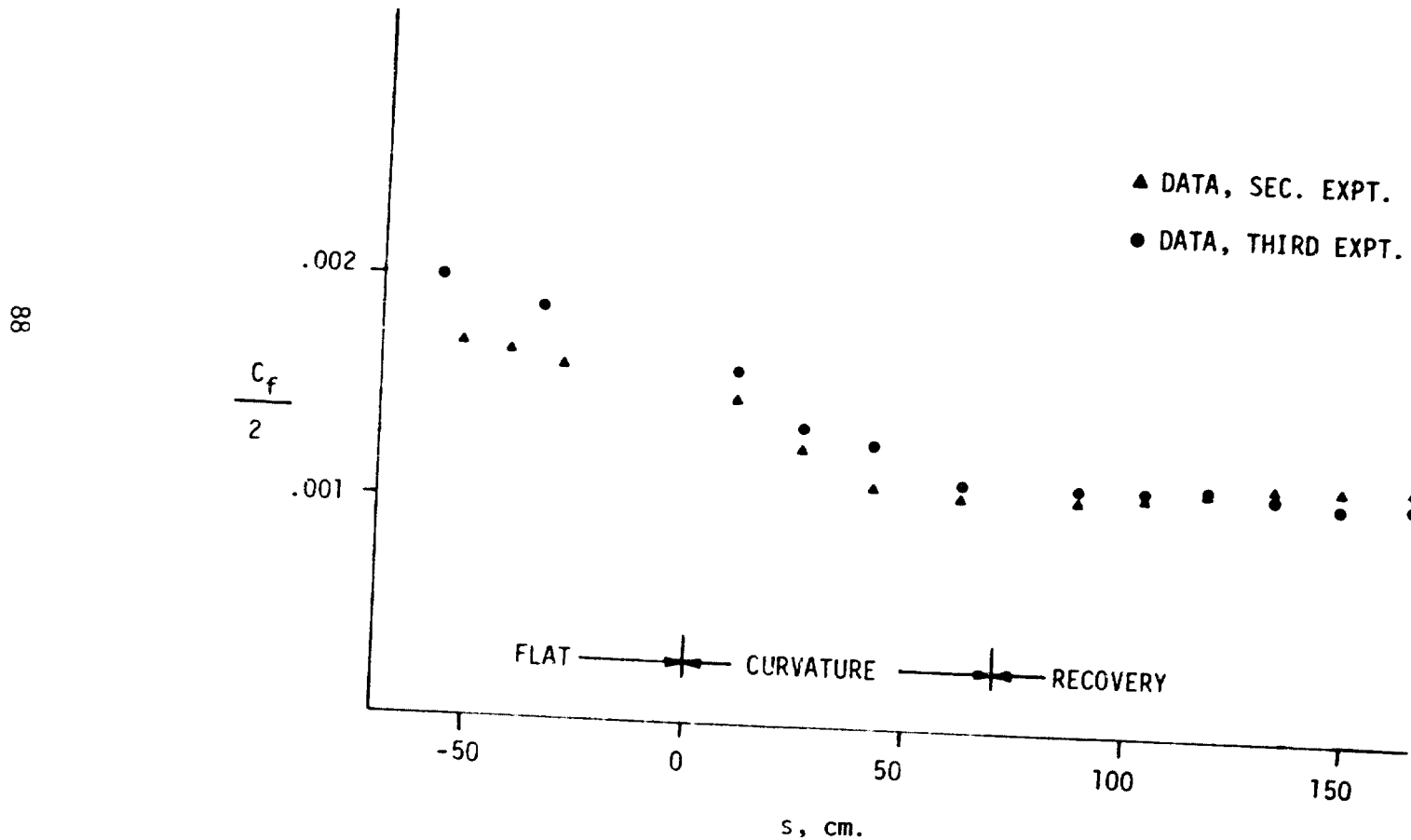
Fig. 52. Comparison of skin-friction curves for second and third experiments

88
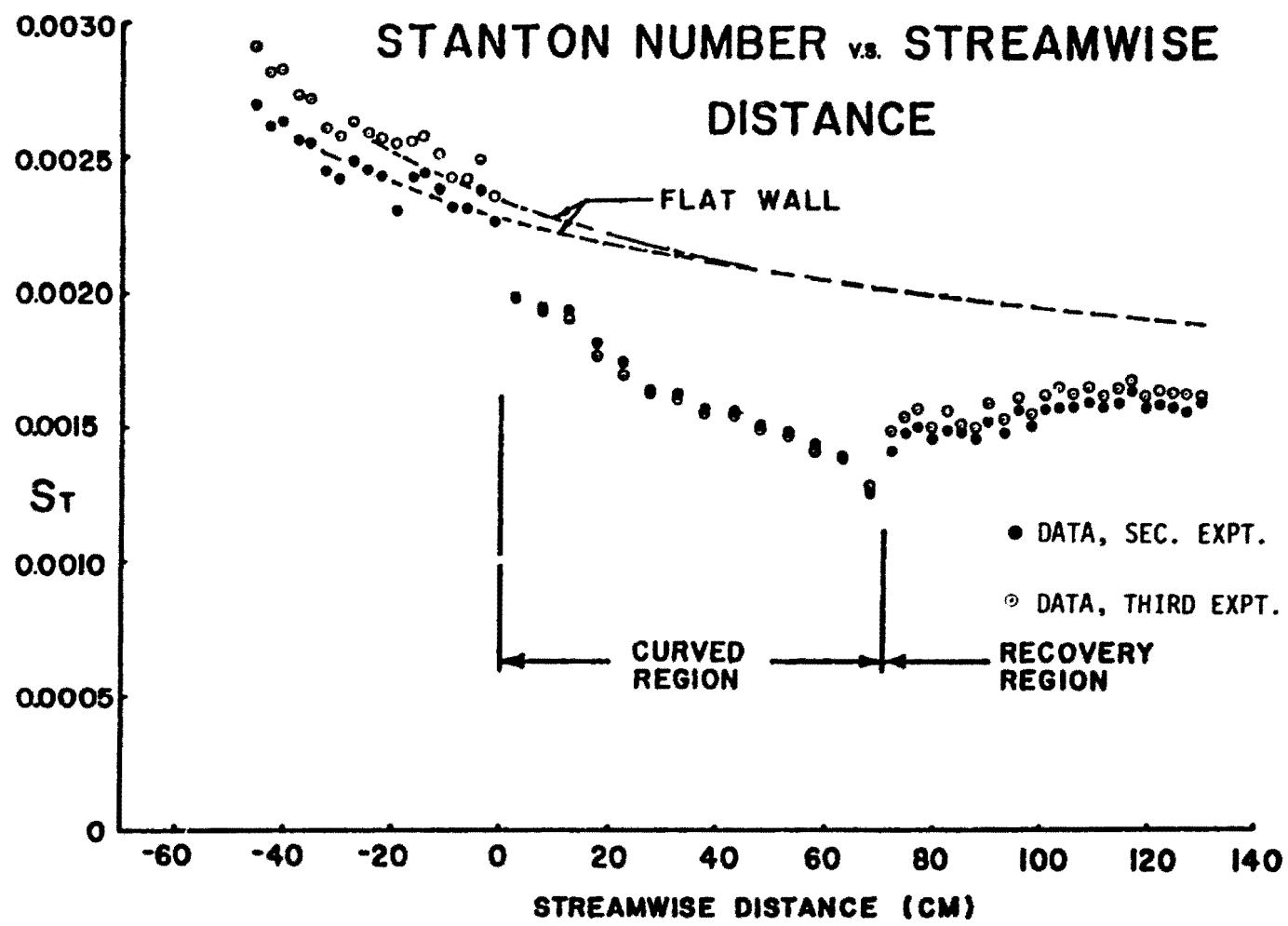
Fig. 53. Comparison of Stanton number from second and third experiments

Chapter 4

DIRECTIONS FOR TURBULENCE MODELING WITH CURVATURE

4.1 Introduction

One of the aims of this project was to translate the experimental data into a simple turbulence model that would be useful in practical engineering calculations. For such a model, it is desirable to keep the number of transport equations to be solved to a minimum. In the author's experience, designers are willing to trade some loss in generality for quick running times and simplified input. For these reasons we chose to use an empirical modification to the mixing-length turbulence model in the boundary layer code STAN5 [1].

The model which has been developed represents a significant improvement over the curvature modeling work done previously at Stanford. In particular, the slow recovery can now be accounted for. Nevertheless, the present model cannot yet be considered complete.

The mixing-length hypothesis uses an empirically prescribed length scale to relate the mean velocity gradient to the Reynolds shear stress, through the formula

$$- \overline{uv} = \ell^2 \frac{\partial U}{\partial y} \left| \frac{\partial U}{\partial y} \right| \tag{4-1}$$

For a flat-wall boundary layer, the length scale is taken as

$$\ell = \kappa y \left[1 - \exp(-y^+/A^+) \right] \tag{4-2}$$

in the wall layers where $y < 0.207 \, \delta$. κ, the Karman constant, is taken to be 0.41, its usual value. In the outer parts of a turbulent boundary layer,

$$\ell = .085 \, \delta , \tag{4-3}$$

where $y > 0.207 \, \delta$. The value of the parameter A^+ is determined from an empirical function. For a flat-plate, turbulent boundary layer,

$A^+ = 25$. For other pressure gradients, etc., the formulation used in STAN5 was also used here.

There have been previous efforts to build simple models of curvature effects. The most successful models have been those based on a scheme proposed by Bradshaw [11]. Bradshaw suggested multiplying the flat-wall mixing length by an empirical function built around the curvature Richardson number:

$$\ell = \ell_o(1-\beta Ri) \tag{4-4}$$

where Ri is the curvature Richardson number, ℓ_o is the standard flat-wall mixing length, and β is an empirical constant[*] obtained from the data. The curvature Richardson number is defined as

$$Ri = \frac{2U/R_{eff}}{\partial U/\partial n} \tag{4-5}$$

The effective radius of curvature, R_{eff}, is computed from a first-order lag equation, which simulates the effect created by a changed radius of curvature with streamwise distance, s.

$$\frac{d(1/R_{eff})}{ds} = \frac{1}{10\delta}\left[\frac{1}{Ro} - \frac{1}{R_{eff}}\right] \tag{4-6}$$

This form of model was used by Cebeci et al. [28], Rastogi and Whitelaw [29], as well as by Johnston and Eide [30].

The Johnston-Eide model also had a feature which allowed it to be used for very strong curvature effects like those shown in the experiments just described. The authors put a restriction on the size of Richardson number in the outer regions of the boundary layer, where the velocity gradient is very small. They used

$$R_I \sim .3\;\frac{2U\delta}{U_{pw}R_o} \tag{4-7}$$

---

[*]Universal values of β are still in question, even for convex walls. Bradshaw suggested $\beta = 2$ for concave and $\beta = 3$ for convex walls.

This allowed them to circumvent a problem which occurs in strong curvature cases. At $\delta/R = 0.10$, the Richardson number becomes large enough half way across the layer, at $n/\delta \approx 0.5$, so that the mixing length calculated from (4-1) becomes negative, an obviously undesirable result.

The models proposed by Launder et al. [31] and Irwin and Smith [32] are based on the flat-plate stress equation model of Launder, Reece and Rodi [33]. Irwin and Smith showed that mild curvature effects could be modeled reasonably well by including the extra curvature-production terms which appear in Reynolds stress transport equations. These terms can be derived directly from the Navier-Stokes equation without resort to a model of turbulence. This is an important point which will be discussed again below. It is difficult to assess the success of this model, because it was used to calculate only one data set -- that of Meroney and Bradshaw [13]. The curvature effects in that experiment were very slight $(\delta/R \approx .01)$ and even a flat-plate model comes close to the data.

Launder et al. applied the concepts developed by Bradshaw to the two-equation turbulence model of Jones-Launder [34]. Since the turbulence-length scale used by this model is determined by the dissipation equation, their approach was to make some of the constants in the modeled equation depend on the curvature Richardson number. Arguing that the curvature correction should scale on turbulent quantities and not mean-flow quantities, they redefined the curvature Richardson number as (for non-swirling flow):

$$ Ri = \frac{q^2}{4\epsilon^2} \left(\frac{U}{R}\right) \frac{\partial[U(R_o+n)]}{\partial n} \qquad (4-8) $$

The agreement with experiments was improved over the Jones-Launder model. Agreement seemed to be about as good as for mixing-length models which use Bradshaw's suggested correction. One wonders, however, whether multi-equation, single-point closure models, in which all length scales and stresses are calculated from data available at a single point in space, will be much more successful than mixing-length models. As has been shown in the data, curvature effects seem to act on the large-scale processes. Mixing-length models, because they must scale ℓ on

δ and on conditions upstream, if a lag equation is used, would seem to have greater potential for getting large-scale eddy conditions into the calculation scheme, given our current state of knowledge.

Another multi-equation model for curvature effects was developed recently by M. M. Gibson and his co-workers at Imperial College [35]. His model, like that of Irwin and Smith, is based on the work of Launder, Reece, and Rodi, but includes curvature-production terms in the set of Reynolds stress equations. However, Gibson's model is apparently different from Irwin & Smith's in the details of the pressure-strain term modeling. Results of computations show that agreement is as good as Irwin-Smith for the weak-curvature Meroney & Bradshaw data and also very good for the data of So & Mellor and the very strong curvature case of Smits, Young, and Bradshaw. Figs. 54 and 55 show the results of Gibson's calculations of the data of the first experiment presented in Chapter 3. Agreement for mean values and turbulent shear stress is very good in the curved region. It is interesting that Gibson's model predicts negative shear stress in the outer region over the convex surface, as was measured. In the recovery region, however, there is poorer agreement between the model and the data. The surprisingly slow recovery process shown in the data is not reproduced well, although it is somewhat better than earlier work at Stanford [36].

The purpose of constructing a new model was to use the insights developed from the data shown in Chapter 3 to improve on the models previously available. It was also deemed desirable to keep the computation scheme as simple as possible, in order to make the code useful to industrial designers. For this reason, it was decided to try to improve the "zero equation" mixing-length methods, which are easy and inexpensive to use but which are not as general as some of the multi-equation Reynolds stress models. It was particularly desirable to find a model which would predict the observed slow recovery from curvature effects.

An analysis of the causes of sudden disappearance of the Reynolds shear stress was carried out by Honami [21], based on the transport equation for $- \overline{uv}$, which is, for curved flow:

93

$$\frac{D\overline{(uv)}}{Dt} = \overline{u^2}\left[\frac{\partial V}{\partial s} - \frac{U}{R}\right] + \left(1 + \frac{n}{R}\right)\overline{v^2}\frac{\partial U}{\partial n} - \frac{U}{R}(\overline{u^2} - \overline{v^2})$$

$$- \overline{\frac{p'}{\rho}\left[\frac{\partial v}{\partial s} + \left(1 + \frac{n}{R}\right)\frac{\partial U}{\partial n}\right]}$$

$$+ \frac{\partial}{\partial s}\left[\overline{\frac{p'v}{\rho}} + \overline{u^2 v}\right] + \left(1 + \frac{n}{R}\right)\frac{\partial}{\partial n}\left[\overline{\frac{p'u}{\rho}} + \overline{uv^2} + \frac{(2\overline{uv^2} - \overline{u^3})}{R}\right]$$

$$- \epsilon \tag{4-9}$$

The terms of RHS have been grouped according to function. On the first line are the production terms. The second line is the pressure-strain term which tends to change the orientation of the turbulent motions. On the third line are the diffusion terms, and the last line is the dissipation term. Over a curved wall the dominant production terms are

$$\mathcal{P} = \overline{v^2}\frac{\partial U}{\partial n} - (2\overline{u^2} - \overline{v^2})\frac{U}{R} \tag{4-10}$$

For a flat wall, of course, only the first of the terms on the RHS is non-zero. The second term in Eqn. (4-10) appears suddenly at the start of curvature, and it tends to decrease the total production rate, since usually $2\overline{u^2} \gg \overline{v^2}$. Honami calculated the size of the production terms for two profiles of the first experiment, one on the flat wall upstream of curvature and one at Station 4, 20° after the start of curvature. Results are plotted in Fig. 56. For the flat-wall profile, the total production is positive at all values of y. For the curved-wall boundary layer, the total production is positive in the inner layer, but in the outer layers the positive and negative production terms are about equal. This shows the reason for the huge change in the outer layer levels of $-\overline{uv}$ near the start of curvature. The negative production balances the positive production, and the dissipation reduces the level to nearly zero.

Soon after the start of curvature, the shear-stress profiles have the same shape, as was pointed out before. Indeed, the changes in shear-stress profiles were slow with respect to s (or turning angle)

94

downstream of the start of curvature for all three data sets. This indicates that a local equilibrium model, like the mixing-length hypothesis, might be successful.

The first step in building such a model was to calculate the actual mixing-length distributions from the experimental data. From the shear-stress and mean-velocity profiles, it is possible to calculate the mixing length, and in Fig. 57 mixing length profiles have been plotted for three stations of the first experiment used previously to represent flat, curved, and recovery profiles. The mean-velocity gradients needed to calculate the mixing length were obtained by differentiating a cubic spline which was fitted close to the data points. Fortunately, very little smoothing was needed to fit the spline. In the profiles of Fig. 57, the great reduction in the length scale of the turbulence which has been observed by all workers in this field is evident.

Even in the curved region, there is a layer close to the wall where the classical mixing-length distribution ($\ell = \kappa n$) holds. In the curved region, however, the mixing length becomes constant closer to the wall. This view is supported by Fig. 58, where ℓ/δ is plotted vs. n/δ at 60 and 80 deg. (Mixing lengths calculated from data taken far out in the boundary layer are not shown because, far from the wall, both the shear stress and velocity gradient are small and the computed mixing lengths show considerable scatter, due to large uncertainties.) The plots show profiles which seem to have two regimes: $\ell = \kappa n$ for n less than 0.07δ and $\ell = 0.025\delta$ for n greater than 0.07δ. The recovery profiles suggest that the point at which the mixing length becomes constant moves slowly back toward the usual value of approximately $.085\delta$. This picture is consistent with the idea that the main effect of the curvature is to confine the turbulent motions close to the wall and to destroy the previously existing large-scale motions. The slow regrowth of the mixing length in recovery is probably associated with the slow reappearance of large-scale structures.

Previous work on mixing-length models at Stanford showed that the effects of longitudinal pressure gradients and transpiration could be correlated by the use of one parameter A^+, which is the effective viscous sublayer thickness that appears in the Van Driest damping

95

scheme. Near a wall the mixing length is modeled as in Eqn. (4-2). To test the possibility that A^+ might be the correlating parameter for curvature effects, the value of A^+ was calculated from the data for each of the stations in the first experiment. The calculation of A^+ is based on the experimentally observed fact that at $y^+ = 3A^+$, the Reynolds number of turbulence, defined as

$$Re_\tau = \frac{\ell_\tau \sqrt{-\ uv}}{\nu} \qquad (4-9)$$

has a value of 31. The length scale in the equation is taken as the Prandtl mixing length. Results are shown in Table 4-1.

Table 4-1

Values of A^+ Calculated from Data of First Experiment

Wall	Flat			Curved				Flat Recovery		
Station	1	2	3	4	5	6	7	8	9	10
A^+	24.9	25.1	24.5	33.8	28.3	28.9	27.6	24.5	24.6	23.8

With the exception of Station 4, which is the first station downstream of the start of curvature, the value of A^+ is changed only slightly for the flat-wall value of 25. This makes sense because, in the sublayer, the normal pressure gradient $\rho U^2/R$, is very small compared to its value in the outer layers. Since the strongest effects are away from the wall, another method of correlation must be found.

4.2 Development of an Outer-Layer Model

The facts that the outer-layer mixing length is so much smaller than $0.085\ \delta$ and that the layer with active shear-stress is also so much smaller than δ suggest that perhaps δ is no longer the appropriate scaling length. In fact, it seems much more likely that the outer-layer mixing length is tied to the width of the active shear-stress layer than to the velocity-gradient layer. Indeed for flat-wall

flow, if a boundary layer were to develop into a free stream which had a slight shear, one would not expect that the boundary layer length scale for active turbulence would extend far into the free stream.

In an unrelated experiment, Kim, Kline, and Johnston [37] found, in a reattached boundary layer downstream of a separation, that the outer-layer eddy viscosity scaled on $(\delta-\delta_1)$, not on δ alone. In their case, as in our recovery flow, a new sub-boundary layer grows slowly out from the wall, downstream of a sudden change of conditions, detachment in [37], removal of stabilizing curvature in our flow. Both observations noted above were combined for our model of mixing length, i.e.,

$$\ell \ \propto \ (\delta_{sl} - \delta_{sl}^{*}) \tag{4-10}$$

where δ_{sl} is the width of the active shear layer and δ_{sl}^{*} is the displacement thickness calculated by integrating out to δ_{sl}.

The problem of how to determine the width of the shear layer was now faced. This can be done very easily but only approximately by eye. Examination of Figs. 21, 42, and 48 shows that δ_{sl} must be about 0.35 δ for the first two experiments and about 0.6 δ for the third experiment. To determine δ_{sl} consistently, the procedure illustrated in Fig. 59 was used. Here δ_{sl} is taken to be the extrapolation of the straight, descending portion of the shear-stress profile. The other parameter, δ_{sl}^{*}, was calculated, once δ_{sl} was determined as:

$$\delta_{sl}^{*} \ = \ \int_{0}^{\delta_{sl}} \left(1 - \frac{U}{U_{pw}}\right) dn \tag{4-11}$$

Figures 60 and 61 show how the mixing length compares in the second and third experiments with $(\delta_{sl} - \delta_{sl}^{*})$. The constant of proportionality is taken as 0.10. Also shown is the average value of the experimentally determined mixing length in the active stress outer region $(n < \delta_{sl})$. The scaling is very good in the curved region, and reasonable in the recovery region, although $(\delta_{sl} - \delta_{sl}^{*})$ recovers slightly faster. The fact that agreement is so good for the mixing length indicates that the mean velocity profiles resulting from integrating this mixing length will be very close indeed.

Examination of Figs. 60 and 61 shows that the suggested scaling method works well when the boundary layer is in quasi-equilibrium in the latter stages of the curve and through the recovery section. It will not be a good predictive tool at the start of curvature where the boundary layer is out of equilibrium. Indeed, the scaling method does not address the question of why the mixing length should drop when the wall suddenly changes from flat to curved. Clearly, another step is necessary to complete the model -- some way is needed to adjust δ_{sl} down at the start of curvature.

Many ideas for ways of adjusting δ_{sl} downward in the non-equilibrium portion of the flow were tested in the code STAN5. The most successful (but still not entirely satisfactory) scheme was based on the work of Gibson [38], who made the observation[*] that there appears to be critical value of the stability parameter S, defined as

$$S = \frac{U/R}{\frac{\partial U}{\partial y}} \tag{4-12}$$

above which shear stress could not sustain itself. Note that the stability parameter, S, is one-half the curvature Richardson number.

Gibson surmised that the shear stress fell to zero whenever S was greater than 0.17. It was then suggested that the data of our experiment could have been predicted by the boundary-layer code STAN5, if it had used the shear-layer mixing-length scaling discussed above, and defined δ_{SL} in the curved region to be the n value where S was equal to 0.17.

To summarize the calculation procedure, upstream of curvature the outer-layer mixing length is determined directly from $(\delta_{sl} - \delta_{sl}^{*})$. At the start of curvature, δ_{sl} is taken to be the n value where s is $S_{critical}$ regardless of the shear stress profile. This reduces the outer-layer mixing length immediately, and δ_{sl} is determined by the S parameter through the curvature. At the end of curvature, the

---

[*] One may attribute the first observation of this type to either L. Prandtl or P. Bradshaw.

calculation switches back to determining δ_{sl} from the shear-stress profile by extrapolation, as in Fig. 59.

The model described above was applied in conjunction with the STAN5 two-dimensional boundary layer method. However, a good fit, in terms of computed mean properties and shear stress, was produced with $S_{critical}$ = 0.11.

Results computed for the first experiment were very encouraging. Fig. 62 shows a plot of the computed $C_f/2$ distribution. These results were very encouraging; the skin friction trends are well represented in the curved region, and the recovery is very slow, as the data say it should be. More importantly, the shear-stress profiles are closely predicted, as shown in Fig. 63.

Figure 64 compares the results of the second experiment to the predictions. The skin friction is again well predicted in the curved region, as would be expected since δ/R is almost the same for the two experiments. The recovery-region skin friction is also well predicted, as are the shear-stress profiles.

Results were not as encouraging for the third experiment, as shown in Fig. 65. The skin friction is overpredicted by about 6% in the curved region. In the recovery region, the calculation shows some recovery; however, the skin-friction data show none. As a result, the predicted skin friction is 25% too high at the end of the recovery region. It may be that some of the disagreement between calculation and experiment in the recovery region of the third experiment is due to the influence of secondary flows, which, as Fig. 47 shows, become large in the last half of the recovery plate. However, it is also clear that the new model does recover too quickly, although it is closer to the data than previous models. The reason for the quick recovery of the model is the fact that the scaling length δ_{sl} is set artificially in the curved region, rather than taken from the calculated shear-stress profile. At the end of the curved region, the program switches back from setting δ_{sl} at the point where $S = 0.11$ to setting δ_{sl} by extrapolating the shear-stress profile. If the mixing lengths calculated by the two methods are not exactly the same, then there is a step change in the calculated turbulence structure which causes either a too quick or a too slow

recovery. In this case, the model for the curved region produced a shear-stress profile (at the end of curvature) with δ_{s1} about equal to .84 δ, whereas the data show δ_{s1} = .56δ. Also shown in Fig. 65 are the results of computing the recovery region flow using, as an initial condition, the data at Station 10. This calculation showed much better agreement. Thus, the key to better agreement in the recovery region is a better method for setting δ_{s1} in the curved region. Efforts to find such a model are continuing.

The model presented above is based on the premise that the near-wall conditions are unaffected (to the level of approximation necessary to get rough agreement with the data). If this idea is true, then one might expect that heat-transfer data could also be predicted to good accuracy by using the above model to calculate the hydrodynamic equations, standard flat-wall energy equation, and turbulent Prandtl number distribution. The turbulent Prandtl number is close to 1.0 in the outer layer, as it should be when the momentum and energy transport are both determined by the turbulence structure. If this is the case, then one would expect the heat and momentum diffusion processes to be affected in the same way by the curvature. To test this assertion, the heat-transfer data from the second experiment was predicted with the new curvature model. Results shown in Fig. 66, show that indeed the Stanton numbers can be predicted with no change to the energy equation, or change from the usual flat-wall turbulent Pr number values.
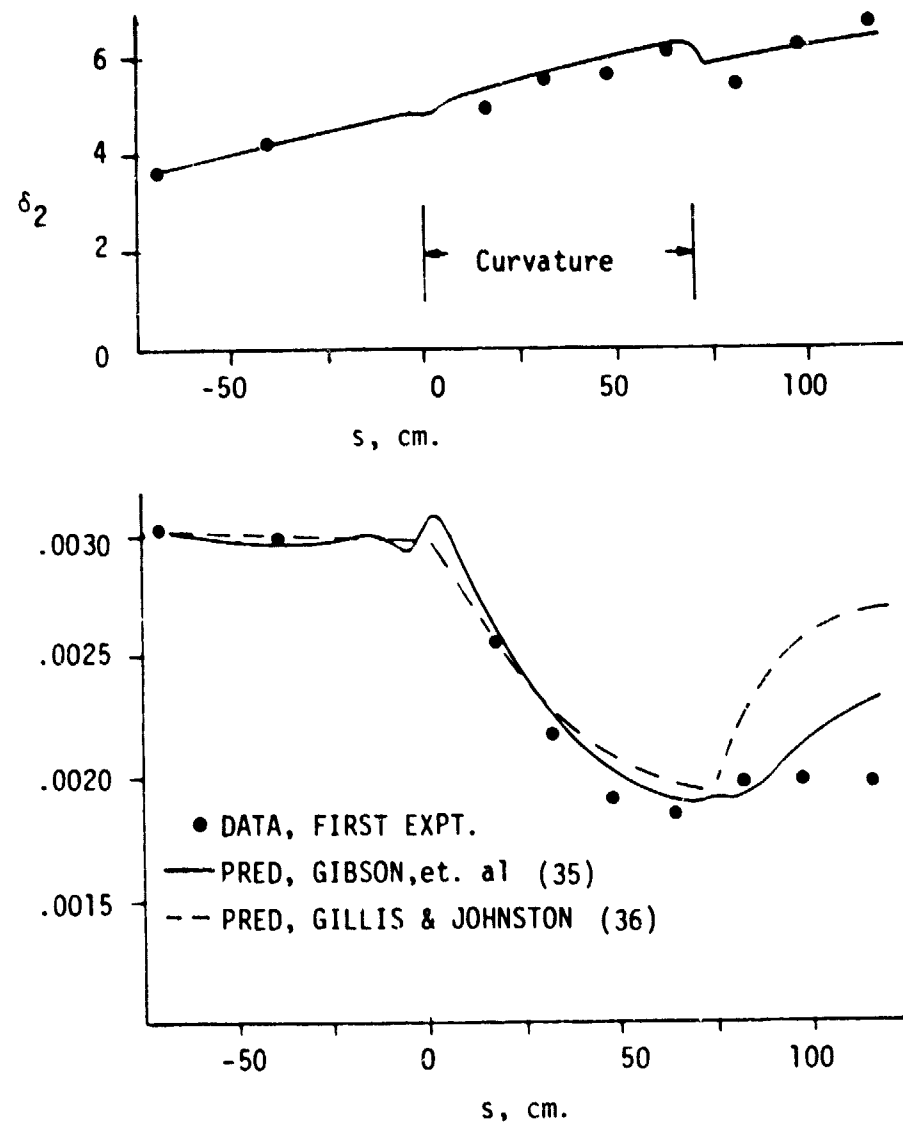
Fig. 54.   Comparison of mean-velocity data from first
experiment to prediction of Gibson

101
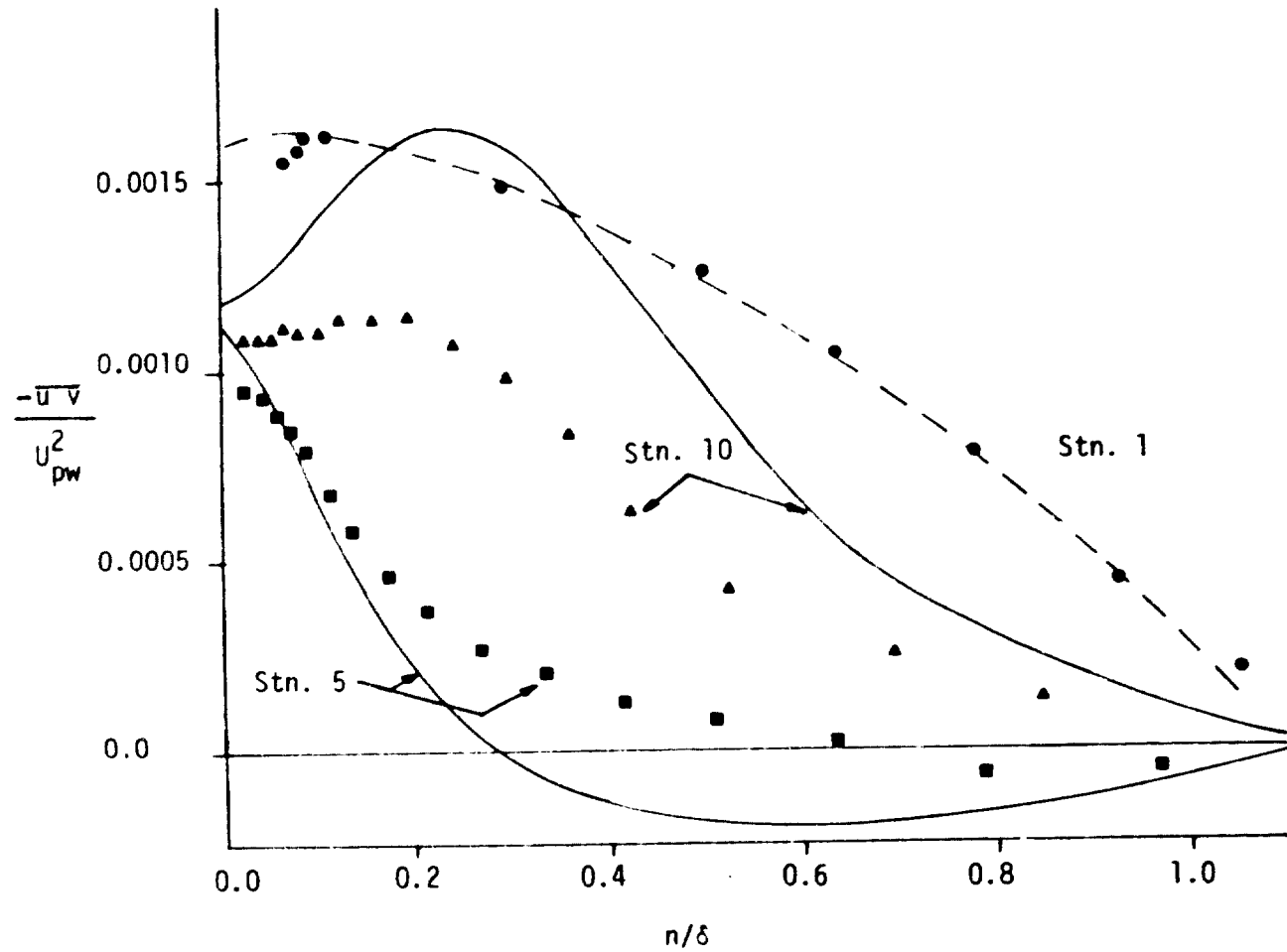
Fig. 55.   Shear-stress profiles for first experiment as predicted by
Gibson compared to data
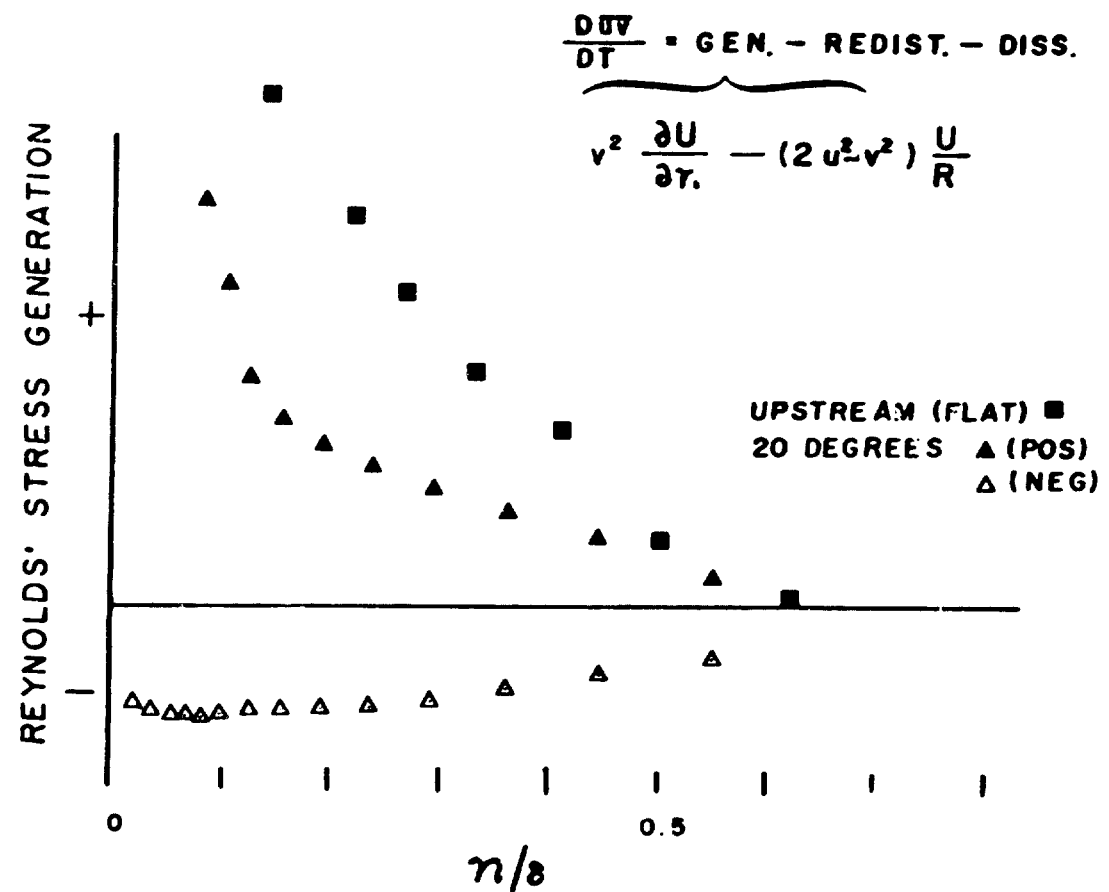
Fig. 56. Shear-stress production profiles on flat wall and after 20° of
curvature, as computed by Honami for data of first experiment
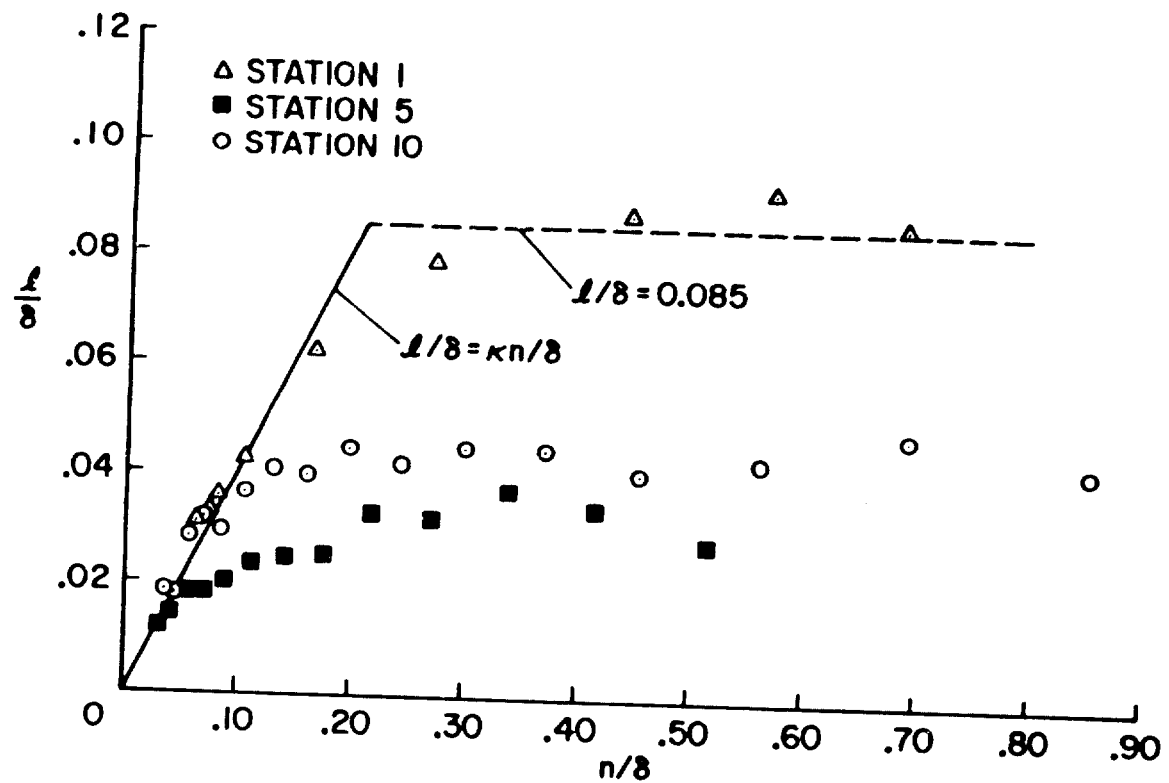
Fig. 57. Mixing-length profiles at representative stations for data of first experiment
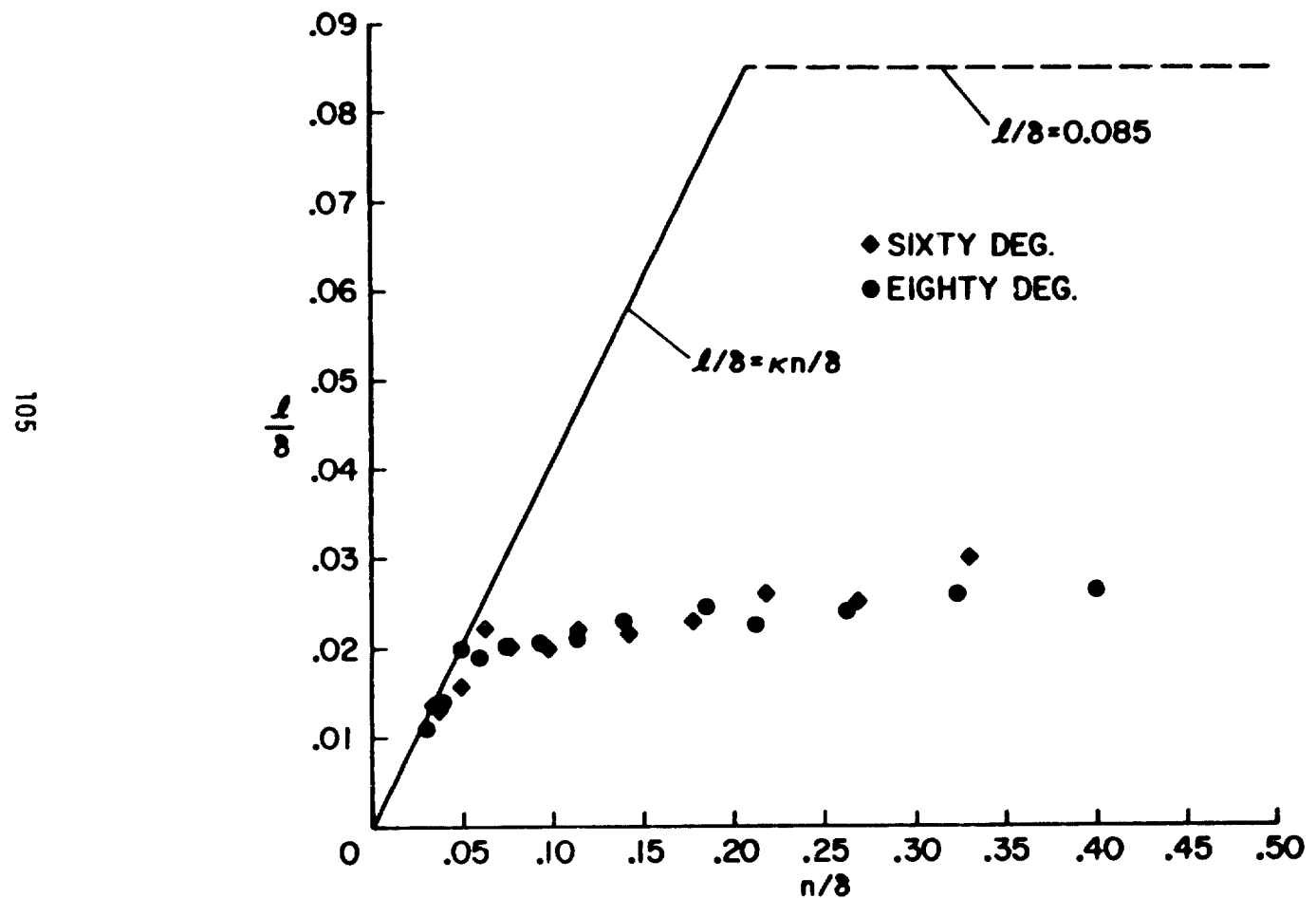
Fig. 58. Mixing-length profiles at stations near the end of curvature for data of first experiment
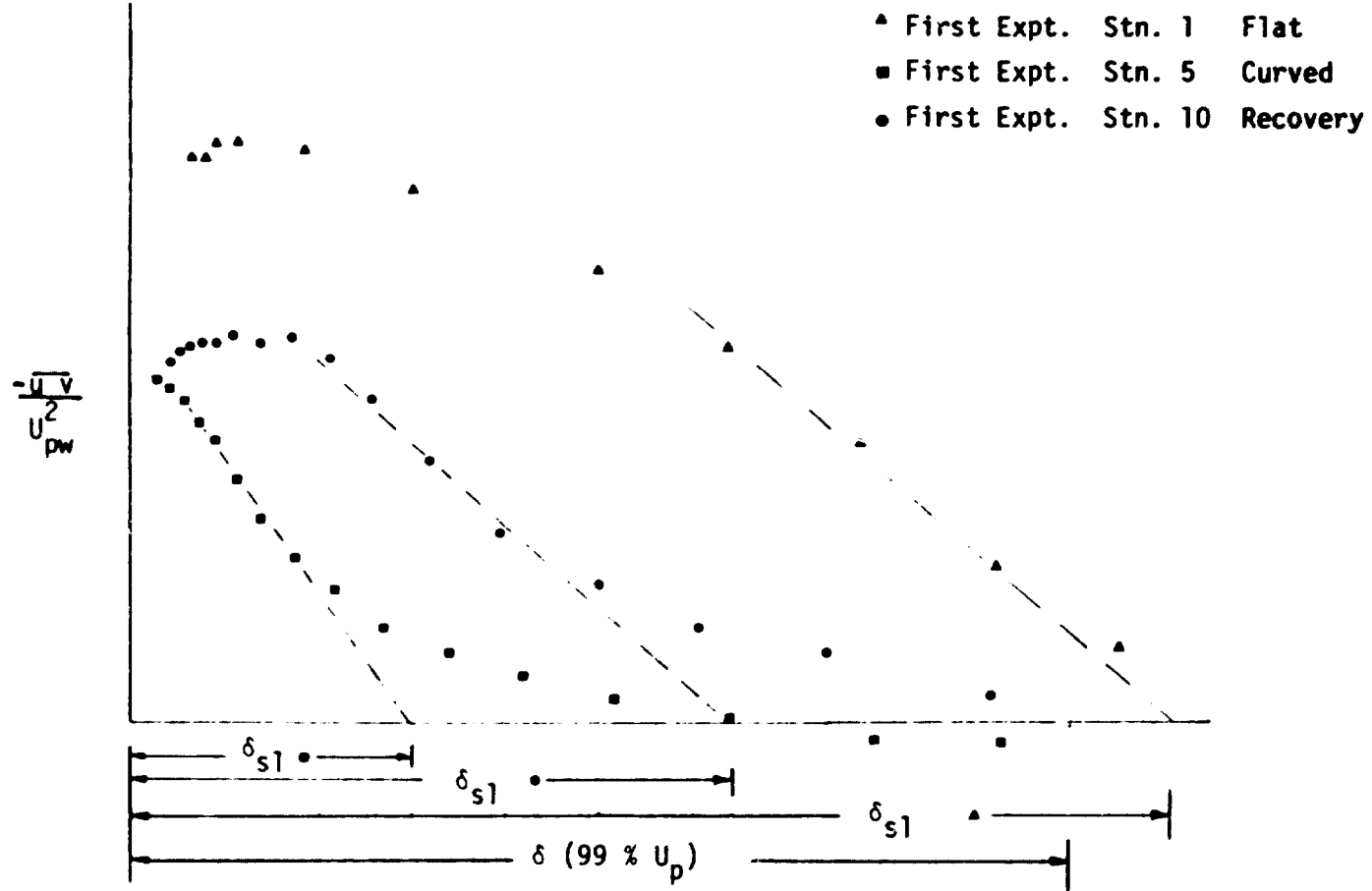
Fig. 59. Method of determining δ_{sl} by extrapolating shear-stress profile
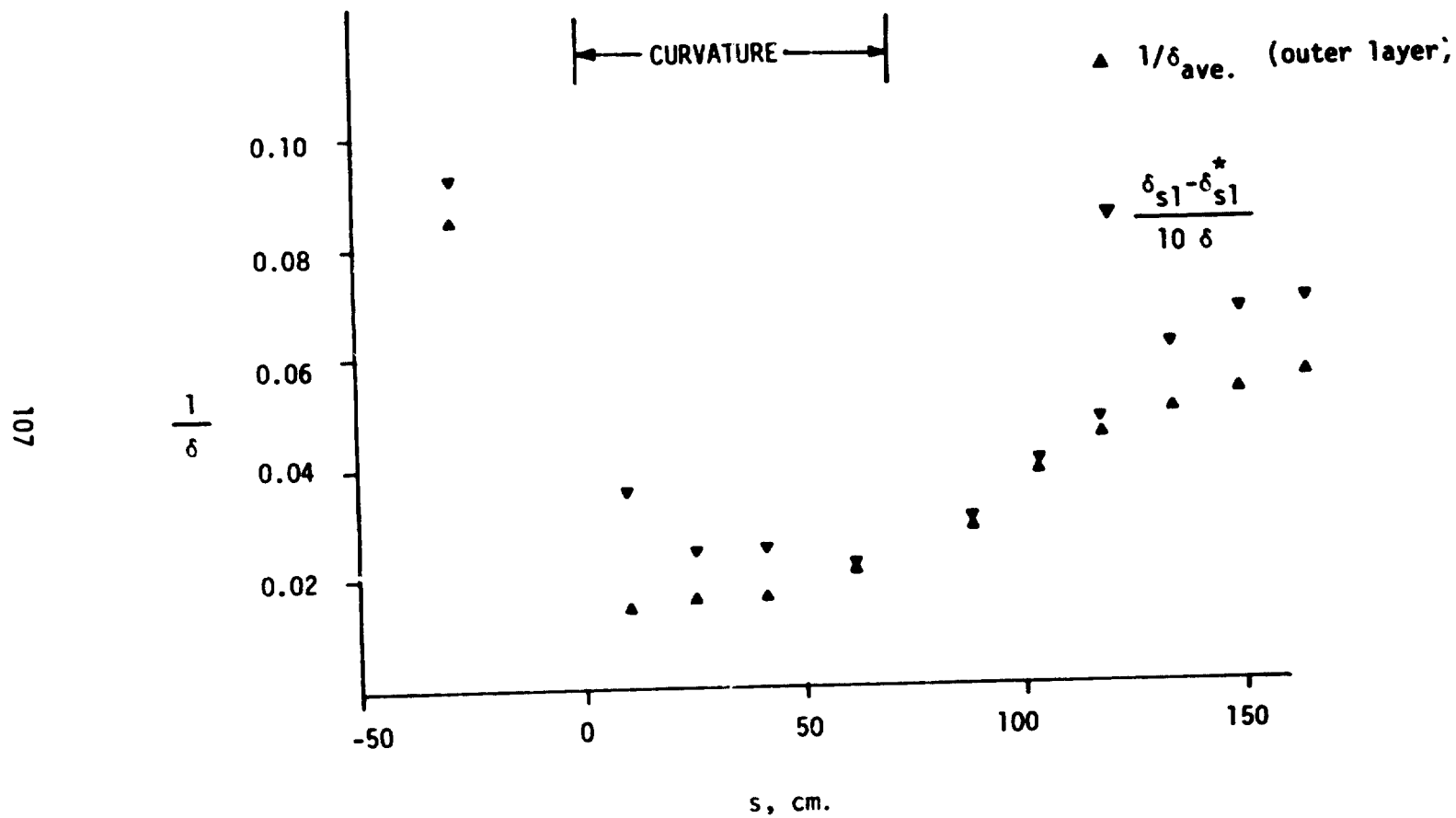
Fig. 60. Comparison of mixing length scaled on shear-layer thickness
with data of second experiment
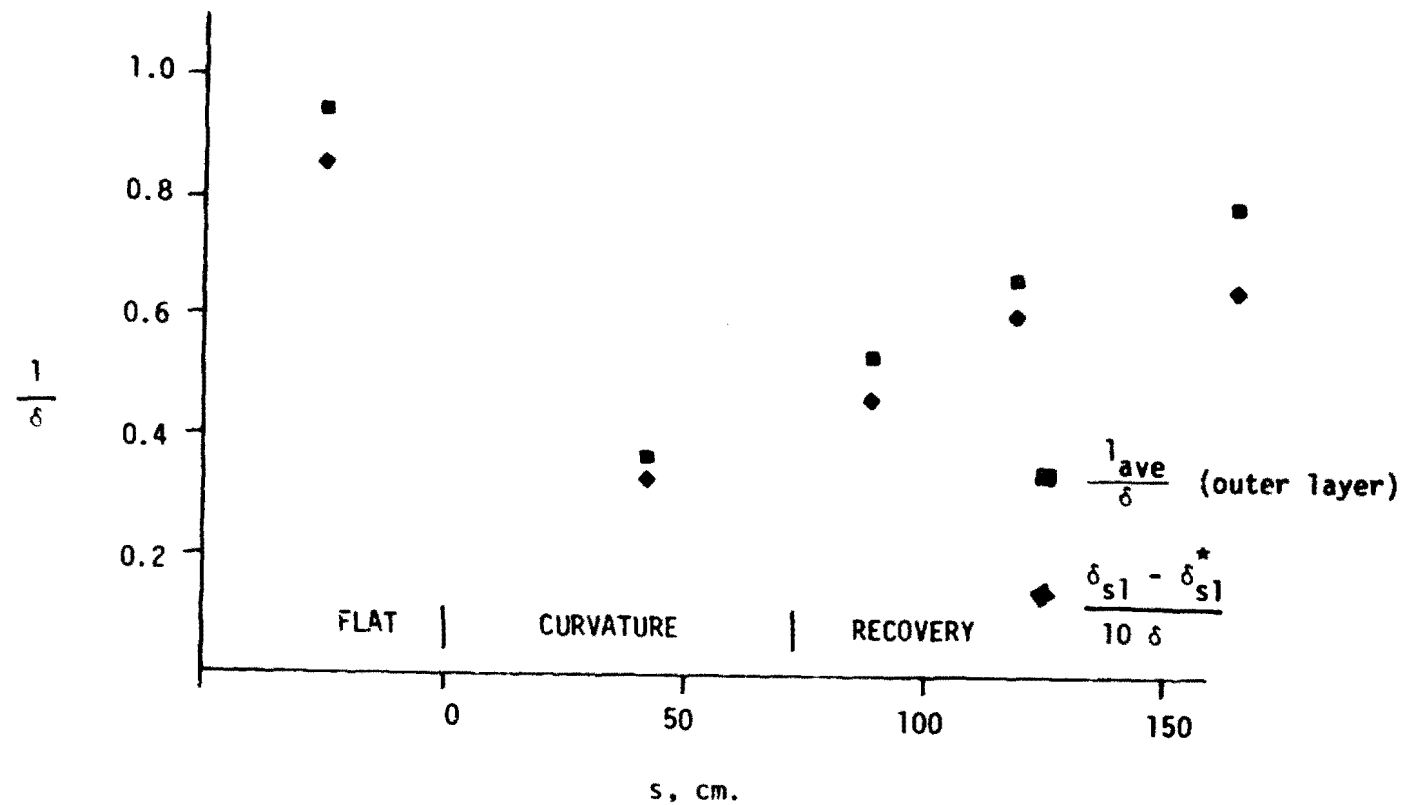
Fig. 61. Comparison of mixing length scaled on shear-layer thickness with data of third experiment
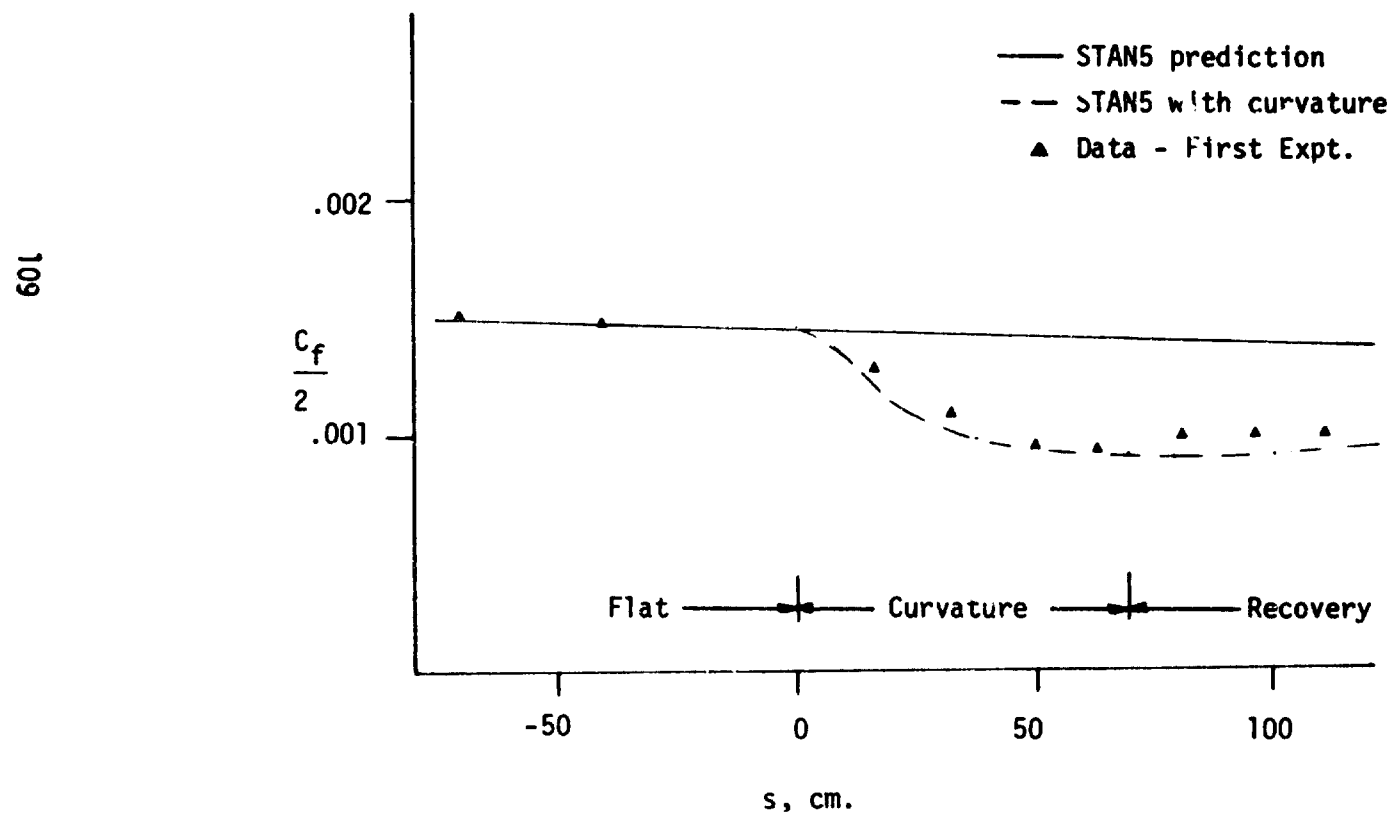
Fig. 62. Skin-friction distribution predicted by stability model compared with data of first experiment
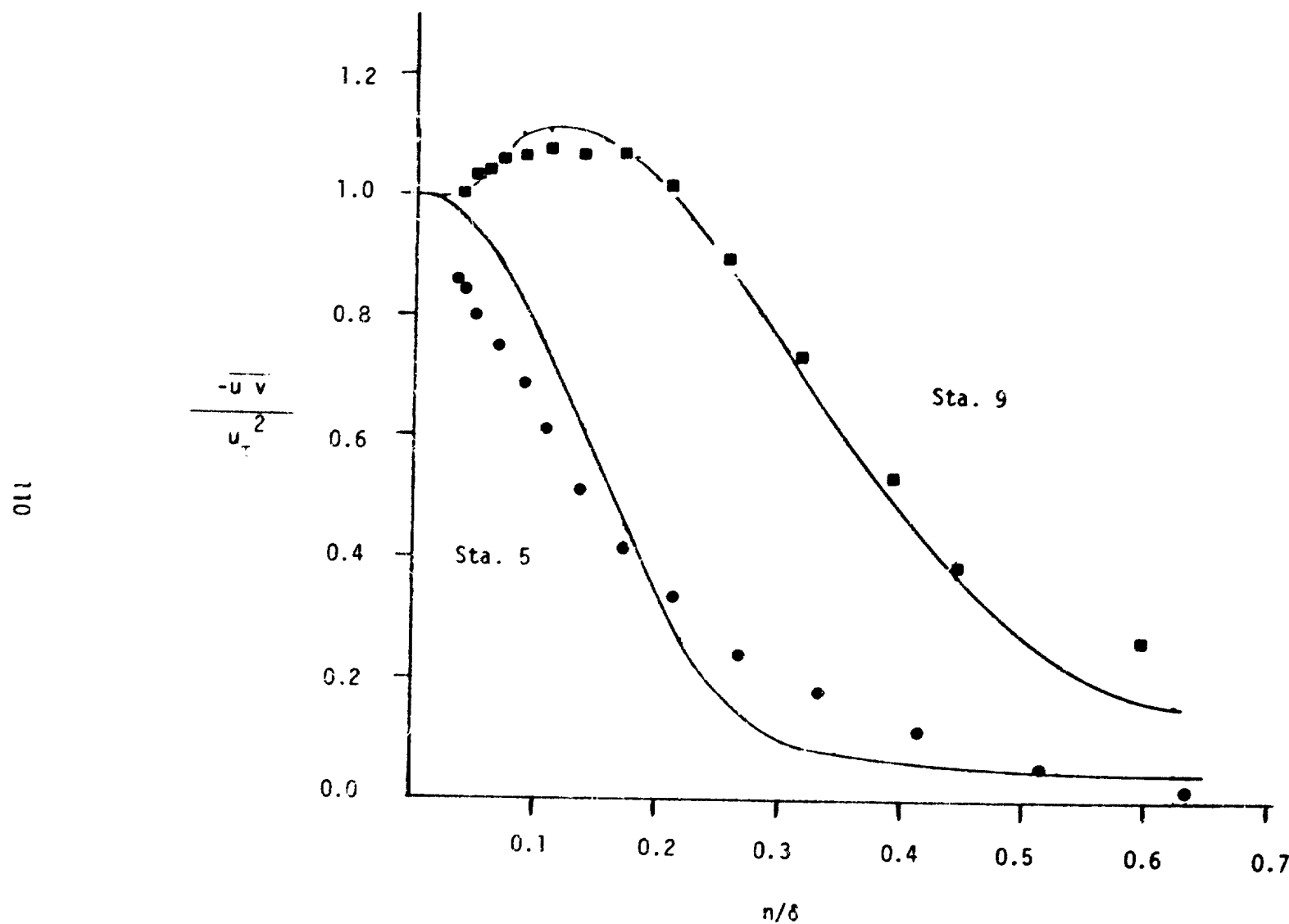
Fig. 63. Predicted shear-stress profiles compared with data of first experiment
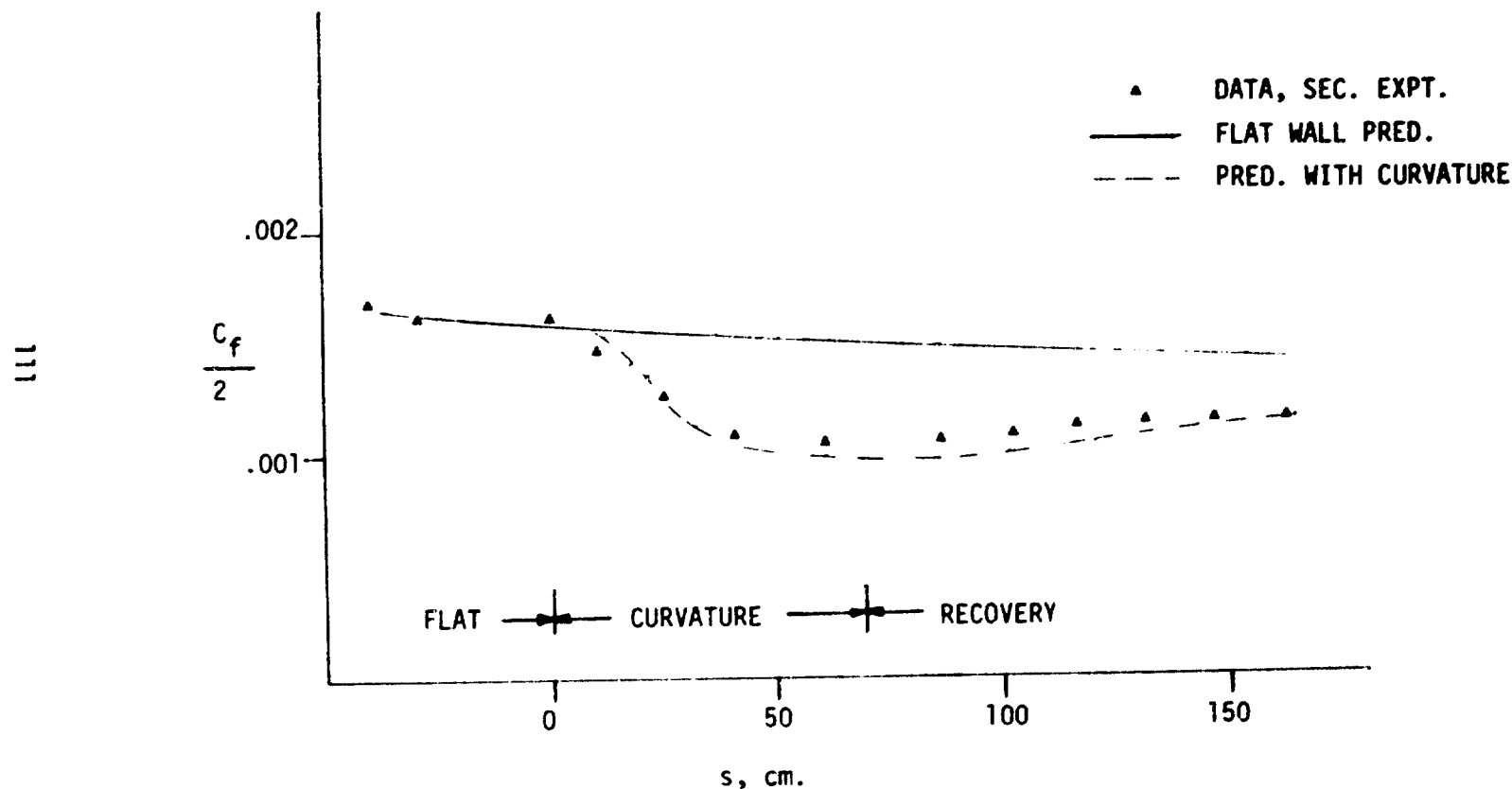
Fig. 64. Skin-friction distribution predicted by stability model compared
with data of second experiment
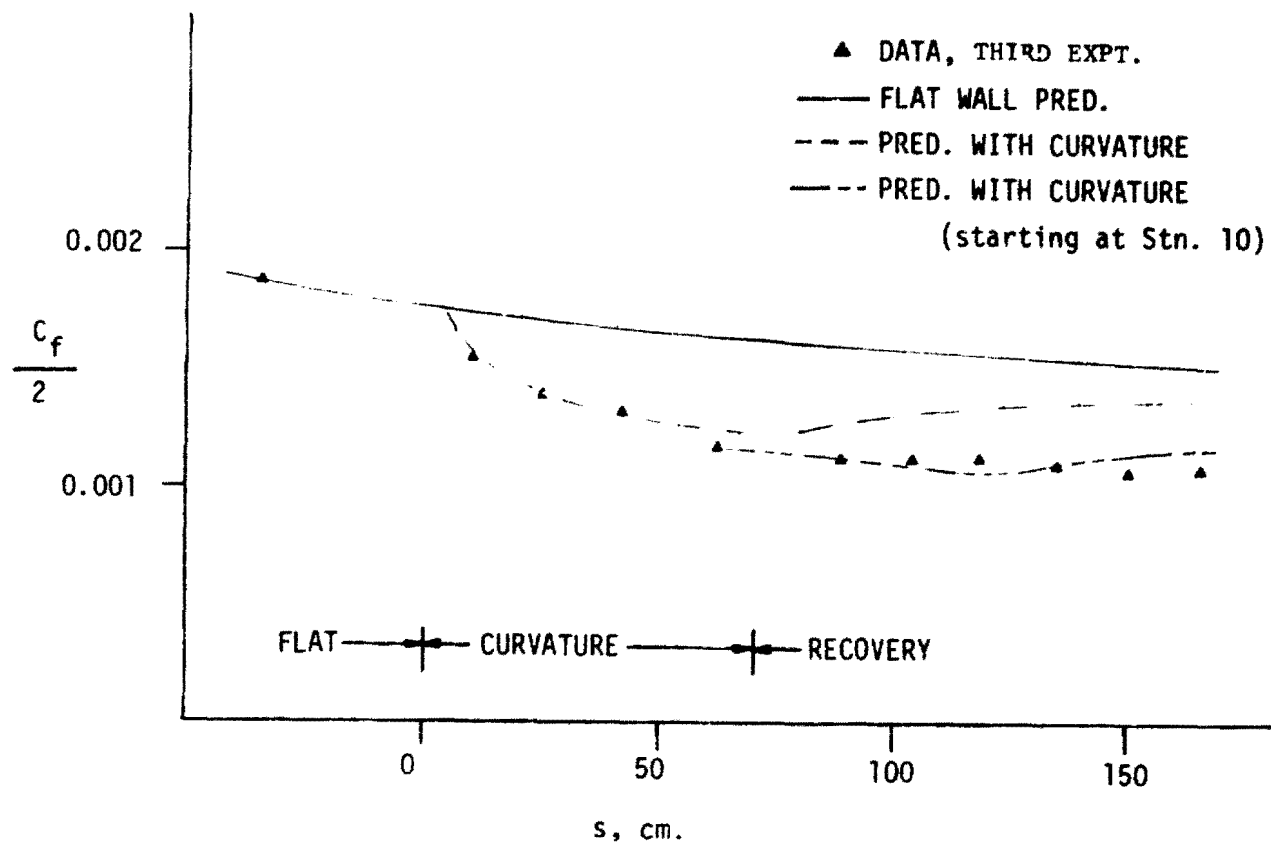
Fig. 65 Skin-friction distribution predicted by stability model
compared with data of third experiment
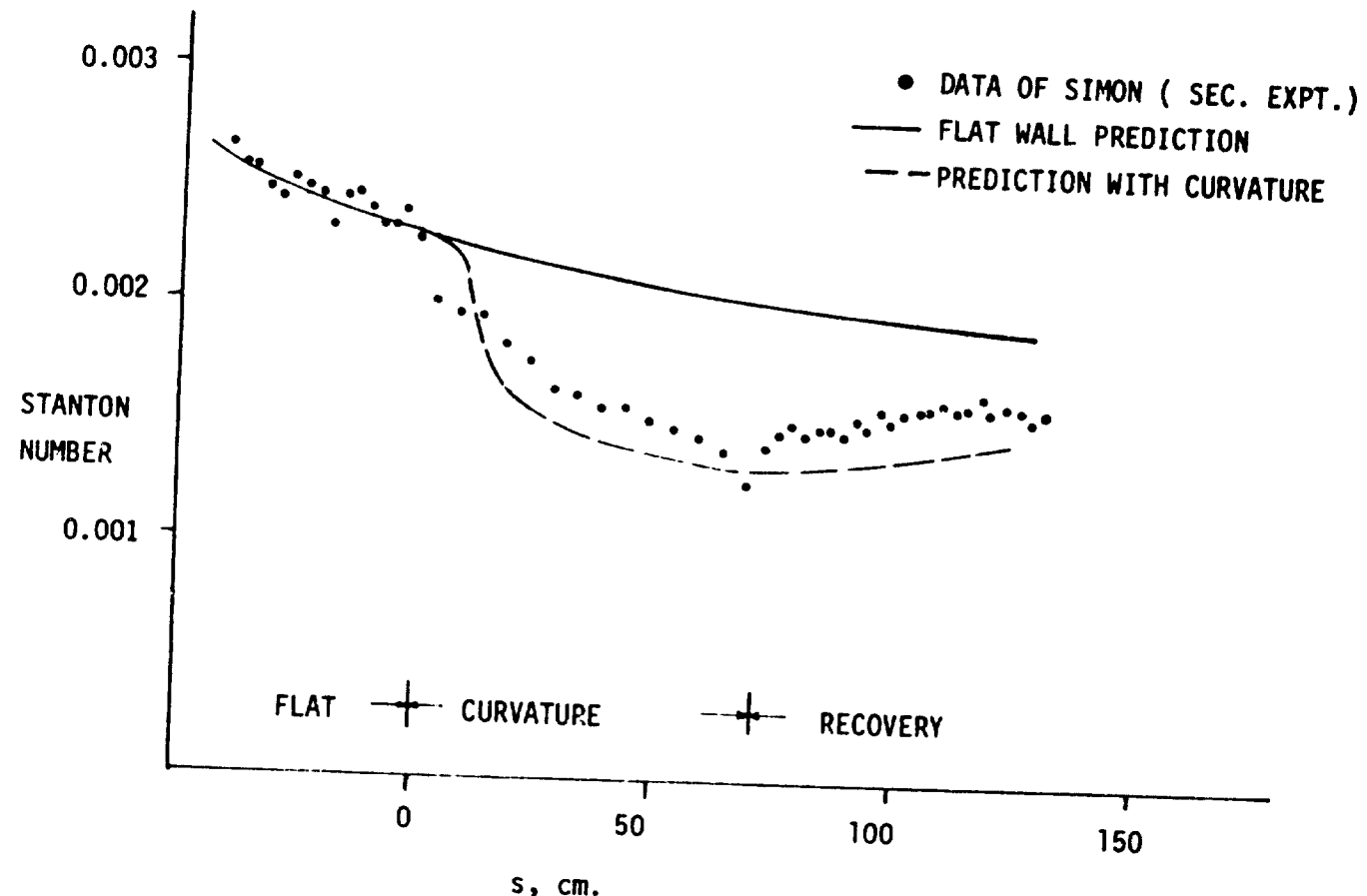
Fig. 66.   Stanton number predicted by stability model with flat-wall turbulent Prandtl number (Pr_t = .86) compared with data of second experiment

Chapter 5

CONCLUSIONS AND RECOMMENDATIONS FOR FURTHER RESEARCH

5.1 Conclusions

This project, like almost all work on turbulent boundary layers, has provided some insights, but it has also served to illustrate the complexity of the turbulence problem. The main conclusions are as follows.

1. The main effect of the introduction of surface curvature is a significant and immediate reduction in the turbulence-length scale (as measured by the mixing length). Once this length scale is reduced, it regrows ery slowly, even if the boundary layer is flowing over a flat surface downstream of significant curvature.

The reduction of eddy-length scale caused by the curvature, through the action of the normal pressure gradient $(\rho U^2/R)$, is accompanied by a collapse of the active shear-stress layer to a thickness less than the thickness δ of the velocity-gradient boundary layer. The width of the velocity-gradient boundary layer is mainly determined by flow upstream of curvature; the width of the active shear layer is chiefly determined by local conditions in the curved region. Once the shear-stress layer has collapsed, it can regrow only at the rate characteristic of a thinner developing boundary layer. This rate is slow enough to account for the slow redevelopment of the shear-stress layer, after curvature, on the flat recovery surface.

After compression of the shear-stress layer, the turbulence at large values of n/δ, beyond the shear-stress layer but within the velocity-gradient layer, is effectively isolated from the wall layers. It has little production and consequently dissipation causes decay of the turbulent energy.

2. Shear-stress profiles taken in the curved regions for our two different sets of initial conditions $(\delta/R = 0.05$ and $\delta/R = 0.10)$, and the data of So & Mellor (with different radius of curvature and free-stream velocity), collapse when $\overline{uv}/u_\tau^2$ is plotted vs. n/R. This behavior indicates that, after the compression of the turbulent shear-

114

stress layer, the large-scale eddies which carry the upstream history of the boundary layer are destroyed and the initial conditions no longer matter. The collapse of profile indicates that there may be an asymptotic shear-stress profile, at least for zero pressure-gradient flow over convex surfaces with δ/R greater than 1/20.

3. In the curved region, the law of the wall fits the data with the same constants used on the flat wall. The log region does not extend as far out in the boundary layer, ending near $y^+ = 100$. Calculation of the effective sublayer thickness shows A^+ is essentially unchanged by curvature. In addition, near the wall, the mixing length still scales a distance from the wall, as it does for no curvature. These observations indicate that the near-wall layers are not as strongly affected by the curvature as is the wake region.

4. It was found that, for this experiment, the outer layer mixing length scaled on the width of the shear-stress layer rather than on the velocity-gradient-layer thickness δ. This fact was used to construct a model of curvature effects which appears to enable one to predict the slow recovery from curvature.

5.2 Recommendations for Further Research

This program has answered some, but hardly all, questions about the effects of convex curvature. Several interesting experiments could be performed to further elucidate curvature effects. First, it would be instructive to see whether, in a tunnel like ours which turned more than 90°, the outer-layer turbulence does indeed decay away completely as the flow goes on in the curved region.

Another good area for investigation is the examination of curvature effects on boundary layers with very small values of δ/R. If the asymptotic state our data indicate does exist, then the shear-stress profile of a very thin boundary layer should grow out until it reaches that state. (In our cases, the profile contracted inward.) The data of Bradshaw and Hoffman indicate that, after a sudden change from flat to mild curvature, δ_{sl} slowly becomes a smaller and smaller fraction of δ as the layer moves downstream. However, the asymptotic limit is not approached, we believe, because the length of curved surface is too

short to allow the layer to get thick enough. It would be interesting to see a curved run long enough to approach the hypothesized asymptotic limit independent of initial conditions.

Finally, a better model for the onset of curvature effects is needed. We feel that such a model should adjust the shear-stress distribution when it is incompatible with the radius of curvature but stop adjusting when $(\delta_{sl}-\delta_{sl}^{*})$ is about ten times the outer-layer mixing length.

Still unanswered are questions about the combined effects of convex curvature with longitudinal pressure gradients, transpiration, or surface roughness. And beyond these is the whole area of concave curvature, which must be explored before the problem can be considered to be in hand.

References

1. Crawford, M. E., and W. M. Kays, "STAN5 -- A Program for Numerical Computation of Two-Dimensional Internal/External Boundary Layer Flow," Thermosciences Division Report HMT-23, Dept. of Mechanical Engrg., Stanford Univesity, Stanford, CA., Dec. 1975. Also NASA CR-2742 (1976).

2. Wilcken, H., "Effects of Curved Surfaces on Turbulent Boundary Layers," NASA TTF 11421, 1967.

3. Wendt, F., "Turbulent Strömungen zwischen zwei rotierenden honaxi-alen Zylindren," Ing.-Arch., Vol. 4, p. 577 (1933).

4. Wattendorf, F. L., "A Study of the Effect of Curvature on Fully Developed Turbulent Flow," Proc. Royal Soc., Vol. 148, 1935.

5. Schmidbauer, H., "Behavior of Turbulent Boundary Layers in Curved Convex Walls," NACA TM 791 (1936).

6. Kreith, F., "The Influence of Curvature on Heat Transfer to Incompressible Fluids," Trans. ASME, Nov. 1955.

7. Eskinazi, S., and H. Yeh, "An Investigation on Fully Developed Turbulent Flows in a Curved Channel," Jour. of Aero. Sciences, Vol. 23, No. 1 (1956).

8. Patel, V. C., "The Effects of Curvature on the Turbulent Boundary Layer," Aero. Research Council, ARC 30427, FM 3974, Aug. 1968.

9. Thomann, H., "Effect of Streamwise Wall Curvature on heat Transfer in a Turbulent Boundry Layer," JFM, Vol. 33, Part 2, 283-292 (1967).

10. So, R. M. C., and G. L. Mellor, "An Experimental Investigation of Turbulent Boundary Layers along Curved Surfaces," NASA-CR-1940 April 1972.

11. Bradshaw, P., "The Analogy between Streamline Curvature and Buoyancy in Turbulent Shear Flow," JFM, Vol. 36, 177-191 (1969).

12. Ellis, L. B., and P. N. Joubert, "Turbulent Shear Flow in a Curved Duct," JFM, Vol. 62, Part 1, 65-84, 1974.

13. Meroney, R. N., and P. Bradshaw, "Turbulent Boundary Layer Growth over a Longitudinally Curved Surface," AIAA Journal, Vol. B, No. 11 (1975).

14. Hoffmann, P. H., and P. Bradshaw, "Turbulent Boundary Layers on Surfaces of Mild Longitudinal Curvature," Imperial College, Aero. Rept. 78-04, Dec. 1978.

15. Castro, I. R., and P. Bradshaw, "The Turbulence Structure of a Highly Curved Mixing Layer," JFM, Vol. 81, Part 1, 155-185 (1977).

16. Ramaprian, B. S., and B. G. Shivaprashad, "Mean Flow Measurements in Turbulent Boundary Layers along Mildely Curved Surfaces," AIAA J., Vol. 15, No. 2 (1977).

17. Ramaprian, B. S., and B. G. Shivaprashad, "The Structure of Turbulent Boundary Layers along Mildly Curved Surfaces," JFM, Vol. 85, 273 (1978).

18. Mayle, R. E., M. F. Blair, and F. C. Kopper, Turbulent Boundary Layer Heat Transfer on Curved Surfaces," ASME J. of Heat Transfer, Vol. 101, No. 3 (1979).

19. Moffat, R. J., and W. M. Kays, "The Turbulent Boundary Layer over a Porous Plate: Experimental Heat Transfer with Uniform Blowing and Suction," Int. J. of Heat and Mass Transfer, Vol. 11, No. 11, 1547-1565 (1968).

20. Simon, T. W., and R. J. Moffat, "Heat Transfer through Turbulent Boundary Layers -- The Effects of Introduction of and Recovery from Convex Curvature," ASME 79-WA/GT-10 (1979).

21. Honami, S., private communication, 1980.

22. Tennekes, H., and J. L. Lumley, A First Course in Turbulence, The MIT Press, Cambridge, 1971.

23. Klebanoff, P. S., "Characteristics of Turbulence in a Boundary Layer with Zero Pressure Gradient," NACA Report 1247, 1955.

24. Bradshaw, P., "Effect of Streamline Curvature on Turbulent Flow," AGARDograph No. 169 (1973).

25. Reynolds, W. C., "Computation of Turbulent Flows," Annual Review of Fluid Mechanics, Vol. 8, 183-207 (1976).

26. Bradshaw, P., D. H. Ferris, and N. D. Atwell, JFM, Vol. 28, No. 593 (1967).

27. Smits, A. J., S. T. B. Young, and P. Bradshaw, "The Effects of Short Regions of High Surface Curvature on Turbulent Boundary Layers," JFM, Vol. 94, Part 2, 243-268 (1979).

28. Cebici, T., R. S. Hirsh and J. H. Whitelaw, "On the Calculation of Laminar and Turbulent Boundary Layers on Longitudinally Curved Surfaces," AIAA Journal, Vol. 17, No. 4 (1978).

29. Rastogi, A. K., and J. H. Whitelaw, "Procedure for Predicting the Influence of Longitudinal Surface Curvature on Boundary Layer Flow," ASME 71-WA/FE-37 (1971).

30. Johnston, J. P., and S. A. Eide, "Turbulent Boundary Layers in Centrifugal Compressor Blades: Prediction of the Effects of Surface Curvature and Rotation," J. of Fluids Engrg., 98(I), 374-381 (1976).

31. Launder, B. E., C. H. Priddin, and B. I. Sharma, "The Calculation of Turbulent Boundary Layers on Spinning and Curved Surfaces," ASME J. of Fluids Engrg., March 1977.

32. Irwin, H.P.A.H., and P. Arnot Smith, "Prediction of the Effect of Streamline Curvature on Turbulence," Physics of Fluids, Vol. 18, No. 6, June 1975.

33. Launder, B. E., G. J. Reese, and W. Rodi, "Progress in the Development of a Reynolds-Stress Turbulence Closure," JFM, Vol. 68, Part 3, 537-566 (1975).

34. Jones, W. P., and Launder, B. E., "The Calculation of Low Reynolds Number Phenomena with a Two-Equation Model of Turbulence," Int. Jour. of Heat and Mass transfer, Vol. 15, 301 (1972).

35. Gibson, M. M., W. P. Jones, and B. A. Younis, "Calculation of Turbulent Boundary Layers on Curved Surfaces," Mech. Engrg. Dept., Imperial College of Science and Tech., Report FS/80/6, Feb. 1980.

36. Gillis, J. C., and J. P. Johnston, "Experiments on the Turbulent Boundary Layer over Convex Walls, and Its Recovery to Flat-Wall Conditions," Selected Papers from the Second International Symposium on Turbulent Shear Flows, Springer-Verlag, 1980.

37. Kim, J., S. J. Kline, and J. P. Johnston, "Investigation of Separation and Reattachment of a Turbulent Shear Layer: Flow over a Backward-Facing Step," Stanford University Dept. of Mech. Engrg., Thermosciences Div., Report MD-37, April 1978.

38. Gibson, M. M., "An Algebraic Stress and Heat-Flux Model for Turbulent Shear Flow with Streamline Curvature," Int. Jour. of Heat and Mass Transfer, Vol. 21, 1609-1617 (1978).

39. Launder, B. E., private communication, 1977.

40. Sabersky, R., A. J. Acosta, and E. G. Hauptmann, Fluid Flow, The Macmillan Co., New York, 1971.

41. Young, A. D., and J. N. Maas, "The Behavior of a Pitot Tube in a Transverse Total-Pressure Gradient," Rep. Memo No. 1770, Aero Res. Council, London (1936).

42. Coles, Donald, "The Young Person's Guide to the Data," Proc. of the 1968 AFOSR-IFP-Stanford Conference, Vol. II, 1-19, 1968.

43. Jørgensen, F. E., "Directional Sensitivity of Wire and Fiber-Film Probes," DISA Information No. 11, May 1971.

44. Anderson, P. S., W. M. Kays, and R. J. Moffat, "The Turbulent Boundary Layer on a Porous Plate: An Experimental Study of the Fluid Mechanics for Adverse Free-Stream Pressure Gradients," Stanford University, Dept. of Mech. Engrg., Thermosciences Div., Report HMT-15, 1972.

45. Hussein, A.K.M.F., and W. C. Reynolds, "The Mechanics of a Perturbation Wave in Turbulent Shear Flow," Report FM-6, Mech. Engrg. Dept., Stanford University, 1970.

46. Taslim, M. E., S. J. Kline, and R. J. Moffat, "Calibration of Hot-Wires and Hot-Films for Velocity Fluctuations," Report TMC-4, Mech. Engrg. Dept., Stanford University (1978).

47. Reynolds, W. C., Solution of Partial Differential Equatins, Dept. of Mech. Engrg., Stanford University, 1978.

Appendix A

THE EFFECT OF SECONDARY FLOW

Any experimenter who studies two-dimensional boundary layer flow on convex surface in a test section of rectangular geometry will have to face the problem of secondary flow. The direction of these flows is shown in Fig. A-1. The sidewalls of the wind tunnel are covered by low-momentum boundarty layer fluid which reacts to the radial pressure gradient created by the curvature. As a result, the side wall boundary layer fluid flows down the sidewall toward the convex surface. When it reaches the surface, it makes a right-angle bend and flows onto the convex surface. Eventually, the secondary flows from the two sidewalls meet on the tunnel centerline. Thus the flow in the test surface boundary layer--off the centerline--flows at an angle toward the centerline. On the centerline, however, the flow is straight, but the boundary layer growth is faster than in the same flow if there were no convergence. There is no way to avoid this problem completely, since it is the radial pressure gradient which both causes the flow to follow the convex surface and also drives the secondary flow down the side walls.

There are a number of devices which one may use to minimize the influence of secondary flows. The most successful trick is to use a tunnel with a large aspect ratio. If the convex surface is twenty or more times as wide as the sidewalls are high, the influence of the secondary flows near the centerline will be small. In the current experiment, the aspect ratio was dictated, at the start, by the flat tunnel upstream of the curve; it was about 3:1. Other experimenters with low aspect ratio tunnels have used various schemes to straighten the flow. Patel [8] used false walls which made the effective sidewall boundary layers thinner, and so reduced the amount of low-momentum fluid subject to the radial pressure gradient. There has been some question about the effectiveness of this technique [24]. So & Mellor [10], in an experiment much like this one, fired jets upwards into the sidewall boundary layer. Mayle [18] used side-wall slots to intercept the secondary flows. Launder [39] used boundary layer fences.

121

We tried several schemes before settling on a layout which used a combination of false walls, fences, and slots. We believe that this combination preserved the flow's two-dimensionality in our test section. In succeeding sections, some of the early experiments with less successful schemes are discussed as background for the presentation of the final results.

Preliminary Data

Before beginning our work on the secondary flows, we made a quick check of the spanwise uniformity of the upstream tunnel by using a Preston tube to measure the skin friction. Results are shown in Fig. A-2. These measurements indicate good spanwise uniformity in the flow upstream of curvature.

For our first attempt, following Patel's scheme to reduce the secondary flows, we narrowed the test channel width at the start of curvature and blew the sidewall boundary layers out of the tunnel (see Fig. A-2). The boundary layers which established themselves on the new sidewalls downstream were then much thinner than the boundary layers on the sidewalls upstream of curvature. We also opened slots in the side walls, as shown below in Fig. A-3. In theory, these slots would intercept the secondary flows as they came down the sidewalls, and blow them out.

The sidewall slots were adjusted as follows. First, the slot was opened fully (about .63 cm), and then a tuft was positioned inside the tunnel, just below the slot. In theory the slot should intercept and blow out only the secondary flow coming down the sidewall from above the slot and not "lift" any fluid from the boundary layer beneath the slot. The slot opening was then narrowed until the tuft below the slot was parallel to the surface. This method generated settings which were repeatable to about ± .25 mm.

The effectiveness of these techniques could be gauged in several ways. With the slots closed (but upstream boundary layers blown out at the start of curvature), the secondary flows were so strong that, near the sidewalls, tufts showed a flow skew angle of up to 30°. When the slot openings were adjusted as described above, the skew angles were

122

small enough that tufts were not reliable indicators. All further measurements of skew angles were made with the Conrad probe described in Appendix E. The Conrad probe gave a good measure of the magnitude of the flow angles, but, to our surprise, we found that the spanwise distribution of integral parameters (δ, δ_1, δ_2) was also an extremely sensitive indicator of the presence of secondary flows. In fact, the spanwise distribution of δ_1 and δ_2 became our final criterion of two-dimensionality. Figs. A-5 and A-6 show flow skew angles at Station 4 (A-5) and Station 9 (A-6) measured after the slots were adjusted. The skew angles at $\pm$ 13 cm are larger near the wall and reach a maximum of seven degrees. Nearer the centerline, the flow is straighter, and the flow on the centerline is straight to within experimental accuracy. In spite of the smallness of the angles, there was significant variation of the spanwise integral properties. Fig. A-7 shows three spanwise profiles of momentum thickness taken at Stations 4, 6, and 9. the influence of the secondary flows (which thickens the boundary layer at a rate which increases off the centerline) is clear.

Lest the reader be led to believe the problem was worse than it was, it must be pointed out that the vertical scale is 50 times the horizontal scale. In fact, at the second downstream (worst) station the variation in δ divided by the channel width is only about 2%. In view of the spanwise difference in integral quantities, it was decided to try other schemes.

We finally decided that further reductions of the effects might be obtained with a boundary layer fence such as the one used by Launder. In the end, three configurations were tried, these are shown in Fig. A-8. We used flow angle measurements to test the effectiveness of these schemes -- no velocity profiles were taken.

For the first experiment with fences, we used the configuration shown in Fig. A-8a, with fences mounted horizontally on the sidewalls, at the same height as the slots. This scheme produced flow angles on the test surface of about the same magnitude as the slots. Upon reflection, we decided that this was due to the position of the fences on the sidewall. We speculated that both the sidewall slots and the fences used by themselves were doing an effective job of stopping the secondary

123

flow coming down the side wall from above, but that our problem was coming from side-wall secondary flow generated below the slots and fences. The slots and fences were located 3.8 cm above the tunnel flow. Since the tunnel was 42 cm wide, this meant that the effective aspect ratio which they created (AR = 6:1) was apparently not sufficiently large. To increase the effective aspect ratio, we lowered the slots one inch on the sidewalls, as shown in Fig. A-8b. This arrangement, however, did not greatly improve things. Finally, we tried mounting low fences on the tunnel floor. This increased the effective aspect ratio to 11:1. At first, this did not prove to be any more effective than any of the other configurations. However, a survey of spanwise static pressure showed that, while the static pressure was very uniform, the static pressure between the fences and the sidewalls was $0.10 \times \rho U_{pw}^2/2$ higher than the centerline wall static. This was interpreted to mean that the secondary flows were in fact stagnating in the regions close to the side walls. We also discovered that if a trip on a barrier was placed just downstream and parallel to the leading edge of the fence, the flow angles were greatly affected. Finally, we decided that there was a small leading edge separation bubble on the fence and that this was thickening the fence boundary layer, as shown on the left, below, in Fig. A-9a.

To avoid this separation bubble, we opened the first sidewall slot, which was just above the fence leading edge. This changed the direction of the flow just upstream of the leading edge and moved the separation bubble to the other side (see Fig. A-9b). This action reduced the flow angles measured 12.7 cm off the centerline by a factor of two.

Final Data

Figures A-10 and A-11 show flow angles measured at Stations 4 and 9, with the last configuration described above. Although near the centerline the flow angles are not much affected, the angles at z = 12.7 cm are much less than with any other flow-control configuration. A complete survey of flow angles was taken and appears in the tabulated data. The worst flow angles were at Station 8, and were about the same as those plotted for Station 9.

124

Figure A-10 is a plot of the spanwise distribution of momentum thickness, which is much more uniform than obtained with the sidewall slots alone. There were no measurements taken at ± 12.7 cm because the boundary layers on the fences distorted the velocity profiles there.

Finally, Figs. A-13 and A-14 show the variation of centerline integral properties in the streamwise direction measured with slots only (A-13) and with fences (A-14). There is little difference between the two plots, leading us to believe that the secondary flows had been reduced to an acceptable level.

HIGH PRESSURE

LOW PRESSURE
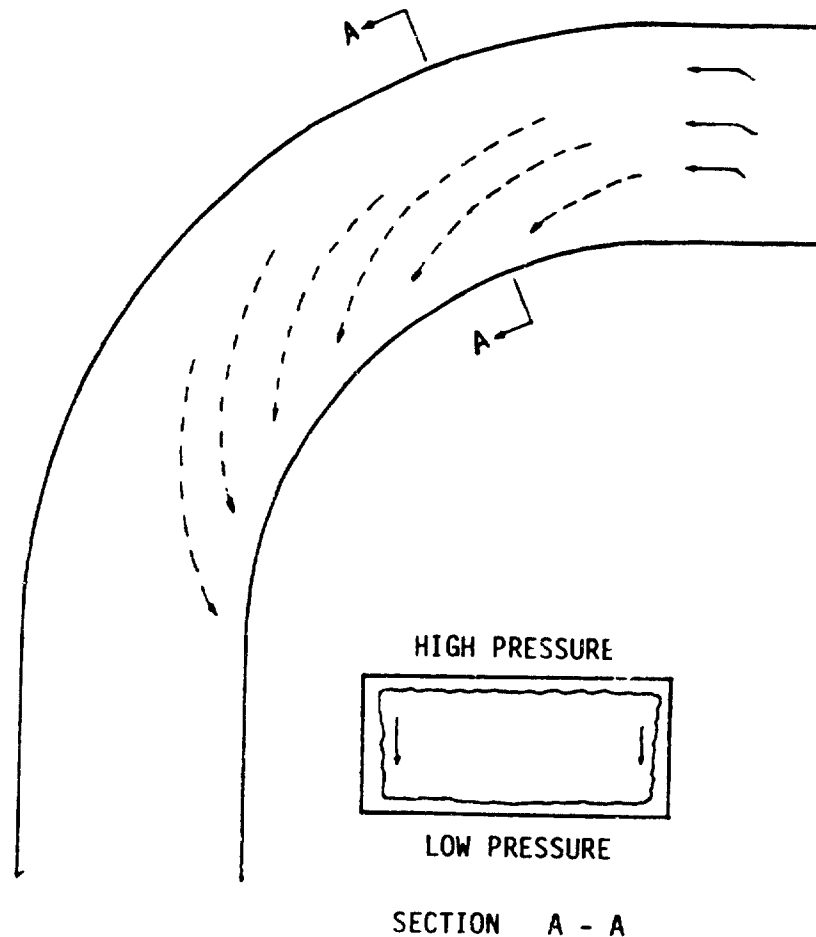
SECTION   A - A

Fig. A-1.   Secondary flows on side walls of curved section
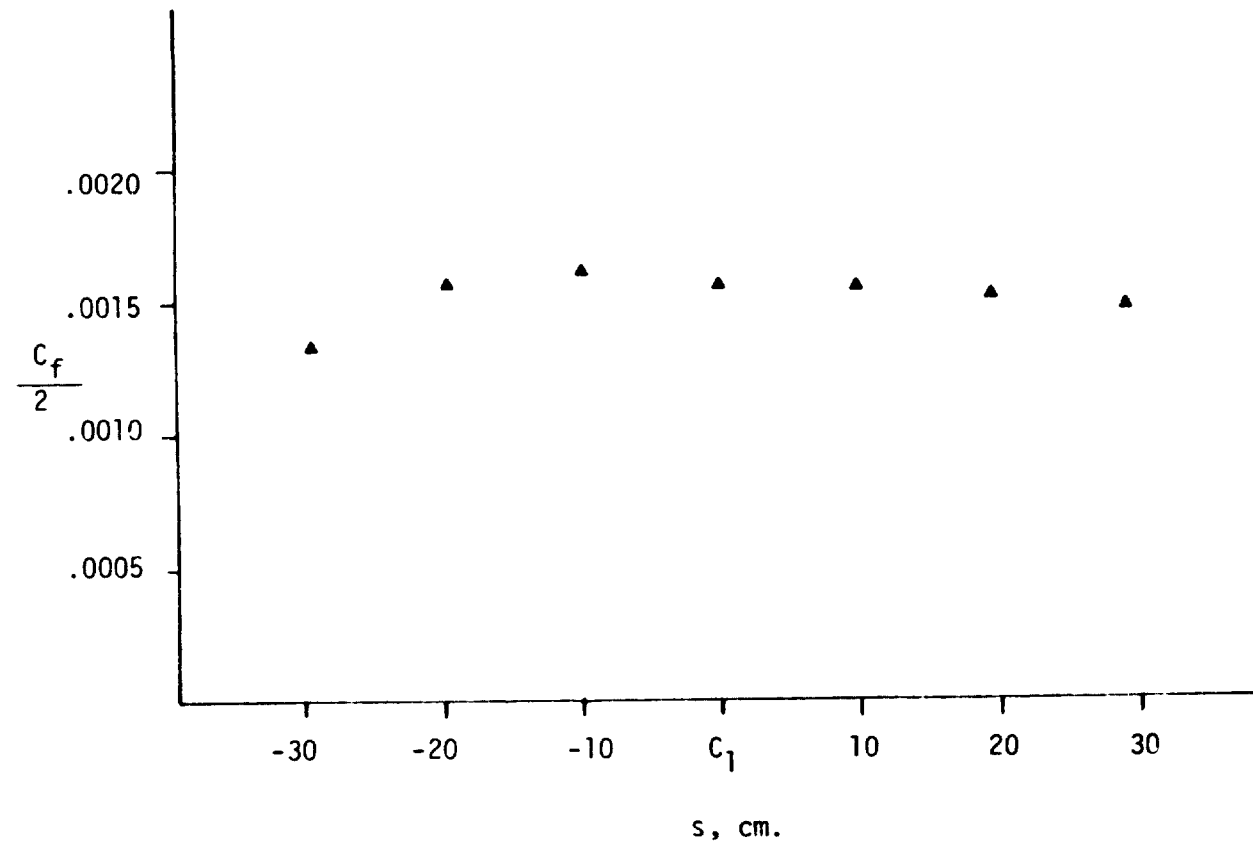
Fig. A-2   Spanwise skin friction measured upstream of curvature with Preston tube

START OF
CURVATURE

FLOW

SPLITTER PLATE

SIDE WALL BOUNDARY LAYER
EXITS TO ATMOSPHERE
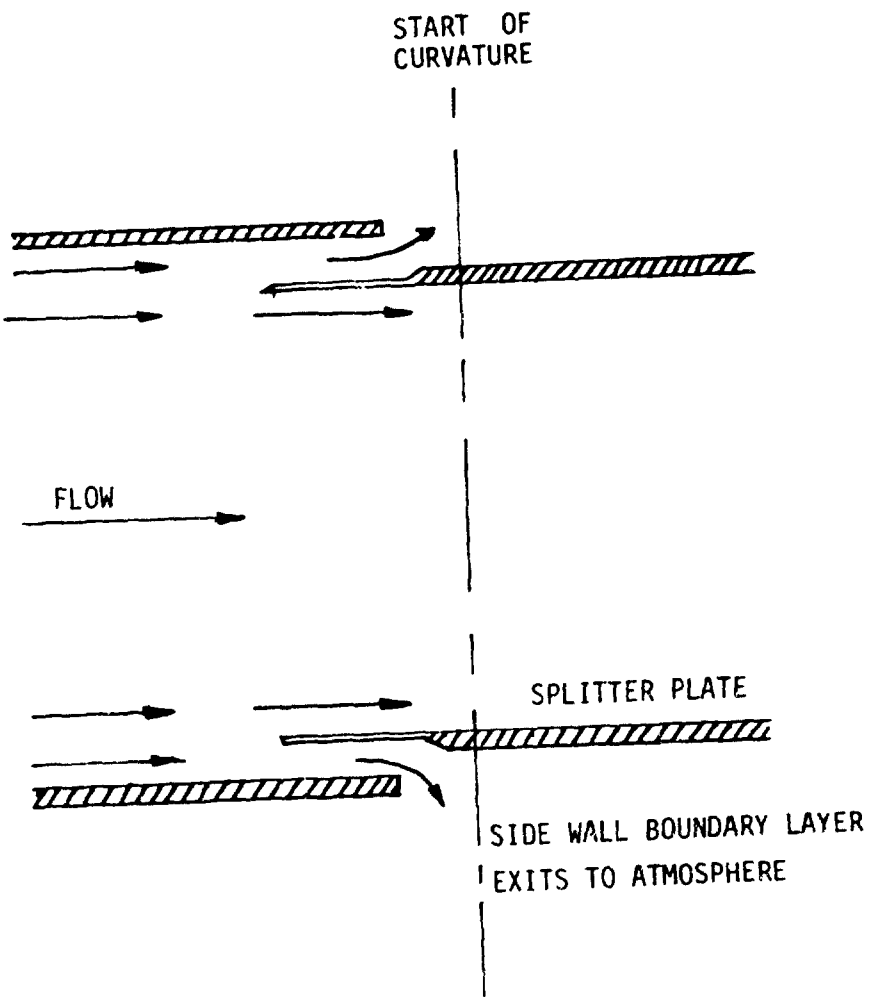
Fig. A-3.   Arrangement to skim upstream boundary layers

SKIM OFF
UPSTREAM
B. LAYERS

SLOTS IN
SIDE WALLS
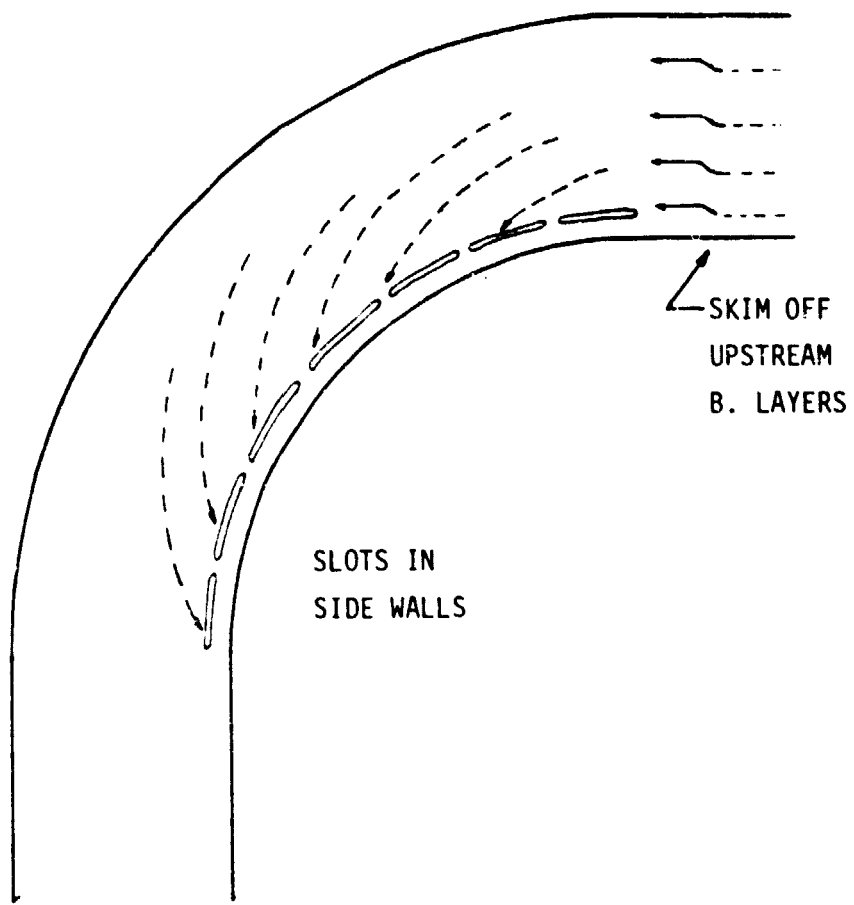
Fig. A-4.   Side-wall slot arrangement to control secondary flows on
first experiment

129
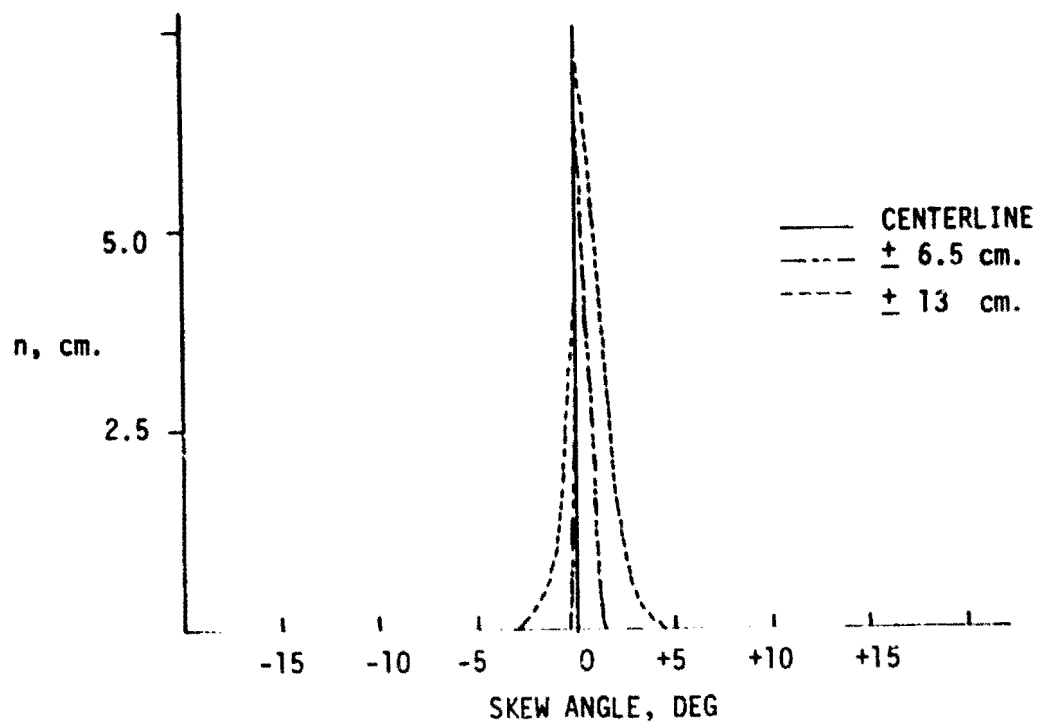
Fig. A-5. Skew-angle profiles at Station 4 (after 20° of turning), with side-wall slots
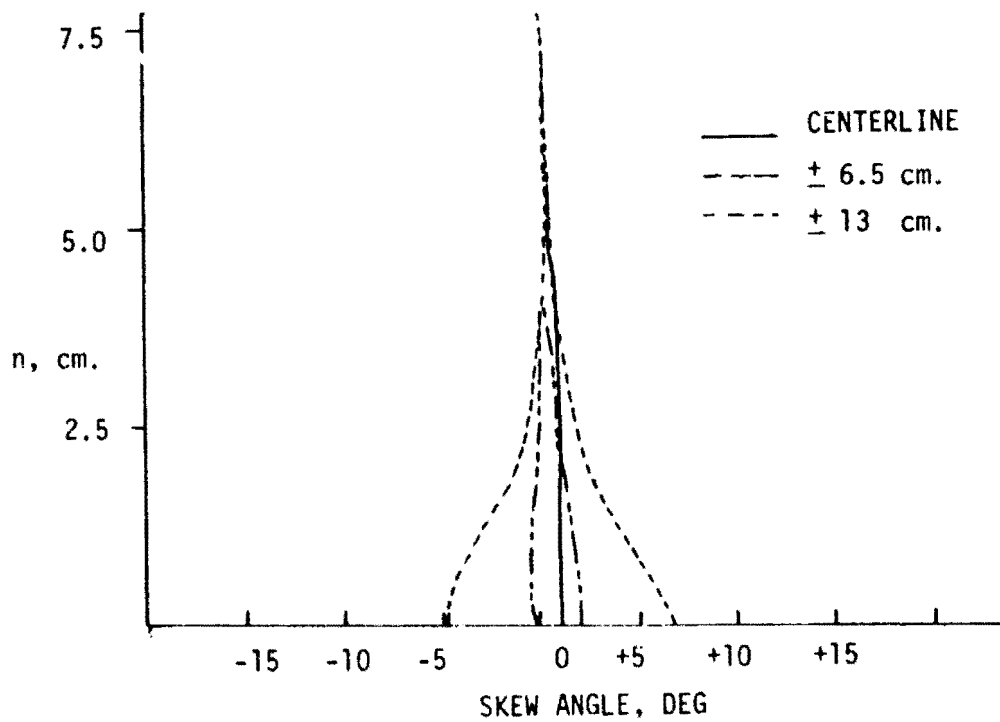
Fig. A-6. Skew-angle profiles at Station 9 (in recovery region) with side-wall slots

131
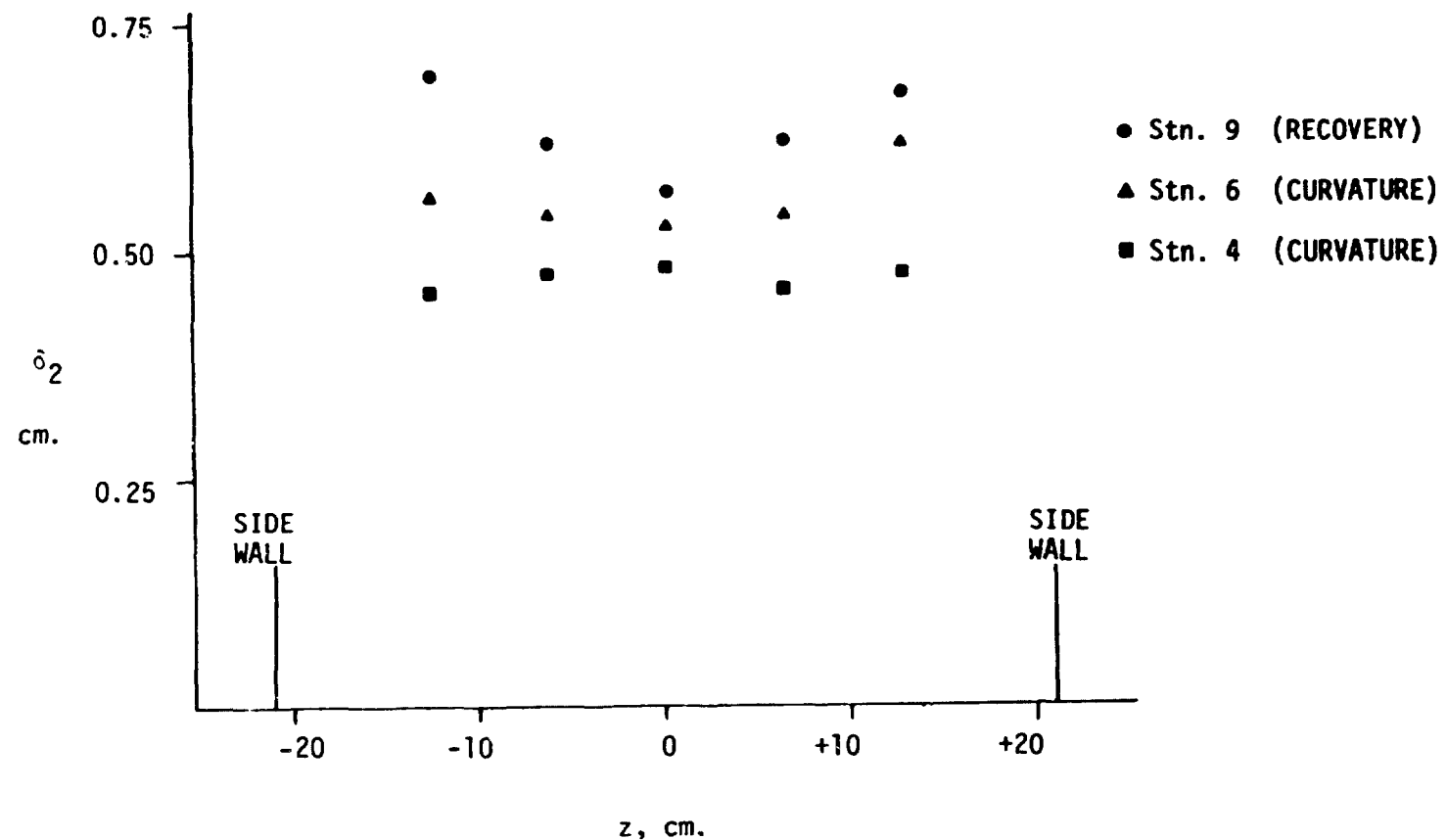
Fig. A-7. Spanwise distribution of momentum thickness at three stations;
data taken using side-wall slots to control secondary flows
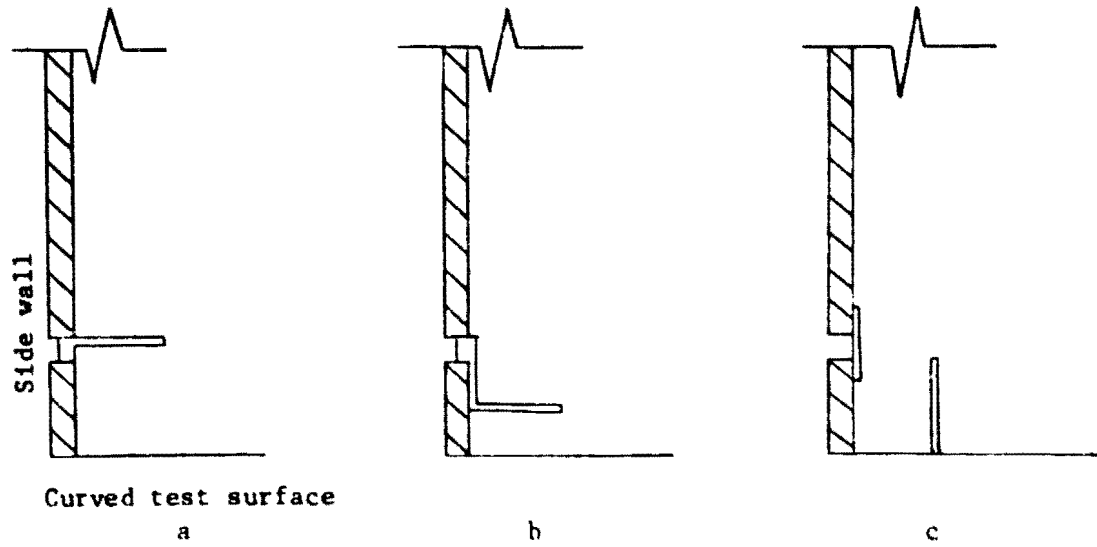
Fig. A-8 Arrangment of Fences
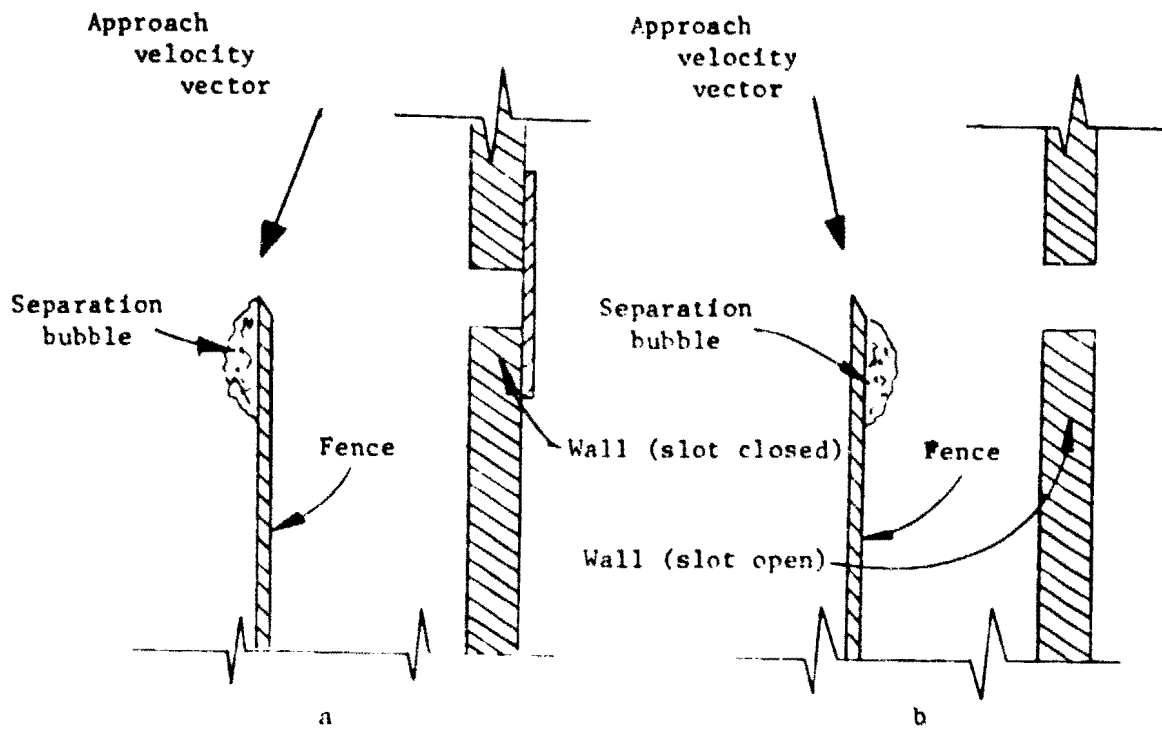
Fig. A-9. Separation bubble on fence leading edge

132
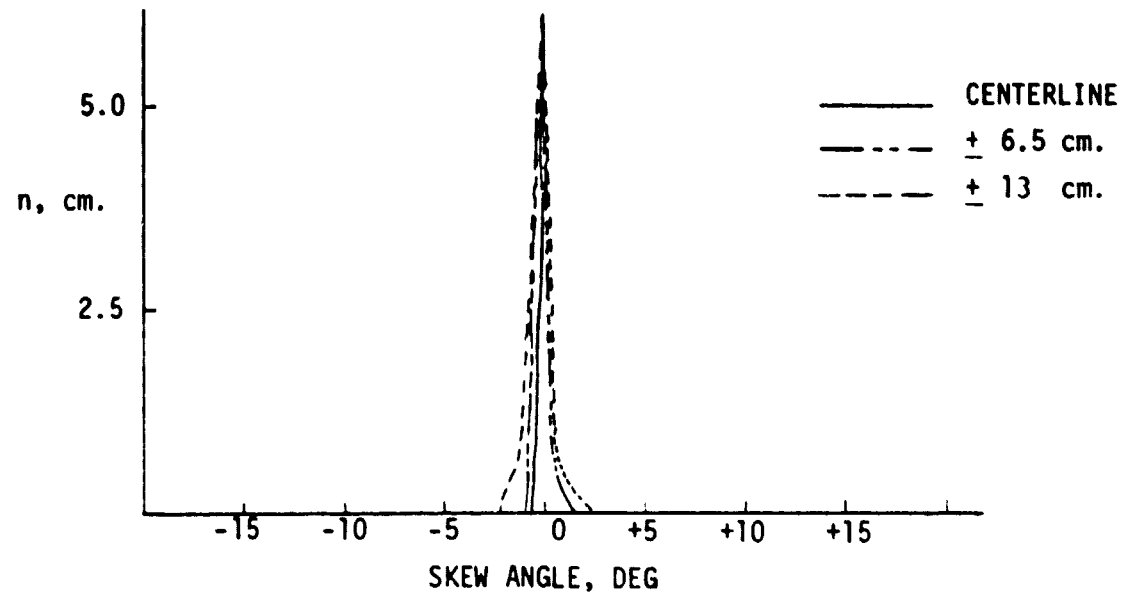
Fig. A-10. Skew-angle profiles for Station 4 (after 40° of curvature), with fences
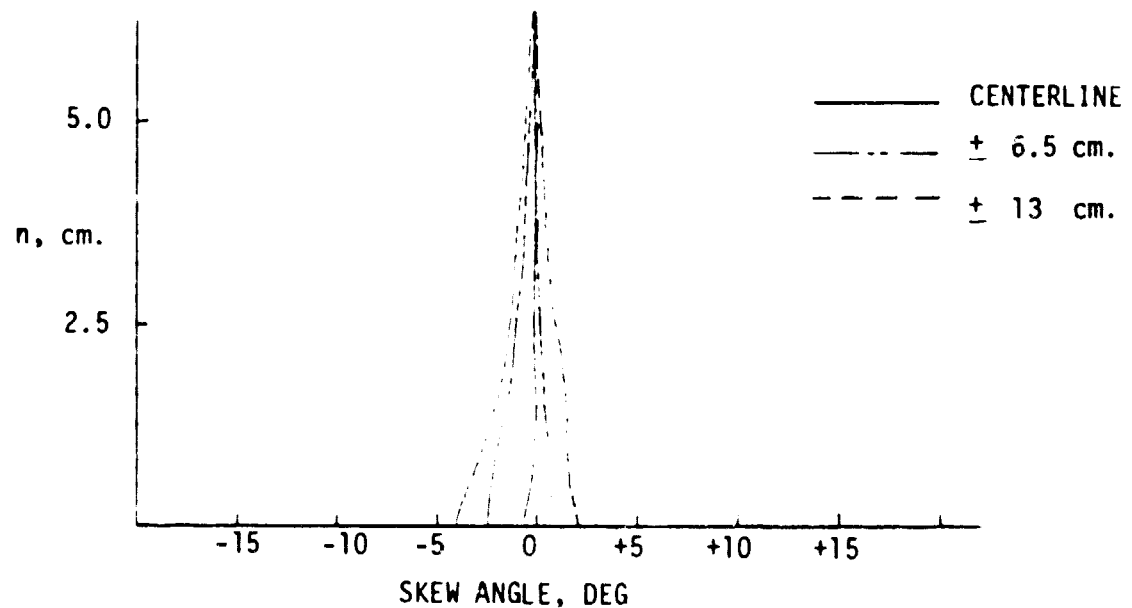
Fig. A-11. Skew-angle profiles for Station 9 (in recovery region), with fences

133
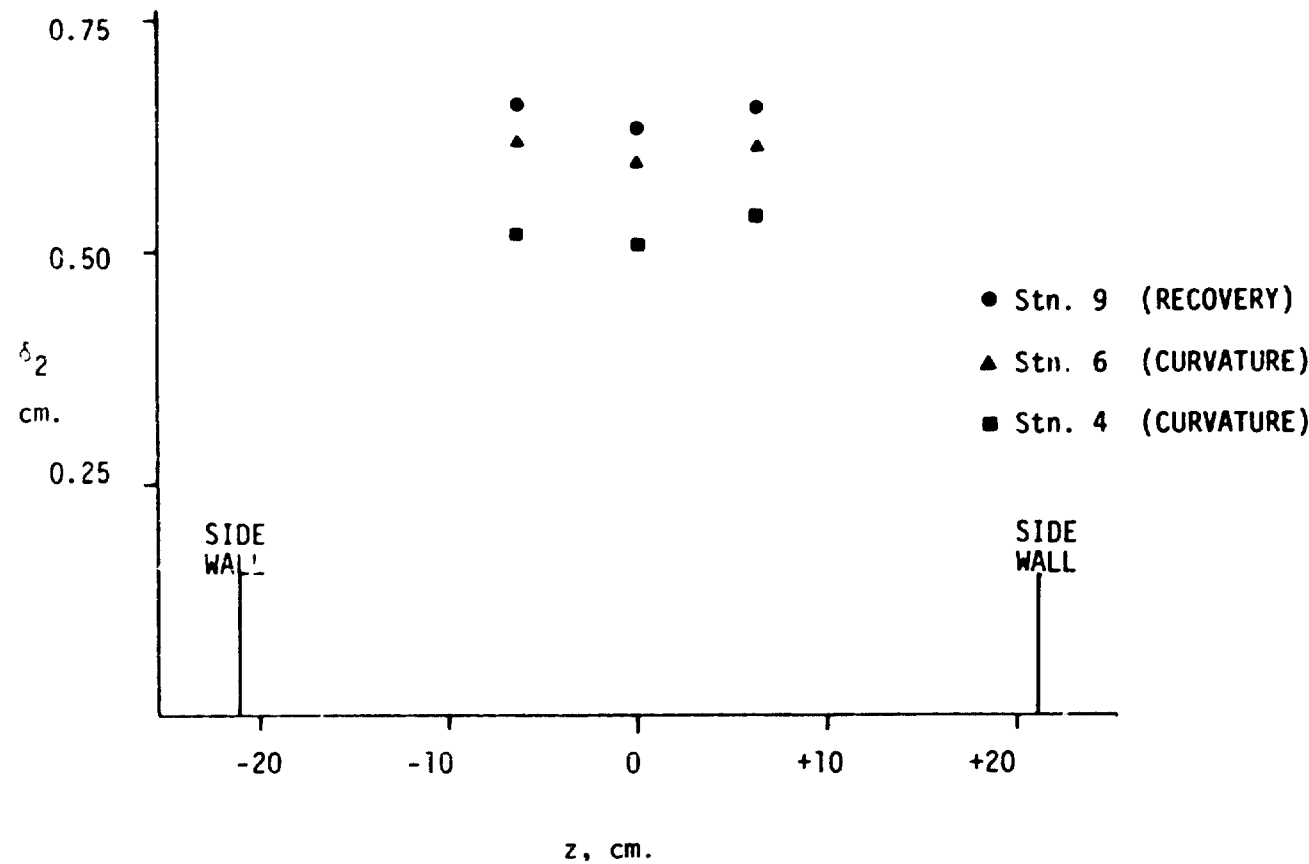
Fig. A-12. Spanwise distribution of momentum thickness with fences
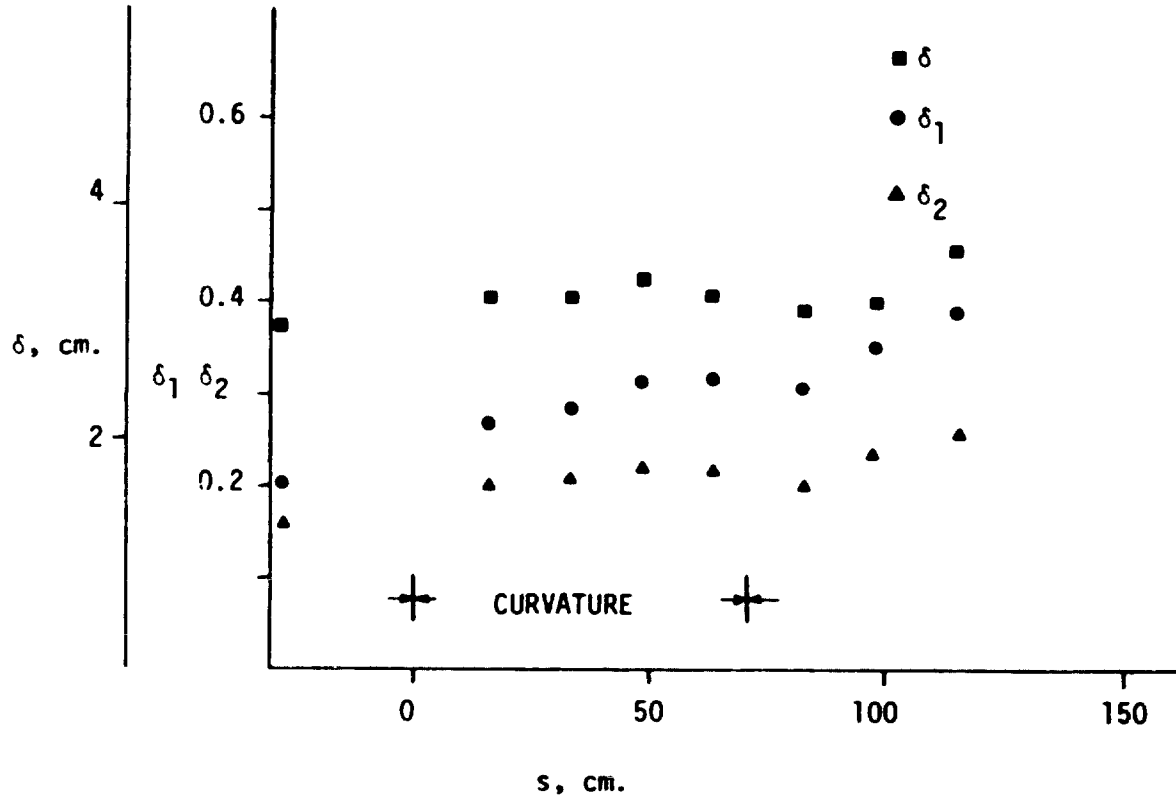
Fig. A-13. Streamwise distribution of momentum thickness with slots
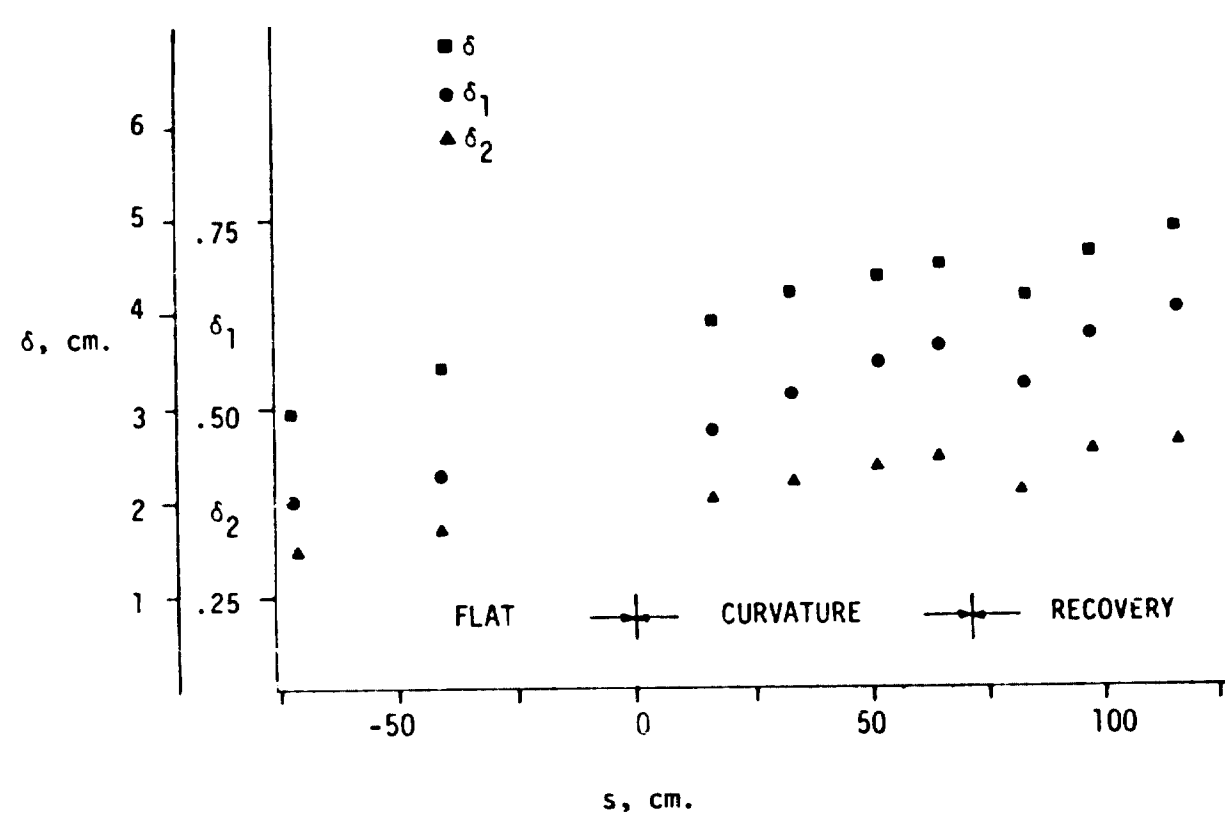
Fig. A-14. Streamwise distribution of momentum thickness with fences

136

Appendix B

MEASUREMENT OF DYNAMIC PRESSURE ON A CURVED WALL

On a flat wall, measurement of dynamic pressure is straightforward. The total pressure is obtained from a total head tube, and the static pressure, which is normally independent of y and z, is measured on a wall at the same x location.

For flow over a curved surface, the problem is more complicated because the static pressure is a function of n, the coordinate normal to the curved surface. In our experiment, we chose to measure the static pressure at the curved surface and then to calculate the static pressure at the n location, where the total head tube was measuring the total pressure (see Fig. B-1).
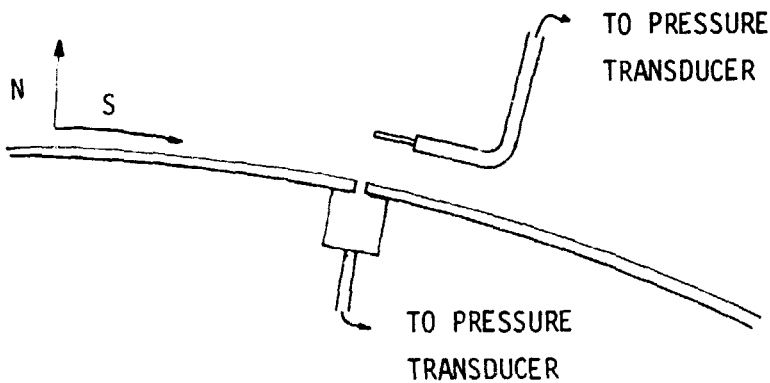
Fig. B-1. Measurement of Wall Static and Total Pressure
in Boundary Layer

To calculate the difference in static pressure between the wall and the measuring station, we first invoke the boundary layer assumption that the static pressure field is imposed by the potential core. For parallel flow,[*] this is

$$\frac{\partial P_s}{\partial n} = \rho \frac{U_p^2(n)}{R(n)} \qquad (B-1)$$

---

[*]Note the assumption of parallel flow is a good approximation in curved boundary layer flows.

137

where P_s is static pressure, ρ is density, R is the local radius of curvature $(R_o + n)$, and U_p is the inviscid velocity. The distribution of U_p is obtained from the irrotationality condition in cylindrical coordinates (see Ref. 39, p. 191).

$$\omega_z = 0 = \frac{1}{R} \frac{\partial (RU_p)}{\partial R} - \frac{1}{R} \frac{\partial (V_p)}{\partial \theta} \tag{B-2}$$

Since V_p is assumed to be zero, Eqn. (B-2) reduces to

$$d(RU_p) = 0 \tag{B-3}$$

This integrates to

$$U_p(n) = \frac{R_o}{R_o + n} U_{pw} \tag{B-4}$$

where U_{pw} is the potential flow velocity at the wall and R_o is the wall radius. With the distribution of U_p in hand, we can substitute into (B-1) and integrate. This gives

$$P_s - P_{sw} = -\frac{\rho U_{pw}^2}{2} \left[1 - \frac{1}{1 + (n/R_o)^2} \right] \tag{B-5}$$

The above equation is not convenient for data reduction because U_{pw} cannot be easily determined. It is a fictitious quantity. To eliminate it, we used another equation derived from considering the reading of a reference pitot tube outside the boundary layer. Designating the reading of this pitot probe as P_r,

$$P_r - P_{sw} = \rho \frac{U_{pw}^2}{2} \tag{B-6}$$

Combining Eqns. (B-6) and (B-5) to eliminate U_{pw}, we have

$$P_s - P_{sw} = (P_{sw} - P_r) \left[1 - \frac{1}{1 + (n/R_o)^2} \right] \tag{B-7}$$

Now, the velocity at the measurement point is

$$U(n) = \frac{2}{\rho} \left[P_t - P_s(n) \right]^{1/2} \tag{B-8}$$

138

By using (B-7), we can finally get U in terms of measurable pressures:

$$U(n) = \sqrt{\frac{2}{\rho}} \left\{ (P_t - P_{sw}) - (P_r - P_{sw}) \left[1 - \frac{1}{(1 + n/R_o)^2} \right] \right\}^{1/2} \quad \text{(B-9)}$$

The reader will doubtless notice that a third pressure, P_r, which is the total pressure in the potential core (not a function of n or s or z) appears. In practice, the pressure difference $(P_r - P_{sw})$ was measured at the start of a profile and at the end. In general, the drift was on the order of 1%. This drift was corrected for in the data-reduction program by using a linearly interpolated value of $(P_r - P_{sw})$. The final confirmation of the whole procedure was the agreement of pitot probe and hot-wire velocity profiles.

Appendix C

DATA-REDUCTION PROGRAMS

This appendix is included to show how the raw data were processed. There are four programs: VELPRO, which deduces mean properties from pitot probe data, SHETWO, which reduces data taken with an x-wire array, MIXLN, which uses an input mean velocity profile and shear stress profile to calculate mean velocity gradients, mixing lengths, and other values; and HWIRE, which reduces horizontal wire data. The programs are described and listed in the dissertation by J. C. Gillis, "Turbulent Boundary Layer on a Convex, Curved Surface," Mechanical Engineering Department, Stanford University, June, 1980.

VELPRO

This program, was written to be as easy to use as possible. It is designed to accept pitot probe data for a flow of air in common English engineering units (dynamic pressure in inches of H_2O and distance from the wall in inches) and to yield mean velocities, all integral thicknesses, the inner coordinates (u^+, y^+), and the skin friction. It is designed to reduce both curved-wall and flat-wall data -- a fact that may make the coding hard for those used to flat walls to interpret. In the output, samples of which are shown in Appendix F, the only difference is the column labeled U/U_p. On a flat wall this would be called U/U_∞ or U/U_{edge}.

The program has a number of subsections which help to avoid inaccuracies. First, the flow temperature ($°F$) and atmospheric pressure (in. Hg) are used to calculate an exact density from the perfect gas law, and the viscosity of air at the temperature of the flow is calculated by linearly interpolating data from Keenen & Kay. Another refinement is the use of a variable value of U_∞ (U_{pw} on a curved wall). The program asks for the freestream dynamic pressure at the time the first data point is taken and at the time the last point is taken, and then interpolates the free-stream pressure for each point.

It has been found that the "effective" position of a pitot probe in a flow with a velocity gradient is slightly different from its geometric

140

center. The program calculates the "effective" distance from the wall (this appears in the output as YCAL) using the correlation developed at MIT by Young and Maas [41]. The "effective" y value is used in calculation of the integral parameters.

The program avoids problems caused by thin boundary layers. If the boundary layer being measured is less than about one-half inch thick, a standard diameter pitot probe (.020 in. or more outside diameter) cannot get data close enough to the wall to calculate accurate integral parameters. The program identifies this problem automatically and treats it in the following way. First, the skin friction is calculated and, from it, the inner coordinates u^+ and y^+. If the lowest value of y^+ is thirty or more, the boundary layer is probably too thin to determine δ_1 and δ_2 accurately. The program then uses the following near-wall integrals first proposed by Coles [42]:

$$\int_0^{50} \frac{U}{u_\tau} \, d\left(\frac{yu_\tau}{\nu}\right) = 540.6$$

$$\int_0^{50} \left(\frac{U}{u_\tau}\right)^2 \, d\left(\frac{yu_\tau}{\nu}\right) = 6546$$

up to the data point nearest $y^+ = 50$, and the trapezoid rule from then on. If the first data point is found to have a y^+ value of less than thirty, the program uses the trapezoid rule all the way from the wall to the freestream.

The skin friction is determined by assuming that the law of the wall holds. With the exception of the Stanton tube, every generally used method of determining skin friction from a mean velocity profile (Preston tube, Clauser plots) uses this assumption. The program uses an iterative procedure which goes as follows. First, at every point in the profile, a value of the friction velocity is calculated by assuming the law of the wall holds. This is done by rewriting the law of the wall as:

$$u_\tau = \frac{U(y)}{\frac{1}{.41} \ln\left(\frac{yu_\tau}{\nu}\right) + 5.0}$$

141

Since the RHS is only weakly dependent on u_τ, a guess (usually u_τ = 2 ft/sec) combined with the measured values of y and $U(y)$ will yield a good approximation to u_τ. Inserting this approximation in the RHS and recomputing will yield a better approximation, and so on to closure. The program quits when successive values of u_τ differ by less than .001 ft/sec. The program then uses u_τ to figure a $C_f/2$ for that y value. This iterative calculation is then repeated at the next larger y. At that point the program has generated a profile of $C_f/2$. Now, if the law of the wall really does hold over some range in y, then over that range the values of $C_f/2$ calculated above ought to be the same. Over a flat, smooth wall, this range is approximately $y^+ = 30$ to $y^+ = 225$ (for a curved wall it is less, approximately $y^+ = 25$ to $y^+ = 90$). The program uses the "profile" of approximate $C_f/2$ to calculate a y^+ value for each y value. It then locates the range of $y^+ = 30$ to $y^+ = 225$ (on a flat wall -- for curved walls the range used is 30 to 90), and then averages the values of $C_f/2$ in this range. This value is then taken as the actual value of $C_f/2$, and the u^+, y^+ values are then recomputed in the normal manner. The values of $C_f/2$ used in the averaging process are then checked for scatter. If any of the averaged $C_f/2$ values are more than 2% different from the average, the program prints out a message -- LARGE SCATTER IN COMPUTED $C_f/2$ VALUES. The program also prints out the $C_f/2$ profile. Output should always be checked to make sure that the log zone has been properly identified and that the average value (printed out next to the momentum thickness Reynolds number) is reasonable. Also, if factors such as roughness or very strong pressure gradients move the log zone, new y^+ values for the estimated log zone should be put in the program. The present program could be improved in its procedure for determination of the log zone. With some effort, a section could be designed to search the $C_f/2$ profile to find the region where it is constant, without any reference to the inner coordinates.

The input nomenclature is shown in Table C-1.

142

Table C-1

Input Nomenclature for VELPRO Quantities
Listed in the Order They Are Read

Input Data	Name in Code	Units
Number of profiles to be reduced	NDS	---
Title -- any title of up to 72 characters	TITLE(I)	---
No. of points in profile	N	---
Flow temperature	TEMP	$°F$
Atmospheric pressure	ATP	in.-Hg
Free-stream dynamic pressure at time of first point	POB	in.-H_2O
Free-stream dynamic pressure at time of last point	POE	in.-H_2O
Outside diameter of pitot probe	OD	ins.
Reciprocal of wall radius of curvature	K	$(ins.)^{-1}$
Distance from wall	Y(I)	ins.
Measured dynamic pressure	TRPR(I)	in.-H_2O

SHETWO

SHETWO reduces the output of a rotatable x-wire using the analysis of Appendix D. this program was not intended to be a general-purpose routine like VELPRO, and the input is pretty much limited to the data-acquisition system described in Appendix D. The inputs to the program are:

1. NPS   No. of points in the profile.

2. C_1 The multiplicative constant in the linearized hot-wire equation.

3. UTAU   The friction velocity from mean-velocity data (ft/sec).

4. UPW   The freestream (or wall potential) velocity (ft/sec)

5. DEL   The boundary layer thickness in the same units as Y.

6. DISP   The displacement thickness (ins).

7. MOMT   The momentum thickness (ins).

8. RE   The momentum thickness Reynolds number.

9. TIME   The integration time (sec).

10. PHIONE and PHITWO -- The wire angles as defined in Appendix D (deg).

MIXLN

This program, like VELPRO, is a general purpose routine designed to compute velocity gradients from an input velocity profile. To do this a SCIP library subroutine, ICSSCU, is used. This subroutine fits a cubic spline near but not necessarily through the data points. The amount of smoothing which is done can be controlled from the driver program MIXLN, by adjusting the value of the parameter SM.

If a shear stress profile is input with the mean velocity profile, the program will not only calculate the mean velocity gradient, but also the mixing length, the turbulence production, and the ratio of the experimental mixing length to the standard mixing-length distribution, assuming an A^+ value of 25. Also computed is the eddy Reynolds number, defined as:

$$R_{eddy} = \frac{\sqrt{uv}\ \ell}{\nu} = \frac{\overline{uv}}{\frac{\partial U}{\partial y}\ \nu}$$

If, as is usually the case, the points where y values of the shear stress profile are not coincident with the y values of the mean velocity profile, the program uses the cubic spline to calculate both the mean velocity and the mean velocity gradient separately.

HWIRE

HWIRE reduces the data from a horizontal wire. It is basically the same program as VELPRO, but the data reduction uses the linearized equation

$$U = C_1 E + C_2$$

for velocity. Besides the quantities calculated by VELPRO, the program also calculates the relative turbulence intensity:

$$TURBIN = \frac{\sqrt{\overline{u^2}}}{U_{pw}} = C_1 \frac{\sqrt{\overline{e^2}}}{U_{pw}}$$

The program will also calculate the isotropic dissipation if the time derivative of the fluctuating hot-wire signal, de/dt, is included

145

in the input data. The quantity printed out as DISP in the output is actually

$$\text{DISP} = \frac{\epsilon}{u_\tau^3 \delta}$$

The dissipation, ϵ, is calculated from the assumption of small-scale isotropy and Taylor's hypothesis.

$$\epsilon \cong 15\nu \overline{\left(\frac{\partial u}{\partial x}\right)^2} = \frac{15\nu}{U^2} \overline{\left(\frac{\partial u}{\partial t}\right)^2}$$

The inputs for HWIRE are the same as for VELPRO, except that mean voltage is read in instead of mean dynamic pressure, and in the two fields following are the true RMS fluctuating voltage and the time-differentiated fluctuating voltage.

146

Appendix D

QUALIFICATION OF X-WIRE TECHNIQUES IN A FULLY DEVELOPED CHANNEL FLOW

A pair of crossed hot wires can, in principle be used directly to measure the Reynolds stresses. For this experiment, however, we chose to prove our techniques by measuring the Reynolds stresses in a turbulent channel flow, where the shear stress distribution is known. This appendix will first describe the analysis which relates the fluctuating wire output to the Reynolds strsses, then describe the actual instruments used, and finally present the data measured in the channel.

Data Reduction

After linearization, the output voltage of each wire is related to the flow velocity by the calibration equation (for definition of variables, see Fig. D-1).

$$U_{meas} = Cal\ 1 \cdot E + Cal\ 2 \tag{D-1}$$

where Cal 1 and Cal 2 are constants. The hot wire responds as if it were being acted on by a velocity, U_{eff}, which is defined by Jorgenson's relation [42].

$$U^2_{eff} = U^2_2 + k^2_1 v^2_2 + k^2_2 w^2 \tag{D-2}$$

U_2, V_2, and W_2 are velocities in wire coordinates; that is, U_2 is the compnent of U_{meas} which is perpendicular to the wire and parallel to the prongs; V_2 is parallel to (along) the wire and in the plane of the prongs; and W_2 is perpendicular to the wire and the prongs. U_2, V_2, and W_2 are related to U_{meas} by the cosine law:

$$U_2 = U_{meas}\ cos\ \phi$$

$$V_2 = U_{meas}\ sin\ \phi \tag{D-3}$$

$$W_2 = 0$$

147

In practice the wire is aligned prior to measurement so that, for the mean velocity, the above relations hold. Substituting (D-3) into (D-2) relates U_{meas} to U_{eff}.

$$U_{eff}^2 = (\cos^2 \phi + k_1^2 \sin^2 \phi)\, U_{meas}^2 \qquad (D-4)$$

In unsteady flow, both U_{eff} and U_{meas} have mean and fluctuating components. The task of relating the fluctuating component of U_{eff} to the turbulence quantities was carried out by Anderson [44]. He gets, for $U \gg V$,

$$U_{eff}^2 = (\bar{U}_{eff} + u_{eff})^2 = A\bar{U}_2 + 2A\bar{U}_2 u + D\bar{U}_2 v + FU\, \bar{w}_2$$

where

$$A = (\cos^2 \phi + k_1^2 \sin^2 \phi) \quad,$$
$$D = (1 - k_1^2)\, \sin 2\phi \cos \theta \quad,$$
$$F = (1 - k_1^2)\, \sin 2\phi \sin \theta \quad,$$

where ϕ is the pitch angle as shown in Fig. D-1 and θ is the roll angle.

Returning to the expression for U_{eff}^2, the square root of the RHS can be taken by first dividing through by the large term $(A\bar{U}^2)$ and then using the binomial theorem. This results in

$$U_{eff} = \sqrt{A}\, \bar{U}_{meas} + \sqrt{A}\, u + \frac{D}{2\sqrt{A}}\, v + \frac{F}{2\sqrt{A}}\, w \qquad (D-5)$$

Now we define

$$u_{eff} = U_{eff} - \sqrt{A}\, \bar{U}_{meas} \qquad (D-6)$$

Then

$$u_{eff} = \sqrt{A}\, u + \frac{D}{2\sqrt{A}}\, v + \frac{F}{2\sqrt{A}}\, w \qquad (D-7)$$

Table D-1

Ratio of Difference between Measured and Predicted
uv to Square of Friction Velocity[*]

| | $\phi = 0°$ | | | | $\phi = 180°$ | |
| | $\phi = 180°$ | | | | $\phi = 0°$ | |
y/h	Turb. Processor	RMS Meter	Wire 1 Slant	Wire 2 Slant	Turb. Processor	RMS Meter
.1	-.031	.007	-.007	.048	-.003	.034
.2	.007	.022	.002	.048	-.016	.028
.3	-.003	.028	.011	.044	.002	.022
.4	-.009	.034	.017	.023	-.017	.005
.5	.009	.016	.006	.014	-.025	.004
.6	-.012	-.005	-.013	-.--0	-.028	-.017
.7	-.020	-.023	-.028	-.014	-.025	-.019
.8	-.009	-.005	-.019	-.013	-.020	-.027
.9	-.012	-.024	-.023	-.020	-.009	-.019

[*]Values are of

$$\frac{\overline{uv}_{x-wire} - \overline{uv}_{Eqn. (D-11)}}{u_\tau^2}$$

151
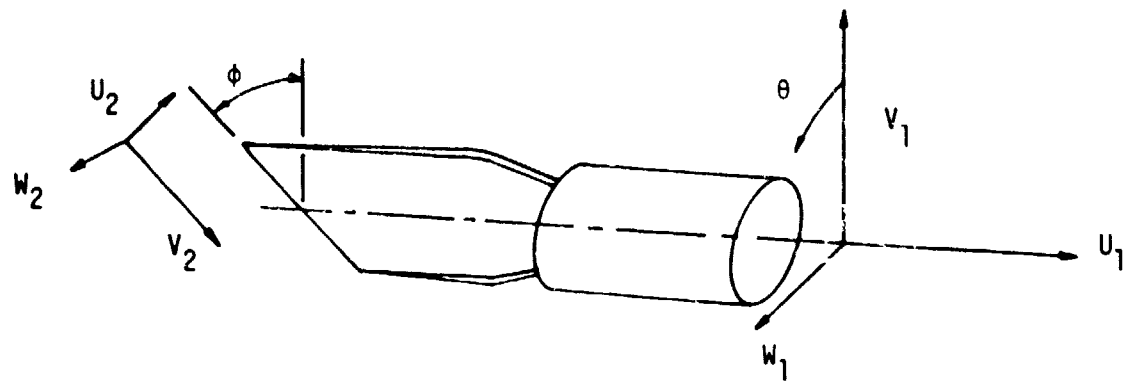
Fig. D-1. Coordinate system for analysis of hot-wire signal
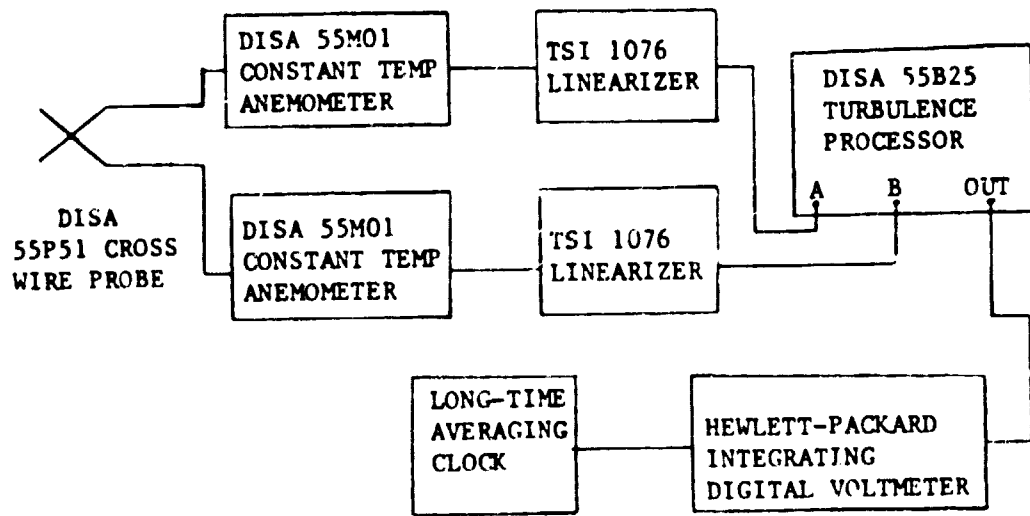
Fig. D-2. Block diagram of instruments for Reynolds stress measurements

152

The AC component of the output of the linearizer is related to the fluctuating component of U_{eff} by

$$u_{eff} = \frac{\partial U_{eff}}{\partial E} e = (\sqrt{A} \text{ Cal 1}) e \qquad (D-8)$$

Inserting (D-8) into (D-7) gives

$$e = \frac{1}{\text{Cal 1}} \left[u + \frac{D}{2A} v + \frac{F}{2A} w \right] \qquad (D-9)$$

(D-9) is the basic equation which is used in the data reduction. When two wires (a and b) are used with $\phi = 45°$ for both and $\theta = 0°$ for one and 180° for the other, the AC outputs can be correlated as

$$(a+b)(a-b) = \left(\frac{4}{\text{Cal 1}} \right)^2 \left[\frac{1 - k_1^2}{(1 + k_1^2)} \overline{uv} \right]$$

In our case, a DISA turbulence processor was used to do the cross-correlation. However, a True RMS meter could also be used since

$$(a+b)(a-b) = a^2 - b^2$$

and this scheme was also used in the channel tests.

Equipment Used

Figure D-2 shows, schematically, the layout of sensors and instruments used to measure the turbulent stresses. The output of the anemometer bridges was linearized, fed to the turbulence processor (which performed the cross-correlations discussed above), and the resulting signal was time-averaged using an integrating digital voltmeter.

The sensor tip was mounted in a probe holder which allowed the sensor to be rotated around an axis parallel to the prongs. The x array could be located in the x-y plane or the y-z plane. This allowed us, in practice, to measure the y-z Reynolds shear stress $(\overline{uw})$ and the y-z Reynolds normal stress. The rotating feature was also useful during qualification -- either of the two wires could be used as a rotatable slant wire to measure the Reynolds stresses independently.

149

Measurements in the Channel

The channel flow we used has been described (and measured) in detail by Hussain [45]. The flow is known to be fully developed and very two-dimensional. The shear-stress distribution is

$$\overline{uv} = \frac{h}{\rho} \frac{dP_t}{dx} [1 - y/h] \tag{D-11}$$

where dP_o/dx is the total (or static) pressure gradient, h is the channel width and y is the distance from the wall. The pressure gradient was measured by taking static pressure measurements at two stations, using a Combist micromanometer. The results are shown in Fig. D-3. The value of $\overline{uv}$ measured with the x-wire is always within $\pm \frac{.03}{2} u_t^2$ of that calculated from Eq. (D-11). In addition, values of u^2 and of $\overline{v^2}$ compare well with those measured by Taslim [46] in the same channel, as shown in Figs. D-4 and D-5.

During these qualification runs, it was discovered that very long averaging times were necessary to avoid large scatter in the data, the minimum acceptable time was 30 sec. For this reason, long averaging times, up to 100 sec., were used during curved-flow data acquisition.

As a further check on the accuracy of measurement, a shear stress profile were taken in which the x-wire array was used in several independent ways. Each of the two wires was used as a rotatable slant wire, an RMS meter was substituted for the DISA turbulence processor, and each of the x-wires was used both at zero and at 180°. All the measured values should agree, and Table D-1 shows that the difference between measured values and values calculated from Eqn. (D-11) is always less than 3 % of u_t^2 at 20:1 odds. The agreement was satisfactory for all configurations.
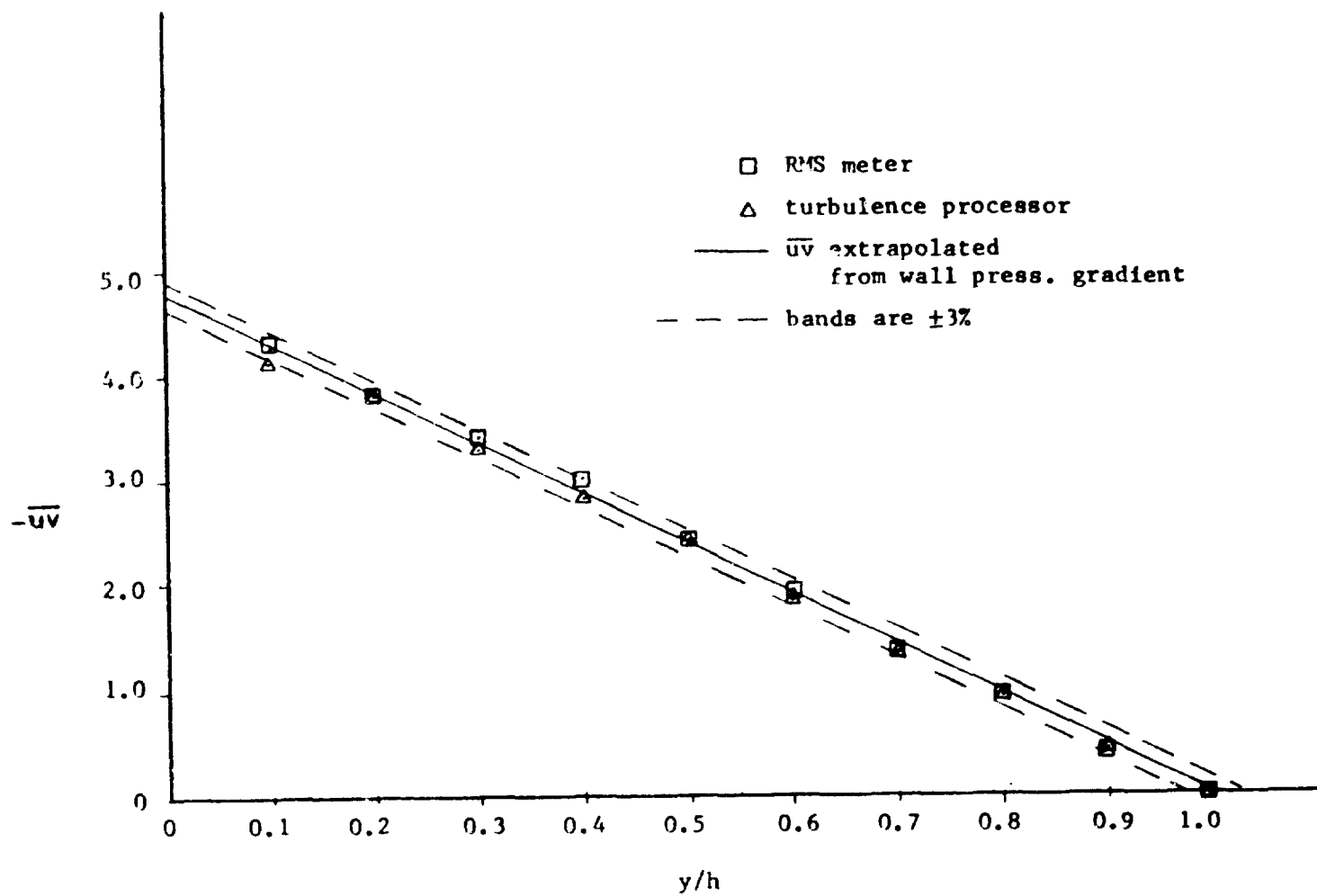
Fig. D-3. Measurements of turbulent shear stress in channel
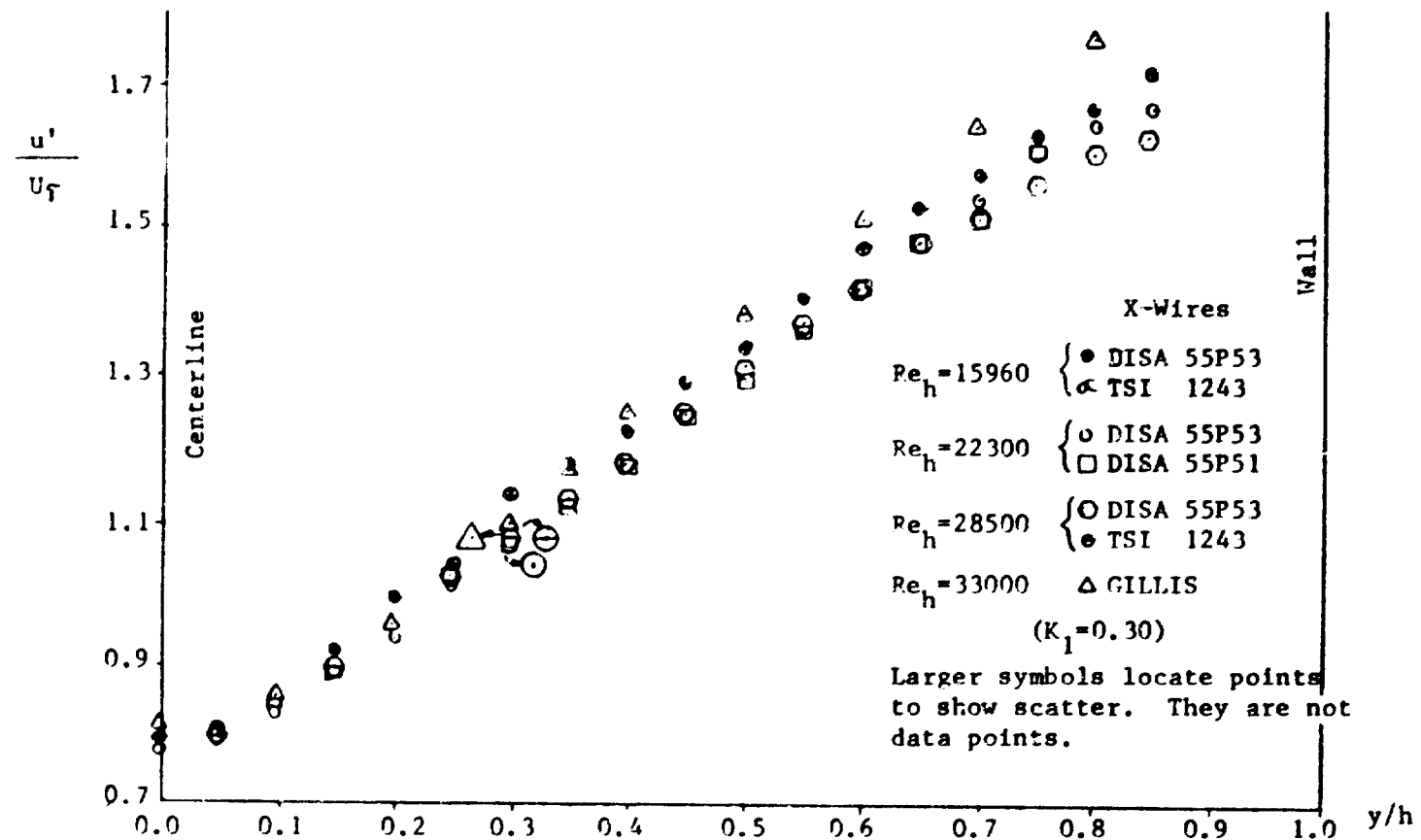
Fig. D-4. Plot of u'/u_τ measured in channel
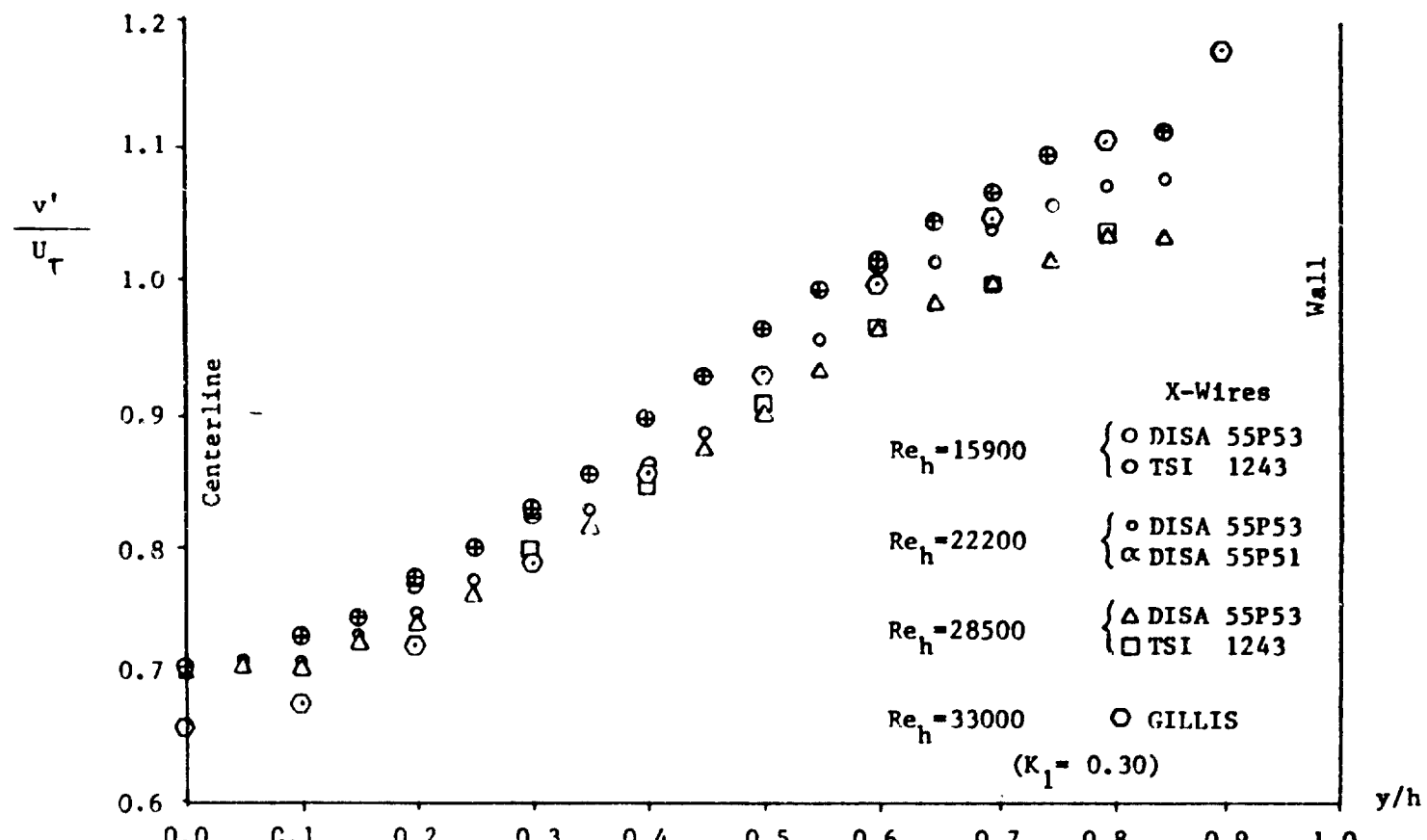
Fig. D-5. Plot of v'/u_τ measured in channel

Appendix E

FLOW-ANGLE MEASUREMENTS

Because the flow over the convex surface is so sensitive to secondary flows, we decided it was wise to measure the flow angle at various points across the boundary layer. To do this we fabricated a two-hole or Conrad probe, the business end of which is pictured in Fig. E-1.

For such a probe, the pressure difference between the two channels should be a linear function of flow angle -- at least for small angles. The response of the probe is shown in Fig. E-2.

Because the slope of calibration curve is a function of the local flow speed, the following procedure was used. First the probe was raised into the free stream and a pointer, attached to the probe shaft, was set to read zero degrees. Then the probe was moved into the boundary layer, and, at every measuring point, the probe shaft was rotated until both tubes read the same pressure. The flow angle relative to the free stream was then read off the pointer. It should be noted, however, that in all cases the free stream flow was parallel to the centerline of the passage within a few degrees.
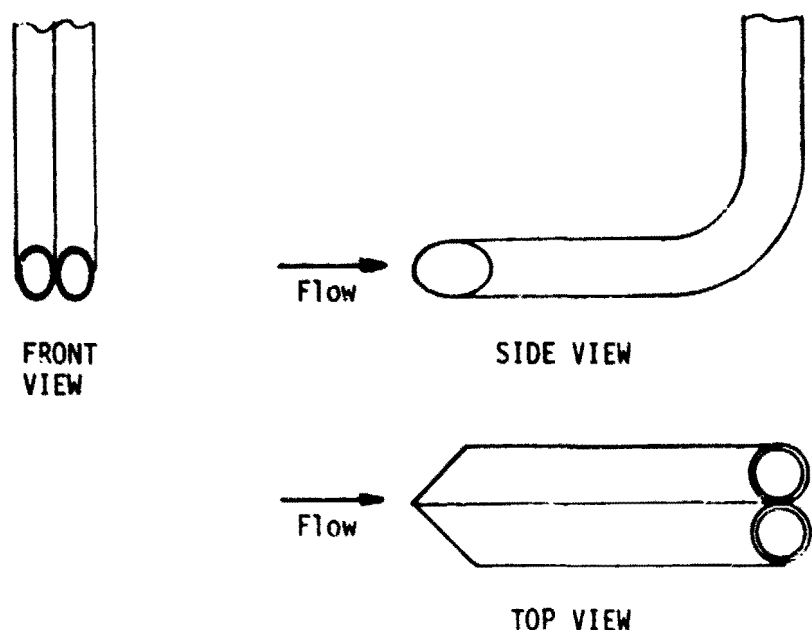
Fig. E-1. Conrad probe
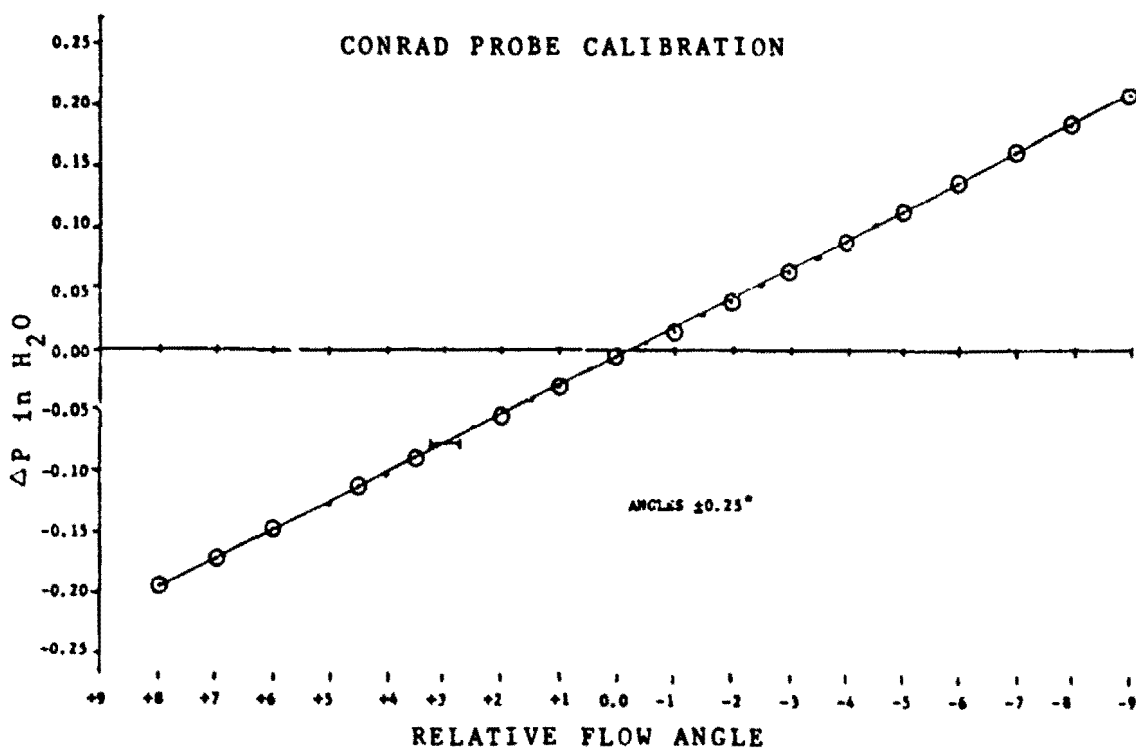
Fig. E-2. Calibration curve for Conrad probe

157

Appendix F

STAN5 SUBROUTINE AUX AFTER CURVATURE MODIFICATIONS

Implementation of the Curvature Model

There are four groups of statements which hav been introduced or modified in Subroutine AUX to model the effects of curvature on turbulence.

The first group is between lines AUX00270 and AUX00280. This group of statements is executed only on the first integration and guesses the value of δ_{s1} and related parameters. δ_{s1} is taken to be the same as δ_{99}, and δ_{s1}^* is taken to be the displacement thickness δ_2. The program also uses the values of $(\delta_{s1}-\delta_{s1}^*)$ from the previous two integrations; and, for the first time step, these are taken as $(\delta-\delta_2)$. This group of statements does not figure in subsequent integrations.

The second set of curvature statements is between AUX01000 and AUX01020. First the values of $(\delta_{s1}-\delta_{s1}^*)$ from the previous three integrations are averaged (this step is taken to improve the stability of the model), and the average value, ALAMA, is used to set the outer layer mixing length as ALAMA/10.

Between statements AUX0124 and AUX0125 is a statement which determines the value of τ^+ (called TPL(I)) at each point for later use.

The fourth group of statements concluded for curvature comes between AUX01560 and AUX01600. This group determines δ_{s1} and then computes δ_{s1}^*. The first set of statements, 1657 to 1667, finds the value of y where the stability parameter s has a value of 0.11. If the wall has convex curvature $(CW < 0)$, then this y value is taken as δ_{s1} and the program skips from 1673 to 1711 to compute δ_{s1}^*. If the wall is flat $(CW = 0)$, then statements 1674 to 1710 determine δ_{s1} from the TPL(1) profile by the method shown in Fig. 61, and as described below.

In the code, the τ^+ profile is first searched to find τ_{max}^+. Then the τ^+ profile is searched again to find points which have τ^+ values between $0.40 * \tau^+$ and $0.90 * \tau_{max}^+$ in a band centered at $0.65\,\tau_{max}^+$ with half width $0.25\,\tau_{max}^+$. If there are fewer than three

158

points in this range, the band is widened by a factor of 1.25 and the profile is searched again. When four or more points have been found, a least-squares routine is used to fit a straight line through them in the τ^{+}-y plane. The intersection of this line with the y axis can be computed directly (statement 1707) and is taken as δ_{sl}.

Once δ_{sl} has been determined, δ_{sl}^{*} is computed in statements 1712 to 1742.

Program Nomenclature

δ_{sl}	SLT
δ_{sl}^{*}	DISSHR
τ^{+}	TPL(I)
$(\delta_{sl}-\delta_{sl}^{*})_{\text{This integration}}$	ALAM
$(\delta_{sl}-\delta_{sl}^{*})_{\text{Last integration}}$	PLAM
$(\delta_{sl}-\delta_{sl}^{*})_{\text{Two integrations ago}}$	PALAM
Average of ALAM, PLAM, & PALAM	ALAMA
s	STAB(I)
$1/R_{o}$	CW (interpolated value)
$1/R_{o}$	CBC (boundary condition read)

In addition, small modifications were made to the input subroutine and the driver program. To read the wall curvature boundary conditions, the read statement for boundary conditions, which normally reads:

90   READ 9(5,580) SIM), RW(MO), AUX2(M), AUX2(M)

was modified to read

90 READ95,5800 X(M), RW(M), AUX2(M), AUX2(M), CBC(M)

159

In the driver program (main), a statement was added to interpolate the local value of wall curvature at the x location of the integration from the boundary condition values of wall radius (CBC(M)) read. This is

$$CW = BCB(M-1) + (CBC(M) - CBC(M-1)) \; 8 \; (XU-X(M-1))/(X(M) - X(M-1))$$

Also, the free constant BXX was not equal to the displacement thickness, DEL2, right after statement 519 in main.

Finally, the common block ADO was enlarged by adding CBC(100),CW after ITKE.

```
      SUBROUTINE AUX                                                    AUX00000
C.....                                                                  AUX00010
      INTEGER GEOM,FLUID,SOURCE(5),SPACE,BOUFOR,OUTPUT,TYPBC            AUX00020
      COMMON/GEN/PEI,AMI,AME,DPDX,XU,XD,XL,DX,INTG,CSALFA,TYPBC(5),     AUX00030
     1MODE,PRT(5),PRE,NXBC,X(100),RH(100),FJ(5,100),GC,CJ,AM(100),PRO,  AUX00040
     2UG(100),PO,SOURCE,RETRAN,NUMRUN,SPACE,RHO,PPLAG,OUTPUT,DELTAX,GV  AUX00050
     3/E/N,NP1,NP2,NP3,NEQ,NPH,KEX,KIN,KASE,KRAD,GEOM,FLUID,BODFOR,YPMIN AUX00060
     4/GG/BETA,GAMA(5),AJI(5),AJE(5),INDI(5),INDE(5),TAU,QWF(5)         AUX00070
     5/V/U(54),F(5,54),R(54),OM(54),Y(54),UGU,UGD,UI,FI(5),FMEAN,TAUW   AUX00080
     6/W/SC(54),AU(54),BU(54),CU(54),A(5,54),B(5,54),C(5,54),SU(5,54),SD AUX00090
     7/L/AK,ALMG,ALMGG,FRA,APL,BPL,AQ,BQ,EMU(54),PREF(5,54),AUXM1       AUX00100
     8/L1/YL,UMAX,UMIN,FR,YIP,YEM,ENFRA,KENT,AUXM2                      AUX00110
     9/P/RHO(54),VISCO(54),PR(5,54),RHOC,VISCOC,PRC(5),T(54),RHOM,BF(54) AUX00120
     1/O/H,REM,CFC,ST(5),LSUB,LVAR,CAY,REH,PPL,GPL,QW(5),KD             AUX00130
     2/CN/AXX,BXX,CXX,DXX,EXX,K1,K2,K3,SP(54),AUX1(100),AUX2(100),YPMAX AUX00140
     3/ADD/RBOM(54),OMD(54),ROMD(54),ITKE,CBC(100),CEFF(54),CLAG,CURV,  AUX00150
     4CW,PL(54)
      DIMENSION DV(54),SHR(54),STAB(54),VELGRD(54),TPL(54)             AUX00160
C.....                                                                  AUX00170
      ITKE=1                                                            AUX00175
      UGG=U(1)+FLOAT(KEX-1)*(U(NP3)-U(1))                              AUX00180
      RHG=RHO(1)+FLOAT(KEX-1)*(RHO(NP3)-RHO(1))                        AUX00190
      AMW=-AME+FLOAT(KEX-1)*(AME+AMI)                                  AUX00200
      RHW=RHO(NP3)+FLOAT(KEX-1)*(RHO(1)-RHO(NP3))                      AUX00210
      VISW=VISCO(NP3)+FLOAT(KEX-1)*(VISCO(1)-VISCO(NP3))              AUX00220
      UTAU=SQRT(GC*TAUW/RHW)                                           AUX00230
      YPUT=RHW*UTAU/VISW                                               AUX00240
      KTHRU=0
      IF (INTG.GT.1) GO TO 10                                          AUX00250
      KOUNT=0                                                          AUX00260
      IF (MODE.EQ.2) KOUNT=1                                           AUX00270
C     ****************************************************************
C     CURVATURE MODIFICATION -- GUESS INITIAL VALUES OF PARAMETERS
      SLT=YL
      DISSHR=BXX
      ALAM=SLT-DISSHR
      PLAM=ALAM
      P2LAM=PLAM
      ISLT=N
      REMS=REM
C     ****************************************************************
    1 RAVG=R(1)                                                        AUX00280
      RHOAV=RHO(1)                                                     AUX00290
      VISAV=VISCO(1)                                                   AUX00300
      KTURB=0                                                          AUX00310
      IF (NPH.EQ.0.AND.MODE.EQ.2.AND.K2.NE.2)WRITE(6,6)               AUX00320
      IF(K2.EQ.2.AND.MODE.EQ.2)WRITE(6,9)                             AUX00330
      IF (NPH.EQ.0.AND.MODE.EQ.2.AND.KD.LT.2) WRITE(6,7)             AUX00340
      IF (NPH.EQ.0.AND.MODE.EQ.2.AND.KD.GE.2) WRITE(6,8)             AUX00350
      IF (NPH.EQ.0) GO TO 10                                          AUX00360
      JTKE=0                                                          AUX00370
      DO 5 J=1,NPH                                                     AUX00380
      IF (SOURCE(J).EQ.2) JTKE=J                                       AUX00390
      IF (J.EQ.JTKE.AND.MODE.EQ.2) WRITE (6,4)                        AUX00400
      IF (J.EQ.JTKE.AND.MODE.EQ.2.AND.K2.EQ.2) WRITE (6,3)           AUX00410
    3 FORMAT(//' K2 SHOULD NOT BE SET EQUAL TO 2 '//)                 AUX00420
    4 FORMAT(' FLOW IS TURBULENT AND PROGRAM IS USING TURBULENT'       AUX00430
     1/' KINETIC-ENERGY TO EVALUATE EDDY VISCOSITY, EXCEPT IN THE'/   AUX00440
     1' WALL FUNCTION WHERE MIXING-LENGTH IS USED.  NOTE THAT THE'/   AUX00450
     1' PRINTED-OUT VALUES OF TKE HAVE NO MEANING IN THE NEAR-WALL'/  AUX00460
     1' REGION, I.E., FOR Y+ LESS THAN B+, OR 2*A+.'/)                AUX00470
    5 IF (SOURCE(J).EQ.2) KTURB=1                                     AUX00480
      IF (MODE.EQ.1) GO TO 10                                          AUX00490
      IF (KTURB.EQ.0.AND.K2.NE.2)WRITE (6,6)                          AUX00500
      IF (KD.LT.2) WRITE (6,7)                                        AUX00510
      IF (KD.GE.2) WRITE (6,8)                                        AUX00520
    6 FORMAT(' FLOW IS TURBULENT AND PROGRAM IS USING THE PRANDTL MIX-' AUX00530
     1/' ING-LENGTH HYPOTHESIS TO EVALUATE EDDY-VISCOSITY'/)          AUX00540
```

161

```
      7 FORMAT(' THE VAN DRIEST SCHEME IS BEING USED TO EVALUATE'          AUX00550
       1/' THE MIXING-LENGTH OR LENGTH-SCALE DAMPING NEAR THE WALL.'/)     AUX00560
      8 FORMAT(' THE EVANS SCHEME IS BEING USED TO EVALUATE THE'           AUX00570
       1/' MIXING-LENGTH OR LENGTH-SCALE DAMPING NEAR THE WALL.'/)         AUX00580
      9 FORMAT(' FLOW IS TURBULENT AND PROGRAM IS USING THE CONSTANT'/     AUX00590
       1' EDDY DIFFUSIVITY OPTION IN THE OUTER REGION'/)                   AUX00600
C.....                                                                     AUX00610
     10 KTHRU=KTHRU+1
        DO 89 I=2,NP1                                                      AUX00620
        YM=0.5*(Y(I+1)+Y(I))                                              AUX00630
        IF (KEX.EQ.1) YM=Y(NP3)-YM                                        AUX00640
        IF (FLUID.EQ.1) GO TO 12                                          AUX00650

        RAVG=0.5*(R(I)+R(I+1))                                           AUX00660
        RHOAV=0.5*(RHO(I)+RHO(I+1))                                      AUX00670
        VISAV=0.5*(VISCO(I)+VISCO(I+1))                                  AUX00680
     12 EMUT=0.                                                           AUX00690
        DV(I)=1.                                                         AUX00700
        IF (MODE.EQ.1) GO TO 50                                         AUX00710
        KOUNT=KOUNT+1                                                   AUX00720
        IF (KOUNT.EQ.1) GO TO 1                                         AUX00730
        IF (KASE.EQ.2) GO TO 25                                         AUX00740
C--------------------------------------- EDDY VISCOSITY DAMPING TERM ----AUX00750
C.....VAN DRIEST DAMPING FUNCTION                                        AUX00760
C.....APL, BPL COMPUTED IN WALL                                          AUX00770
        IF (FLUID.NE.1) YPUT=SQRT(RHOAV*TAUW*GC)/VISAV                   AUX00780
        YLOC=YM*YPUT                                                    AUX00790
        IF (KD.GT.1) GO TO 15                                           AUX00800
        IF (YLOC/APL.GT.10.) GO TO 25                                   AUX00810
        DV(I)=1.-1./EXP(YLOC/APL)                                       AUX00820
        GO TO 22                                                        AUX00830
C.....EVANS DAMPING FUNCTION                                             AUX00840
     15 DV(I)=YLOC/BPL                                                   AUX00850
     20 IF(DV(I).GT.1.) DV(I)=1.                                         AUX00860
C.....LOWER LIMIT VALUE DAMPING TERM                                     AUX00870
     22 IF (DV(I).LT.0.0001) DV(I)=0.0001                               AUX00880
     25 CONTINUE                                                        AUX00890
C--------------------------------------------- PRANDTL MIXING LENGTH ----AUX00900
        IF (I.GT.2) GO TO 30                                            AUX00910
        IF (GEOM.EQ.4.OR.GEOM.EQ.5) GO TO 30                           AUX00920
        IF (REM.LE.100..OR.K2.EQ.3) GO TO 30                           AUX00930
C.....EMPIRICAL CORRELATION FOR ALMG FOR WALL FLOWS                     AUX00940
C.....THIS CORRELATION THEN OVERRIDES THE INPUT ALMGG                   AUX00950
        AMOR=AME/RHO(1)                                                AUX00960
        IF (KIN.EQ.1) AMOR=AMI/RHO(NP3)                               AUX00970
        ALMG=ALMGG*(1.-67.5*AMOR/UGU)                                 AUX00980
        IF (ALMG.LT.ALMGG) ALMG=ALMGG                                 AUX00990
C.....COMPUTE MIXING LENGTH                                             AUX01000
C     ********************************************************
C     CURVATURE MODIFICATION TO WAKE MIXING LENGTH
        ALAMA=(ALAM+PLAM+P2LAM)/3.
     30 AL=ALMG*ALAMA*1.1765                                           AUX01010
        ALMAX=AL
C     ********************************************************
        IF (KASE.EQ.1.AND.YM.LT.AL/AK) AL=AK*YM                       AUX01020
        IF(KASE.EQ.1.AND.K2.EQ.2)AL=AK*YM                            AUX01030
        IF (KTURB.EQ.1.AND.KASE.EQ.2) GO TO 40                       AUX01040
        IF(KASE.EQ.2)GO TO 35                                        AUX01050
        YTKE=Y(I)*YPUT                                               AUX01502
        IF (KEX.EQ.1)YTKE=(Y(NP3)-Y(I+1))*YPUT                       AUX01054
        IF(KTURB.EQ.1.AND.KD.LE.1.AND.YTKE.GE.2.*APL)GO TO 40        AUX01060
        IF(KTURB.EQ.1.AND.KD.GE.2.AND.YTKE.GE.BPL)GO TO 40          AUX01070
     35 EMUT=RHOAV*AL*AL*ABS((U(I+1)-U(I))/(Y(I+1)-Y(I)))*DV(I)*DV(I) AUX01080
        PL(I)=AL/YL
        SP(2)=BXX
        SP(3)=SLT
        IF(K2.NE.2.OR.KASE.EQ.2)GO TO 36                             AUX01090
        EMUTC=(AQ*REM**BQ)*VISAV                                     AUX01100
        IF(EMUT.GT.EMUTC)EMUT=EMUTC                                  AUX01110
```

162

```
        IF(YM.GT.0.4*YL)EMUT=EMUTC                                    AUX01120
     36 IF(KTURB.NE.1)GO TO 50                                        AUX01130
C.....ADJUSTMENT OF TKE IN NEAR-WALL REGION                           AUX01140
        FJJAVE=((AK*EMUT)/(AQ*RHOAV*AL*DV(I)))**2                     AUX01150
        F(JTKE,I)=FJJAVE                                              AUX01160
        ITKE=I                                                        AUX01161
        IF (KEX.EQ.1.AND.ITKE.EQ.1) ITKE=I                           AUX01162
        GO TO 50                                                      AUX01170
C.....COMPUTE EDDY VISCOSITY USING TURBULENT KINETIC ENERGE EQN       AUX01180
     40 FJJAVE=ABS(0.5*(F(JTKE,I+1)+F(JTKE,I)))                       AUX01190
        EMUT=AQ*RHOAV*AL*DV(I)*SQRT(FJJAVE)/AK                        AUX01200
C----------------------------------------- EFFECTIVE VISCOSITY ----AUX01210
     50 EMU(I)=EMUT+VISAV                                             AUX01220
        IF (NPH.EQ.0.AND.KASE.EQ.1) T(I)=ABS(EMU(I)*(U(I+1)-U(I))/    AUX01230
       1(Y(I+1)-Y(I)))/(GC*TAUW)                                     AUX01240
        TPL(I)=ABS(EMU(I)*(U(I+1)-U(I))/(Y(I+1)-Y(I)))/(GC*TAUW)
        VELGPD(I)=(U(I+1)-U(I))/(Y(I+1)-Y(I))
        IF (NPH.EQ.0) GO TO 89                                        AUX01250
C--------------------------- TURBULENT PRANDTL/SCHMIDT NUMBER ----AUX01260
        EDR=EMUT/VISAV                                                AUX01270
        DO 88 J=1,NPH                                                 AUX01280
        IF (MODE.EQ.1) GO TO 80                                       AUX01290
        JPHI=1                                                        AUX01300
        IF (SOURCE(J).GT.0) JPHI=SOURCE(J)                            AUX01310
        GO TO (62,68,62,62), JPHI                                     AUX01320
C.....                                                                AUX01330
C.....STAGNATION ENERGY EQN, TURBULENT PRANDTL NUMBER                 AUX01340
     62 PRTJ=PRT(J)                                                   AUX01350
        IF (KASE.EQ.2.OR.K3.EQ.3) GO TO 70                            AUX01360
C.....THE FOLLOWING IS THE FREE CONSTANT IN THE TURBULENT PRANDTL     AUX01370
C.....NUMBER EQUATION. EXPERIENCE MAY SUGGEST A DIFFERENT VALUE.      AUX01380
        CT = 0.2                                                      AUX01390
        PETC=EDR*CT*(PR(J,I+1)+PR(J,I))/2.                            AUX01400
        IF(PETC.LT..001)PETC=.001                                     AUX01410
        IF(PETC.GT.100.)GO TO 69                                      AUX01420
        ALPHA=SQRT(1./PRTJ)                                           AUX01430
        AOP=ALPHA/PETC                                                AUX01440
        IF(AOP.GT.10.)AOP=10.                                         AUX01450
        PRTJ=1./(1./(2.*PRTJ)+ALPHA*PETC-PETC*PETC*(1.-EXP(-AOP)))    AUX01460
        GO TO 69                                                      AUX01470
C.....TURBULENT KINETIC ENERGY EQN, TURB PRANDTL NUMBER               AUX01480
     68 PRTJ=PRT(J)                                                   AUX01490
C--------------------------- EFFECIVE PRANDTL/SCHMIDT NUMBER ----AUX01500
     69 IF(KIN.EQ.1.AND.I.EQ.2)GO TO 88                               AUX01510
        IF(KEX.EQ.1.AND.I.EQ.NP1)GO TO 88                            AUX01520
     70 PREF(J,I)=(1.0+EDR)/(EDR/PRTJ+1.0/(0.5*(PR(J,I+1)+PR(J,I))))  AUX01530
        GO TO 88                                                      AUX01540
C.....LAMINAR EFFECTIVE PRANDTL NUMBER                                AUX01550
     80 PREF(J,I)=0.5*(PR(J,I+1)+PR(J,I))                             AUX01560
     88 CONTINUE
     89 CONTINUE
        Y11=0.00
        IF(CW.GE.0.0) GO TO 91
        DO 90 I=2,NP1
        IF(Y11.GT.0.0) GO TO 90
        VELGPD(I)=(U(I)-U(I-1))/(Y(I)-Y(I-1))
        STAB(I)=CW*U(I)/VELGPD(I)
        IF(STAB(I).GT.-.11) GO TO 90
        Y11=(-.11-STAB(I-1))/(STAB(I)-STAB(I-1))
        SLT=Y11*(Y(I)-Y(I-1))+Y(I-1)
     90 CONTINUE
     91 P2LAM=PLAM
        PLAM=SLT-DISSHR
        IF(Y11.GT.0) GO TO 102
        NPSHR=NP1-1
        TAUMAX=0.0
        DO 92  I=3,NPSHR
```

```
      DO 92 I=2 ...
   92 IF(TPL(I).GT.TAUMAX) TAUMAX=TPL(I)
      CNTR=0.65
      BAND=0.25
   93 KLUNK=0
      NFIT=0
      SUM1=0.0
      SUM2=0.0
      SUM3=0.0
      SUM4=0.0
      DO 94 I=1,NPSHR
      UPPER=(CNTR+BAND)*TAUMAX
      ALOWR=(CNTR-BAND)*TAUMAX
      IF(KLUNK.GT.0) GO TO 94
      NSRC=NP1-I
      IF(TPL(NSRC).GE.(0.93*TAUMAX)) KLUNK=1
      IF(TPL(NSRC).GT.UPPER.OR.TPL(NSRC).LT.ALOWR) GO TO 94
      NFIT=NFIT+1
      SUM1=SUM1+Y(NSRC)
      SUM2=SUM2+TPL(NSRC)
      SUM3=SUM3+TPL(NSRC)*Y(NSPC)
      SUM4=SUM4+TPL(NSRC)*TPL(NSRC)
   94 CONTINUE
      ANUM=SUM3-(SUM1*SUM2/NFIT)
      DENUM=SUM4-(SUM2*SUM2/NFIT)
      IF(DENUM.LE.0.0) WRITE(6,96) (I,Y(I),U(I),TPL(I), I=1,NPSHR)
      IF(BAND.GT.0.50) GO TO 100
      IF(DENUM.GT.0.0.AND.NFIT.GT.2) GO TO 100
   96 FORMAT(2X,I3,4X,F9.5,4X,F7.2,4X,F7.4)
      BAND=BAND*1.25
      GO TO 93
  100 SLT=(SUM1-SUM2*(ANUM/DENUM))/NFIT
      IF(INTG.GT.19.AND.INTG.LT.30) WRITE(6,97) (I,Y(I),U(I),
     1TPL(I),VELGRD(I),PL(I), I=1,NPSHR)
   97 FORMAT(2X,I3,4X,F9.5,4X,F7.2,4X,F7.4,4X,F7.0,4X,F7.4)
  102 IF(SLT.GT.1.2*YL) SLT=1.2*YL
C     FIND NEW DELTASTAR BASED ON SHEAR LAYER THICKNESS
C      FIND NEW EDGE VELOCITY

      KSLT=0
      DO 103 I=2,NP1
      IF(KSLT.EQ.0.AND.Y(I).GT.SLT) ISLT=I
      IF(Y(I).GT.SLT) KSLT=1
  103 CONTINUE
      IF(KSLT.EQ.0) GO TO 105
      USLT=UGU
      DISSHR=(1.-U(2)/USLT)*(Y(2)/2)
      DMOMT=(U(2)/USLT)*DISSHR
      ISLT1=ISLT-1
      DO 104 I=3,ISLT1
      DISSHR=DISSHR+((1.-U(I-1)/USLT)+(1.-U(I)/USLT))
     1*(Y(I)-Y(I-1))/2.
      DMT1=(U(I)/USLT)*(1.-(U(I)/USLT))
      DMT2=(U(I-1)/USLT)*(1.-(U(I-1)/USLT))
  104 DMOMT=DMOMT+(DMT1+DMT2)*(Y(I)-Y(I-1))/2.
      DISSHR=DISSHR+(1.-U(ISLT1)/USLT)*(SLT-Y(ISLT1))/2.
      DMINC=(U(ISLT1)/USLT)*(1.-U(ISLT1)/USLT)*(SLT-Y(ISLT1))/2.
      DMOMT=DMOMT+DMINC
      REMS=DMOMT*USLT*RHO(1)/VISCO(1)
  105 IF(KSLT.EQ.0) DISSHR=BXX
      ALAM=SLT-DISSHR
      IF(INTG.GT.0.AND.INTG.LT.299) WRITE(6,106) INTG,SLT,DISSHR,
     1YL,NFIT,REMS,ALMAX,KTHRU
  106 FORMAT(1X,'INTG =',I4,3X,'SLT =',F8.5,3X,'DISSHR =',F8.5,3X,
     1'DEL99=',F7.4,3X,'KFIT=',I2,4X,'REMS=',F7.2,4X,'LMAX=',F7.4,
     22X,'KTHRU=',I3)
      IF(ABS(ALAM-P2LAM).LE.(0.05*YL)) ALAM=(PLAM+ALAM)/2.
  108 CONTINUE
      DO 110 I=2,NP1                                                    AUX01600
      RHOAV=(RHO(I)+RHO(I+1))/2.                                        AUX01610
```

```
      RAVG=(R(1)+R(I+1))/2.                                      AUX01620
C.....ADJUSTMENT OF EMU AT 2.5 AND N+1.5                         AUX01630
      IF (I.GT.2) GO TO 110                                      AUX01640
      IF (KIN.NE.1) GO TO 109                                    AUX01650
      IF (BETA.LT.0.02.OR.BETA.GT.0.9) GO TO 110                 AUX01660
      EMU(2)=TAU*(Y(2)+Y(3))/(BETA*(U(2)+U(3)))                  AUX01670
  109 IF (KEX.NE.1) GO TO 110                                    AUX01680
      IF (BETA.LT.0.02.OR.BETA.GT.0.9) GO TO 110                 AUX01690
      EMU(NP1)=TAU*(Y(NP3)-0.5*(Y(NP1)+Y(NP2))/                  AUX01700
     1          (BETA*0.5*(U(NP1)+U(NP2)))                       AUX01710
C.....COMPUTE SMALL C'S                                          AUX01720
  110 SC(I)=RAVG*RAVG*RHOAV*0.5*(U(I+1)+U(I))*EMU(I)/(PEI*PEI)   AUX01730
      IF (NEQ.EQ.1) GO TO 300                                    AUX01740
C---------------------------------------------- SOURCE TERMS ----AUX01745
      DO 200 I=3,NP1                                             AUX01750
      DO 150 J=1,NPH                                             AUX01760
      SU(J,I)=0.                                                 AUX01770
      SD=0.                                                      AUX01780
      IF (SOURCE(J).EQ.0) GO TO 150                              AUX01790
      NSOR=SOURCE(J)                                             AUX01800
      GO TO (115,130,115,120), NSOR                             AUX01810
C-------------------------------- STAGNATION ENERGY EQN SOURCE ----AUX01820
  115 IF (I.EQ.2) PREF(J,1)=PREF(J,2)                           AUX01830
      PREFF=(PREF(J,I)+PREF(J,I-1))*0.5                          AUX01840
      CS=SC(I)*(U(I+1)*U(I+1)-U(I)*U(I))*ROMD(I)                 AUX01850
      CS = CS-SC(I-1)*(U(I)*U(I)-U(I-1)*U(I-1))*ROMD(I-1)        AUX01860
      CS=(1.-1./PREFF  )*CS*RBOM(I)                              AUX01870
      SU(J,I) = CS/(GC*CJ)+BF(I)/(CJ*RHO(I))                     AUX01880
  120 IF (U(I).LT.0.0001) GO TO 125                              AUX01890
      IF (SOURCE(J).EQ.3) SU(J,I)=SU(J,I)+AUXM2/(RHO(I)*U(I))    AUX01900
      IF (SOURCE(J).EQ.4) SU(J,I)=AUXM2/(RHO(I)*U(I))            AUX01910
  125 SD=0.                                                      AUX01920
      GO TO 150                                                  AUX01930
C----------------------- TURBULENT KINETIC ENERGY EQUATION SOURCE ----AUX01940
  130 AL=ALMG*YL                                                 AUX01950
      IF (KASE.EQ.2) GO TO 140                                   AUX01960
      YMQ=Y(I)                                                   AUX01970
      IF (KEX.EQ.1) YMQ=Y(NP3)-Y(I)                             AUX01980
      IF (YMQ.LT.AL/AK) AL=AK*YMQ                               AUX01990
  140 DU2DOM=.5*((U(I+1)*U(I+1)-U(I)*U(I))*ROMD(I)+             AUX02000
     1  (U(I)*U(I)-U(I-1)*U(I-1))*ROMD(I-1))                     AUX02010
      DVQ=.5*(DV(I)+DV(I-1))                                     AUX02020
      FJ2=ABS(F(J,I))                                            AUX02030
      PROD=AQ*AL*DVQ*SQRT(FJ2)*(RHO(I)*R(I)/PEI)**2/(U(I)*AK*4.)* AUX02040
     1 DU2DOM**2                                                 AUX02050
      DISS=BQ*AK*FJ2**1.5/(AL*DVQ*U(I))                          AUX02060
      IF(DISS*DX.GT.FJ2)DISS=FJ2/DX                              AUX02070
      SU(J,I)=PROD-DISS                                          AUX02080
      FGT=F(J,NP3)                                               AUX02090
      IF(KIN.EQ.2)FGT=F(J,1)                                     AUX02100
      IF(KIN.EQ.3)FGT=0.0                                        AUX02110
      IF(F(J,I).LT.FGT)SU(J,I)=PROD                              AUX02120
      SD=0.0                                                     AUX02130
      GO TO 150                                                  AUX02140
C.....ADD OTHER SOURCE FUNCTIONS HERE                            AUX02150
C.....CHANGE 'COMPUTED GO TO' STATEMENT TO INCLUDE               AUX02160
C.....SOURCE FUNCTION STATEMENT NUMBERS.  LIKEWISE,              AUX02170
C.....CHANGE TURBULENT PR/SC NUMBER 'COMPUTED GO TO '            AUX02180
C.....STATEMENT NUMBERS.                                         AUX02190
  150 CONTINUE                                                   AUX02200
  200 CONTINUE                                                   AUX02210
  300 CONTINUE                                                   AUX02220
      RETURN                                                     AUX02230
      END                                                        AUX02240
```

165

Appendix G

THE PARABOLICITY OF THE BOUNDARY LAYER EQUATIONS
FOR PARALLEL FLOW OVER A CURVED SURFACE

This section is included as a justification for using a parabolic marching scheme (STAN5) to solve the boundary layer equations over a curved wall. In the modeling done elsewhere in this thesis, the effects of curvature appear implicitly in the turbulence model, and the standard linear momentum and continuity equations are then solved. For very strong curvature, however, it seems clear that the normal direction momentum equation will have to be solved too. As a first step towards developing such a computation scheme, the parabolicity of a set of equations in which the normal momentum equation was taken to be

$$\frac{\partial P}{\partial n} = \rho \frac{U^2}{R} \tag{G-1}$$

was investigated. In the proposed computation, this would be solved with the continuity and s component equation for momentum,

$$\frac{\partial U}{\partial s} + \left(1 + \frac{n}{R}\right)\frac{\partial V}{\partial n} + \frac{V}{R} = 0 \tag{G-2}$$

$$U\frac{\partial U}{\partial s} + V\frac{\partial U}{\partial n} = -\frac{1}{\rho}\frac{\partial P}{\partial s} - \frac{\partial \overline{uv}}{\partial n} + \nu\frac{\partial}{\partial n}\left[\frac{\partial U}{\partial n}\right] \tag{G-3}$$

Reynolds [47] found a method which finds the characteristics which reveal the nature of the equation set. The first step is to introduce a new variable W, which replaces the normal gradient of U and converts 1-3 into a set of four first-order equations:

$$W = \frac{\partial U}{\partial n} \tag{G-4}$$

$$U\frac{\partial U}{\partial s} + V\frac{\partial U}{\partial n} = -\frac{1}{\rho}\frac{\partial P}{\partial s} - \frac{\partial \overline{uv}}{\partial n} + \nu\frac{\partial W}{\partial n} \tag{G-5}$$

$$\frac{U^2}{R} = \frac{1}{\rho}\frac{\partial P}{\partial n} \tag{G-6}$$

$$\frac{\partial U}{\partial s} = -\frac{V}{R} + \left[\left(1 + \frac{n}{R}\right)\frac{\partial V}{\partial n}\right] \tag{G-7}$$

It is now assumed that $\overline{uv}$ is modeled as an algebraic function of W $(\overline{uv} = \kappa^2 n^2 W^2)$ and that the four remaining independent variables U, V, P and W are themselves functions of two new variables ξ and η. The chain rule is then used extensively to make transformations such as

$$\frac{\partial U}{\partial s} = \frac{\partial U}{\partial \xi}\frac{\partial \xi}{\partial s} + \frac{\partial U}{\partial \eta}\frac{\partial \eta}{\partial s} \tag{G-8}$$

This . to the following set of equations.

$$U\left[\frac{\partial U}{\partial \xi}\frac{\partial \xi}{\partial s} + \frac{\partial u}{\partial \eta}\frac{\partial \eta}{\partial s}\right] + V\left[\frac{\partial U}{\partial \xi}\frac{\partial \xi}{\partial n} + \frac{\partial U}{\partial \eta}\frac{\partial \eta}{\partial n}\right] = -\frac{1}{\rho}\left[\frac{\partial P}{\partial \xi}\frac{\partial \xi}{\partial s} + \frac{\partial P}{\partial \eta}\frac{\partial \eta}{\partial s}\right] \tag{G-9}$$

$$- 2n\kappa^2 W^2 - 2\kappa^2 W\left[\frac{\partial W}{\partial \xi}\frac{\partial \xi}{\partial n} + \frac{\partial W}{\partial \eta}\frac{\partial \eta}{\partial n}\right] + \nu\left[\frac{\partial W}{\partial \xi}\frac{\partial \xi}{\partial n} + \frac{\partial W}{\partial \eta}\frac{\partial \eta}{\partial n}\right]$$

$$\left[\frac{\partial U}{\partial \xi}\frac{\partial \xi}{\partial n} + \frac{\partial U}{\partial \eta}\frac{\partial \eta}{\partial n}\right] = W \tag{G-10}$$

$$\frac{U^2}{R} = \frac{1}{\rho}\left[\frac{\partial P}{\partial \xi}\frac{\partial \xi}{\partial n} + \frac{\partial P}{\partial \eta}\frac{\partial \eta}{\partial n}\right] \tag{G-11}$$

$$\left[\frac{\partial U}{\partial \xi}\frac{\partial \xi}{\partial s} + \frac{\partial U}{\partial \eta}\frac{\partial \eta}{\partial s}\right] + \left[1 + \frac{n}{R}\right]\left[\frac{\partial V}{\partial \xi}\frac{\partial \xi}{\partial n} + \frac{\partial V}{\partial \eta}\frac{\partial \eta}{\partial n}\right] + \frac{V}{R} = 0 \tag{G-12}$$

Now these four equations are combined into one by multiplying each by an arbitrary constant C_1 times Eq. (9), C_2 times Eq. (10), C_3 times Eq. (11), and C_4 times Eq. (12). The four equations are then added together to produce:

$$\frac{\partial U}{\partial \xi}\left[C_1 U\frac{\partial \xi}{\partial s} + C_1 V\frac{\partial \xi}{\partial n} + C_2\frac{\partial \xi}{\partial n} + C_4\frac{\partial \xi}{\partial s}\right] + \frac{\partial U}{\partial \eta}\left[C_1 U\frac{\partial \eta}{\partial s} + C_1 V\frac{\partial \eta}{\partial n} + C_2\frac{\partial \eta}{\partial n}\right.$$

$$\left. + C_4\frac{\partial \eta}{\partial s}\right] + \frac{\partial P}{\partial \xi}\left[\frac{C_1}{\rho}\frac{\partial \xi}{\partial s} - \frac{C_3}{\rho}\frac{\partial \xi}{\partial n}\right] + \frac{\partial P}{\partial \eta}\left[\frac{C_1}{\rho}\frac{\partial \eta}{\partial s} - \frac{C_3}{\rho}\frac{\partial \eta}{\partial n}\right]$$

$$+ \frac{\partial W}{\partial \xi}\left[2C_1\kappa^2 W\frac{\partial \eta}{\partial n} - C_1\nu\frac{\partial \eta}{\partial n}\right] + \frac{\partial V}{\partial \xi}\left[C_4\left(1 + \frac{n}{R}\right)\frac{\partial \xi}{\partial n}\right] + \frac{\partial V}{\partial \eta} \tag{G-13}$$

$$\cdot\left[C_4\left(1 + \frac{n}{R}\right)\frac{\partial \eta}{\partial n}\right] + \left[2C_1 n\kappa^2 W^2 - C_2 W + C_3\frac{U^2}{R} + C_4\frac{V}{R}\right] = 0$$

167

Now the equations of the characteristic lines are obtained by set-
ting one of the partials with respect to a characteristic, say $\partial/\partial\eta$,
to zero. This leads to an equation for a line of constant η. Doing
this gives four equations which can be used to find C_1 through C_4.

$$C_1 U \frac{\partial\eta}{\partial s} + C_1 V \frac{\partial\eta}{\partial n} + C_2 \frac{\partial\eta}{\partial n} + C_4 \frac{\partial\eta}{\partial s} = 0 \qquad (G-14)$$

$$\frac{C_1}{\rho} \frac{\partial\eta}{\partial s} - \frac{C_3}{\rho} \frac{\partial\eta}{\partial n} = 0 \qquad (G-15)$$

$$C_4 \left[1 + \frac{n}{R} \right] \frac{\partial\eta}{\partial n} = 0 \qquad (G-16)$$

$$2C_1 \kappa^2 W \frac{\partial\eta}{\partial n} - C_1 v \frac{\partial\eta}{\partial n} = 0 \qquad (G-17)$$

These equations can be rewritten in matrix form as.

$$\begin{bmatrix} U \frac{\partial\eta}{\partial s} + V \frac{\partial\eta}{\partial n} & \frac{\partial\eta}{\partial n} & 0 & \frac{\partial\eta}{\partial s} \\[2ex] \frac{1}{\rho} \frac{\partial\eta}{\partial s} & 0 & -\frac{1}{\rho} \frac{\partial\eta}{\partial n} & 0 \\[2ex] 0 & 0 & 0 & \left[1 + \frac{n}{R} \right] \frac{\partial\eta}{\partial n} \\[2ex] (2\kappa^2 W - v) \frac{\partial\eta}{\partial n} & 0 & 0 & 0 \end{bmatrix} \begin{bmatrix} C_1 \\[2ex] C_2 \\[2ex] C_3 \\[2ex] C_4 \end{bmatrix} = 0$$
$$(G-18)$$

The determinant of the coefficient matrix, which must equal zero, is

$$\frac{\partial\eta}{\partial n}^4 \left[\frac{1 + n/R}{\rho} (2\kappa^2 W - v) \right] = 0 \qquad (G-19)$$

Since in the above equation the term in the brackets is generally
different from zero, one concludes that

$$\frac{\partial\eta}{\partial n} = 0 \qquad (G-20)$$

It is interesting to note that if the viscous and turbulent stress terms
were zero, the characteristic line would not be defined. This is as it
should be, since the potential flow equations are elliptic and have
imaginary characteristics. In the present case, however, we have that

168

$$\frac{\partial \eta}{\partial n} = 0 \qquad\qquad (G-21)$$

Now, the procedure of Reynolds for finding the characteristic lines is now to write an equation for a line segment of a characteristic.

$$d\eta = \frac{\partial \eta}{\partial n} dn + \frac{\partial \eta}{\partial s} ds \qquad\qquad (G-22)$$

Since this is an equation for a characteristic line, which is a line of constant η, $d\eta$ must be zero. But it has been shown that $\partial \eta / \partial n$ is also zero. For the above equation to balance, then, it must be that ds is zero. That is, lines of constant η have the equation: s equals a constant. They are lines normal to the surface.

To find the other characteristic, it is necessary to consider traveling along constant ξ lines. This leads to four more equations.

$$\begin{bmatrix} U\frac{\partial \xi}{\partial s} + V\frac{\partial \xi}{\partial n} & \frac{\partial \xi}{\partial n} & 0 & \frac{\partial \xi}{\partial s} \\ \frac{1}{\rho}\frac{\partial \xi}{\partial s} & 0 & \frac{-1}{\rho}\frac{\partial \xi}{\partial n} & 0 \\ 0 & 0 & 0 & 1 + \frac{n}{R}\frac{\partial \xi}{\partial n} \\ (2\kappa^2 W \frac{\partial \xi}{\partial s} - v) & 0 & 0 & 0 \end{bmatrix} \begin{bmatrix} c_1 \\ c_2 \\ c_3 \\ c \end{bmatrix} = 0 \qquad (G-23)$$

This yields, as before, an equation analogous to Eq. (21).

$$\frac{\partial \xi}{\partial n} = 0 \qquad\qquad (G-24)$$

And so we find that lines of constant ξ are lines of constant s. The two sets of characteristic lines are coincident, which implies that the equations are parabolic.

It should be pointed out that this result is not dependent on what sort of substitution is made for $\overline{uv}$ in the s component momentum equation.

Appendix H

CALCULATION OF BOUNDARY LAYER MASS FLUX ON A CURVED WALL

The rate of entrainment of freestream fluid into a boundary layer is defined as the rate growth of boundary layer mass flux. For a two-dimensional, incompressible boundary layer, the entrainment per unit width is:

$$E(x) = \frac{d}{dx} \int_0^\delta \rho U dy = \frac{d}{dx} \rho \int_0^\delta U dy \tag{H-1}$$

On a flat wall the integral in the above expression can be recast in terms of standard integral parameters, as follows. First, multiply and divide by U_∞:

$$I = \int_0^\delta U \, dy = U_\infty \int_0^\delta \frac{U}{U_\infty} dy \tag{H-2}$$

Now add and subtract 1 from the integrand:

$$I = U_\infty \int_0^\delta \left[(1-1) + \frac{U}{U_\infty} dy \right] = U_\infty \left[\int_0^\delta 1 dy - \int_0^\delta 1 - \frac{U}{U_\infty} dy \right] \tag{H-3}$$

which reduces to

$$I = U_\infty [\delta - \delta^*] \tag{H-4}$$

Over a curved wall, the situation is slightly more complicated. The definition of entrainment is, of course, the same. Now, however, there is no single scaling velocity, U_∞. The first step is to add and subtract the potential flow velocity, which is a function of n.

$$I = \int_0^\delta U \, dn = \int_0^\delta (U_p - U_p + U) \, dn \tag{H-5}$$

$$I = \int_0^\delta U_p dn - \int_0^\delta (U_p - U) \, dn \tag{H-6}$$

The second integral on the RHS is (as has been pointed out by Honami) the mass flux deficit of the boundary layer. This can be used to define the displacement thickness as:

$$\int_0^\delta (U_p - U) \, dn = \int_0^{\delta_1} (U_p - U) \, dn \qquad (H\text{-}7)$$

Equation (I-6) can then be written as

$$I = \int_0^\delta U_p \, dn - \int_0^{\delta_1} U_p \, dn \qquad (H\text{-}8)$$

Over a curved wall, we have

$$U_p = U_{pw} \frac{Ro}{Ro + n} \qquad (H\text{-}9)$$

where Ro is the wall radius of curvature.

Substituting in and performing the integration leads directly to a simple expression:

$$E = \frac{d}{dx} \left[U_{pw} \, \rho \, Ro \, \ell n \, \frac{Ro + \delta}{Ro + \delta_1} \right] \qquad (H\text{-}10)$$

This is the expression used to generate Figures 15 and 35.

Appendix I

TABULATED DATA

Notes for Tabulated Data

1. **Mean Velocity Profiles -- Pitot Probes**

   a. y/DEL is y/δ.

   b. U/U_p is U divided by the local potential flow velocity, not U divided by U_{pw}.

   c. DY PR is the measured dynamic pressure -- total pressure minus wall static pressure -- in centimeters of water.

2. **Hot-Wire Data**

   a. TURBIN is the measured turbulence intensity, $\sqrt{\overline{u^2}}/U_{pw}$.

   b. DISP is the non-dimensional dissipation $\varepsilon\delta/u_\tau^3$.

3. **Shear-Stress Profiles**

   a. UTSQ is $(u_\tau)^2$.

   b. A is the structural coefficient $-uv/q^2$.

   c. SHEAR CORR is

   $$-\overline{uv}/\sqrt{\overline{u^2}} \cdot \sqrt{\overline{v^2}}\ .$$

   d. ANISOTROPY is b^2, where b_{ij} is the second rank tensor calculated from the Reynolds stress tensor R_{ij} as

   $$b_{ij} = \frac{R_{ij} - q^2\frac{\delta_{ij}}{3}}{q^2}\ .$$

   where δ_{ij} is the Kroneker Delta and q^2 is R_{ij}.

4. **Mixing Length Profiles**

   a. UCAL is the value of U/U_{pw} calculated by the system.

   b. PROD is the production term in the TKE equation, non-dimensionalized as

172

$$\frac{\overline{uv}}{u_\tau^2} \cdot \frac{\partial(U/U_{pw})}{\partial(y/\delta)} \quad .$$

c. L/LO is the measured mixing length divided by the flat-wall mixing length, where LO is given by 0.41n (or 0.41y), when n (or y) is less than 0.085δ, and LO equals 0.085δ for n (or y) greater than 0.085.

d. RIC is the Richardson number.

e. ED RE is the eddy Reynolds number, where eddy Reynolds number is

$$L \sqrt{\overline{uv}}/\nu \quad .$$

f. VELGRD is the velocity gradient non-dimensionalized as

$$\frac{\partial(U/U_{pw})}{\partial(y/\delta)} \quad .$$

173

Wall static pressure distribution -- FIRST EXPERIMENT

TAP	s, cm	C_p
0	- 15.54	0.00
1	- 9.53	.006
2	- 7.62	.014
3	- 5.08	.021
4	- 2.54	.012
5	0.0	- .006
6	2.54	- .022
7	5.08	- .029
8	7.62	- .016
9	10.16	.003
10	13.34	.004
11	17.78	- .004
12	22.86	- .005
13	27.94	.002
14	33.02	.002
15	38.10	.001
16	43.10	- .001
17	48.26	.001
18	53.34	.006
19	59.69	.009
20	63.50	.001
21	66.04	- .007
22	68.58	- .008
23	71.12	- .004
24	73.66	.002
25	76.20	.005
26	78.74	.006
27	81.28	.004
28	83.82	.001
29	86.36	.000
30	88.90	.000
31	93.98	.000
32	96.52	.004
33	99.06	- .002
34	104.14	- .001
35	109.22	- .002
36	114.30	- .001
37	119.38	- .001
38	124.46	.000

$$C_p = \frac{P - P_{TAP_0}}{\tfrac{1}{2} \rho U_{pw}^2}$$

$s = 0$ at start of curvature

174

EXPT. 1, FLOW SKEW ANGLE (REL. TO FREE STRM.) AT STN. 4
FLOW ANGLE IN DEG, Z IN CM.

N/DEL	Z=-12.5	Z=-6.2	Z=0.0	Z=6.2	Z=12.5
0.98	0.00	0.00	0.00	0.00	0.00
0.81	0.08	-0.16	-0.04	-0.17	-0.17
0.65	0.42	0.04	-0.08	-0.21	-0.08
0.49	0.62	0.00	0.00	-0.12	-0.25
0.33	0.71	0.08	-0.04	-0.17	-0.42
0.26	0.87	0.25	-0.01	-0.13	-0.38
0.20	1.03	0.27	0.27	-0.22	-0.60
0.13	1.06	0.18	0.18	-0.32	-0.82
0.07	1.22	0.22	0.34	-0.28	-1.08

EXPT. 1, FLOW SKEW ANGLE (REL. TO FREE STRM. AT STN. 5
FLOW ANGLE Z IN CM.

N/DEL	Z=-12.5	Z= -6.2	Z = 0.0	Z = 6.2	Z=12.5
0.91	0.025	-0.50	-0.80	-0.63	-1.54
0.75	0.33	-0.41	-0.79	-0.67	-1.42
0.60	0.42	-0.33	-0.83	-0.83	-1.46
0.45	0.62	-0.37	-0.75	-0.88	-1.63
0.30	0.71	-0.16	-0.67	-0.92	-1.67
0.24	0.87	-0.26	-0.63	-0.88	-1.76
0.18	0.90	-0.22	-0.60	-1.10	-1.73
0.12	1.06	-0.07	-0.57	-1.19	-2.19
0.06	1.72	-0.15	-0.53	-1.53	-2.66

EXPT. 1, FLOW SKEW ANGLE (REL. TO FREE STRM.) AT STN. 6
FLOW ANGLE Z IN CM.

N/DEL	Z=-12.5	Z= -6.2	Z = 0.0	Z = 6.2	Z=12.5
0.87	0.00	0.00	-0.12	-0.62	-1.00
0.73	0.12	-0.12	-0.25	-0.87	-1.37
0.58	0.25	0.00	-0.25	-1.00	-1.75
0.44	0.50	0.00	-0.25	-1.25	-2.00
0.29	0.75	0.12	-0.25	-1.50	-2.37
0.23	0.75	0.00	-0.38	-1.62	-2.62
0.17	1.00	0.12	-0.37	-1.75	-3.25
0.12	1.50	0.50	-0.50	-1.87	-3.50
0.06	2.38	0.87	-0.38	-2.00	-4.50

EXPT. 1, FLOW SKEW ANGLE (REL. TO FREE STRM.) AT STN. 7
FLOW ANGLE Z IN CM.

N/DEL	Z=-12.5	Z= -6.2	Z = 0.0	Z = 6.2	Z=12.5
0.85	-0.13	-1.13	-1.00	-1.75	-2.00
0.71	0.21	-1.17	-0.79	-2.00	-2.25
0.56	0.42	-0.83	-0.83	-2.12	-2.62
0.42	0.75	-0.63	-0.75	-2.25	-3.25
0.28	1.08	-0.29	-0.67	-2.62	-4.00
0.23	1.37	-0.13	-0.51	-2.75	-4.14
0.17	1.67	-0.10	-0.60	-2.87	-4.50
0.11	2.06	0.31	-0.57	-3.00	-5.00
0.06	2.47	0.47	-0.66	-3.00	-5.25

EXPT. 1, FLOW SKEW ANGLE (REL. TO FREE STRM.) AT STN. 8
FLOW ANGLE Z IN CM.

N/DEL	Z=-12.5	Z= -6.2	Z = 0.0	Z = 6.2	Z=12.5
0.91	0.13	-0.63	-0.13	-0.25	-0.50
0.76	0.46	-0.29	-0.04	-0.04	-0.92
0.61	0.92	-0.08	0.04	-0.21	-1.08
0.46	1.38	0.25	0.25	-0.25	-1.75
0.30	2.08	0.83	0.08	-0.54	-2.29
0.24	2.62	1.12	0.12	-0.63	-2.63
0.12	3.31	1.56	0.06	-0.82	-2.82
0.06	4.22	1.59	0.22	-1.03	-3.16

EXPT. 1, FLOW SKEW ANGLE (REL. TO FREE STRM.) AT STN. 9
FLOW ANGLE Z IN CM.

N/DEL	Z=-12.5	Z= -6.2	Z = 0.0	Z = 6.2	Z=12.5
0.83	0.38	-0.75	0.00	0.25	0.00
0.69	0.58	-0.67	0.08	0.08	-0.17
0.55	0.79	-0.46	0.04	-0.04	-1.00
0.41	1.25	-0.13	0.13	-0.13	-1.00
0.28	1.83	0.21	0.08	-0.29	-1.17
0.22	2.12	0.49	0.12	-0.38	-1.26
0.17	2.40	0.65	0.15	-0.60	-1.23
0.11	2.81	0.81	0.18	-0.57	-1.32
0.06	3.22	0.84	0.34	-0.41	-1.53

EXPT. 1, FLOW SKEW ANGLE (REL. TO FREE STRM.) AT STN. 10
FLOW ANGLE Z IN CM.

N/DEL	Z=-12.5	Z= -6.2	Z = 0.0	Z = 6.2	Z=12.5
0.78	-0.63	-0.50	-0.25	-0.38	-0.50
0.65	-0.54	-0.54	0.29	-0.42	-0.79
0.52	-0.33	-0.33	-0.33	-0.83	-1.33
0.39	0.25	-0.13	-0.25	-0.38	-1.75
0.26	1.08	0.08	-0.29	-0.92	-1.79
0.21	1.24	0.12	-0.26	-1.01	-1.76
0.16	1.65	0.40	-0.35	-1.10	-1.85
0.10	1.93	0.68	-0.44	-1.19	-1.94
0.05	2.34	0.72	-0.41	-1.28	-2.03

FIRST EXPT., STN 1, S = -71.75 CM.,   UPW = 16.00 M/SEC

PT	Y/DEL	U/UP	DY PR	YPLUS	UPLUS	CF/2
1	0.016	0.433	0.292	19.	11.2	0.00130
2	0.020	0.453	0.320	23.	11.7	0.00132
3	0.024	0.493	0.378	28.	12.7	0.00143
4	0.030	0.522	0.424	35.	13.5	0.00147
5	0.036	0.545	0.462	43.	14.0	0.00150
6	0.043	0.564	0.495	51.	14.5	0.00151
7	0.052	0.581	0.526	61.	15.0	0.00151
8	0.061	0.597	0.554	71.	15.4	0.00151
9	0.069	0.606	0.572	81.	15.6	0.00150
10	0.080	0.621	0.599	94.	16.0	0.00150
11	0.101	0.642	0.640	118.	16.6	0.00150
12	0.129	0.666	0.688	151.	17.2	0.00150
13	0.164	0.691	0.742	192.	17.8	0.00151
14	0.211	0.720	0.805	247.	18.6	0.00153
15	0.270	0.752	0.876	316.	19.4	0.00156
16	0.345	0.787	0.960	404.	20.3	0.00160
17	0.443	0.831	1.069	518.	21.4	0.00167
18	0.568	0.877	1.191	665.	22.6	0.00174
19	0.693	0.919	1.308	811.	23.7	0.00182
20	0.822	0.956	1.415	963.	24.7	0.00189
21	0.935	0.980	1.486	1095.	25.3	0.00192
22	1.003	0.990	1.516	1174.	25.5	0.00193
23	1.202	0.999	1.542	1407.	25.8	0.00189
24	1.323	1.000	1.544	1549.	25.8	0.00186

DISP. THICKNESS = 0.504 CM.   MOMT. THICKESS =0.370 CM.

SHAPE FACTOR = 1.362   DELTA 99 = 2.938 CM.

MOMENTUM THICKNESS REYNOLDS NO. = 3802.   CF/2 = 0.00150

FIRST EXPT., STN 2, S = -41.27 CM., UPW = 16.00 M/SEC

PT	Y/DEL	U/UP	DY PR	YPLUS	UPLUS	CF/2
1	0.013	0.443	0.302	19.	11.6	0.00134
2	0.016	0.481	0.356	23.	12.6	0.00144
3	0.020	0.503	0.389	28.	13.1	0.00146
4	0.025	0.514	0.406	35.	13.4	0.00142
5	0.029	0.545	0.457	42.	14.3	0.00148
6	0.035	0.562	0.485	50.	14.7	0.00148
7	0.042	0.575	0.508	60.	15.0	0.00146
8	0.049	0.589	0.533	70.	15.4	0.00146
9	0.056	0.600	0.554	80.	15.7	0.00146
10	0.065	0.613	0.579	93.	16.0	0.00146
11	0.082	0.633	0.617	117.	16.6	0.00145
12	0.104	0.655	0.660	149.	17.1	0.00145
13	0.133	0.679	0.711	190.	17.8	0.00145
14	0.171	0.791	0.757	244.	18.3	0.00145
15	0.219	0.733	0.828	311.	19.2	0.00148
16	0.280	0.764	0.899	398.	20.0	0.00151
17	0.359	0.803	0.993	511.	21.0	0.00156
18	0.460	0.847	1.107	656.	22.2	0.00163
19	0.561	0.885	1.209	800.	23.2	0.00170
20	0.666	0.923	1.313	949.	24.1	0.00176
21	0.759	0.952	1.397	1081.	24.9	0.00182
22	0.813	0.964	1.435	1158.	25.2	0.00184
23	0.974	0.989	1.509	1388.	25.9	0.00186
24	1.072	0.994	1.524	1528.	26.0	0.00184
25	1.177	0.993	1.524	1677.	26.0	0.00181
26	1.282	0.994	1.527	1827.	26.0	0.00178

DISP. THICKNESS = 0.593 CM.   MOMT. THICKESS = 0.439 CM.

SHAPE FACTOR = 1.350   DELTA 99 = 3.625 CM.

MOMENTUM THICKNESS REYNOLDS NO. = 4517.   CF/2 = 0.00146

FIRST EXPT., STN 4, S = 16.20 CM.,   UPW = 16.09 M/SEC

PT	Y/DEL	U/UP	DY PR	YPLUS	UPLUS	CF/2
1	0.012	0.371	0.221	18.	10.5	0.00100
2	0.014	0.410	0.269	21.	11.6	0.00111
3	0.017	0.438	0.307	26.	12.3	0.00115
4	0.021	0.474	0.361	33.	13.4	0.00123
5	0.026	0.492	0.389	39.	13.9	0.00124
6	0.031	0.507	0.414	47.	14.3	0.00124
7	0.037	0.522	0.439	56.	14.7	0.00124
8	0.043	0.540	0.470	65.	15.2	0.00125
9	0.049	0.554	0.495	75.	15.6	0.00126
10	0.058	0.569	0.523	88.	16.0	0.00127
11	0.072	0.595	0.574	110.	16.7	0.00129
12	0.091	0.622	0.627	139.	17.4	0.00130
13	0.117	0.652	0.691	178.	18.2	0.00133
14	0.149	0.684	0.762	228.	19.1	0.00136
15	0.190	0.713	0.831	290.	19.8	0.00137
16	0.244	0.743	0.984	372.	20.5	0.00138
17	0.313	0.777	0.988	477.	21.3	0.00140
18	0.402	0.814	1.085	613.	22.2	0.00142
19	0.490	0.848	1.173	747.	22.9	0.00145
20	0.582	0.882	1.265	887.	23.7	0.00148
21	0.662	0.909	1.336	1009.	24.2	0.00150
22	0.710	0.925	1.379	1082.	24.5	0.00152
23	0.851	0.964	1.483	1296.	25.3	0.00155
24	0.937	0.982	1.532	1427.	25.5	0.00155
25	1.029	0.994	1.562	1567.	25.6	0.00153
26	1.120	0.993	1.560	1707.	25.4	0.00148
27	1.224	1.000	1.580	1865.	25.4	0.00146

DISP. THICKNESS = 0.720 CM.   MOMT. THICKESS =0.523 CM.

SHAPE FACTOR = 1.377   DELTA 99 = 4.149 CM.

MOMENTUM THICKNESS REYNOLDS NO. = 5424.   CF/2 = 0.00125

FIRST EXPT., STN 5, S = 33.65 CM., UPW = 16.15 M/SEC

PT	Y/DEL	U/UP	DY PR	YPLUS	UPLUS	CF/2
1	0.011	0.336	0.180	16.	10.2	0.00085
2	0.014	0.372	0.221	20.	11.3	0.00094
3	0.017	0.403	0.259	24.	12.2	0.00100
4	0.021	0.427	0.292	30.	13.0	0.00103
5	0.025	0.447	0.320	36.	13.6	0.00105
6	0.030	0.466	0.348	43.	14.1	0.00107
7	0.036	0.480	0.371	52.	14.6	0.00107
8	0.042	0.494	0.394	60.	15.0	0.00108
9	0.048	0.507	0.414	69.	15.4	0.00108
10	0.057	0.523	0.442	81.	15.8	0.00109
11	0.072	0.549	0.488	103.	16.6	0.00111
12	0.091	0.577	0.541	129.	17.4	0.00114
13	0.115	0.609	0.605	165.	18.3	0.00118
14	0.148	0.645	0.678	211.	19.4	0.00122
15	0.188	0.684	0.765	269.	20.5	0.00127
16	0.241	0.721	0.851	344.	21.5	0.00131
17	0.309	0.761	0.947	442.	22.5	0.00135
18	0.397	0.801	1.049	567.	23.5	0.00138
19	0.483	0.838	1.143	691.	24.4	0.00142
20	0.574	0.872	1.232	821.	25.2	0.00145
21	0.633	0.898	1.303	934.	25.8	0.00147
22	0.700	0.915	1.346	1001.	26.1	0.00149
23	0.839	0.957	1.458	1200.	27.0	0.00152
24	0.923	0.978	1.514	1321.	27.4	0.00154
25	1.014	0.992	1.552	1450.	27.6	0.00153
26	1.105	0.998	1.567	1580.	27.5	0.00150
27	1.207	1.000	1.572	1726.	27.4	0.00146

DISP. THICKNESS = 0.789 CM.   MOMT. THICKESS =0.552 CM.

SHAPE FACTOR = 1.429   DELTA 99 = 4.208 CM.

MOMENTUM THICKNESS REYNOLDS NO. = 5711.   CF/2 = 0.00108

FIRST EXPT., STN 6, S = 50.80 CM., UPW = 16.10 M/SEC

PT	Y/DEL	U/UP	DY FR	YPLUS	UPLUS	CF/2
1	0.011	0.301	0.145	15.	9.7	0.00070
2	0.013	0.336	0.180	19.	10.9	0.00079
3	0.016	0.365	0.213	23.	11.8	0.00085
4	0.020	0.394	0.249	29.	12.8	0.00090
5	0.024	0.414	0.274	34.	13.4	0.00092
6	0.029	0.432	0.300	41.	14.0	0.00094
7	0.035	0.446	0.320	49.	14.4	0.00094
8	0.041	0.461	0.343	57.	14.9	0.00095
9	0.046	0.472	0.361	65.	15.2	0.00096
10	0.055	0.488	0.336	77.	15.7	0.00097
11	0.069	0.509	0.422	97.	16.4	0.00097
12	0.087	0.536	0.470	122.	17.2	0.00100
13	0.111	0.569	0.531	156.	18.3	0.00104
14	0.142	0.607	0.605	200.	19.4	0.00109
15	0.181	0.650	0.693	254.	20.7	0.00116
16	0.232	0.693	0.790	326.	22.0	0.00122
17	0.297	0.742	0.902	417.	23.4	0.00129
18	0.381	0.786	1.011	535.	24.6	0.00133
19	0.464	0.822	1.102	653.	25.5	0.00137
20	0.551	0.857	1.194	775.	26.4	0.00140
21	0.628	0.885	1.267	883.	27.0	0.00143
22	0.673	0.901	1.308	945.	27.4	0.00145
23	0.806	0.945	1.425	1133.	28.4	0.00149
24	0.887	0.969	1.488	1247.	28.9	0.00151
25	0.974	0.987	1.537	1369.	29.2	0.00151
26	1.061	0.996	1.560	1491.	29.3	0.00149
27	1.160	0.999	1.567	1630.	29.1	0.00145
28	1.305	1.000	1.570	1834.	28.8	0.00139

DISP. THICKNESS = 0.872 CM.   MOMT. THICKESS = 0.592 CM.

SHAPE FACTOR = 1.474   DELTA 99 = 4.380 CM.

MOMENTUM THICKNESS REYNOLDS NO. = 6156.   CF/2 = 0.00095

FIRST EXPT., STN 7, S = 64.13 CM., UPW = 16.08 M/SEC

PT	Y/DEL	U/UP	DY PR	YPLUS	UPLUS	CF/2
1	0.011	0.303	0.147	15.	9.9	0.00071
2	0.013	0.338	0.183	18.	11.1	0.00080
3	0.016	0.367	0.216	23.	12.0	0.00086
4	0.020	0.392	0.246	28.	12.8	0.00089
5	0.024	0.411	0.272	34.	13.5	0.00092
6	0.028	0.426	0.292	40.	13.9	0.00092
7	0.034	0.440	0.312	48.	14.4	0.00092
8	0.040	0.453	0.333	56.	14.8	0.00093
9	0.045	0.465	0.351	64.	15.2	0.00093
10	0.053	0.476	0.368	76.	15.5	0.00093
11	0.067	0.497	0.404	96.	16.2	0.00094
12	0.085	0.524	0.450	121.	17.1	0.00096
13	0.108	0.554	0.505	154.	18.0	0.00100
14	0.138	0.591	0.577	197.	19.2	0.00105
15	0.176	0.631	0.658	251.	20.4	0.00110
16	0.226	0.679	0.759	322.	21.8	0.00117
17	0.289	0.729	0.874	412.	23.3	0.00125
18	0.371	0.777	0.991	528.	24.6	0.00131
19	0.452	0.815	1.087	644.	25.6	0.00135
20	0.537	0.850	1.176	765.	26.5	0.00138
21	0.611	0.877	1.247	871.	27.2	0.00141
22	0.655	0.895	1.293	933.	27.6	0.00143
23	0.785	0.939	1.410	1118.	28.6	0.00147
24	0.864	0.963	1.471	1230.	29.1	0.00149
25	0.948	0.982	1.521	1351.	29.5	0.00150
26	1.033	0.995	1.554	1471.	29.6	0.00149
27	1.129	1.000	1.567	1608.	29.5	0.00145

DISP. THICKNESS = 0.911 CM.   MOMT. THICKESS =0.612 CM.

SHAPE FACTOR = 1.489   DELTA 99 = 4.499 CM.

MOMENTUM THICKNESS REYNOLDS NO. = 6363.   CF/2 = 0.00093

FIRST EXPT., STN 8, S = 81.91 CM., UPW = 16.02 M/SEC

PT	Y/DEL	U/UP	DY PR	YPLUS	UPLUS	CF/2
1	0.012	0.336	0.175	16.	10.6	0.00085
2	0.014	0.360	0.201	19.	11.3	0.00089
3	0.017	0.390	0.236	23.	12.3	0.00096
4	0.021	0.415	0.267	29.	13.0	0.00099
5	0.026	0.430	0.287	35.	13.5	0.00100
6	0.030	0.443	0.305	42.	13.9	0.00099
7	0.037	0.458	0.325	50.	14.4	0.00100
8	0.043	0.467	0.338	58.	14.7	0.00099
9	0.049	0.477	0.353	67.	15.0	0.00099
10	0.057	0.491	0.373	78.	15.4	0.00099
11	0.072	0.510	0.404	98.	16.0	0.00100
12	0.091	0.534	0.442	125.	16.8	0.00101
13	0.117	0.564	0.493	160.	17.7	0.00105
14	0.149	0.602	0.561	204.	18.9	0.00111
15	0.190	0.648	0.650	260.	20.3	0.00119
16	0.243	0.698	0.754	333.	21.9	0.00129
17	0.312	0.755	0.884	427.	23.7	0.00140
18	0.400	0.812	1.021	547.	25.5	0.00152
19	0.487	0.852	1.123	666.	26.7	0.00158
20	0.579	0.885	1.212	791.	27.8	0.00164
21	0.659	0.908	1.278	901.	28.5	0.00167
22	0.707	0.923	1.318	966.	29.0	0.00170
23	0.846	0.961	1.430	1156.	30.2	0.00177
24	0.931	0.980	1.486	1273.	30.8	0.00179
25	1.022	0.993	1.527	1398.	31.2	0.00181
26	1.114	0.999	1.544	1522.	31.4	0.00180
27	1.217	1.000	1.547	1664.	31.4	0.00177

DISP. THICKNESS = 0.805 CM.   MOMT. THICKESS = 0.543 CM.

SHAPE FACTOR = 1.481   DELTA 99 = 4.173 CM.

MOMENTUM THICKNESS REYNOLDS NO. = 5586.   CF/2 = 0.00101

FIRST EXPT., STN 9, S = 97.16 CM., UPW = 16.00 M/SEC

PT	Y/DEL	U/UP	DY PR	YPLUS	UPLUS	CF/2
1	0.010	0.320	0.160	16.	10.1	0.00079
2	0.013	0.347	0.188	19.	11.0	0.00085
3	0.015	0.383	0.229	23.	12.1	0.00094
4	0.019	0.408	0.259	29.	12.9	0.00097
5	0.023	0.427	0.284	35.	13.5	0.00099
6	0.028	0.443	0.305	41.	14.0	0.00100
7	0.033	0.459	0.328	49.	14.5	0.00101
8	0.039	0.470	0.343	58.	14.8	0.00100
9	0.044	0.478	0.356	66.	15.1	0.00099
10	0.051	0.490	0.373	77.	15.5	0.00100
11	0.064	0.505	0.396	96.	16.0	0.00099
12	0.082	0.524	0.427	123.	16.6	0.00099
13	0.105	0.549	0.467	158.	17.4	0.00101
14	0.135	0.575	0.513	202.	18.2	0.00103
15	0.172	0.611	0.579	257.	19.3	0.00108
16	0.220	0.653	0.660	330.	20.6	0.00115
17	0.283	0.706	0.772	423.	22.3	0.00125
18	0.362	0.762	0.899	542.	24.1	0.00135
19	0.441	0.812	1.021	661.	25.7	0.00146
20	0.524	0.851	1.123	784.	26.9	0.00153
21	0.597	0.880	1.199	893.	27.8	0.00158
22	0.640	0.895	1.240	957.	28.3	0.00161
23	0.767	0.936	1.356	1147.	29.6	0.00169
24	0.843	0.958	1.420	1262.	30.3	0.00172
25	0.926	0.978	1.478	1385.	30.9	0.00176
26	1.009	0.991	1.519	1509.	31.4	0.00177
27	1.102	0.999	1.542	1649.	31.6	0.00177
28	1.240	1.000	1.544	1855.	31.6	0.00173

DISP. THICKNESS = 0.940 CM.   MOMT. THICKESS =0.629 CM.

SHAPE FACTOR = 1.495   DELTA 99 = 4.609 CM.

MOMENTUM THICKNESS REYNOLDS NO. = 6456.   CF/2 = 0.00100

FIRST EXPT., STN 10, S = 112.4 CM., UPW = 16.10 M/SEC

PT	Y/DEL	U/UP	DY PR	YPLUS	UPLUS	CF/2
1	0.010	0.334	0.175	16.	10.6	0.00084
2	0.012	0.365	0.208	19.	11.6	0.00091
3	0.015	0.390	0.239	23.	12.4	0.00096
4	0.018	0.405	0.257	29.	12.9	0.00095
5	0.022	0.430	0.290	35.	13.7	0.00099
6	0.026	0.443	0.307	41.	14.1	0.00099
7	0.031	0.457	0.328	50.	14.6	0.00099
8	0.036	0.466	0.340	58.	14.8	0.00098
9	0.042	0.478	0.358	66.	15.2	0.00099
10	0.048	0.488	0.373	77.	15.5	0.00098
11	0.061	0.505	0.399	97.	16.1	0.00098
12	0.078	0.522	0.427	123.	16.6	0.00098
13	0.100	0.545	0.465	158.	17.3	0.00099
14	0.127	0.570	0.508	201.	18.1	0.00101
15	0.163	0.600	0.564	258.	19.1	0.00104
16	0.208	0.636	0.632	330.	20.2	0.00109
17	0.267	0.682	0.726	423.	21.7	0.00117
18	0.342	0.734	0.843	542.	23.4	0.00126
19	0.417	0.783	0.958	661.	24.9	0.00136
20	0.495	0.830	1.077	785.	26.4	0.00146
21	0.564	0.864	1.168	894.	27.5	0.00153
22	0.605	0.882	1.217	958.	28.1	0.00156
23	0.725	0.927	1.344	1148.	29.5	0.00165
24	0.797	0.950	1.410	1263.	30.2	0.00169
25	0.875	0.970	1.471	1387.	30.9	0.00173
26	0.953	0.983	1.511	1511.	31.3	0.00174
27	1.042	0.996	1.549	1651.	31.7	0.00175
28	1.172	1.000	1.562	1657.	31.8	0.00173

DISP. THICKNESS = 1.008 CM.   MOMT. THICKESS = 0.672 CM.

SHAPE FACTOR = 1.501   DELTA 99 = 4.875 CM.

MOMENTUM THICKNESS REYNOLDS NO. = 6943.   CF/2 = 0.00099

FIRST EXPT., SINGLE WIRE DATA AT STN. 1, S = -71.75 CM.

PT	Y/DEL	U/UP	YPLUS	UPLUS	TURB.IN.	DISP
1	0.005	0.213	6.	5.5	0.0670	10.1
2	0.010	0.299	11.	7.7	0.0896	17.8
3	0.015	0.407	18.	10.5	0.0962	15.6
4	0.021	0.461	24.	11.9	0.0935	14.5
5	0.025	0.497	29.	12.8	0.0901	13.4
6	0.031	0.525	36.	13.6	0.0863	12.6
7	0.037	0.547	44.	14.1	0.0835	12.0
8	0.045	0.568	52.	14.7	0.0811	11.3
9	0.053	0.585	62.	15.1	0.0788	10.5
10	0.062	0.600	73.	15.5	0.0777	9.9
11	0.071	0.610	83.	15.8	0.0768	9.5
12	0.084	0.623	98.	16.1	0.0753	8.8
13	0.106	0.646	124.	16.7	0.0745	7.9
14	0.134	0.673	156.	17.4	0.0732	6.8
15	0.170	0.695	199.	18.0	0.0718	6.1
16	0.218	0.728	255.	18.8	0.0705	5.2
17	0.278	0.758	325.	19.6	0.0686	4.7
18	0.356	0.794	416.	20.5	0.0657	4.0
19	0.456	0.837	533.	21.6	0.0608	3.3
20	0.586	0.885	684.	22.9	0.0551	2.6
21	0.714	0.928	834.	24.0	0.0461	1.9
22	0.848	0.963	990.	24.9	0.0365	1.3
23	0.964	0.987	1127.	25.5	0.0250	0.9
24	1.034	0.993	1208.	25.7	0.0191	0.8
25	1.239	1.000	1447.	25.9	0.0049	0.6
26	1.364	0.986	1593.	25.5	0.0023	0.5

FIRST EXPT., SINGLE WIRE DATA AT STN. 2, S = -41.27 CM.

PT	Y/DEL	U/UP	YPLUS	UPLUS	TURE.IN.	DISP
1	0.005	0.233	6.	6.0	0.0744	20.6
2	0.009	0.340	11.	8.8	0.0943	20.1
3	0.013	0.417	17.	10.8	0.0974	18.2
4	0.018	0.466	23.	12.1	0.0945	16.7
5	0.022	0.499	28.	12.9	0.0919	15.2
6	0.027	0.522	35.	13.5	0.0876	14.7
7	0.033	0.541	42.	14.0	0.0855	13.9
8	0.039	0.563	50.	14.6	0.0820	13.2
9	0.047	0.578	60.	15.0	0.0797	12.4
10	0.055	0.594	70.	15.4	0.0785	11.6
11	0.062	0.605	81.	15.7	0.0777	11.2
12	0.073	0.621	95.	16.1	0.0781	10.3
13	0.093	0.643	120.	16.7	0.0757	9.2
14	0.117	0.666	151.	17.3	0.0748	8.0
15	0.149	0.691	192.	17.9	0.0740	7.2
16	0.191	0.716	247.	18.6	0.0726	6.3
17	0.244	0.745	314.	19.3	0.0702	5.6
18	0.311	0.778	402.	20.2	0.0685	4.9
19	0.400	0.808	516.	21.0	0.0652	4.3
20	0.513	0.863	662.	22.4	0.0591	3.4
21	0.625	0.902	807.	23.4	0.0535	2.8
22	0.742	0.935	958.	24.3	0.0457	2.1
23	0.844	0.965	1090.	25.0	0.0378	1.6
24	0.905	0.978	1168.	25.4	0.0306	1.3
25	1.085	1.001	1400.	26.0	0.0159	0.9
26	1.194	1.001	1541.	26.0	0.0065	0.7
27	1.311	1.000	1692.	25.9	0.0028	0.7
28	1.428	0.996	1843.	25.8	0.0014	0.7

FIRST EXPT., SINGLE WIRE DATA AT STN. 3, S = -0.96 CM.

PT	Y/DEL	U/UP	YPLUS	UPLUS	TURB.IN.	DISP
1	0.003	0.170	5.	4.4	0.0525	8.0
2	0.007	0.228	11.	5.9	0.0688	8.7
3	0.011	0.365	17.	9.5	0.0930	22.3
4	0.015	0.432	24.	11.2	0.0950	22.3
5	0.018	0.480	29.	12.5	0.0913	19.2
6	0.022	0.511	36.	13.3	0.0870	18.1
7	0.026	0.538	43.	14.0	0.0833	16.5
8	0.032	0.563	51.	14.6	0.0826	15.1
9	0.038	0.580	61.	15.1	0.0788	14.2
10	0.044	0.591	72.	15.4	0.0757	13.8
11	0.050	0.603	82.	15.7	0.0749	12.9
12	0.059	0.618	96.	16.1	0.0743	11.7
13	0.075	0.641	122.	16.7	0.0721	10.1
14	0.095	0.673	153.	17.5	0.0692	8.4
15	0.120	0.691	195.	18.0	0.0678	7.2
16	0.155	0.720	251.	18.7	0.0655	6.1
17	0.197	0.738	319.	19.2	0.0645	5.6
18	0.252	0.774	408.	20.1	0.0611	4.8
19	0.323	0.804	524.	20.9	0.0585	4.3
20	0.414	0.840	672.	21.9	0.0554	3.7
21	0.505	0.854	820.	22.2	0.0537	3.5
22	0.600	0.910	973.	23.7	0.0437	2.5
23	0.682	0.948	1107.	24.7	0.0390	2.0
24	0.732	0.973	1187.	25.3	0.0355	1.8
25	0.877	0.976	1422.	25.4	0.0224	1.3
26	0.965	0.984	1565.	25.6	0.0153	1.0
27	1.060	1.000	1719.	26.0	0.0085	0.8
28	1.154	0.996	1872.	25.9	0.0038	0.8

FIRST EXPT., SINGLE WIRE DATA AT STN. 4, S = 16.09 CM.

PT	Y/DEL	U/UP	YPLUS	UPLUS	TURB.IN.	DISP
1	0.004	0.110	5.	2.8	0.0308	20.7
2	0.019	0.402	21.	10.2	0.0791	11.2
3	0.014	0.350	16.	8.8	0.0879	17.5
4	0.019	0.418	21.	10.6	0.0892	17.5
5	0.023	0.467	26.	11.8	0.0854	16.0
6	0.029	0.502	32.	12.7	0.0805	15.2
7	0.035	0.535	39.	13.5	0.0773	14.6
8	0.041	0.553	46.	14.0	0.0720	12.9
9	0.050	0.581	55.	14.7	0.0674	12.1
10	0.058	0.591	65.	15.0	0.0656	11.8
11	0.066	0.610	74.	15.4	0.0668	10.8
12	0.078	0.634	87.	16.0	0.0641	10.1
13	0.098	0.662	110.	16.7	0.0627	9.0
14	0.124	0.686	139.	17.4	0.0610	7.8
15	0.158	0.699	176.	17.7	0.0602	7.5
16	0.202	0.760	226.	19.2	0.0555	4.9
17	0.258	0.784	288.	19.8	0.0537	4.5
18	0.329	0.825	369.	20.9	0.0518	3.6
19	0.423	0.864	473.	21.9	0.0508	3.4
20	0.542	0.886	607.	22.4	0.0477	3.0
21	0.661	0.935	740.	23.7	0.0459	2.6
22	0.785	0.941	878.	23.8	0.0434	2.3
23	0.893	0.955	999.	24.1	0.0404	2.1
24	0.958	0.978	1071.	24.7	0.0392	1.9
25	1.147	1.032	1284.	26.1	0.0291	1.3
26	1.263	1.038	1413.	26.2	0.0215	1.1
27	1.387	1.045	1552.	26.4	0.0152	0.9
28	1.511	1.022	1690.	25.9	0.0110	0.9
29	1.651	1.027	1847.	26.0	0.0049	0.8
30	1.857	1.000	2078.	25.3	0.0030	0.8

FIRST EXPT,. SINGLE WIRE DATA AT STN. 5, 3 = 33.65 CM.

PT	Y/DEL	U/UP	YPLUS	UPLUS	TURB.IN.	DISP
1	0.004	0.158	4.	4.2	0.0485	19.7
2	0.010	0.263	10.	6.9	0.0760	18.7
3	0.015	0.359	15.	9.5	0.0849	16.6
4	0.020	0.412	21.	10.9	0.0837	16.4
5	0.024	0.445	25.	11.7	0.0807	15.1
6	0.031	0.490	31.	12.9	0.0773	13.5
7	0.037	0.497	38.	13.1	0.0726	14.0
8	0.044	0.531	45.	14.0	0.0695	11.8
9	0.052	0.551	54.	14.5	0.0675	12.0
10	0.061	0.566	63.	14.9	0.0648	10.9
11	0.070	0.575	72.	15.2	0.0641	11.1
12	0.082	0.601	84.	15.8	0.0623	9.8
13	0.104	0.619	106.	16.3	0.0593	8.7
14	0.131	0.665	134.	17.5	0.0589	7.4
15	0.167	0.683	171.	18.0	0.0558	6.7
16	0.214	0.749	219.	19.7	0.0525	4.9
17	0.273	0.764	279.	20.1	0.0471	4.1
18	0.348	0.816	357.	21.5	0.0438	3.2
19	0.447	0.875	458.	23.1	0.0404	2.5
20	0.574	0.908	587.	23.9	0.0369	2.3
21	0.700	0.934	716.	24.6	0.0356	2.2
22	0.831	0.963	850.	25.4	0.0332	1.9
23	0.945	0.977	967.	25.7	0.0316	1.8
24	1.013	0.993	1037.	26.2	0.0305	1.7
25	1.214	1.025	1243.	27.0	0.0258	1.4
26	1.336	1.030	1368.	27.1	0.0209	1.2
27	1.467	1.044	1502.	27.5	0.0134	1.0
28	1.747	0.999	1788.	26.3	0.0048	0.9
29	1.965	1.000	2011.	26.4	0.0031	0.9

FIRST EXPT., SINGLE WIRE DATA AT STN. 6, S = 50.80 CM.

PT	Y/DEL	U/UP	YPLUS	UPLUS	TURB.IN.	DISP
1	0.004	0.190	4.	5.3	0.0588	23.3
2	0.009	0.209	9.	5.9	0.0646	22.1
3	0.013	0.296	14.	8.3	0.0797	20.8
4	0.018	0.384	20.	10.8	0.0803	17.0
5	0.022	0.401	24.	11.3	0.0783	17.9
6	0.027	0.439	30.	12.4	0.0738	16.6
7	0.033	0.468	36.	13.2	0.0694	15.6
8	0.039	0.484	43.	13.6	0.0665	15.1
9	0.047	0.494	51.	13.9	0.0637	15.0
10	0.054	0.523	60.	14.7	0.0614	13.8
11	0.062	0.536	68.	15.1	0.0595	13.0
12	0.073	0.559	80.	15.7	0.0578	11.9
13	0.092	0.585	101.	16.5	0.0562	10.8
14	0.116	0.617	128.	17.4	0.0536	9.1
15	0.148	0.656	163.	18.5	0.0517	7.6
16	0.190	0.699	209.	19.7	0.0491	6.2
17	0.242	0.742	266.	20.9	0.0432	4.9
18	0.310	0.789	340.	22.2	0.0415	3.8
19	0.397	0.836	436.	23.5	0.0368	2.9
20	0.510	0.877	560.	24.7	0.0322	2.5
21	0.622	0.913	682.	25.7	0.0302	2.3
22	0.738	0.937	810.	26.4	0.0286	2.2
23	0.840	0.964	922.	27.1	0.0271	2.1
24	0.900	0.973	988.	27.4	0.0261	2.0
25	1.079	1.003	1184.	28.2	0.0226	1.7
26	1.188	1.010	1303.	28.4	0.0191	1.6
27	1.304	1.023	1431.	28.8	0.0156	1.4
28	1.421	1.023	1559.	28.8	0.0101	1.3
29	1.553	1.013	1704.	28.5	0.0094	1.2
30	1.747	1.000	1917.	28.2	0.0067	1.2

FIRST EXPT., SINGLE WIRE DATA AT STN. 7, S = 64.13 CM.

PT	Y/DEL	U/UP	YPLUS	UPLUS	TURB.IN.	DISP
1	0.004	0.211	4.	5.8	0.0648	16.9
2	0.009	0.287	9.	8.0	0.0783	17.1
3	0.014	0.351	14.	9.7	0.0812	14.5
4	0.019	0.400	19.	11.1	0.0787	14.9
5	0.023	0.428	24.	11.9	0.0748	13.9
6	0.028	0.459	30.	12.7	0.0705	12.7
7	0.034	0.480	36.	13.3	0.0674	12.3
8	0.040	0.500	42.	13.8	0.0646	11.8
9	0.048	0.514	51.	14.2	0.0617	11.4
10	0.056	0.534	59.	14.8	0.0591	10.7
11	0.064	0.548	68.	15.2	0.0572	10.3
12	0.076	0.560	80.	15.5	0.0563	9.9
13	0.096	0.583	101.	16.2	0.0548	9.2
14	0.121	0.615	127.	17.0	0.0534	8.2
15	0.154	0.649	162.	18.0	0.0514	7.2
16	0.197	0.673	208.	18.6	0.0504	6.6
17	0.251	0.739	264.	20.5	0.0470	4.9
18	0.321	0.790	338.	21.9	0.0423	3.8
19	0.412	0.836	434.	23.1	0.0363	3.0
20	0.529	0.883	557.	24.5	0.0319	2.3
21	0.644	0.919	679.	25.5	0.0289	2.1
22	0.765	0.940	806.	26.0	0.0274	2.0
23	0.871	0.962	917.	26.6	0.0266	1.9
24	0.933	0.977	983.	27.1	0.0260	1.8
25	1.118	1.013	1178.	28.0	0.0232	1.6
26	1.231	1.037	1297.	28.7	0.0209	1.5
27	1.352	1.031	1424.	28.5	0.0167	1.4
28	1.472	1.044	1551.	28.9	0.0125	1.3
29	1.609	1.031	1695.	28.5	0.0093	1.2
30	1.810	1.012	1907.	28.0	0.0099	1.2

FIRST EXPT., SINGLE WIRE DATA AT STN. 8, S = 81.91 CM.

PT	Y/DEL	U/UP	YPLUS	UPLUS	TURB.IN.	DISP
1	0.003	0.142	4.	4.7	0.0459	31.3
2	0.007	0.212	9.	7.0	0.0649	30.0
3	0.010	0.281	14.	9.2	0.0741	26.8
4	0.014	0.335	19.	11.0	0.0733	24.8
5	0.017	0.366	23.	12.0	0.0703	23.0
6	0.021	0.390	29.	12.8	0.0650	22.0
7	0.025	0.403	35.	13.2	0.0628	21.2
8	0.030	0.420	41.	13.8	0.0599	19.9
9	0.036	0.433	49.	14.2	0.0575	19.2
10	0.041	0.444	58.	14.6	0.0564	19.2
11	0.047	0.453	66.	14.9	0.0554	18.3
12	0.056	0.471	77.	15.4	0.0542	17.2
13	0.070	0.492	98.	16.1	0.0533	15.8
14	0.089	0.516	123.	16.9	0.0534	14.6
15	0.113	0.541	157.	17.8	0.0519	13.2
16	0.145	0.578	201.	19.0	0.0510	11.3
17	0.185	0.622	256.	20.4	0.0482	9.2
18	0.236	0.671	328.	22.0	0.0444	7.1
19	0.303	0.725	421.	23.8	0.0381	5.1
20	0.389	0.786	540.	25.8	0.0302	3.4
21	0.474	0.820	659.	26.9	0.0255	2.8
22	0.563	0.860	782.	28.2	0.0230	2.5
23	0.640	0.890	890.	29.2	0.0231	2.3
24	0.687	0.907	954.	29.8	0.0228	2.2
25	0.823	0.946	1143.	31.0	0.0213	2.1
26	0.906	0.968	1258.	31.8	0.0189	1.9
27	0.994	0.989	1381.	32.5	0.0151	1.8
28	1.083	1.000	1504.	32.8	0.0117	1.7
29	1.184	0.999	1644.	32.8	0.0121	1.7
30	1.332	0.993	1850.	32.6	0.0138	1.7

FIRST EXPT., SINGLE WIRE DATA AT STN. 9, S = 97.16 CM.

PT	Y/DEL	U/UP	YPLUS	UPLUS	TURB.IN.	DISP
1	0.003	0.124	4.	3.9	0.0563	72.2
2	0.006	0.255	9.	8.0	0.0766	38.4
3	0.009	0.333	14.	10.4	0.0794	34.4
4	0.012	0.377	19.	11.8	0.0751	31.1
5	0.014	0.393	23.	12.3	0.0733	30.0
6	0.018	0.414	29.	12.9	0.0693	28.7
7	0.021	0.437	34.	13.6	0.0671	25.9
8	0.025	0.451	41.	14.1	0.0647	25.2
9	0.030	0.464	49.	14.5	0.0622	24.0
10	0.035	0.477	57.	14.9	0.0599	23.0
11	0.040	0.485	66.	15.1	0.0587	22.2
12	0.047	0.495	77.	15.4	0.0584	21.6
13	0.060	0.513	98.	16.0	0.0568	19.8
14	0.076	0.537	123.	16.8	0.0568	17.8
15	0.096	0.555	157.	17.3	0.0564	17.0
16	0.124	0.586	201.	18.3	0.0566	15.3
17	0.158	0.618	256.	19.3	0.0556	14.0
18	0.201	0.658	327.	20.5	0.0539	12.1
19	0.258	0.708	420.	22.1	0.0504	9.5
20	0.332	0.767	539.	23.9	0.0430	6.3
21	0.404	0.810	657.	25.3	0.0358	4.3
22	0.480	0.842	780.	26.3	0.0312	3.5
23	0.546	0.878	887.	27.4	0.0258	2.8
24	0.586	0.897	951.	28.0	0.0258	2.7
25	0.702	0.928	1140.	29.0	0.0228	2.4
26	0.772	0.950	1254.	29.7	0.0208	2.3
27	0.848	0.972	1377.	30.3	0.0175	2.1
28	0.924	0.981	1500.	30.6	0.0131	2.0
29	1.010	0.991	1640.	30.9	0.0094	2.0
30	1.136	1.000	1845.	31.2	0.0110	2.0

FIRST EXPT., SINGLE WIRE DATA AT STN. 10, S = 112.4 CM.

PT	Y/DEL	U/UP	YPLUS	UPLUS	TURB.IN.	DISP
1	0.003	0.153	4.	4.8	0.0505	34.7
2	0.006	0.250	9.	7.9	0.0760	31.3
3	0.010	0.319	14.	10.1	0.0815	27.6
4	0.013	0.363	20.	11.5	0.0781	25.4
5	0.016	0.385	24.	12.2	0.0772	23.5
6	0.020	0.417	30.	13.2	0.0729	21.8
7	0.024	0.430	36.	13.6	0.0698	21.4
8	0.028	0.444	43.	14.1	0.0674	20.7
9	0.034	0.461	51.	14.6	0.0648	18.9
10	0.039	0.470	60.	14.9	0.0634	18.2
11	0.045	0.481	68.	15.3	0.0629	17.7
12	0.053	0.493	80.	15.6	0.0622	16.9
13	0.067	0.513	101.	16.3	0.0605	15.1
14	0.085	0.531	128.	16.8	0.0603	13.9
15	0.108	0.549	162.	17.4	0.0658	12.8
16	0.138	0.577	208.	18.3	0.0597	11.8
17	0.176	0.609	265.	19.3	0.0598	11.0
18	0.225	0.647	339.	20.5	0.0594	9.9
19	0.289	0.696	436.	22.1	0.0573	8.6
20	0.371	0.745	559.	23.6	0.0543	7.0
21	0.452	0.793	681.	25.2	0.0476	5.3
22	0.536	0.843	809.	26.7	0.0420	3.6
23	0.610	0.875	920.	27.7	0.0374	2.9
24	0.654	0.891	987.	28.3	0.0357	2.6
25	0.784	0.940	1182.	29.8	0.0301	2.2
26	0.863	0.956	1301.	30.3	0.0262	2.0
27	0.948	0.974	1429.	30.9	0.0231	1.9
28	1.032	1.000	1557.	31.7	0.0203	1.8
29	1.128	0.999	1701.	31.7	0.0182	1.8
30	1.269	0.993	1914.	31.5	0.0215	2.0
31	1.410	0.997	2127.	31.6	0.0245	2.0

FIRST EXPT., REYNOLDS' STRESSES AT STN. 1, S = -71.75 CM.

OUTPUT NONDIMENSIONALIZED ON FRICTION VELOCITY

PT	Y/DEL	UV/UTSQ	USQ/UTSQ	VSQ/UTSQ	WSQ/UTSQ	QSQ/UTSQ	A	SHEAR CORR	ANISOTROPY
1	0.067	1.0095	3.838	1.522	2.345	7.705	0.131	0.418	0.034
2	0.073	1.0187	3.787	1.509	2.256	7.552	0.135	0.426	0.036
3	0.081	1.0403	3.674	1.474	2.221	7.369	0.141	0.447	0.040
4	0.103	1.0422	3.618	1.481	2.136	7.235	0.144	0.450	0.042
5	0.165	1.0213	3.474	1.520	2.034	7.028	0.145	0.444	0.042
6	0.270	0.9585	3.128	1.466	1.913	6.507	0.147	0.448	0.043
7	0.443	0.8067	2.467	1.324	1.659	5.450	0.148	0.446	0.044
8	0.568	0.6660	1.988	1.048	1.329	4.365	0.153	0.461	0.047
9	0.692	0.4953	1.416	0.920	0.970	.306	0.150	0.434	0.045
10	0.822	0.2800	0.872	0.527	0.583	1.982	0.141	0.413	0.040
11	0.935	0.1322	0.444	0.393	0.315	1.152	0.115	0.316	0.026

DISPLACEMENT THICKNESS = 0.503 CM.   MOMENTUM THICKNESS = 0.371 CM.   DELTA 99 = 2.939 CM.

MOMENTUM THICKNESS REYNOLDS NO. = 3769.   UTAU = 0.622 M/SEC   UPW = 16.00 M/SEC

OUTPUT NONDIMENSIONALIZED ON WALL VELOCITY

PT	Y/DEL	UV/UPWS	USQ/UPWS	VSQ/UPWS	WSQ/UPWS	QSQ/UPWS
1	0.067	0.00152	0.00579	0.00230	0.00354	0.01163
2	0.073	0.00154	0.00572	0.00228	0.00341	0.01140
3	0.081	0.00157	0.00555	0.00223	0.00335	0.01113
4	0.103	0.00157	0.00546	0.00224	0.00323	0.01092
5	0.165	0.00154	0.00525	0.00229	0.00307	0.01061
6	0.270	0.00145	0.00472	0.00221	0.00289	0.00983
7	0.443	0.00122	0.00373	0.00200	0.00250	0.00823
8	0.568	0.00101	0.00300	0.00158	0.00201	0.00659
9	0.692	0.00075	0.00214	0.00139	0.00146	0.00499
10	0.822	0.00042	0.00132	0.00080	0.00088	0.00299
11	0.935	0.00020	0.00067	0.00059	0.00048	0.00174

FIRST EXPT., REYNOLDS' STRESSES AT STN. 2, S = -41.27 CM.

OUTPUT NONDIMENSIONALIZED ON FRICTION VELOCITY

PT	Y/DEL	UV/UTSQ	USQ/UTSQ	VSQ/UTSQ	WSQ/UTSQ	QSQ/UTSQ	A	SHEAR CORR	ANISOTROPY
1	0.061	0.9765	4.210	1.695	2.713	8.618	0.113	0.366	0.026
2	0.079	0.9650	4.112	1.604	2.555	8.271	0.117	0.376	0.027
3	0.098	0.9793	4.018	1.613	2.406	8.037	0.122	0.385	0.030
4	0.120	0.9808	3.935	1.570	2.353	7.858	0.125	0.395	0.031
5	0.148	0.9915	3.879	1.584	2.262	7.725	0.128	0.400	0.033
6	0.183	0.9686	3.736	1.583	2.219	7.538	0.128	0.398	0.033
7	0.226	0.9843	3.519	1.592	2.195	7.306	0.135	0.416	0.036
8	0.279	0.9522	3.310	1.551	2.148	7.009	0.136	0.420	0.037
9	0.344	0.9015	3.052	1.475	2.041	6.568	0.137	0.425	0.038
10	0.424	0.8201	2.707	1.360	1.866	5.933	0.138	0.427	0.038
11	0.523	0.6959	2.266	1.181	1.613	5.060	0.138	0.425	0.038
12	0.644	0.5067	1.667	0.929	1.223	3.819	0.133	0.407	0.035
13	0.796	0.2882	0.971	0.575	0.712	2.258	0.128	0.386	0.033
14	0.981	0.0590	0.259	0.223	0.208	0.690	0.086	0.245	0.015
15	1.210	-0.0124	0.020	0.030	0.011	0.061	-0.205	-0.506	0.084

DISPLACEMENT THICKNESS = 0.572 CM.   MOMENTUM THICKNESS = 0.419 CM.   DELTA 99 = 3.429 CM.

MOMENTUM THICKNESS REYNOLDS NO. = 4312.   UTAU = 0.614 M/SEC   UPW = 15.91 M/SEC

OUTPUT NONDIMENSIONALIZED ON WALL VELOCITY

PT	Y/DEL	UV/UPWS	USQ/UPWS	VSQ/UPWS	WSQ/UPWS	QSQ/UPWS
1	0.061	0.00145	0.00627	0.00253	0.00404	0.01284
2	0.079	0.00144	0.00613	0.00239	0.00381	0.01232
3	0.098	0.00146	0.00599	0.00240	0.00358	0.01198
4	0.120	0.00146	0.00586	0.00234	0.00351	0.01171
5	0.148	0.00148	0.00578	0.00236	0.00337	0.01151
6	0.183	0.00144	0.00557	0.00236	0.00331	0.01123
7	0.226	0.00147	0.00524	0.00237	0.00327	0.01069
8	0.279	0.00142	0.00493	0.00231	0.00320	0.01044
9	0.344	0.00134	0.00455	0.00220	0.00304	0.00979
10	0.424	0.00122	0.00403	0.00203	0.00278	0.00884
11	0.523	0.00104	0.00338	0.00176	0.00240	0.00754
12	0.644	0.00075	0.00248	0.00138	0.00182	0.00569
13	0.796	0.00043	0.00145	0.00086	0.00106	0.00336
14	0.981	0.00009	0.00039	0.00033	0.00031	0.00103
15	1.210	-0.00002	0.00003	0.00004	0.00002	0.00009

FIRST EXPT., REYNOLDS' STRESSES AT STN. 3, S = -6.19 CM.

OUTPUT NONDIMENSIONALIZED ON FRICTION VELOCITY

PT	Y/DEL	UV/UTSQ	USQ/UTSQ	VSQ/UTSQ	WSQ/UTSQ	QSQ/UTSQ	A	SHEAR CORR	ANISOTROPY
1	0.050	1.0261	4.504	1.678	2.720	8.901	0.115	0.373	0.027
2	0.055	1.0007	4.403	1.674	2.659	8.737	0.115	0.369	0.026
3	0.069	0.9795	4.306	1.581	2.512	8.399	0.117	0.375	0.027
4	0.085	0.9661	4.152	1.532	2.401	8.084	0.120	0.383	0.029
5	0.105	0.9392	3.999	1.516	2.283	7.798	0.120	0.381	0.029
6	0.129	0.9590	3.923	1.500	2.266	7.689	0.125	0.395	0.031
7	0.159	0.9053	3.483	1.480	2.103	7.066	0.128	0.399	0.033
8	0.197	0.9138	3.348	1.475	2.094	6.917	0.132	0.411	0.035
9	0.243	0.8813	3.184	1.455	2.010	6.649	0.133	0.409	0.035
10	0.299	0.8566	2.867	1.413	1.959	6.239	0.137	0.426	0.038
11	0.369	0.8255	2.646	1.346	1.836	5.829	0.142	0.437	0.040
12	0.455	0.7118	2.272	1.204	1.656	5.132	0.139	0.430	0.038
13	0.561	0.5706	1.814	1.001	1.359	4.175	0.137	0.423	0.037
14	0.693	0.3799	1.229	0.705	0.900	2.835	0.134	0.408	0.036
15	0.855	0.1582	0.505	0.377	0.393	1.276	0.124	0.362	0.031
16	1.054	0.0106	0.105	0.104	0.079	0.288	0.037	0.101	0.003

DISPLACEMENT THICKNESS = 0.610 CM.   MOMENTUM THICKNESS = 0.442 CM.   DELTA 99 = 3.937 CM.

MOMENTUM THICKNESS REYNOLDS NO. = 4622.   UTAU = 0.618 M/SEC   UPW = 16.05 M/SEC

OUTPUT NONDIMENSIONALIZED ON WALL VELOCITY

PT	Y/DEL	UV/UPWS	USQ/UPWS	VSQ/UPWS	WSQ/UPWS	QSQ/UPWS
1	0.050	0.00152	0.00667	0.00248	0.00403	0.01318
2	0.055	0.00148	0.00652	0.00248	0.00394	0.01294
3	0.069	0.00145	0.00638	0.00234	0.00372	0.01244
4	0.085	0.00143	0.00615	0.00227	0.00355	0.01197
5	0.105	0.00139	0.00592	0.00225	0.00338	0.01155
6	0.129	0.00142	0.00581	0.00222	0.00336	0.01139
7	0.159	0.00134	0.00516	0.00219	0.00311	0.01046
8	0.197	0.00135	0.00496	0.00218	0.00310	0.01024
9	0.243	0.00131	0.00471	0.00215	0.00298	0.00985
10	0.299	0.00127	0.00425	0.00209	0.00290	0.00924
11	0.369	0.00122	0.00392	0.00199	0.00272	0.00863
12	0.455	0.00105	0.00336	0.00178	0.00245	0.00760
13	0.561	0.00084	0.00269	0.00148	0.00201	0.00618
14	0.693	0.00056	0.00182	0.00104	0.00133	0.00420
15	0.855	0.00023	0.00075	0.00056	0.00058	0.00189
16	1.054	0.00002	0.00016	0.00015	0.00012	0.00043

FIRST EXPT., REYNOLDS' STRESSES AT STN. 4, S = 16.20 CM. (20.6 DEG)

OUTPUT NONDIMENSIONALIZED ON FRICTION VELOCITY

PT	Y/DEL	UV/UTSQ	USQ/UTSQ	VSQ/UTSQ	WSQ/UTSQ	QSQ/UTSQ	A	SHEAR CORR	ANISOTROPY
1	0.034	0.6544	3.004	1.363	2.007	6.375	0.103	0.323	0.021
2	0.046	0.6238	2.939	1.270	1.882	6.091	0.102	0.323	0.021
3	0.057	0.6009	2.876	1.214	1.781	5.871	0.102	0.322	0.021
4	0.070	0.5523	2.781	1.157	1.724	5.662	0.098	0.308	0.019
5	0.087	0.4917	2.734	1.079	1.647	5.460	0.090	0.286	0.016
6	0.107	0.3993	2.591	1.013	1.586	5.191	0.077	0.246	0.012
7	0.131	0.3084	2.501	0.954	1.517	4.972	0.062	0.200	0.008
8	0.162	0.2091	2.363	0.913	1.435	4.711	0.044	0.142	0.004
9	0.201	0.1480	2.240	0.907	1.401	4.547	0.033	0.104	0.002
10	0.247	0.0876	2.171	0.893	1.344	4.409	0.020	0.063	0.001
11	0.305	0.0494	2.086	0.903	1.312	4.301	0.011	0.036	0.000
12	0.376	0.0135	1.957	0.877	1.269	4.103	0.003	0.010	0.000
13	0.464	-0.0140	1.808	0.824	1.183	3.815	-0.004	-0.011	0.000
14	0.572	-0.0377	1.579	0.746	1.042	3.367	-0.011	-0.035	0.000
15	0.706	-0.0674	1.257	0.595	0.793	2.645	-0.025	-0.078	0.001
16	0.871	-0.0713	0.943	0.485	0.583	2.011	-0.035	-0.105	0.003
17	1.074	-0.0453	0.315	0.239	0.208	0.762	-0.059	-0.165	0.007
18	1.325	-0.0086	0.036	0.050	0.028	0.115	-0.075	-0.202	0.011

DISPLACEMENT THICKNESS = 0.681 CM.   MOMENTUM THICKNESS = 0.493 CM.   DELTA 99 = 3.863 CM.

MOMENTUM THICKNESS REYNOLDS NO. = 5066.   UTAU = 0.575 M/SEC   UPW = 16.09 M/SEC

OUTPUT NONDIMENSIONALIZED ON WALL VELOCITY

PT	Y/DEL	UV/UPWS	USQ/UPWS	VSQ/UPWS	WSQ/UPWS	QSQ/UPWS
1	0.034	0.00084	0.00384	0.00174	0.00257	0.00816
2	0.046	0.00080	0.00376	0.00163	0.00241	0.00779
3	0.057	0.00077	0.00368	0.00155	0.00228	0.00751
4	0.070	0.00071	0.00356	0.00148	0.00221	0.00724
5	0.087	0.00063	0.00350	0.00138	0.00211	0.00699
6	0.107	0.00051	0.00332	0.00130	0.00203	0.00664
7	0.131	0.00039	0.00320	0.00122	0.00194	0.00636
8	0.162	0.00027	0.00302	0.00117	0.00184	0.00603
9	0.201	0.00019	0.00287	0.00116	0.00179	0.00582
10	0.247	0.00011	0.00278	0.00114	0.00172	0.00564
11	0.305	0.00006	0.00267	0.00115	0.00168	0.00550
12	0.376	0.00002	0.00250	0.00112	0.00162	0.00525
13	0.464	-0.00002	0.00231	0.00105	0.00151	0.00488
14	0.572	-0.00005	0.00202	0.00095	0.00133	0.00431
15	0.706	-0.00009	0.00161	0.00076	0.00102	0.00338
16	0.871	-0.00009	0.00121	0.00062	0.00075	0.00257
17	1.074	-0.00006	0.00040	0.00031	0.00027	0.00098
18	1.325	-0.00001	0.00005	0.00006	0.00004	0.00015

FIRST EXPT., REYNOLDS' STRESSES AT STN. 5, S = 33.65 CM. (42.8 DEG)

OUTPUT NONDIMENSIONALIZED ON FRICTION VELOCITY

PT	Y/DEL	UV/UTSQ	USQ/UTSQ	VSQ/UTSQ	WSQ/UTSQ	QSQ/UTSQ	A	SHEAR CORR	ANISOTROPY
1	0.031	0.8604	3.044	1.624	2.093	6.761	0.127	0.387	0.032
2	0.041	0.8412	2.966	1.523	2.061	6.549	0.128	0.396	0.033
3	0.051	0.8064	2.821	1.367	1.933	6.121	0.132	0.411	0.035
4	0.069	0.7508	2.725	1.275	1.833	5.832	0.129	0.403	0.033
5	0.087	0.6990	2.571	1.189	1.765	5.525	0.127	0.400	0.032
6	0.110	0.6111	2.334	1.067	1.626	5.027	0.122	0.387	0.030
7	0.138	0.5159	2.075	0.941	1.492	4.508	0.114	0.369	0.026
8	0.173	0.4152	1.825	0.848	1.354	4.027	0.103	0.334	0.021
9	0.216	0.3282	1.563	0.764	1.237	3.564	0.092	0.300	0.017
10	0.269	0.2412	1.343	0.712	1.121	3.176	0.076	0.247	0.012
11	0.334	0.1813	1.198	0.703	1.066	2.966	0.061	0.198	0.007
12	0.415	0.1179	1.118	0.713	1.001	2.832	0.042	0.132	0.003
13	0.514	0.0598	1.008	0.700	0.913	2.621	0.023	0.071	0.001
14	0.637	0.0136	0.867	0.666	0.768	2.301	0.006	0.018	0.000
15	0.789	-0.0390	0.619	0.542	0.499	1.660	-0.023	-0.067	0.001
16	0.975	-0.0426	0.199	0.280	0.188	0.667	-0.064	-0.180	0.008
17	1.217	-0.0109	0.018	0.073	0.041	0.132	-0.082	-0.297	0.014
18	1.490	-0.0036	0.017	0.023	0.015	0.054	-0.067	-0.187	0.009

DISPLACEMENT THICKNESS = 0.787 CM.   MOMENTUM THICKNESS = 0.551 CM.   DELTA 99 = 4.209 CM.

MOMENTUM THICKNESS REYNOLDS NO. = 5709.   UTAU = 0.528 M/SEC   UPW = 16.15 M/SEC

OUTPUT NONDIMENSIONALIZED ON WALL VELOCITY

PT	Y/DEL	UV/UPWS	USQ/UPWS	VSQ/UPWS	WSQ/UPWS	QSQ/UPWS
1	0.031	0.00092	0.00326	0.00174	0.00224	0.00723
2	0.041	0.00090	0.00317	0.00163	0.00220	0.00700
3	0.051	0.00086	0.00302	0.00146	0.00207	0.00655
4	0.069	0.00080	0.00291	0.00136	0.00196	0.00624
5	0.087	0.00075	0.00275	0.00127	0.00189	0.00591
6	0.110	0.00065	0.00250	0.00114	0.00174	0.00538
7	0.138	0.00055	0.00222	0.00101	0.00160	0.00482
8	0.173	0.00044	0.00195	0.00091	0.00145	0.00431
9	0.216	0.00035	0.00167	0.00082	0.00132	0.00381
10	0.269	0.00026	0.00144	0.00076	0.00120	0.00340
11	0.334	0.00019	0.00128	0.00075	0.00114	0.00317
12	0.415	0.00013	0.00120	0.00076	0.00107	0.00303
13	0.514	0.00006	0.00108	0.00075	0.00098	0.00280
14	0.637	0.00001	0.00093	0.00071	0.00082	0.00246
15	0.789	-0.00004	0.00066	0.00058	0.00053	0.00178
16	0.975	-0.00005	0.00021	0.00030	0.00020	0.00071
17	1.217	-0.00001	0.00002	0.00008	0.00004	0.00014
18	1.490	-0.00000	0.00002	0.00002	0.00002	0.00006

FIRST EXPT., REYNOLDS' STRESSES AT STN. 6, S = 50.80 CM. (64.7 DEG)

OUTPUT NONDIMENSIONALIZED ON FRICTION VELOCITY

PT	Y/DEL	UV/UTSQ	USQ/UTSQ	VSQ/UTSQ	WSQ/UTSQ	QSQ/UTSQ	A	SHEAR CORR	ANISOTROPY
1	0.034	0.8464	3.296	1.828	2.439	7.564	0.112	0.345	0.025
2	0.041	0.8064	3.166	1.649	2.381	7.196	0.112	0.353	0.025
3	0.050	0.7811	3.098	1.569	2.327	6.994	0.112	0.354	0.025
4	0.062	0.7473	3.025	1.502	2.230	6.757	0.111	0.351	0.024
5	0.076	0.7115	2.988	1.441	2.168	6.598	0.108	0.343	0.023
6	0.094	0.6588	2.815	1.331	2.079	6.226	0.106	0.340	0.022
7	0.116	0.6156	2.649	1.238	1.940	5.827	0.106	0.340	0.022
8	0.143	0.5017	2.430	1.097	1.813	5.341	0.094	0.307	0.018
9	0.177	0.4237	2.211	0.964	1.609	4.783	0.089	0.290	0.016
10	0.218	0.3204	1.883	0.800	1.386	4.069	0.079	0.261	0.012
11	0.269	0.2298	1.547	0.677	1.220	3.444	0.067	0.225	0.009
12	0.331	0.1792	1.270	0.591	1.062	2.923	0.061	0.207	0.003
13	0.409	0.1391	1.097	0.554	0.959	2.610	0.053	0.179	0.006
14	0.504	0.1138	0.976	0.544	0.886	2.406	0.047	0.156	0.004
15	0.622	0.1033	0.861	0.539	0.813	2.213	0.047	0.152	0.004
16	0.767	0.0527	0.647	0.517	0.589	1.754	0.030	0.091	0.002
17	0.946	-0.0053	0.270	0.369	0.263	0.902	-0.006	-0.017	0.000
18	1.167	-0.0179	0.057	0.058	0.046	0.161	-0.111	-0.310	0.025

DISPLACEMENT THICKNESS = 0.874 CM.   MOMENTUM THICKNESS = 0.442 CM.   DELTA 99 = 4.387 CM.

MOMENTUM THICKNESS REYNOLDS NO. = 6163.   UTAU = 0.482 M/SEC   UPW = 16.10 M/SEC

OUTPUT NONDIMENSIONALIZED ON WALL VELOCITY

PT	Y/DEL	UV/UPWS	USQ/UPWS	VSQ/UPWS	WSQ/UPWS	QSQ/UPWS
1	0.034	0.00076	0.00295	0.00164	0.00218	0.00677
2	0.041	0.00072	0.00283	0.00148	0.00213	0.00644
3	0.050	0.00070	0.00277	0.00140	0.00208	0.00626
4	0.062	0.00067	0.00271	0.00134	0.00200	0.00605
5	0.076	0.00064	0.00267	0.00129	0.00194	0.00590
6	0.094	0.00059	0.00252	0.00119	0.00186	0.00557
7	0.116	0.00055	0.00237	0.00111	0.00174	0.00521
8	0.143	0.00045	0.00217	0.00098	0.00162	0.00478
9	0.177	0.00038	0.00198	0.00086	0.00144	0.00428
10	0.218	0.00029	0.00168	0.00072	0.00124	0.00364
11	0.269	0.00021	0.00138	0.00061	0.00109	0.00308
12	0.331	0.00016	0.00114	0.00053	0.00095	0.00262
13	0.409	0.00012	0.00098	0.00050	0.00086	0.00233
14	0.504	0.00010	0.00087	0.00049	0.00079	0.00215
15	0.622	0.00009	0.00077	0.00048	0.00073	0.00198
16	0.767	0.00005	0.00058	0.00046	0.00053	0.00157
17	0.946	-0.00000	0.00024	0.00033	0.00024	0.00081
18	1.167	-0.00002	0.00005	0.00005	0.00004	0.00014

FIRST EXPT., REYNOLDS' STRESSES AT STN. 7, S = 64.13 CM. (81.6 DEG)

OUTPUT NONDIMENSIONALIZED ON FRICTION VELOCITY

PT	Y/DEL	UV/UTSQ	USQ/UTSQ	VSQ/UTSQ	WSQ/UTSQ	QSQ/UTSQ	A	SHEAR CORR	ANISOTROPY
1	0.029	0.8723	3.076	1.625	2.149	6.851	0.127	0.390	0.032
2	0.040	0.8625	2.854	1.484	2.071	6.409	0.135	0.419	0.036
3	0.049	0.8301	2.774	1.429	1.982	6.185	0.134	0.417	0.036
4	0.060	0.8139	2.705	1.368	1.918	5.991	0.137	0.426	0.037
5	0.075	0.7858	2.589	1.313	1.861	5.763	0.136	0.426	0.037
6	0.092	0.7404	2.497	1.239	1.808	5.544	0.134	0.421	0.036
7	0.113	0.6722	2.374	1.170	1.718	5.261	0.128	0.403	0.033
8	0.140	0.5884	2.176	1.053	1.607	4.837	0.122	0.389	0.030
9	0.172	0.4928	1.941	0.924	1.458	4.323	0.114	0.368	0.026
10	0.213	0.3733	1.653	0.782	1.260	3.694	0.101	0.328	0.020
11	0.262	0.2560	1.356	0.628	1.057	3.041	0.084	0.277	0.014
12	0.323	0.1643	1.113	0.496	0.884	2.493	0.066	0.221	0.009
13	0.399	0.0969	0.931	0.424	0.765	2.121	0.046	0.154	0.004
14	0.492	0.0676	0.858	0.406	0.711	1.975	0.034	0.115	0.002
15	0.607	0.0549	0.773	0.395	0.627	1.795	0.031	0.099	0.002
16	0.749	0.0432	0.620	0.386	0.472	1.478	0.029	0.088	0.002
17	0.924	0.0175	0.313	0.324	0.251	0.887	0.020	0.055	0.001
18	1.140	-0.0226	0.060	0.108	0.059	0.228	-0.099	-0.280	0.020
19	1.406	-0.0268	0.054	0.111	0.072	0.237	-0.113	-0.346	0.026

DISPLACEMENT THICKNESS = 0.909 CM.   MOMENTUM THICKNESS = 0.612 CM.   DELTA 99 = 4.493 CM.

MOMENTUM THICKNESS REYNOLDS NO. = 6352.   UTAU = 0.490 M/SEC   UPW = 16.08 M/SEC

OUTPUT NONDIMENSIONALIZED ON WALL VELOCITY

PT	Y/DEL	UV/UPWS	USQ/UPWS	VSQ/UPWS	WSQ/UPWS	QSQ/UPWS
1	0.029	0.00081	0.00286	0.00151	0.00200	0.00637
2	0.040	0.00080	0.00265	0.00138	0.00193	0.00596
3	0.049	0.00077	0.00258	0.00133	0.00184	0.00575
4	0.060	0.00076	0.00252	0.00127	0.00178	0.00557
5	0.075	0.00073	0.00241	0.00122	0.00173	0.00536
6	0.092	0.00069	0.00232	0.00115	0.00168	0.00516
7	0.113	0.00063	0.00221	0.00109	0.00160	0.00489
8	0.140	0.00055	0.00202	0.00098	0.00149	0.00450
9	0.172	0.00046	0.00181	0.00086	0.00136	0.00402
10	0.213	0.00035	0.00154	0.00073	0.00117	0.00344
11	0.262	0.00024	0.00126	0.00058	0.00098	0.00283
12	0.323	0.00015	0.00104	0.00046	0.00082	0.00232
13	0.399	0.00009	0.00087	0.00039	0.00071	0.00197
14	0.492	0.00006	0.00080	0.00038	0.00066	0.00184
15	0.607	0.00005	0.00072	0.00037	0.00058	0.00167
16	0.749	0.00004	0.00058	0.00036	0.00044	0.00137
17	0.924	0.00002	0.00029	0.00030	0.00023	0.00083
18	1.140	-0.00002	0.00006	0.00010	0.00005	0.00021
19	1.406	-0.00002	0.00005	0.00010	0.00007	0.00022

FIRST EXPT., REYNOLDS' STRESSES AT STN. 8, S = 81.91 CM.

OUTPUT NONDIMENSIONALIZED ON FRICTION VELOCITY

PT	Y/DEL	UV/UTSQ	USQ/UTSQ	VSQ/UTSQ	WSQ/UTSQ	QSQ/UTSQ	A	SHEAR CORR	ANISOTROPY
1	0.043	1.0042	3.601	1.573	2.428	7.603	0.132	0.422	0.035
2	0.052	1.0331	3.454	1.605	2.325	7.384	0.141	0.441	0.040
3	0.065	1.0470	3.368	1.613	2.297	7.278	0.144	0.449	0.041
4	0.080	1.0719	3.418	1.638	2.266	7.322	0.146	0.453	0.043
5	0.099	1.0699	3.332	1.667	2.285	7.284	0.147	0.454	0.043
6	0.122	1.0809	3.383	1.682	2.245	7.310	0.148	0.453	0.044
7	0.151	1.0610	3.301	1.653	2.246	7.200	0.147	0.454	0.043
8	0.186	1.0699	3.244	1.605	2.231	7.080	0.151	0.469	0.046
9	0.229	1.0162	3.054	1.514	2.132	6.699	0.152	0.473	0.046
10	0.283	0.8977	2.767	1.329	1.913	6.009	0.149	0.468	0.045
11	0.349	0.7365	2.240	1.045	1.566	4.850	0.152	0.481	0.046
12	0.430	0.5315	1.591	0.748	1.185	3.524	0.151	0.487	0.045
13	0.530	0.3901	1.185	0.569	0.942	2.697	0.145	0.475	0.042
14	0.654	0.2628	0.797	0.405	0.711	1.913	0.137	0.462	0.038
15	0.807	0.2030	0.649	0.372	0.561	1.581	0.128	0.413	0.033
16	0.996	0.0936	0.380	0.342	0.332	1.054	0.079	0.232	0.013
17	1.229	-0.0916	0.232	0.341	0.231	0.804	-0.114	-0.325	0.026

DISPLACEMENT THICKNESS = 0.803 CM.   MOMENTUM THICKNESS = 0.541 CM.   DELTA 99 = 4.168 CM.

MOMENTUM THICKNESS REYNOLDS NO. = 5574.   UTAU = 0.504 M/SEC   UPW = 16.02 M/SEC

OUTPUT NONDIMENSIONALIZED ON WALL VELOCITY

PT	Y/DEL	UV/UPWS	USQ/UPWS	VSQ/UPWS	WSQ/UPWS	QSQ/UPWS
1	0.043	0.00099	0.00357	0.00156	0.00240	0.00753
2	0.052	0.00103	0.00342	0.00159	0.00230	0.00731
3	0.065	0.00104	0.00333	0.00160	0.00227	0.00720
4	0.080	0.00106	0.00338	0.00162	0.00224	0.00725
5	0.099	0.00106	0.00330	0.00165	0.00226	0.00721
6	0.122	0.00107	0.00335	0.00167	0.00222	0.00724
7	0.151	0.00105	0.00327	0.00164	0.00222	0.00713
8	0.186	0.00106	0.00321	0.00159	0.00221	0.00701
9	0.229	0.00101	0.00302	0.00150	0.00211	0.00663
10	0.283	0.00099	0.00274	0.00130	0.00189	0.00595
11	0.349	0.00073	0.00222	0.00103	0.00155	0.00480
12	0.430	0.00053	0.00158	0.00074	0.00117	0.00349
13	0.530	0.00039	0.00117	0.00056	0.00093	0.00267
14	0.654	0.00026	0.00079	0.00040	0.00070	0.00189
15	0.807	0.00020	0.00064	0.00037	0.00056	0.00157
16	0.996	0.00008	0.00038	0.00034	0.00033	0.00104
17	1.229	-0.00009	0.00023	0.00034	0.00023	0.00080

FIRST EXPT., REYNOLDS' STRESSES AT STN. 9, S = 97.16 CM.

OUTPUT NONDIMENSIONALIZED ON FRICTION VELOCITY

PT	Y/DEL	UV/UTSQ	USQ/UTSQ	VSQ/UTSQ	WSQ/UTSQ	QSQ/UTSQ	A	SHEAR CORR	ANISOTROPY
1	0.039	1.0012	3.579	1.566	2.415	7.561	0.132	0.423	0.035
2	0.048	1.0348	3.433	1.598	2.312	7.344	0.141	0.442	0.040
3	0.059	1.0437	3.348	1.606	2.285	7.238	0.144	0.450	0.042
4	0.073	1.0684	3.397	1.631	2.255	7.282	0.147	0.454	0.043
5	0.090	1.0665	3.312	1.659	2.273	7.244	0.147	0.455	0.043
6	0.111	1.0773	3.362	1.674	2.233	7.270	0.148	0.454	0.044
7	0.137	1.0576	3.281	1.646	2.234	7.161	0.148	0.455	0.044
8	0.169	1.0665	3.225	1.598	2.219	7.042	0.151	0.470	0.046
9	0.208	1.0131	3.036	1.507	2.121	6.664	0.152	0.474	0.046
10	0.256	0.8955	2.751	1.324	1.904	5.979	0.150	0.469	0.045
11	0.316	0.7354	2.228	1.042	1.559	4.828	0.152	0.483	0.046
12	0.390	0.5319	1.584	0.747	1.181	3.512	0.151	0.489	0.046
13	0.446	0.3916	1.181	0.570	0.940	2.690	0.146	0.477	0.042
14	0.594	0.2651	0.796	0.407	0.710	1.913	0.139	0.466	0.038
15	0.732	0.2058	0.648	0.374	0.561	1.583	0.130	0.418	0.034
16	0.903	0.0872	0.382	0.344	0.334	1.060	0.082	0.241	0.014
17	1.114	-0.0867	0.235	0.343	0.234	0.811	-0.107	-0.305	0.023

DISPLACEMENT THICKNESS = 0.935 CM.   MOMENTUM THICKNESS = 0.625 CM.   DELTA 99 = 4.595 CM.

MOMENTUM THICKNESS REYNOLDS NO. =64200.   UTAU = 0.506 M/SEC   UPW = 16.00 M/SEC

OUTPUT NONDIMENSIONALIZED ON WALL VELOCITY

PT	Y/DEL	UV/UPWS	USQ/UPWS	VSQ/UPWS	WSQ/UPWS	QSQ/UPWS
1	0.039	0.00100	0.00358	0.00157	0.00244	0.00756
2	0.048	0.00103	0.00343	0.00160	0.00235	0.00734
3	0.059	0.00104	0.00335	0.00161	0.00228	0.00724
4	0.073	0.00107	0.00340	0.00163	0.00225	0.00728
5	0.090	0.00107	0.00331	0.00166	0.00227	0.00724
6	0.111	0.00108	0.00336	0.00167	0.00223	0.00727
7	0.137	0.00106	0.00328	0.00165	0.00223	0.00716
8	0.169	0.00107	0.00322	0.00160	0.00222	0.00704
9	0.208	0.00101	0.00303	0.00151	0.00212	0.00665
10	0.256	0.00090	0.00275	0.00132	0.00190	0.00598
11	0.316	0.00074	0.00223	0.00104	0.00156	0.00483
12	0.390	0.00053	0.00158	0.00075	0.00118	0.00351
13	0.446	0.00039	0.00118	0.00057	0.00094	0.00269
14	0.594	0.00027	0.00080	0.00041	0.00071	0.00191
15	0.732	0.00021	0.00065	0.00037	0.00056	0.00158
16	0.903	0.00009	0.00038	0.00034	0.00033	0.00106
17	1.114	-0.00009	0.00023	0.00034	0.00023	0.00081

FIRST EXPT., REYNOLDS' STRESSES AT STN. 10, S = 112.4 CM.

OUTPUT NONDIMENSIONALIZED ON FRICTION VELOCITY

PT	Y/DEL	UV/UTSQ	USQ/UTSQ	VSQ/UTSQ	WSQ/UTSQ	QSQ/UTSQ	A	SHEAR CORR	ANISOTROPY
1	0.036	1.1050	4.016	1.640	2.468	8.124	0.136	0.431	0.037
2	0.045	1.1060	3.848	1.621	2.403	7.872	0.141	0.443	0.039
3	0.056	1.1070	3.772	1.641	2.336	7.749	0.143	0.445	0.041
4	0.069	1.1267	3.758	1.646	2.365	7.769	0.145	0.453	0.042
5	0.084	1.1237	3.735	1.675	2.302	7.713	0.146	0.449	0.042
6	0.104	1.1375	3.707	1.714	2.341	7.762	0.147	0.451	0.043
7	0.129	1.1661	3.681	1.725	2.334	7.739	0.151	0.463	0.045
8	0.159	1.1661	3.664	1.735	2.334	7.734	0.151	0.462	0.045
9	0.196	1.1484	3.627	1.711	2.332	7.670	0.150	0.461	0.045
10	0.242	1.1020	3.469	1.632	2.257	7.359	0.150	0.463	0.045
11	0.298	1.0173	3.115	1.481	2.099	6.695	0.152	0.474	0.046
12	0.368	0.8615	2.698	1.249	1.799	5.747	0.150	0.469	0.045
13	0.454	0.6575	2.025	0.922	1.401	4.348	0.151	0.481	0.046
14	0.560	0.4564	1.325	0.607	1.029	2.961	0.154	0.509	0.048
15	0.691	0.3233	0.931	0.451	0.765	2.166	0.149	0.494	0.045
16	0.852	0.1567	0.60·	0.449	0.501	1.551	0.101	0.302	0.020
17	1.051	-0.1025	0.350	0.476	0.342	1.168	-0.088	-0.251	0.015

DISPLACEMENT THICKNESS = 1.006 CM.   MOMENTUM THICKNESS = 0.671 CM.   DELTA 99 = 4.872 CM.

MOMENTUM THICKNESS REYNOLDS NO. = 6932.   UTAU = 0.507 M/SEC   UPW = 16.10 M/SEC

OUTPUT NONDIMENSIONALIZED ON WALL VELOCITY

PT	Y/DEL	UV/UPWS	USQ/UPWS	VSQ/UPWS	WSQ/UPWS	QSQ/UPWS
1	0.036	0.00109	0.00398	0.00162	0.00244	0.00805
2	0.045	0.00110	0.00381	0.00161	0.00238	0.00780
3	0.056	0.00110	0.00374	0.00163	0.00231	0.00768
4	0.069	0.00112	0.00372	0.00163	0.00234	0.00769
5	0.084	0.00111	0.00370	0.00166	0.00228	0.00764
6	0.104	0.00113	0.00367	0.00170	0.00232	0.00769
7	0.129	0.00115	0.00365	0.00171	0.00231	0.00767
8	0.159	0.00115	0.00363	0.00172	0.00231	0.00766
9	0.196	0.00114	0.00359	0.00169	0.00231	0.00760
10	0.242	0.00109	0.00344	0.00162	0.00224	0.00729
11	0.298	0.00101	0.00308	0.00147	0.00208	0.00663
12	0.368	0.00085	0.00267	0.00124	0.00178	0.00569
13	0.454	0.00065	0.00201	0.00091	0.00139	0.00431
14	0.560	0.00045	0.00131	0.00060	0.00102	0.00293
15	0.691	0.00032	0.00094	0.00045	0.00075	0.00215
16	0.852	0.00016	0.00060	0.00044	0.00050	0.00154
17	1.051	-0.00010	0.00035	0.00047	0.00034	0.00116

STATEMENTS EXECUTED= 5326

CORE USAGE   OBJECT CODE= 5992 BYTES,ARRAY AREA= 2032 BYTES,TOTAL AREA AVAILABLE= 147456 BYTES

DIAGNOSTICS   NUMBER OF ERRORS= 0, NUMBER OF WARNINGS= 1, NUMBER OF EXTENSIONS= 0

COMPILE TIME= 0.05 SEC,EXECUTION TIME= 0.29 SEC, 14.57.52 FRIDAY 30 MAY 80 WATFIV

FIRST EXPT., STN. 1, S = -71.75 CM.

PT	Y/DEL	U/UPH	UCALC	VELGRAD
1	0.000	0.000	0.070	20.108
2	0.017	0.435	0.381	14.745
3	0.020	0.455	0.423	12.814
4	0.024	0.495	0.469	10.259
5	0.030	0.524	0.520	6.941
6	0.037	0.547	0.558	4.162
7	0.043	0.566	0.578	2.650
8	0.052	0.584	0.596	1.414
9	0.061	0.599	0.606	0.959
10	0.069	0.608	0.613	0.883
11	0.081	0.623	0.624	0.921
12	0.102	0.644	0.644	0.936
13	0.129	0.668	0.667	0.808
14	0.165	0.693	0.693	0.654
15	0.212	0.722	0.722	0.569
16	0.271	0.753	0.753	0.494
17	0.347	0.789	0.789	0.460
18	0.445	0.832	0.832	0.403
19	0.571	0.878	0.878	0.352
20	0.696	0.921	0.921	0.318
21	0.826	0.957	0.957	0.242
22	0.940	0.981	0.981	0.175
23	1.008	0.991	0.991	0.113
24	1.207	0.999	0.999	0.006
25	1.329	1.000	1.000	0.000

PT	Y/DEL	UCAL/UP	VELGRAD	MIX LN/DEL	PROD	L/LO	RIC	BETA	ED.RE
1	0.067	0.611	0.895	0.0448	23.73	1.701	0.0000	0.0	111.24
2	0.073	0.617	0.893	0.0446	24.16	1.538	0.0000	0.0	111.21
3	0.081	0.624	0.921	0.0437	25.44	1.345	0.0000	0.0	110.16
4	0.103	0.645	0.933	0.0432	25.82	1.030	0.0000	0.0	108.92
5	0.165	0.693	0.654	0.0610	17.73	0.902	0.0000	0.0	152.31
6	0.270	0.753	0.495	0.0780	12.61	0.918	0.0000	0.0	188.73
7	0.443	0.831	0.405	0.0875	8.68	1.029	0.0000	0.0	194.13
8	0.568	0.877	0.351	0.0917	6.21	1.079	0.0000	0.0	184.90
9	0.692	0.920	0.320	0.0867	4.21	1.020	0.0000	0.0	150.72
10	0.802	0.956	0.243	0.0858	1.81	1.009	0.0000	0.0	112.16
11	0.935	0.980	0.179	0.0804	0.63	0.945	0.0000	0.0	72.17

FIRST EXPT., STN. 2, S = -41.27 CM.

PT	Y/DEL	U/UFW	UCALC	VELGRAD
1	0.000	0.000	0.064	25.823
2	0.014	0.445	0.389	18.092
3	0.017	0.483	0.439	14.734
4	0.021	0.505	0.489	10.555
5	0.026	0.516	0.531	6.590
6	0.031	0.547	0.557	4.011
7	0.037	0.564	0.575	2.214
8	0.044	0.577	0.587	1.313
9	0.052	0.591	0.596	1.082
10	0.059	0.602	0.604	1.121
11	0.069	0.616	0.615	1.160
12	0.087	0.636	0.636	1.069
13	0.110	0.658	0.658	0.903
14	0.141	0.683	0.683	0.644
15	0.181	0.704	0.705	0.575
16	0.231	0.737	0.737	0.601
17	0.296	0.765	0.768	0.446
18	0.379	0.807	0.807	0.469
19	0.593	0.890	0.890	0.35
20	0.704	0.929	0.928	0.326
21	0.802	0.957	0.957	0.255
22	0.869	0.970	0.970	0.204
23	1.030	0.994	0.994	0.081
24	1.133	0.999	0.999	0.017
25	1.244	0.999	0.999	-0.001
26	1.355	1.000	1.000	0.000

PT	Y/DEL	UCAL/UP	VELGRAD	MIX LN/DEL	PROD	L/LO	RIC	BETA	ED.RE
1	0.061	0.606	1.138	0.0335	28.78	1.389	0.0000	0.0	91.71
2	0.079	0.627	1.125	0.0337	28.11	1.055	0.0000	0.0	91.70
3	0.098	0.647	0.983	0.0339	24.94	0.972	0.0000	0.0	106.46
4	0.120	0.667	0.834	0.0458	21.20	0.933	0.0000	0.0	125.63
5	0.148	0.687	0.581	0.0661	14.93	1.090	0.0000	0.0	182.24
6	0.183	0.706	0.589	0.0645	14.77	0.860	0.0000	0.0	175.82
7	0.226	0.734	0.628	0.0610	16.00	0.718	0.0000	0.0	167.61
8	0.279	0.761	0.440	0.0856	10.86	1.007	0.0000	0.0	231.18
9	0.344	0.791	0.477	0.0769	11.13	0.905	0.0000	0.0	202.16
10	0.424	0.827	0.419	0.0834	8.91	0.981	0.0000	0.0	205.99
11	0.523	0.865	0.364	0.0885	6.56	1.041	0.0000	0.0	204.37
12	0.644	0.908	0.345	0.0796	4.53	0.937	0.0000	0.0	156.91
13	0.796	0.955	0.261	0.0793	1.95	0.933	0.0000	0.0	117.83
14	0.981	0.989	0.114	0.0824	0.17	0.970	0.0000	0.0	55.44
15	1.210	0.999	-0.006	0.0000	0.00	0.000	0.0000	0.0	0.00

FIRST EXPT., STN. 3, S = - 6.20 CM.

PT	Y/DEL	U/UPW	UCALC	VELGRAD
1	0.000	0.000	0.076	24.619
2	0.003	0.171	0.149	24.241
3	0.007	0.229	0.243	22.755
4	0.011	0.367	0.330	20.187
5	0.015	0.434	0.404	16.740
6	0.018	0.481	0.450	13.946
7	0.023	0.513	0.509	9.713
8	0.027	0.540	0.542	6.980
9	0.032	0.565	0.570	4.420
10	0.039	0.582	0.592	2.264
11	0.045	0.594	0.603	1.449
12	0.052	0.605	0.612	1.174
13	0.061	0.620	0.623	1.241
14	0.077	0.643	0.645	1.462
15	0.097	0.676	0.673	1.192
16	0.123	0.694	0.696	0.762
17	0.158	0.722	0.721	0.595
18	0.201	0.741	0.742	0.520
19	0.257	0.777	0.777	0.569
20	0.330	0.807	0.807	0.396
21	0.424	0.843	0.843	0.212
22	0.517	0.857	0.857	0.356
23	0.614	0.914	0.914	0.559
24	0.693	0.952	0.952	0.494
25	0.748	0.977	0.977	0.371
26	0.897	0.979	0.979	-0.026
27	0.987	0.988	0.988	0.185
28	1.084	1.004	1.004	0.070
29	1.181	1.000	1.000	0.000

PT	Y/DEL	UCAL/UP	VELGRAD	MIX LN/DEL	PROD	L/LO	RIC	BETA	ED.RE
1	0.050	0.610	1.202	0.0324	32.04	1.652	0.0000	0.0	105.58
2	0.055	0.616	1.175	0.0328	30.55	1.499	0.0000	0.0	105.34
3	0.069	0.633	1.370	0.0278	34.87	0.995	0.0000	0.0	88.40
4	0.085	0.656	1.463	0.0258	36.74	0.745	0.0000	0.0	81.63
5	0.105	0.681	0.951	0.0392	23.20	0.912	0.0000	0.0	122.16
6	0.129	0.700	0.773	0.0488	19.26	0.922	0.0000	0.0	153.47
7	0.159	0.722	0.582	0.0629	13.70	0.964	0.0000	0.0	192.21
8	0.197	0.740	0.488	0.0754	11.58	0.934	0.0000	0.0	231.75
9	0.243	0.768	0.645	0.0560	14.76	0.659	0.0000	0.0	169.06
10	0.299	0.796	0.377	0.0944	8.39	1.111	0.0000	0.0	280.85
11	0.369	0.824	0.427	0.0818	9.17	0.962	0.0000	0.0	238.78
12	0.455	0.847	0.090	0.3610	1.66	4.247	0.0000	0.0	978.66
13	0.561	0.880	0.633	0.0459	9.39	0.540	0.0000	0.0	111.44
14	0.693	0.950	0.476	0.0499	4.69	0.587	0.0000	0.0	98.78
15	0.855	0.982	-0.104	-0.1471	-0.43	*****	0.0000	0.0	-188.05
16	1.054	1.000	0.152	0.0260	0.04	0.306	0.0000	0.0	8.60

PT	Y/DEL	U/UPW	UCALC	VELGRAD
1	0.000	0.000	0.073	22.222
2	0.013	0.375	0.339	16.921
3	0.015	0.414	0.371	15.226
4	0.018	0.442	0.413	12.616
5	0.023	0.478	0.466	8.696
6	0.028	0.496	0.501	5.684
7	0.033	0.512	0.524	3.658
8	0.039	0.527	0.541	2.271
9	0.046	0.545	0.554	1.571
10	0.053	0.559	0.565	1.382
11	0.062	0.574	0.577	1.402
12	0.078	0.601	0.600	1.421
13	0.098	0.627	0.627	1.266
14	0.125	0.658	0.658	1.043
15	0.160	0.690	0.690	0.789
16	0.205	0.720	0.720	0.582
17	0.262	0.750	0.750	0.485
18	0.337	0.784	0.784	0.419
19	0.432	0.821	0.821	0.374
20	0.526	0.856	0.856	0.372
21	0.625	0.891	0.891	0.316
22	0.712	0.917	0.917	0.319
23	0.767	0.934	0.934	0.322
24	0.914	0.973	0.973	0.214
25	1.006	0.991	0.991	0.175
26	1.105	1.003	1.003	0.038
27	1.203	1.002	1.002	0.009
28	1.315	1.010	1.010	0.000

PT	Y/DEL	UCAL/UP	VELGRAD	MIX LN/DEL	PROD	L/LO	RIC	BETA	ED.RE
1	0.034	0.528	3.360	0.0088	68.16	0.739	0.0000	0.0	19.29
2	0.046	0.554	1.571	0.0184	30.39	1.052	0.0000	0.0	39.34
3	0.057	0.570	1.375	0.0206	25.62	0.918	0.0000	0.0	43.29
4	0.070	0.593	1.449	0.0188	24.72	0.668	0.0000	0.0	37.87
5	0.087	0.612	1.356	0.0189	23.66	0.533	0.0000	0.0	35.90
6	0.107	0.638	1.190	0.0194	14.73	0.443	0.0000	0.0	33.26
7	0.131	0.664	0.997	0.0204	9.53	0.379	0.0000	0.0	30.64
8	0.162	0.691	0.776	0.0215	5.02	0.324	0.0000	0.0	26.68
9	0.201	0.718	0.593	0.0237	2.72	0.288	0.0000	0.0	24.76
10	0.247	0.743	0.502	0.0215	1.36	0.253	0.0000	0.0	17.27
11	0.305	0.770	0.448	0.0182	0.69	0.214	0.0000	0.0	10.99
12	0.376	0.800	0.391	0.0110	0.17	0.129	0.0000	0.0	3.50
13	0.464	0.833	0.373	0.0115	-0.16	0.136	0.0000	0.0	3.67
14	0.572	0.873	0.360	0.0097	-0.42	0.232	0.0000	0.0	10.39
15	0.706	0.915	0.312	0.0303	-0.65	0.357	0.0000	0.0	21.30
16	0.871	0.963	0.233	0.0417	-0.51	0.490	0.0000	0.0	30.03
17	1.074	1.001	0.099	0.0785	-0.14	0.923	0.0000	0.0	45.17

FIRST EXPT., STN. 5, S = 33.65 CM.

PT	Y/DEL	U/UPW	UCALC	VELGRAD
1	0.000	0.000	0.074	20.995
2	0.011	0.336	0.290	16.787
3	0.014	0.372	0.337	14.372
4	0.017	0.402	0.376	11.862
5	0.021	0.426	0.417	8.793
6	0.025	0.446	0.447	6.278
7	0.030	0.465	0.472	3.993
8	0.036	0.478	0.491	2.367
9	0.042	0.492	0.503	1.629
10	0.048	0.505	0.511	1.390
11	0.057	0.520	0.524	1.381
12	0.072	0.545	0.545	1.470
13	0.090	0.572	0.571	1.376
14	0.115	0.603	0.602	1.132
15	0.148	0.636	0.637	0.964
16	0.189	0.672	0.672	0.770
17	0.241	0.705	0.705	0.549
18	0.309	0.740	0.740	0.443
19	0.396	0.772	0.772	0.346
20	0.483	0.802	0.802	0.317
21	0.574	0.828	0.828	0.247
22	0.653	0.846	0.846	0.254
23	0.700	0.859	0.859	0.256
24	0.839	0.887	0.887	0.174
25	0.924	0.900	0.900	0.115
26	1.014	0.906	0.906	0.019
27	1.104	0.905	0.905	-0.043
28	1.207	0.899	0.899	-0.068
29	1.500	0.877	0.877	0.000

PT	Y/DEL	UCAL/UP	VELGRAD	MIX LN/DEL	PROD	L/LO	RIC	BETA	ED.RE
1	0.031	0.476	3.646	0.0088	*****	0.826	0.0243	7.2	21.32
2	0.041	0.501	1.705	0.0185	46.01	1.215	0.0541	-4.0	44.58
3	0.054	0.520	1.360	0.0228	35.00	1.076	0.0700	-1.1	53.75
4	0.069	0.541	1.464	0.0204	34.99	0.734	0.0677	3.9	46.29
5	0.087	0.567	1.407	0.0205	31.22	0.577	0.0737	5.7	44.87
6	0.110	0.597	1.174	0.0229	22.56	0.510	0.0924	5.3	47.06
7	0.133	0.627	0.994	0.0249	15.99	0.441	0.1139	4.9	47.06
8	0.173	0.660	0.867	0.0256	11.01	0.360	0.1364	4.7	43.14
9	0.216	0.691	0.609	0.0324	5.87	0.381	0.1996	3.1	48.53
10	0.269	0.720	0.518	0.0326	3.56	0.383	0.2413	2.6	41.83
11	0.334	0.750	0.395	0.0371	1.94	0.437	0.3211	1.8	41.43
12	0.415	0.779	0.345	0.0341	1.05	0.401	0.3742	1.6	30.50
13	0.514	0.811	0.295	0.0281	0.42	0.331	0.4456	1.5	17.73
14	0.637	0.842	0.241	0.0162	0.07	0.191	0.5462	1.5	4.82
15	0.789	0.878	0.191	0.0353	-0.14	0.416	0.6816	0.9	18.20
16	0.975	0.905	0.058	0.1216	0.04	1.431	1.5484	-0.3	65.55
17	1.206	0.899	-0.068	-0.0577	0.06	*****	******	0.0	-17.15
18	1.490	0.878	-0.077	-0.0272	0.02	*****	******	0.0	-4.33

FIRST EXPT., STN. 6, S = 50.80 CM.

PT	Y/DEL	U/UPW	UCALC	VELGRAD
1	0.000	0.000	0.077	18.486
2	0.011	0.300	0.268	15.083
3	0.013	0.336	0.297	13.779
4	0.016	0.364	0.335	11.699
5	0.020	0.393	0.377	9.022
6	0.024	0.412	0.408	6.698
7	0.029	0.431	0.435	4.462
8	0.035	0.443	0.457	2.743
9	0.041	0.459	0.470	1.848
10	0.046	0.470	0.478	1.502
11	0.054	0.485	0.489	1.280
12	0.069	0.506	0.508	1.252
13	0.087	0.531	0.531	1.322
14	0.111	0.563	0.562	1.254
15	0.142	0.599	0.599	1.106
16	0.181	0.639	0.639	0.908
17	0.231	0.678	0.678	0.707
18	0.297	0.720	0.720	0.558
19	0.380	0.759	0.759	0.368
20	0.464	0.785	0.786	0.322
21	0.550	0.813	0.813	0.299
22	0.627	0.834	0.834	0.252
23	0.805	0.876	0.876	0.217
24	0.894	0.892	0.892	0.159
25	0.973	0.901	0.901	0.059
26	1.060	0.903	0.903	-0.025
27	1.153	0.898	0.898	-0.067
28	1.303	0.887	0.887	0.000

PT	Y/DEL	UCAL/UP	VELGRAD	MIX LN/DEL	PROD	L/LO	RIC	BETA	ED.RE
1	0.034	0.454	2.961	0.0104	*****	0.880	0.0296	4.0	23.25
2	0.041	0.470	1.848	0.0162	60.67	1.079	0.0489	-1.6	35.48
3	0.050	0.484	1.359	0.0017	42.75	1.133	0.0681	-1.9	46.76
4	0.062	0.499	1.270	0.0235	36.84	0.956	0.0774	0.6	49.43
5	0.076	0.517	1.295	0.0218	36.96	0.710	0.0761	3.8	44.69
6	0.094	0.541	1.317	0.0206	34.77	0.537	0.0782	5.9	40.68
7	0.116	0.569	1.226	0.0214	30.08	0.450	0.0881	6.2	40.83
8	0.143	0.600	1.102	0.0215	21.86	0.367	0.1030	6.2	37.02
9	0.177	0.635	0.933	0.0233	15.41	0.321	0.1277	5.3	36.93
10	0.218	0.669	0.737	0.0257	8.98	0.302	0.1683	4.1	35.38
11	0.269	0.703	0.631	0.0254	5.40	0.299	0.2043	3.4	29.59
12	0.331	0.733	0.469	0.0302	2.97	0.355	0.2816	2.3	31.07
13	0.409	0.768	0.330	0.0377	1.43	0.444	0.4007	1.4	34.25
14	0.504	0.799	0.330	0.0341	1.20	0.402	0.4148	1.4	28.02
15	0.622	0.833	0.252	0.0426	0.74	0.501	0.5424	0.9	33.30
16	0.767	0.868	0.227	0.0333	0.31	0.397	0.6126	1.0	18.86
17	0.946	0.899	0.091	0.0268	-0.00	0.315	1.2393	0.6	4.74
18	1.167	0.897	-0.068	-0.0060	0.12	*****	******	0.0	-21.51

FIRST EXPT., STN. 7, S = 64.13 CM.

PT	Y/DEL	U/UPW	UCALC	VELGRAD
1	0.000	0.000	0.077	18.728
2	0.011	0.303	0.270	15.134
3	0.013	0.338	0.299	13.759
4	0.016	0.366	0.337	11.578
5	0.020	0.391	0.377	8.804
6	0.024	0.411	0.408	6.427
7	0.028	0.425	0.429	4.556
8	0.034	0.439	0.450	2.674
9	0.040	0.452	0.463	1.685
10	0.045	0.463	0.471	1.311
11	0.053	0.473	0.480	1.131
12	0.067	0.495	0.496	1.209
13	0.085	0.520	0.519	1.306
14	0.108	0.549	0.549	1.250
15	0.138	0.584	0.584	1.063
16	0.177	0.621	0.621	0.910
17	0.226	0.664	0.664	0.804
18	0.290	0.708	0.708	0.597
19	0.371	0.749	0.749	0.431
20	0.453	0.781	0.781	0.342
21	0.537	0.807	0.807	0.284
22	0.612	0.827	0.827	0.281
23	0.656	0.840	0.840	0.278
24	0.786	0.872	0.872	0.212
25	0.865	0.886	0.866	0.158
26	0.950	0.897	0.897	0.094
27	1.034	0.902	0.902	0.011
28	1.130	0.899	0.899	0.000

PT	Y/DEL	UCAL/UP	VELGRAD	MIX LN/DEL	PROD	L/LO	RIC	BETA	ED.RE
1	0.029	0.434	4.168	0.0070	*****	0.727	0.0207	13.2	15.55
2	0.040	0.463	1.685	0.0172	48.87	1.169	0.0540	-3.1	38.04
3	0.049	0.475	1.175	0.0243	32.35	1.285	0.0790	-3.6	52.52
4	0.060	0.488	1.153	0.0246	31.29	1.032	0.0826	-0.4	52.85
5	0.075	0.506	1.274	0.0218	33.30	0.719	0.0776	3.6	45.95
6	0.092	0.528	1.303	0.0207	32.10	0.552	0.0792	5.7	42.39
7	0.113	0.555	1.222	0.0211	27.29	0.455	0.0884	6.2	41.14
8	0.140	0.586	1.049	0.0230	20.33	0.401	0.1081	5.5	42.09
9	0.172	0.617	0.916	0.0242	14.79	0.343	0.1296	5.1	40.66
10	0.213	0.653	0.847	0.0229	10.35	0.269	0.1476	4.9	33.65
11	0.262	0.691	0.681	0.0238	5.68	0.280	0.1915	3.8	29.30
12	0.323	0.727	0.514	0.0257	2.72	0.302	0.2613	2.7	25.78
13	0.399	0.761	0.396	0.0265	1.25	0.312	0.3459	2.0	21.17
14	0.492	0.793	0.311	0.0293	0.68	0.344	0.4455	1.5	20.19
15	0.607	0.826	0.279	0.0301	0.49	0.354	0.5063	1.3	19.20
16	0.749	0.863	0.229	0.0337	0.30	0.397	0.6211	1.0	19.72
17	0.924	0.894	0.111	0.0530	0.03	0.623	1.1077	0.3	23.56
18	1.140	0.899	-0.001	-3.2332	0.01	*****	3.5801	10.9	-472.97
19	1.406	0.897	-0.009	-0.3078	0.03	*****	4.2884	1.1	-63.66

FIRST EXPT., STN. 8, S =   81.91 CM.

PT	Y/DEL	U/UPW	UCALC	VELGRAD
1	0.000	0.000	0.074	19.910
2	0.012	0.337	0.295	15.326
3	0.014	0.360	0.324	13.742
4	0.017	0.390	0.361	11.296
5	0.021	0.414	0.400	8.272
6	0.026	0.430	0.434	5.261
7	0.030	0.443	0.451	3.536
8	0.037	0.456	0.469	1.730
9	0.043	0.465	0.477	1.114
10	0.049	0.476	0.483	0.969
11	0.057	0.488	0.491	1.021
12	0.072	0.508	0.508	1.152
13	0.091	0.531	0.530	1.145
14	0.117	0.558	0.558	1.098
15	0.149	0.594	0.594	1.085
16	0.191	0.637	0.637	0.948
17	0.244	0.683	0.683	0.819
18	0.312	0.735	0.735	0.687
19	0.400	0.784	0.784	0.438
20	0.488	0.815	0.815	0.303
21	0.579	0.840	0.840	0.232
22	0.660	0.857	0.857	0.200
23	0.707	0.866	0.866	0.205
24	0.847	0.892	0.892	0.149
25	0.932	0.902	0.902	0.088
26	1.004	0.907	0.907	0.017
27	1.115	0.905	0.905	-0.046
28	1.219	0.899	0.899	-0.076
29	1.550	0.874	0.874	0.000

PT	Y/DEL	UCAL/UP	VELGRAD	MIX LN/DEL	PROD	L/LO	RIC	BETA	ED.RE
1	0.043	0.477	1.114	0.0290	36.09	1.820	0.0774	-10.6	67.62
2	0.052	0.486	0.976	0.0331	31.41	1.650	0.0897	-7.2	77.19
3	0.065	0.500	1.107	0.0296	36.81	1.144	0.0815	-1.8	69.96
4	0.080	0.517	1.171	0.0281	39.33	0.869	0.0797	1.6	66.74
5	0.099	0.539	1.112	0.0295	36.83	0.730	0.0874	3.1	69.70
6	0.122	0.564	1.105	0.0291	35.18	0.583	0.0919	4.5	67.54
7	0.151	0.596	1.080	0.0291	32.61	0.470	0.0991	5.3	65.81
8	0.186	0.632	0.988	0.0309	26.27	0.406	0.1167	5.1	66.69
9	0.229	0.670	0.833	0.0328	18.91	0.386	0.1418	4.3	64.98
10	0.283	0.714	0.761	0.0317	13.06	0.373	0.1649	3.8	55.07
11	0.349	0.758	0.577	0.0356	6.91	0.419	0.2264	2.6	52.68
12	0.430	0.796	0.371	0.0437	2.53	0.514	0.3542	1.4	51.10
13	0.530	0.827	0.277	0.0484	1.16	0.570	0.4738	0.9	46.74
14	0.654	0.855	0.199	0.0596	0.54	0.701	0.6414	0.5	50.77
15	0.807	0.885	0.173	0.0622	0.34	0.732	0.7341	0.4	48.35
16	0.996	0.906	0.039	0.1376	-0.04	1.619	1.8644	-0.3	53.00
17	1.208	0.899	-0.076	-0.1134	0.38	*****	******	0.0	-70.26
18	1.372	0.887	-0.073	-0.1512	0.60	*****	******	0.0	-119.45
19	1.516	0.877	-0.071	-0.1961	0.96	*****	******	0.0	-197.41

FIRST EXPT., STN. 9, S = 97.16 CM.

PT	Y/DEL	U/UPW	UCALC	VELGRAD
1	0.000	0.000	0.077	20.270
2	0.011	0.322	0.285	16.249
3	0.013	0.349	0.316	14.718
4	0.016	0.385	0.357	12.287
5	0.019	0.410	0.390	9.908
6	0.023	0.429	0.424	7.124
7	0.028	0.444	0.453	4.491
8	0.033	0.461	0.470	2.754
9	0.039	0.471	0.483	1.589
10	0.044	0.480	0.490	1.156
11	0.051	0.492	0.497	0.932
12	0.065	0.507	0.509	0.915
13	0.082	0.526	0.526	1.020
14	0.105	0.550	0.549	0.985
15	0.135	0.577	0.577	0.910
16	0.173	0.612	0.612	0.898
17	0.221	0.654	0.654	0.876
18	0.283	0.707	0.707	0.789
19	0.363	0.763	0.763	0.657
20	0.443	0.813	0.813	0.562
21	0.526	0.853	0.853	0.418
22	0.599	0.881	0.881	0.358
23	0.642	0.896	0.896	0.342
24	0.769	0.937	0.937	0.301
25	0.846	0.959	0.959	0.269
26	0.929	0.979	0.979	0.202
27	1.012	0.992	0.992	0.115
28	1.106	0.999	0.999	0.038
29	1.244	1.000	1.000	0.000

PT	Y/DEL	UCAL/UP	VELGRAD	MIX LN/DEL	PROD	L/LO	RIC	BETA	ED.RE
1	0.039	0.483	1.589	0.0199	50.48	1.373	0.0000	0.0	50.18
2	0.048	0.494	0.994	0.0324	32.63	1.739	0.0000	0.0	82.97
3	0.059	0.504	0.884	0.0365	29.29	1.553	0.0000	0.0	94.04
4	0.073	0.517	0.979	0.0334	33.22	1.128	0.0000	0.0	86.94
5	0.090	0.534	1.029	0.0317	34.84	0.863	0.0000	0.0	82.57
6	0.111	0.555	0.955	0.0344	32.66	0.756	0.0000	0.0	89.90
7	0.137	0.579	0.912	0.0357	30.60	0.635	0.0000	0.0	92.43
8	0.169	0.608	0.902	0.0362	30.55	0.522	0.0000	0.0	94.17
9	0.208	0.643	0.873	0.0364	28.07	0.429	0.0000	0.0	92.42
10	0.256	0.685	0.855	0.0350	24.28	0.412	0.0000	0.0	83.44
11	0.316	0.731	0.705	0.0384	16.42	0.452	0.0000	0.0	83.04
12	0.390	0.781	0.644	0.0357	10.83	0.420	0.0000	0.0	65.57
13	0.481	0.833	0.485	0.0407	5.99	0.478	0.0000	0.0	63.94
14	0.594	0.879	0.360	0.0450	3.00	0.529	0.0000	0.0	58.07
15	0.732	0.926	0.315	0.0452	2.02	0.532	0.0000	0.0	51.29
16	0.903	0.973	0.230	0.0399	0.61	0.469	0.0000	0.0	29.09
17	1.114	0.999	0.033	0.2869	-0.10	3.375	0.0000	0.0	217.89

215

FIRST EXPT., STN. 10, S = 112.40 CM.

PT	Y/DEL	U/UPW	UCALC	VELGRAD
1	0.000	0.000	0.073	23.441
2	0.010	0.335	0.290	18.170
3	0.012	0.365	0.324	15.981
4	0.015	0.391	0.367	12.653
5	0.018	0.405	0.401	9.640
6	0.022	0.431	0.432	6.402
7	0.026	0.444	0.453	4.085
8	0.031	0.458	0.468	2.302
9	0.037	0.467	0.479	1.333
10	0.042	0.479	0.485	1.100
11	0.048	0.489	0.491	1.052
12	0.061	0.505	0.505	1.069
13	0.079	0.523	0.523	1.083
14	0.099	0.546	0.545	0.981
15	0.127	0.570	0.570	0.854
16	0.163	0.601	0.601	0.819
17	0.208	0.636	0.636	0.776
18	0.267	0.682	0.682	0.752
19	0.343	0.735	0.735	0.659
20	0.418	0.783	0.783	0.628
21	0.496	0.830	0.830	0.556
22	0.565	0.865	0.865	0.468
23	0.605	0.883	0.883	0.430
24	0.725	0.928	0.928	0.325
25	0.798	0.950	0.950	0.283
26	0.876	0.970	0.970	0.216
27	0.954	0.984	0.984	0.159
28	1.043	0.996	0.996	0.091
29	1.173	1.000	1.000	0.000

PT	Y/DEL	UCAL/UP	VELGRAD	MIX LN/DEL	PROD	L/LO	RIC	BETA	ED.RE
1	0.036	0.477	1.423	0.0032	49.76	1.744	0.0000	0.0	64.76
2	0.044	0.487	1.071	0.0308	37.46	1.815	0.0000	0.0	86.02
3	0.056	0.500	1.063	0.0311	37.15	1.391	0.0000	0.0	86.73
4	0.069	0.514	1.077	0.0309	38.33	1.106	0.0000	0.0	87.14
5	0.084	0.530	1.076	0.0302	38.31	0.902	0.0000	0.0	87.18
6	0.104	0.550	0.936	0.0357	33.62	0.839	0.0000	0.0	101.15
7	0.129	0.572	0.855	0.0396	31.54	0.749	0.0000	0.0	113.62
8	0.159	0.598	0.829	0.0409	30.59	0.627	0.0000	0.0	117.16
9	0.196	0.627	0.770	0.0436	27.91	0.543	0.0000	0.0	123.99
10	0.242	0.663	0.782	0.0420	27.09	0.494	0.0000	0.0	116.79
11	0.298	0.704	0.703	0.0450	22.58	0.529	0.0000	0.0	120.30
12	0.363	0.751	0.644	0.0448	17.20	0.527	0.0000	0.0	109.24
13	0.454	0.805	0.610	0.0410	12.21	0.482	0.0000	0.0	86.57
14	0.560	0.863	0.473	0.0431	6.31	0.507	0.0000	0.0	74.44
15	0.691	0.917	0.352	0.0482	3.24	0.567	0.0000	0.0	69.11
16	0.852	0.964	0.245	0.0426	0.86	0.501	0.0000	0.0	37.63
17	1.051	0.997	0.080	0.1516	-0.38	1.783	0.0000	0.0	156.33

STATEMENTS EXECUTED= 55819

CORE USAGE   OBJECT CODE= 17736 BYTES,ARRAY AREA=   8968 BYTES,TOTAL AREA AVAILABLE= 147456 BYTES

DIAGNOSTICS   NUMBER OF ERRORS=   0, NUMBER OF WARNINGS=   0, NUMBER OF EXTENSIONS=   0

216

Wall static pressure distribution -- SECOND EXPERIMENT

TAP	s, cm	C_p
1	- 82.55	0.00
2	- 59.69	.006
3	- 26.67	.002
4	- 8.89	.025
5	2.54	- .014
6	7.62	- .018
7	12.70	- .006
8	17.78	.006
9	22.86	.005
10	27.94	.000
11	33.02	- .003
12	38.10	.001
13	43.18	.000
14	48.26	.002
15	53.34	.005
16	58.42	- .002
17	63.50	- .020
18	68.58	- .021
19	76.96	.019
20	87.12	.006
21	98.55	.000
22	129.03	- .002
23	159.51	- .002
24	189.97	- .007

$$C_p = \frac{P - P_{TAP_1}}{\frac{1}{2} \rho U_{pw}^2}$$

s = 0 at start of curvature

SEC. EXPT., STN 1, S=-118.74 CM., UPW=14.94 M/SEC

PT	Y/DEL	U/UP	DY PR	YPLUS	UPLUS	CF/2
1	0.022	0.503	0.333	19.	11.6	0.00172
2	0.040	0.603	0.478	36.	13.9	0.00193
3	0.058	0.642	0.541	51.	14.8	0.00193
4	0.075	0.667	0.584	66.	15.4	0.00191
5	0.104	0.695	0.635	91.	16.0	0.00188
6	0.127	0.713	0.668	112.	16.5	0.00187
7	0.155	0.732	0.704	137.	16.9	0.00186
8	0.189	0.752	0.742	167.	17.3	0.00185
9	0.232	0.773	0.785	205.	17.8	0.00185
10	0.286	0.795	0.831	252.	18.3	0.00185
11	0.353	0.823	0.889	311.	19.0	0.00187
12	0.434	0.852	0.952	383.	19.6	0.00190
13	0.536	0.883	1.024	472.	20.4	0.00194
14	0.660	0.925	1.123	582.	21.3	0.00201
15	0.814	0.966	1.224	717.	22.3	0.00208
16	1.002	0.990	1.288	883.	22.8	0.00209
17	1.237	1.000	1.313	1090.	23.1	0.00204
18	1.526	1.000	1.313	1345.	23.1	0.00195
19	1.882	1.000	1.313	1658.	23.1	0.00188

DISP. THICKNESS = 0.322 CM.   MOMT. THICKESS =0.248 CM.

SHAPE FACTOR = 1.300   DELTA 99 = 2.206 CM.

MOMENTUM THICKNESS REYNOLDS NO. = 2282.   CF/2 = 0.00188

SEC. EXPT., STN 2, S=-74.29 CM., UPW=15.11 M/SEC

PT	Y/DEL	U/UP	DY PR	YPLUS	UPLUS	CF/2
1	0.016	0.441	0.262	19.	10.6	0.00138
2	0.030	0.565	0.429	34.	13.6	0.00172
3	0.043	0.607	0.495	49.	14.6	0.00175
4	0.056	0.632	0.536	64.	15.2	0.00174
5	0.078	0.665	0.594	89.	16.0	0.00174
6	0.095	0.683	0.627	109.	16.4	0.00173
7	0.116	0.704	0.665	133.	16.9	0.00173
8	0.141	0.724	0.704	162.	17.4	0.00173
9	0.174	0.746	0.747	199.	17.9	0.00174
10	0.214	0.770	0.795	245.	18.5	0.00175
11	0.263	0.795	0.848	301.	19.1	0.00176
12	.324	0.820	0.902	371.	19.7	0 00177
13	0.400	0.849	0.968	458.	20.4	0.00181
14	0.492	0.881	1.041	564.	21.1	0.00184
15	0.607	0.915	1.123	695.	21.9	0.00189
16	0.748	0.951	1.214	857.	22.8	0.00194
17	0.923	0.985	1.300	1057.	23.6	0.00198
18	1.139	1.000	1.341	1304.	24.0	0.00195
19	1.404	1.001	1.344	1608.	24.0	0.00188
20	1.733	1.000	1.341	1984.	24.0	0.00180
21	2.138	1.000	1.341	2447.	24.0	0.00173

DISP. THICKNESS = 0.422 CM.   MOMT. THICKESS =0.322 CM.

SHAPE FACTOR = 1.312   DELTA 99 = 2.955 CM.

MOMENTUM THICKNESS REYNOLDS NO. = 2989.   CF/2 = 0.00174

SEC. EXPT., STN 3, S=-52.70 CM.,   UPW=15.12 M/SEC

PT	Y/DEL	U/UP	DY PR	YPLUS	UPLUS	CF/2
1	0.015	0.439	0.259	18.	10.7	0.00137
2	0.027	0.560	0.422	34.	13.6	0.00170
3	0.039	0.593	0.480	49.	14.5	0.00170
4	0.050	0.624	0.523	63.	15.2	0.00170
5	0.070	0.654	0.574	88.	15.9	0.00169
6	0.086	0.674	0.610	107.	16.4	0.00169
7	0.105	0.694	0.648	131.	16.9	0.00169
8	0.127	0.713	0.683	159.	17.3	0.00169
9	0.157	0.735	0.726	196.	17.9	0.00169
10	0.193	0.757	0.770	241.	18.4	0.00169
11	0.238	0.783	0.823	297.	19.0	0.00171
12	0.292	0.808	0.876	366.	19.6	0.00173
13	0.369	0.835	0.937	451.	20.3	0.00175
14	0.444	0.866	1.008	556.	21.1	0.00179
15	0.548	0.899	1.087	685.	21.9	0.00183
16	0.675	0.934	1.171	844.	22.7	0.00187
17	0.833	0.969	1.262	1042.	23.6	0.00192
18	1.027	0.993	1.326	1285.	24.1	0.00193
19	1.267	1.000	1.344	1585.	24.3	0.00187
20	1.563	1.000	1.344	1955.	24.3	0.00180
21	1.928	0.999	1.341	2412.	24.3	0.00173

DISP. THICKNESS = 0.470 CM.   MOMT. THICKESS =0.359 CM.

SHAPE FACTOR = 1.308   DELTA 99 = 3.277 CM.

MOMENTUM THICKNESS REYNOLDS NO. = 3332.   CF/2 = 0.00169

SEC. EXPT., STN 4, S=-41.28 CM., UPW=15.16 M/SEC

PT	Y/DEL	U/UP	DY PR	YPLUS	UPLUS	CF/2
1	0.014	0.436	0.259	19.	10.7	0.00135
2	0.025	0.557	0.422	34.	13.6	0.00167
3	0.037	0.595	0.483	49.	14.6	0.00169
4	0.049	0.619	0.521	63.	15.1	0.00167
5	0.068	0.649	0.574	88.	15.9	0.00166
6	0.082	0.669	0.610	108.	16.4	0.00166
7	0.101	0.687	0.643	132.	16.8	0.00166
8	0.123	0.707	0.681	160.	17.3	0.00166
9	0.151	0.729	0.724	197.	17.9	0.00166
10	0.186	0.751	0.767	243.	18.4	0.00167
11	0.229	0.775	0.818	299.	19.0	0.00168
12	0.282	0.802	0.874	368.	19.6	0.00170
13	0.347	0.829	0.935	454.	20.3	0.00173
14	0.428	0.859	1.003	559.	21.0	0.00176
15	0.528	0.891	1.079	689.	21.8	0.00179
16	0.650	0.925	1.163	849.	22.7	0.00184
17	0.802	0.963	1.260	1048.	23.6	0.00189
18	0.990	0.990	1.331	1293.	24.2	0.00191
19	1.220	1.000	1.359	1594.	24.5	0.00187
20	1.506	1.001	1.361	1967.	24.5	0.00180
21	1.857	1.000	1.359	2426.	24.5	0.00173

DISP. THICKNESS = 0.491 CM.   MOMT. THICKESS =0.375 CM.

SHAPE FACTOR = 1.310   DELTA 99 = 3.401 CM.

MOMENTUM THICKNESS REYNOLDS NO. = 3528.   CF/2 = 0.00167

221

SEC. EXPT., STN 5, S=-29.84 CM., UPW=15.03 M/SEC

PT	Y/DEL	U/UP	DY PR	YPLUS	UPLUS	CF/2
1	0.013	0.429	0.246	18.	10.7	0.00132
2	0.024	0.540	0.391	33.	13.5	0.00160
3	0.034	0.579	0.450	48.	14.4	0.00162
4	0.044	0.603	0.488	62.	15.0	0.00161
5	0.062	0.634	0.538	86.	15.8	0.00160
6	0.076	0.653	0.572	105.	16.3	0.00160
7	0.092	0.676	0.612	128.	16.9	0.00161
8	0.112	0.694	0.645	156.	17.3	0.00161
9	0.138	0.714	0.683	192.	17.8	0.00161
10	0.169	0.738	0.729	236.	18.4	0.00162
11	0.209	0.762	0.777	291.	19.0	0.00163
12	0.257	0.788	0.831	358.	19.6	0.00165
13	0.317	0.815	0.889	442.	20.3	0.00168
14	0.390	0.846	0.958	544.	21.1	0.00171
15	0.481	0.879	1.034	671.	21.9	0.00176
16	0.593	0.914	1.118	827.	22.8	0.00180
17	0.732	0.952	1.212	1021.	23.7	0.00186
18	0.902	0.982	1.288	1259.	24.5	0.00189
19	1.113	1.000	1.336	1553.	24.9	0.00187
20	1.373	1.001	1.339	1915.	25.0	0.00180
21	1.694	1.000	1.336	2363.	24.9	0.00173

DISP. THICKNESS = 0.535 CM.   MOMT. THICKESS =0.405 CM.

SHAPE FACTOR = 1.321   DELTA 99 = 3.730 CM.

MOMENTUM THICKNESS REYNOLDS NO. = 3778.   CF/2 = 0.00161

SEC. EXPT., STN 7, S=10.39 CM. (13 DEG), UPW=15.00 M/SEC

PT	Y/DEL	U/UP	DY PR	YPLUS	UPLUS	CF/2
1	0.010	0.395	0.218	18.	10.3	0.00114
2	0.018	0.506	0.358	32.	13.2	0.00142
3	0.026	0.549	0.422	46.	14.3	0.00146
4	0.034	0.576	0.465	60.	15.0	0.00147
5	0.047	0.613	0.528	84.	15.9	0.00149
6	0.058	0.635	0.566	103.	16.4	0.00150
7	0.070	0.658	0.610	125.	17.0	0.00151
8	0.085	0.678	0.648	152.	17.5	0.00151
9	0.105	0.697	0.686	187.	18.0	0.00150
10	0.129	0.719	0.732	230.	18.5	0.00150
11	0.159	0.740	0.777	284.	19.0	0.00150
12	0.196	0.764	0.828	349.	19.5	0.00150
13	0.242	0.790	0.886	431.	20.1	0.00151
14	0.298	0.818	0.950	531.	20.6	0.00152
15	0.368	0.850	1.024	655.	21.3	0.00153
16	0.453	0.884	1.105	807.	22.0	0.00155
17	0.559	0.921	1.191	996.	22.6	0.00157
18	0.690	0.948	1.257	1228.	23.0	0.00155
19	0.851	0.957	1.280	1515.	22.8	0.00147
20	1.049	1.001	1.379	1869.	23.4	0.00148
21	1.295	1.001	1.379	2305.	22.9	0.00136
22	1.598	1.000	1.377	2844.	22.2	0.00124

DISP. THICKNESS = 0.676 CM.   MOMT. THICKESS =0.514 CM.

SHAPE FACTOR = 1.314   DELTA 99 = 4.879 CM.

MOMENTUM THICKNESS REYNOLDS NO. = 4889.   CF/2 = 0.00147

SEC. EXPT., STN 8, S=25.19 CM. (31 DEG), UPW=15.14 M/SEC

PT	Y/DEL	U/UP	DY PR	YPLUS	UPLUS	CF/2
1	0.010	0.316	0.140	15.	9.6	0.00080
2	0.019	0.418	0.244	28.	12.6	0.00103
3	0.027	0.455	0.290	40.	13.7	0.00106
4	0.036	0.480	0.323	52.	14.5	0.00108
5	0.050	0.512	0.368	72.	15.4	0.00109
6	0.061	0.532	0.399	88.	16.0	0.00110
7	0.075	0.554	0.434	108.	16.7	0.00112
8	0.091	0.577	0.472	131.	17.3	0.00114
9	0.112	0.610	0.528	161.	18.3	0.00119
10	0.137	0.643	0.587	198.	19.2	0.00124
11	0.168	0.677	0.650	243.	20.1	0.00128
12	0.207	0.713	0.721	299.	21.1	0.00133
13	0.255	0.746	0.790	368.	22.0	0.00137
14	0.314	0.780	0.864	454.	22.9	0.00140
15	0.387	0.816	0.942	560.	23.8	0.00143
16	0.477	0.852	1.024	689.	24.6	0.00146
17	0.589	0.894	1.120	851.	25.5	0.00149
18	0.727	0.938	1.222	1050.	26.4	0.00152
19	0.896	0.980	1.318	1294.	27.2	0.00154
20	1.105	1.000	1.361	1597.	27.2	0.00148
21	1.364	1.000	1.361	1970.	26.6	0.00136
22	1.683	1.000	1.361	2431.	25.8	0.00124

DISP. THICKNESS = 0.814 CM.   MOMT. THICKESS =0.569 CM.

SHAPE FACTOR = 1.430   DELTA 99 = 4.632 CM.

MOMENTUM THICKNESS REYNOLDS NO. = 5376.   CF/2 = 0.00109

224

SEC. EXPT., STN 9, S=41.48 CM. (52 DEG), UPW=15.13 M/SEC

PT	Y/DEL	U/UP	DY PR	YPLUS	UPLUS	CF/2
1	0.010	0.312	0.135	15.	9.4	0.00078
2	0.019	0.418	0.241	28.	12.6	0.00103
3	0.027	0.455	0.287	39.	13.8	0.00106
4	0.035	0.480	0.320	51.	14.5	0.00108
5	0.049	0.510	0.363	72.	15.4	0.00109
6	0.060	0.532	0.396	88.	16.0	0.00110
7	0.073	0.555	0.432	107.	16.7	0.00112
8	0.089	0.578	0.470	130.	17.4	0.00114
9	0.110	0.608	0.521	160.	18.2	0.00118
10	0.135	0.641	0.579	196.	19.2	0.00123
11	0.166	0.677	0.645	241.	20.2	0.00128
12	0.204	0.709	0.709	297.	21.0	0.00132
13	0.251	0.744	0.780	365.	22.0	0.00136
14	0.309	0.777	0.851	450.	22.8	0.00139
15	0.382	0.814	0.932	555.	23.7	0.00142
16	0.470	0.850	1.013	684.	24.6	0.00145
17	0.580	0.892	1.107	844.	25.5	0.00148
18	0.715	0.935	1.206	1041.	26.4	0.00151
19	0.882	0.978	1.306	1284.	27.2	0.00153
20	1.088	0.999	1.351	1584.	27.2	0.00148
21	1.343	1.000	1.354	1954.	26.6	0.00136
22	1.657	1.000	1.354	2411.	25.8	0.00124

DISP. THICKNESS = 0.825 CM.   MOMT. THICKESS =0.577 CM.

SHAPE FACTOR = 1.429   DELTA 99 = 4.705 CM.

MOMENTUM THICKNESS REYNOLDS NO. = 5414.   CF/2 = 0.00109

SEC. EXPT., STN 10, S=61.72 CM. (78 DEG), UFW=15.25 M/SEC

PT	Y/DEL	U/UP	DY PR	YPLUS	UPLUS	CF/2
1	0.010	0.309	0.135	15.	9.5	0.00077
2	0.019	0.410	0.236	27.	12.6	0.00099
3	0.027	0.449	0.284	39.	13.8	0.00104
4	0.035	0.474	0.317	51.	14.5	0.00105
5	0.048	0.504	0.361	71.	15.4	0.00106
6	0.059	0.523	0.389	87.	15.9	0.00107
7	0.072	0.542	0.419	106.	16.5	0.00108
8	0.088	0.563	0.455	129.	17.1	0.00109
9	0.108	0.590	0.500	159.	17.9	0.00112
10	0.133	0.622	0.556	195.	18.8	0.00117
11	0.163	0.658	0.622	240.	19.8	0.00122
12	0.201	0.695	0.693	295.	20.9	0.00127
13	0.247	0.733	0.772	364.	21.9	0.00132
14	0.304	0.772	0.853	448.	22.9	0.00137
15	0.376	0.808	0.935	552.	23.9	0.00141
16	0.463	0.845	1.019	680.	24.7	0.00143
17	0.571	0.886	1.113	840.	25.6	0.00147
18	0.704	0.929	1.212	1036.	26.5	0.00149
19	0.868	0.974	1.316	1277.	27.4	0.00152
20	1.071	0.999	1.372	1576.	27.5	0.00147
21	1.321	1.000	1.374	1944.	26.9	0.00136
22	1.631	0.999	1.372	2399.	26.1	0.00124

DISP. THICKNESS = 0.861 CM.   MOMT. THICKESS =0.597 CM.

SHAPE FACTOR = 1.442   DELTA 99 = 4.780 CM.

MOMENTUM THICKNESS REYNOLDS NO. = 5637.   CF/2 = 0.00106

SEC. EXPT., STN 12, S=88.47 CM., UPW=14.97 M/SEC

PT	Y/DEL	U/UP	DY PR	YPLUS	UPLUS	CF/2
1	0.010	0.310	0.127	15.	9.5	0.00078
2	0.019	0.409	0.221	27.	12.6	0.00100
3	0.027	0.445	0.262	38.	13.7	0.00103
4	0.035	0.468	0.290	50.	14.4	0.00104
5	0.048	0.492	0.320	69.	15.1	0.00104
6	0.059	0.508	0.340	84.	15.6	0.00103
7	0.072	0.525	0.363	103.	16.1	0.00104
8	0.088	0.546	0.394	126.	16.8	0.00106
9	0.108	0.567	0.424	155.	17.4	0.00107
10	0.133	0.597	0.470	190.	18.4	0.00112
11	0.164	0.633	0.528	234.	19.5	0.00118
12	0.202	0.668	0.589	288.	20.6	0.00124
13	0.248	0.714	0.673	355.	22.0	0.00133
14	0.306	0.761	0.765	437.	23.4	0.00142
15	0.377	0.808	0.861	539.	24.9	0.00151
16	0.464	0.851	0.955	663.	26.2	0.00159
17	0.573	0.890	1.044	819.	27.4	0.00165
18	0.706	0.932	1.146	1010.	28.7	0.00172
19	0.871	0.975	1.252	1245.	30.0	0.00179
20	1.074	0.999	1.316	1536.	30.7	0.00180
21	1.325	1.001	1.321	1895.	30.8	0.00174
22	1.636	1.000	1.318	2338.	30.8	0.00167

DISP. THICKNESS = 0.879 CM.   MOMT. THICKESS =0.597 CM.

SHAPE FACTOR = 1.473   DELTA 99 = 4.766 CM.

MOMENTUM THICKNESS REYNOLDS NO. = 5507.   CF/2 = 0.00106

SEC. EXPT., STN 13, S=103.71 CM., UPW=14.97 M/SEC

PT	Y/DEL	U/UP	DY PR	YPLUS	UPLUS	CF/2
1	0.010	0.319	0.135	15.	9.7	0.00081
2	0.018	0.420	0.234	27.	12.7	0.00104
3	0.026	0.457	0.277	39.	13.9	0.00108
4	0.034	0.477	0.302	51.	14.5	0.00108
5	0.048	0.505	0.338	71.	15.3	0.00108
6	0.058	0.520	0.358	86.	15.8	0.00107
7	0.071	0.536	0.381	105.	16.3	0.00108
8	0.087	0.554	0.406	128.	16.8	0.00108
9	0.107	0.576	0.439	158.	17.5	0.00110
10	0.131	0.600	0.478	194.	18.2	0.00112
11	0.161	0.628	0.523	239.	19.1	0.00116
12	0.199	0.661	0.579	294.	20.0	0.00121
13	0.245	0.700	0.650	362.	21.2	0.00128
14	0.301	0.747	0.739	446.	22.6	0.00137
15	0.372	0.798	0.843	550.	24.2	0.00147
16	0.458	0.844	0.945	677.	25.6	0.00156
17	0.565	0.888	1.046	835.	26.9	0.00164
18	0.697	0.930	1.146	1030.	28.2	0.00171
19	0.859	0.971	1.250	1270.	29.4	0.00178
20	1.060	0.998	1.321	1567.	30.3	0.00179
21	1.307	1.001	1.328	1933.	30.4	0.00173
22	1.613	1.000	1.326	2386.	30.3	0.00167
23	1.839	1.000	1.326	2721.	30.3	0.00163

DISP. THICKNESS = 0.897 CM.   MOMT. THICKESS =0.612 CM.

SHAPE FACTOR = 1.466   DELTA 99 = 4.833 CM.

MOMENTUM THICKNESS REYNOLDS NO. = 5679.   CF/2 = 0.00109

SEC. EXPT., STN 14, S=118.95 CM., UPW=15.01 M/SEC

PT	Y/DEL	U/UP	DY PR	YPLUS	UPLUS	CF/2
1	0.010	0.333	0.147	15.	9.9	0.00088
2	0.018	0.433	0.249	28.	12.9	0.00110
3	0.025	0.469	0.292	39.	13.9	0.00113
4	0.033	0.491	0.320	51.	14.6	0.00114
5	0.046	0.516	0.353	71.	15.3	0.00113
6	0.056	0.532	0.376	87.	15.8	0.00113
7	0.069	0.548	0.399	106.	16.3	0.00113
8	0.084	0.566	0.424	130.	16.8	0.00113
9	0.103	0.584	0.452	159.	17.4	0.00113
10	0.127	0.607	0.488	196.	18.0	0.00115
11	0.156	0.633	0.531	241.	18.8	0.00118
12	0.192	0.661	0.579	297.	19.6	0.00122
13	0.237	0.695	0.640	366.	20.7	0.00127
14	0.291	0.737	0.719	451.	21.9	0.00134
15	0.359	0.782	0.810	556.	23.2	0.00143
16	0.443	0.834	0.919	685.	24.8	0.00153
17	0.546	0.882	1.029	845.	26.2	0.00163
18	0.673	0.924	1.130	1043.	27.5	0.00170
19	0.830	0.963	1.227	1286.	28.6	0.00176
20	1.024	0.994	1.306	1586.	29.5	0.00178
21	1.264	1.001	1.323	1957.	29.7	0.00174
22	1.559	1.000	1.321	2414.	29.7	0.00167
23	1.778	0.999	1.318	2754.	29.7	0.00163

DISP. THICKNESS = 0.923 CM.   MOMT. THICKESS =0.638 CM.

SHAPE FACTOR = 1.447   DELTA 99 = 4.999 CM.

MOMENTUM THICKNESS REYNOLDS NO. = 5867.   CF/2 = 0.00113

229

SEC. EXPT., STN 15, S=124.79 CM., UPW=14.97 M/SEC

PT	Y/DEL	U/UP	DY PR	YPLUS	UPLUS	CF/2
1	0.010	0.335	0.147	15.	9.9	0.00088
2	0.018	0.437	0.251	28.	12.9	0.00112
3	0.025	0.473	0.295	39.	14.0	0.00115
4	0.033	0.495	0.323	51.	14.6	0.00115
5	0.046	0.520	0.356	71.	15.4	0.00114
6	0.056	0.536	0.378	87.	15.9	0.00114
7	0.068	0.552	0.401	106.	16.3	0.00114
8	0.083	0.568	0.424	130.	16.8	0.00114
9	0.102	0.588	0.455	159.	17.4	0.00115
10	0.125	0.611	0.490	196.	18.0	0.00116
11	0.154	0.634	0.528	242.	18.7	0.00118
12	0.190	0.661	0.574	298.	19.5	0.00121
13	0.234	0.694	0.632	367.	20.5	0.00126
14	0.288	0.729	0.698	452.	21.5	0.00132
15	0.355	0.772	0.782	557.	22.8	0.00139
16	0.437	0.823	0.889	686.	24.3	0.00150
17	0.540	0.874	1.003	847.	25.8	0.00160
18	0.666	0.920	1.113	1044.	27.2	0.00168
19	0.821	0.960	1.212	1288.	28.4	0.00175
20	1.013	0.992	1.293	1588.	29.3	0.00178
21	1.249	1.002	1.318	1959.	29.6	0.00174
22	1.542	1.001	1.316	2418.	29.6	0.00167
23	1.758	1.000	1.313	2758.	29.5	0.00163

DISP. THICKNESS = 0.941 CM.   MOMT. THICKESS =0.651 CM.

SHAPE FACTOR = 1.445   DELTA 99 = 5.057 CM.

MOMENTUM THICKNESS REYNOLDS NO. = 5968.   CF/2 = 0.00115

SEC. EXPT., STN 16, S=149.43 CM., UPW=14.98 M/SEC

PT	Y/DEL	U/UP	DY PR	YPLUS	UPLUS	CF/2
1	0.009	0.333	0.147	15.	9.8	0.00087
2	0.017	0.438	0.254	28.	12.9	0.00112
3	0.024	0.476	0.300	40.	14.1	0.00116
4	0.032	0.495	0.325	52.	14.6	0.00115
5	0.044	0.522	0.361	72.	15.4	0.00115
6	0.054	0.538	0.384	88.	15.9	0.00115
7	0.066	0.554	0.406	107.	16.4	0.00114
8	0.080	0.569	0.429	131.	16.8	0.00114
9	0.099	0.588	0.457	161.	17.4	0.00114
10	0.121	0.607	0.488	198.	17.9	0.00115
11	0.150	0.630	0.526	244.	18.6	0.00117
12	0.184	0.657	0.572	300.	19.4	0.00120
13	0.227	0.689	0.627	370.	20.3	0.00125
14	0.280	0.723	0.691	456.	21.4	0.00130
15	0.345	0.764	0.772	562.	22.6	0.00137
16	0.425	0.811	0.869	692.	23.9	0.00146
17	0.525	0.861	0.980	854.	25.4	0.00156
18	0.647	0.913	1.102	1054.	27.0	0.00166
19	0.798	0.956	1.209	1299.	28.3	0.00173
20	0.984	0.989	1.293	1603.	29.2	0.00177
21	1.214	1.002	1.326	1977.	29.6	0.00174
22	1.498	1.001	1.323	2440.	29.6	0.00167
23	1.708	1.000	1.321	2782.	29.5	0.00163

DISP. THICKNESS = 0.973 CM.   MOMT. THICKESS =0.674 CM.

SHAPE FACTOR = 1.444   DELTA 99 = 5.204 CM.

MOMENTUM THICKNESS REYNOLDS NO. = 6234.   CF/2 = 0.00115

SEC. EXPT., STN 17, S=164.67 CM., UPW=14.96 M/SEC

PT	Y/DEL	U/UP	DY PR	YPLUS	UPLUS	CF/2
1	0.009	0.343	0.155	15.	10.1	0.00091
2	0.016	0.446	0.262	28.	13.1	0.00115
3	0.024	0.481	0.305	40.	14.1	0.00118
4	0.031	0.503	0.333	52.	14.7	0.00118
5	0.043	0.527	0.366	72.	15.5	0.00116
6	0.052	0.543	0.389	88.	15.9	0.00116
7	0.063	0.557	0.409	108.	16.3	0.00115
8	0.077	0.573	0.432	132.	16.8	0.00115
9	0.095	0.593	0.462	162.	17.4	0.00116
10	0.117	0.612	0.493	199.	17.9	1.00116
11	0.144	0.633	0.528	245.	18.6	0 00118
12	0.177	0.657	0.569	302.	19.3	0.00120
13	0.219	0.686	0.620	372.	20.1	0.00123
14	0.269	0.719	0.681	459.	21.1	0.00128
15	0.332	0.758	0.757	566.	22.2	0.00135
16	0.409	0.801	0.846	697.	23.5	0.00142
17	0.505	0.853	0.958	860.	25.0	0.00153
18	0.623	0.904	1.077	1060.	26.5	0.00163
19	0.768	0.950	1.189	1307.	27.9	0.00171
20	0.947	0.987	1.283	1613.	28.9	0.00176
21	1.169	1.001	1.321	1989.	28.9	0.00174
22	1.442	1.001	1.321	2455.	29.4	0.00167
23	1.644	1.000	1.318	2800.	29.3	0.00163

DISP. THICKNESS = 0.998 CM.   MOMT. THICKESS =0.696 CM.

SHAPE FACTOR = 1.434   DELTA 99 = 5.406 CM.

MOMENTUM THICKNESS REYNOLDS NO. = 6431.   CF/2 = 0.00116

SEC. EXPT., SINGLE WIRE DATA AT STN. 3, S = -52.70 CM.

PT	Y/DEL	U/UP	YPLUS	UPLUS	TURB.IN.
1	0.004	0.124	5.	3.1	0.0322
2	0.005	0.169	7.	4.2	0.0561
3	0.008	0.253	10.	6.3	0.0860
4	0.010	0.319	13.	7.9	0.0985
5	0.023	0.508	28.	12.5	0.1019
6	0.034	0.565	43.	14.0	0.0930
7	0.046	0.601	58.	14.8	0.0880
8	0.066	0.640	83.	15.8	0.0856
9	0.083	0.663	103.	16.4	0.0816
10	0.102	0.683	128.	16.9	0.0804
11	0.126	0.704	157.	17.4	0.0785
12	0.155	0.730	194.	18.0	0.0768
13	0.192	0.753	240.	18.6	0.0742
14	0.238	0.779	297.	19.2	0.0722
15	0.293	0.805	366.	19.9	0.0682
16	0.362	0.833	452.	20.6	0.0655
17	0.446	0.864	557.	21.3	0.0596
18	0.551	0.898	688.	22.2	0.0539
19	0.679	0.934	848.	23.1	0.0466
20	0.838	0.969	1047.	23.9	0.0349
21	1.035	0.994	1292.	24.6	0.0169
22	1.276	1.000	1594.	24.7	0.0079
23	1.575	1.000	1966.	24.7	0.0060

SEC. EXPT., SINGLE WIRE DATA AT STN. 6, S = 0.0 CM

PT	Y/DEL	U/UP	YPLUS	UPLUS	TURB.IN.
1	0.003	0.116	5.	2.9	0.0200
2	0.005	0.129	8.	3.2	0.0354
3	0.007	0.205	9.	5.1	0.0674
4	0.009	0.289	12.	7.2	0.0906
5	0.020	0.498	27.	12.4	0.0972
6	0.030	0.558	42.	13.9	0.0881
7	0.040	0.591	56.	14.7	0.0870
8	0.058	0.631	80.	15.7	0.0844
9	0.072	0.651	100.	16.3	0.0832
10	0.089	0.673	124.	16.8	0.0813
11	0.109	0.695	152.	17.3	0.0818
12	0.135	0.718	188.	17.9	0.0808
13	0.166	0.743	233.	18.5	0.0795
14	0.206	0.767	288.	19.1	0.0789
15	0.254	0.792	355.	19.8	0.0751
16	0.313	0.820	438.	20.5	0.0730
17	0.386	0.849	540.	21.2	0.0684
18	0.477	0.881	667.	22.0	0.0639
19	0.588	0.915	822.	22.8	0.0563
20	0.726	0.949	1015.	23.7	0.0487
21	0.896	0.980	1252.	24.5	0.0370
22	1.105	1.000	1545.	25.0	0.0199
23	1.363	1.000	1906.	25.0	0.0079

SEC. EXPT., SINGLE WIRE DATA AT STN. 7, S = 10.39 CM. (13.25 DEG)

PT	Y/DEL	U/UP	YPLUS	UPLUS	TURB.IN.
1	0.003	0.127	4.	3.4	0.0421
2	0.004	0.165	6.	4.4	0.0591
3	0.006	0.231	9.	6.2	0.0800
4	0.008	0.288	11.	7.7	0.0908
5	0.018	0.448	25.	12.0	0.0908
6	0.028	0.506	38.	13.5	0.0828
7	0.036	0.541	50.	14.5	0.0774
8	0.052	0.584	72.	15.6	0.0732
9	0.065	0.608	90.	16.2	0.0716
10	0.081	0.634	112.	16.9	0.0690
11	0.099	0.658	137.	17.5	0.0648
12	0.123	0.680	170.	18.0	0.0643
13	0.151	0.702	210.	18.6	0.0632
14	0.187	0.726	259.	19.1	0.0620
15	0.231	0.752	320.	19.7	0.0613
16	0.285	0.779	395.	20.4	0.0597
17	0.352	0.811	487.	21.1	0.0577
18	0.434	0.845	601.	21.8	0.0540
19	0.535	0.881	741.	22.5	0.0471
20	0.661	0.920	915.	23.3	0.0440
21	0.815	0.958	1128.	23.9	0.0354
22	1.005	0.991	1393.	24.3	0.0202
23	1.241	1.003	1719.	24.1	0.0083
24	1.531	1.003	2121.	23.6	0.0048
25	1.890	1.000	2617.	22.8	0.0043

SEC. EXPT., SINGLE WIRE DATA AT STN. 8, S = 25.20 CM. (32.08 DEG)

PT	Y/DEL	U/UP	YPLUS	UPLUS	TURB.IN.
1	0.003	0.103	4.	3.0	0.0281
2	0.004	0.129	6.	3.8	0.0402
3	0.006	0.185	8.	5.4	0.0636
4	0.007	0.236	11.	6.9	0.0759
5	0.017	0.398	25.	11.7	0.0813
6	0.025	0.458	37.	13.4	0.0725
7	0.034	0.492	50.	14.4	0.0682
8	0.049	0.532	72.	15.6	0.0631
9	0.061	0.560	90.	16.4	0.0608
10	0.075	0.587	111.	17.1	0.0586
11	0.093	0.615	136.	17.9	0.0570
12	0.115	0.646	169.	18.8	0.0527
13	0.142	0.678	208.	19.7	0.0495
14	0.175	0.709	257.	20.5	0.0467
15	0.216	0.739	318.	21.3	0.0445
16	0.267	0.770	392.	22.1	0.0428
17	0.329	0.801	484.	22.8	0.0417
18	0.406	0.836	597.	23.6	0.0404
19	0.500	0.872	736.	24.4	0.0378
20	0.618	0.911	909.	25.3	0.0351
21	0.762	0.951	1121.	26.0	0.0306
22	0.940	0.986	1383.	26.5	0.0187
23	1.161	1.000	1707.	26.4	0.0079
24	1.431	1.000	2106.	25.8	0.0049

SEC. EXPT., SINGLE WIRE DATA AT STN. 9, S = 41.48 CM. (52.82 DEG)

PT	Y/DEL	U/UP	YPLUS	UPLUS	TURB.IN.
1	0.003	0.088	4.	2.8	0.0196
2	0.004	0.102	5.	3.2	0.0323
3	0.005	0.150	8.	4.7	0.0526
4	0.007	0.198	10.	6.3	0.0676
5	0.016	0.355	23.	11.2	0.0777
6	0.024	0.413	34.	13.0	0.0699
7	0.032	0.446	46.	14.0	0.0646
8	0.046	0.484	66.	15.2	0.0594
9	0.057	0.510	82.	16.0	0.0570
10	0.070	0.536	102.	16.8	0.0556
11	0.086	0.565	125.	17.7	0.0541
12	0.107	0.597	155.	18.7	0.0516
13	0.133	0.632	192.	19.7	0.0491
14	0.163	0.668	236.	20.8	0.0451
15	0.201	0.705	291.	21.8	0.0410
16	0.248	0.739	360.	22.8	0.0371
17	0.306	0.776	443.	23.8	0.0343
18	0.378	0.814	548.	24.7	0.0324
19	0.466	0.851	675.	25.7	0.0303
20	0.576	0.893	833.	26.6	0.0282
21	0.710	0.939	1028.	27.6	0.0242
22	0.876	0.978	1268.	28.3	0.0172
23	1.130	1.003	1636.	28.3	0.0065
24	1.334	1.000	1931.	27.7	0.0049

SEC. EXPT., SINGLE WIRE DATA AT STN. 10, S = 61.72 CM. (78.57 DEG)

PT	Y/DEL	U/UP	YPLUS	UPLUS	TURB.IN.
1	0.003	0.083	4.	2.6	0.0162
2	0.004	0.120	6.	3.8	0.0366
3	0.006	0.175	8.	5.6	0.0548
4	0.008	0.222	10.	7.1	0.0661
5	0.016	0.359	22.	11.4	0.0685
6	0.024	0.413	33.	13.1	0.0599
7	0.032	0.443	45.	14.1	0.0540
8	0.047	0.479	64.	15.2	0.0489
9	0.058	0.501	79.	15.9	0.0470
10	0.071	0.525	98.	16.6	0.0458
11	0.088	0.550	120.	17.4	0.0445
12	0.108	0.580	148.	18.3	0.0432
13	0.134	0.614	183.	19.3	0.0410
14	0.165	0.653	226.	20.4	0.0382
15	0.204	0.692	279.	21.6	0.0338
16	0.251	0.732	344.	22.7	0.0298
17	0.310	0.772	424.	23.8	0.0283
18	0.382	0.810	524.	24.8	0.0272
19	0.471	0.849	645.	25.8	0.0259
20	0.581	0.891	797.	26.7	0.0245
21	0.717	0.935	983.	27.7	0.0223
22	0.885	0.980	1212.	28.6	0.0155
23	1.091	0.998	1496.	28.5	0.0052
24	1.346	1.000	1845.	27.9	0.0041

SEC. EXPT., SINGLE WIRE DATA AT STN. 12, S = 88.47 CM.

PT	Y/DEL	U/UP	YPLUS	UPLUS	TURB.IN.
1	0.003	0.096	4.	3.0	0.0260
2	0.004	0.118	6.	3.7	0.0391
3	0.005	0.169	8.	5.3	0.0596
4	0.007	0.225	10.	7.0	0.0745
5	0.015	0.374	23.	11.6	0.0818
6	0.022	0.421	35.	13.1	0.0741
7	0.030	0.451	47.	14.0	0.0689
8	0.043	0.483	67.	15.0	0.0642
9	0.053	0.503	84.	15.6	0.0628
10	0.066	0.521	103.	16.2	0.0620
11	0.081	0.542	127.	16.8	0.0615
12	0.101	0.567	158.	17.6	0.0618
13	0.124	0.598	194.	18.6	0.0612
14	0.154	0.633	241.	19.7	0.0597
15	0.189	0.674	296.	20.9	0.0541
16	0.233	0.718	366.	22.3	0.0485
17	0.288	0.765	451.	23.8	0.0401
18	0.355	0.809	557.	25.1	0.0324
19	0.438	0.851	686.	26.4	0.0278
20	0.541	0.890	848.	27.7	0.0256
21	0.667	0.931	1046.	28.9	0.0243
22	0.823	0.972	1290.	30.2	0.0184
23	1.061	0.996	1663.	31.0	0.0083
24	1.253	1.000	1964.	31.1	0.0057
25	1.547	1.000	2424.	31.1	0.0056

SEC. EXPT., SINGLE WIRE DATA AT STN. 13, S = 103.71 CM.

PT	Y/DEL	U/UP	YPLUS	UPLUS	TURB.IN.
1	0.003	0.103	4.	3.1	0.0311
2	0.004	0.131	6.	4.0	0.0454
3	0.005	0.191	8.	5.8	0.0681
4	0.007	0.239	10.	7.2	0.0800
5	0.015	0.386	23.	11.7	0.0868
6	0.023	0.439	35.	13.3	0.0794
7	0.031	0.467	47.	14.2	0.0744
8	0.044	0.498	68.	15.1	0.0691
9	0.055	0.517	84.	15.7	0.0681
10	0.068	0.536	104.	16.3	0.0667
11	0.083	0.555	128.	16.8	0.0658
12	0.103	0.578	159.	17.5	0.0655
13	0.127	0.603	196.	18.3	0.0648
14	0.157	0.632	242.	19.2	0.0638
15	0.194	0.665	299.	20.2	0.0600
16	0.240	0.704	369.	21.4	0.0578
17	0.296	0.750	455.	22.8	0.0527
18	0.365	0.799	562.	24.3	0.0447
19	0.450	0.846	692.	25.7	0.0347
20	0.555	0.890	855.	27.0	0.0286
21	0.685	0.930	1055.	28.2	0.0262
22	0.845	0.968	1301.	29.4	0.0199
23	1.043	0.996	1606.	30.3	0.0098
24	1.287	1.000	1981.	30.4	0.0061
25	1.589	1.000	2444.	30.4	0.0062

240

SEC. EXPT., SINGLE WIRE DATA AT STN. 14, S = 118.95 CM.

PT	Y/DEL	U/UP	YPLUS	UPLUS	TURB.IN.
1	0.003	0.117	5.	3.6	0.0389
2	0.004	0.151	6.	4.6	0.0534
3	0.005	0.213	8.	6.5	0.0744
4	0.007	0.262	11.	8.0	0.0841
5	0.015	0.394	24.	12.0	0.0865
6	0.023	0.442	36.	13.4	0.0793
7	0.030	0.470	48.	14.3	0.0746
8	0.044	0.501	68.	15.2	0.0797
9	0.054	0.518	85.	15.7	0.0697
10	0.067	0.537	105.	16.3	0.0687
11	0.082	0.554	129.	16.8	0.0681
12	0.101	0.576	159.	17.5	0.0673
13	0.125	0.599	196.	18.2	0.0673
14	0.155	0.627	242.	19.1	0.0662
15	0.191	0.659	299.	20.0	0.0635
16	0.235	0.692	369.	21.0	0.0616
17	0.290	0.733	454.	22.3	0.0588
18	0.358	0.782	561.	23.8	0.0532
19	0.441	0.833	691.	25.3	0.0460
20	0.544	0.882	853.	26.8	0.0351
21	0.671	0.925	1053.	28.1	0.0293
22	0.828	0.962	1298.	29.2	0.0238
23	1.022	0.994	1602.	30.2	0.0122
24	1.260	1.000	1976.	30.4	0.0064
25	1.555	1.000	2438.	30.4	0.0067

SEC. EXPT., SINGLE WIRE DATA AT STN. 15, S = 124.79 CM.

PT	Y/DEL	U/UP	YPLUS	UPLUS	TURB.IN.
1	0.002	0.113	4.	3.4	0.0328
2	0.003	0.172	6.	5.2	0.0572
3	0.005	0.224	8.	6.7	0.0735
4	0.006	0.274	10.	8.2	0.0826
5	0.014	0.406	23.	12.2	0.0843
6	0.022	0.440	35.	13.2	0.0789
7	0.029	0.479	47.	14.3	0.0724
8	0.042	.510	67.	15.3	0.0689
9	0.052	0.525	84.	15.7	0.0675
10	0.064	0.544	103.	16.3	0.0666
11	0.079	0.562	127.	16.8	0.0658
12	0.098	0.579	157.	17.3	0.0649
13	0.121	0.601	194.	18.0	0.0644
14	0.149	0.627	240.	18.8	0.0636
15	0.184	0.655	296.	19.6	0.0610
16	0.228	0.688	366.	20.6	0.0594
17	0.281	0.723	451.	21.7	0.0578
18	0.346	0.768	557.	23.0	0.0539
19	0.427	0.816	686.	24.4	0.0491
20	0.527	0.871	847.	26.1	0.0400
21	0.651	0.917	1046.	27.5	0.0300
22	0.803	0.957	1290.	28.7	0.0236
23	0.991	0.990	1592.	29.6	0.0137
24	1.222	1.000	1964.	29.9	0.0065
25	1.508	0.999	2423.	29.9	0.0065

SEC. EXPT., SINGLE WIRE DATA AT STN. 16, S = 149.43 CM.

PT	Y/DEL	U/UP	YPLUS	UPLUS	TURB.IN.
1	0.002	0.101	4.	3.0	0.0274
2	0.004	0.149	6.	4.5	0.0499
3	0.005	0.207	9.	6.2	0.0700
4	0.006	0.256	11.	7.7	0.0792
5	0.014	0.397	24.	12.0	0.0845
6	0.020	0.447	36.	13.5	0.0771
7	0.027	0.474	48.	14.3	0.0735
8	0.039	0.506	69.	15.3	0.0704
9	0.048	0.522	85.	15.7	0.0686
10	0.060	0.540	105.	16.3	0.0681
11	0.073	0.560	129.	16.9	0.0671
12	0.090	0.579	159.	17.5	0.0669
13	0.112	0.603	197.	18.2	0.0666
14	0.138	0.625	243.	18.8	0.0661
15	0.170	0.653	300.	19.7	0.0642
16	0.210	0.683	370.	20.6	0.0629
17	0.258	0.718	456.	21.7	0.0610
18	0.319	0.761	563.	22.9	0.0583
19	0.393	0.807	694.	24.3	0.0544
20	0.485	0.859	856.	25.9	0.0469
21	0.598	0.911	1057.	27.5	0.0359
22	0.738	0.953	1303.	28.7	0.0271
23	0.951	0.986	1679.	29.7	0.0167
24	1.123	1.000	1983.	30.2	0.0071
25	1.386	0.999	2447.	30.1	0.0069

SEC. EXPT., SINGLE WIRE DATA AT STN. 17, S = 164.67 CM.

PT	Y/DEL	U/UP	YPLUS	UPLUS	TURB.IN.
1	0.002	0.090	4.	2.7	0.0141
2	0.004	0.122	6.	3.7	0.0387
3	0.005	0.178	8.	5.4	0.0600
4	0.006	0.222	10.	6.7	0.0736
5	0.013	0.384	22.	11.6	0.0842
6	0.020	0.433	34.	13.0	0.0787
7	0.027	0.469	45.	14.1	0.0742
8	0.038	0.503	64.	15.1	0.0712
9	0.048	0.518	80.	15.6	0.0704
10	0.059	0.538	99.	16.2	0.0683
11	0.072	0.555	121.	16.7	0.0680
12	0.089	0.574	150.	17.3	0.0678
13	0.111	0.597	185.	18.0	0.0674
14	0.136	0.621	228.	18.7	0.0673
15	0.168	0.645	282.	19.4	0.0666
16	0.208	0.674	347.	20.3	0.0660
17	0.256	0.711	428.	21.4	0.0635
18	0.316	0.749	529.	22.6	0.0609
19	0.389	0.795	651.	23.9	0.0571
20	0.481	0.844	804.	25.4	0.0510
21	0.593	0.898	992.	27.0	0.0413
22	0.731	0.944	1223.	28.4	0.0297
23	0.902	0.981	1509.	29.6	0.0201
24	1.113	1.000	1862.	30.1	0.0071
25	1.373	1.000	2298.	30.1	0.0062

SECOND EXPT., REYNOLDS STRESSES AT STN. 3, S = -52.70 CM.

OUTPUT NONDIMENSIONALIZED ON FRICTION VELOCITY

PT	Y/DEL	UV/UTSQ	USQ/UTSQ	VSQ/UTSQ	WSG/UTSQ	QSQ/UTSQ	A	SHEAR CORR	ANISOTROPY
1	0.062	0.9329	3.562	1.520	2.137	7.219	0.129	0.401	0.033
2	0.083	0.9538	3.441	1.351	2.078	6.870	0.139	0.442	0.039
3	0.103	0.9228	3.356	1.317	1.991	6.664	0.138	0.439	0.038
4	0.126	0.9288	3.287	1.327	1.911	6.525	0.142	0.445	0.041
5	0.156	0.9126	3.185	1.343	1.835	6.362	0.143	0.441	0.041
6	0.193	0.9093	3.048	1.258	1.789	6.095	0.149	0.464	0.045
7	0.238	0.8607	2.831	1.234	1.719	5.784	0.149	0.461	0.044
8	0.293	0.7702	2.554	1.185	1.629	5.368	0.143	0.443	0.041
9	0.362	0.7209	2.254	1.157	1.527	4.938	0.146	0.446	0.043
10	0.446	0.6865	2.045	1.013	1.392	4.450	0.154	0.477	0.048
11	0.551	0.5765	1.665	0.951	1.194	3.810	0.151	0.458	0.046
12	0.679	0.4604	1.338	0.736	0.938	3.012	0.153	0.464	0.047
13	0.838	0.1721	0.525	0.371	0.350	1.246	0.138	0.390	0.038
14	1.034	0.0338	0.093	0.127	0.091	0.311	0.109	0.311	0.024
15	1.275	0.0196	0.036	0.045	0.031	0.112	0.175	0.492	0.062

DISPLACEMENT THICKNESS = 0.465 CM.   MOMENTUM THICKNESS = 0.356 CM.   DELTA 99 = 3.256 CM.

MOMENTUM THICKNESS REYNOLDS NO. = 3291.   UTAU = 0.624 M/SEC   UPW = 15.12 M/SEC

OUTPUT NONDIMENSIONALIZED ON WALL VELOCITY

PT	Y/DEL	UV/UPWS	USQ/UPWS	VSQ/UPWS	WSQ/UPWS	QSQ/UFWS
1	0.062	0.00159	0.00606	0.00258	0.00363	0.01227
2	0.083	0.00162	0.00595	0.00230	0.00353	0.01168
3	0.103	0.00157	0.00571	0.00224	0.00338	0.01133
4	0.126	0.00158	0.00559	0.00226	0.00325	0.01109
5	0.156	0.00155	0.00541	0.00228	0.00312	0.01082
6	0.193	0.00155	0.00518	0.00214	0.00304	0.01036
7	0.238	0.00146	0.00481	0.00210	0.00292	0.00983
8	0.293	0.00131	0.00434	0.00202	0.00277	0.00913
9	0.362	0.00123	0.00383	0.00197	0.00260	0.00840
10	0.446	0.00117	0.00348	0.00172	0.00237	0.00757
11	0.551	0.00098	0.00283	0.00162	0.00203	0.00648
12	0.679	0.00078	0.00227	0.00125	0.00160	0.00512
13	0.838	0.00029	0.00089	0.00063	0.00060	0.00212
14	1.034	0.00006	0.00016	0.00022	0.00015	0.00053
15	1.275	0.00003	0.00006	0.00008	0.00005	0.00019

SECOND EXPT., REYNOLDS STRESSES AT STN. 4, S = -41.28 CM.

OUTPUT NONDIMENSIONALIZED ON FRICTION VELOCITY

PT	Y/DEL	UV/UTSQ	USQ/UTSQ	VSQ/UTSQ	WSQ/UTSQ	QSQ/UTSQ	A	SHEAR CORR	ANISOTROPY
1	0.059	0.9681	3.870	1.526	2.362	7.758	0.125	0.398	0.031
2	0.080	0.9654	3.660	1.389	2.175	7.224	0.134	0.428	0.036
3	0.099	0.9647	3.550	1.363	2.071	6.984	0.138	0.439	0.038
4	0.121	0.9407	3.534	1.335	1.943	6.813	0.138	0.433	0.038
5	0.149	0.9312	3.407	1.315	1.903	6.625	0.141	0.440	0.040
6	0.184	0.9052	3.273	1.281	1.835	6.388	0.142	0.442	0.040
7	0.228	0.8758	3.077	1.273	1.762	6.112	0.143	0.443	0.041
8	0.281	0.8122	2.777	1.210	1.685	5.672	0.143	0.447	0.041
9	0.347	0.7623	2.498	1.131	1.581	5.209	0.146	0.454	0.043
10	0.427	0.6330	2.134	1.036	1.420	4.590	0.149	0.459	0.044
11	0.527	0.5675	1.760	0.889	1.196	3.845	0.148	0.454	0.044
12	0.650	0.4239	1.318	0.704	0.893	2.915	0.145	0.440	0.042
13	0.802	0.2516	0.795	0.463	0.523	1.780	0.141	0.415	0.040
14	0.990	0.0889	0.260	0.222	0.181	0.664	0.134	0.370	0.036
15	1.220	0.0082	0.035	0.052	0.030	0.117	0.070	0.192	0.010
16	1.506	0.0007	0.011	0.010	0.005	0.027	0.025	0.063	0.001

DISPLACEMENT THICKNESS = 0.490 CM.   MOMENTUM THICKNESS = 0.376 CM.   DELTA 99 = 3.401 CM.

MOMENTUM THICKNESS REYNOLDS NO. = 3528.   UTAU = 0.620 M/SEC   UPW = 15.17 M/SEC

OUTPUT NONDIMENSIONALIZED ON WALL VELOCITY

PT	Y/DEL	UV/UPWS	USQ/UPWS	VSQ/UPWS	WSQ/UPWS	QSQ/UPWS
1	0.059	0.00162	0.00646	0.00255	0.00394	0.01295
2	0.080	0.00161	0.00611	0.00232	0.00363	0.01206
3	0.099	0.00161	0.00593	0.00227	0.00346	0.01166
4	0.121	0.00157	0.00590	0.00223	0.00324	0.01137
5	0.149	0.00155	0.00569	0.00220	0.00318	0.01106
6	0.184	0.00151	0.00546	0.00214	0.00306	0.01066
7	0.228	0.00146	0.00514	0.00213	0.00294	0.01020
8	0.281	0.00136	0.00464	0.00202	0.00281	0.00947
9	0.347	0.00127	0.00417	0.00189	0.00264	0.00870
10	0.427	0.00114	0.00356	0.00173	0.00237	0.00766
11	0.527	0.00095	0.00294	0.00148	0.00200	0.00642
12	0.650	0.00071	0.00220	0.00118	0.00149	0.00487
13	0.802	0.00042	0.00133	0.00077	0.00087	0.00297
14	0.990	0.00015	0.00043	0.00037	0.00030	0.00111
15	1.220	0.00001	0.00006	0.00009	0.00005	0.00019
16	1.506	0.00000	0.00002	0.00002	0.00001	0.00004

SECOND EXPT., REYNOLDS STRESSES AT STN. 5: S = -29.84 CM.

OUTPUT NONDIMENSIONALIZED ON FRICTION VELOCITY

PT	Y/DEL	UV/UTSQ	USQ/UTSQ	VSQ/UTSQ	WSQ/UTSQ	QSQ/UTSQ	A	SHEAR CORR	ANISOTROPY
1	0.091	0.9912	3.861	1.457	2.216	7.534	0.132	0.418	0.035
2	0.112	0.9855	3.749	1.407	2.115	7.271	0.136	0.429	0.037
3	0.138	0.9847	3.617	1.383	2.025	7.024	0.140	0.440	0.039
4	0.170	0.9588	3.475	1.359	1.932	6.766	0.142	0.441	0.040
5	0.210	0.9285	3.236	1.319	1.889	6.444	0.144	0.449	0.042
6	0.259	0.8729	2.997	1.276	1.777	6.051	0.144	0.446	0.042
7	0.320	0.8203	2.708	1.206	1.689	5.603	0.146	0.454	0.043
8	0.395	0.7330	2.344	1.102	1.525	4.971	0.147	0.456	0.043
9	0.487	0.6183	1.927	0.953	1.317	4.196	0.147	0.456	0.043
10	0.600	0.4783	1.468	0.771	1.018	3.257	0.147	0.450	0.043
11	0.741	0.3189	0.959	0.533	0.644	2.136	0.149	0.446	0.045
12	0.914	0.1428	0.375	0.271	0.258	0.904	0.158	0.448	0.050
13	1.128	0.0447	0.055	0.073	0.049	0.177	0.253	0.710	0.128
14	1.391	0.0000	0.013	0.014	0.007	0.034	0.000	0.000	0.000

DISPLACEMENT THICKNESS = 0.533 CM.   MOMENTUM THICKNESS = 0.404 CM.   DELTA 99 = 3.680 CM.

MOMENTUM THICKNESS REYNOLDS NO. = 3766.   UTAU = 0.604 M/SEC   UPW = 15.04 M/SEC

OUTPUT NONDIMENSIONALIZED ON WALL VELOCITY

PT	Y/DEL	UV/UPWS	USQ/UPWS	VSQ/UPWS	WSQ/UPWS	QSQ/UPWS
1	0.091	0.00160	0.00622	0.00235	0.00357	0.01213
2	0.112	0.00159	0.00604	0.00227	0.00341	0.01171
3	0.138	0.00159	0.00582	0.00223	0.00326	0.01131
4	0.170	0.00154	0.00560	0.00219	0.00311	0.01090
5	0.210	0.00150	0.00521	0.00212	0.00304	0.01038
6	0.259	0.00141	0.00483	0.00206	0.00286	0.00974
7	0.320	0.00132	0.00436	0.00194	0.00272	0.00902
8	0.395	0.00118	0.00377	0.00177	0.00246	0.00800
9	0.487	0.00100	0.00310	0.00153	0.00212	0.00676
10	0.600	0.00077	0.00236	0.00124	0.00164	0.00524
11	0.741	0.00051	0.00154	0.00086	0.00104	0.00344
12	0.914	0.00023	00060	0.00044	0.00042	0.00146
13	1.128	0.00007	0.00009	0.00012	0.00008	0.00028
14	1.391	0.00000	0.00002	0.00002	0.00001	0.00006

SECOND EXPT., REYNOLDS STRESSES AT STN. 6, S = 0.0 CM. (0.0 DEG)

OUTPUT NONDIMENSIONALIZED ON FRICTION VELOCITY

PT	Y/DEL	UV/UTSQ	USQ/UTSQ	VSQ/UTSQ	WSQ/UTSQ	QSQ/UTSQ	A	SHEAR CORR	ANISOTROPY
1	0.047	0.9693	3.852	1.393	2.298	7.543	0.128	0.418	0.033
2	0.060	0.9654	3.527	1.454	2.234	7.215	0.134	0.426	0.036
3	0.072	0.9926	3.569	1.449	2.185	7.204	0.138	0.436	0.038
4	0.089	0.9872	3.470	1.474	2.126	7.070	0.140	0.436	0.039
5	0.110	0.9926	3.444	1.495	2.098	7.037	0.141	0.437	0.040
6	0.135	0.9942	3.391	1.504	2.077	6.972	0.143	0.440	0.041
7	0.167	0.9397	3.248	1.500	2.022	6.770	0.139	0.426	0.039
8	0.206	0.9202	3.088	1.470	1.939	6.497	0.142	0.432	0.040
9	0.254	0.8681	2.887	1.425	1.880	6.192	0.140	0.428	0.039
10	0.314	0.8136	2.700	1.370	1.800	5.869	0.139	0.423	0.038
11	0.387	0.7170	2.393	1.268	1.670	5.331	0.134	0.412	0.036
12	0.478	0.6205	2.060	1.132	1.495	4.686	0.132	0.406	0.035
13	0.589	0.5099	1.665	0.945	1.242	3.852	0.132	0.407	0.035
14	0.727	0.3682	1.236	0.701	0.889	2.826	0.130	0.396	0.034
15	0.896	0.1837	0.681	0.423	0.477	1.582	0.116	0.342	0.027
16	1.106	0.0483	0.207	0.192	0.140	0.539	0.090	0.242	0.016
17	1.364	-0.0008	0.022	0.039	0.019	0.080	-0.010	-0.027	0.000

DISPLACEMENT THICKNESS = 0.551 CM.   MOMENTUM THICKNESS = 0.404 CM.   DELTA 99 = 3.754 CM.

MOMENTUM THICKNESS REYNOLDS NO. = 3763.   UTAU = 0.581 M/SEC   UPW = 15.00 M/SEC

OUTPUT NONDIMENSIONALIZED ON WALL VELOCITY

PT	Y/DEL	UV/UPWS	USQ/UPWS	VSQ/UPWS	WSQ/UPWS	QSQ/UPWS
1	0.047	0.00145	0.00578	0.00209	0.00345	0.01132
2	0.060	0.00145	0.00529	0.00218	0.00335	0.01083
3	0.072	0.00149	0.00536	0.00217	0.00328	0.01081
4	0.089	0.00148	0.00521	0.00221	0.00319	0.01061
5	0.110	0.00149	0.00517	0.00224	0.00315	0.01056
6	0.135	0.00149	0.00509	0.00226	0.00312	0.01046
7	0.167	0.00141	0.00487	0.00225	0.00304	0.01016
8	0.206	0.00138	0.00463	0.00221	0.00291	0.00975
9	0.254	0.00130	0.00433	0.00214	0.00282	0.00929
10	0.314	0.00122	0.00405	0.00206	0.00270	0.00881
11	0.387	0.00108	0.00359	0.00190	0.00251	0.00800
12	0.478	0.00093	0.00309	0.00170	0.00224	0.00703
13	0.589	0.00077	0.00250	0.00142	0.00186	0.00578
14	0.727	0.00055	0.00186	0.00105	0.00133	0.00424
15	0.896	0.00028	0.00102	0.00064	0.00072	0.00237
16	1.106	0.00007	0.00031	0.00029	0.00021	0.00081
17	1.364	-0.00000	0.00003	0.00006	0.00003	0.00012

SECOND EXPT., REYNOLDS STRESSES AT STN. 7, S = 10.39 CM. (12.80 DEG)

OUTPUT NONDIMENSIONALIZED ON FRICTION VELOCITY

PT	Y/DEL	UV/UTSQ	USQ/UTSQ	VSQ/UTSQ	WSQ/UTSQ	QSQ/UTSQ	A	SHEAR CORR	ANISOTROPY
1	0.036	0.7506	2.979	1.309	1.944	6.232	0.120	0.380	0.029
2	0.043	0.7090	2.853	1.240	1.839	5.931	0.120	0.377	0.029
3	0.056	0.6215	2.755	1.112	1.726	5.593	0.111	0.355	0.025
4	0.069	0.5442	2.664	1.028	1.642	5.334	0.102	0.329	0.021
5	0.084	0.4746	2.588	0.982	1.563	5.134	0.092	0.298	0.017
6	0.104	0.4075	2.537	0.961	1.507	5.005	0.081	0.261	0.013
7	0.129	0.4114	2.493	0.981	1.501	4.975	0.083	0.263	0.014
8	0.159	0.3366	2.439	0.996	1.472	4.906	0.069	0.216	0.009
9	0.196	0.3072	2.374	0.992	1.463	4.829	0.064	0.200	0.008
10	0.242	0.2740	2.260	0.974	1.437	4.670	0.059	0.185	0.007
11	0.298	0.2306	2.090	0.927	1.350	4.367	0.053	0.166	0.006
12	0.368	0.1872	1.896	0.847	1.229	3.972	0.047	0.148	0.004
13	0.453	0.1456	1.574	0.733	1.085	3.392	0.043	0.136	0.004
14	0.559	0.0945	1.222	0.570	0.821	2.613	0.036	0.113	0.003
15	0.690	0.0345	0.773	0.397	0.496	1.666	0.021	0.062	0.001
16	0.851	0.0051	0.285	0.199	0.199	0.683	0.007	0.021	0.000
17	1.049	0.0000	0.050	0.064	0.049	0.163	0.000	0.000	0.000

DISPLACEMENT THICKNESS = 0.676 CM.   MOMENTUM THICKNESS = 0.513 CM.   DELTA 99 = 4.879 CM.

MOMENTUM THICKNESS REYNOLDS NO. = 4889.   UTAU = 0.584 M/SEC   UPW = 15.23 M/SEC

OUTPUT NONDIMENSIONALIZED ON WALL VELOCITY

PT	Y/DEL	UV/UPWS	USQ/UPWS	VSQ/UPWS	WSQ/UPWS	QSQ/UPWS
1	0.036	0.00110	0.00438	0.00192	0.00286	0.00916
2	0.043	0.00104	0.00419	0.00152	0.00270	0.00872
3	0.056	0.00091	0.00405	0.00163	0.00254	0.00822
4	0.069	0.00080	0.00391	0.00151	0.00241	0.00784
5	0.094	0.00070	0.00380	0.00144	0.00230	0.00754
6	0.104	0.00060	0.00373	0.00141	0.00221	0.00736
7	0.129	0.00060	0.00366	0.00144	0.00221	0.00731
8	0.159	0.00049	0.00358	0.00146	0.00216	0.00721
9	0.196	0.00045	0.00349	0.00146	0.00215	0.00710
10	0.242	0.00040	0.00332	0.00143	0.00211	0.00686
11	0.298	0.00034	0.00307	0.00136	0.00198	0.00642
12	0.368	0.00028	0.00279	0.00124	0.00181	0.00584
13	0.453	0.00021	0.00231	0.00108	0.00159	0.00499
14	0.559	0.00014	0.00180	0.00084	0.00121	0.00384
15	0.690	0.00005	0.00114	0.00058	0.00073	0.00245
16	0.851	0.00001	0.00042	0.00029	0.00029	0.00100
17	1.049	0.00000	0.00007	0.00009	0.00007	0.00024

SECONO EXPT., REYNOLDS STRESSES AT STN. 8, S = 25.19 CM. (31.7 DEG)

OUTPUT NONDIMENSIONALIZED ON FRICTION VELOCITY

PT	Y/DEL	UV/UTSQ	USQ/UTSQ	VSQ/UTSQ	WSQ/UTSQ	QSQ/UTSQ	A	SHEAR CORP	ANISOTROPY
1	0.046	0.8868	2.672	1.462	2.048	6.181	0.143	0.449	0.041
2	0.060	0.8052	2.446	1.328	1.930	5.704	0.141	0.447	0.040
3	0.074	0.7325	2.312	1.241	1.811	5.364	0.137	0.432	0.037
4	0.091	0.6579	2.160	1.139	1.718	5.016	0.131	0.420	0.034
5	0.112	0.5594	1.997	1.047	1.601	4.646	0.120	0.387	0.029
6	0.138	9.4529	1.770	0.967	1.497	4.234	0.107	0.346	0.023
7	0.171	0.3494	1.648	0.881	1.390	3.919	0.089	0.290	0.016
8	0.211	0.2458	1.501	0.852	1.307	3.660	0.067	0.217	0.009
9	0.260	0.1443	1.408	0.845	1.254	3.507	0.041	0.132	0.003
10	0.320	0.0776	1.332	0.843	1.181	3.356	0.023	0.073	0.001
11	0.395	0.0229	1.270	0.841	1.127	3.238	0.007	0.022	0.000
12	0.487	-0.0408	1.144	0.793	1.023	2.960	-0.014	-0.043	0.000
13	0.601	-0.0916	0.979	0.691	0.824	2.494	-0.037	-0.111	0.003
14	0.742	-0.1354	0.707	0.537	0.570	1.814	-0.075	-0.220	0.011
15	0.915	-0.0975	0.281	0.293	0.237	0.812	-0.120	-0.340	0.029
16	1.129	-0.0099	0.046	0.087	0.029	0.162	-0.055	-0.141	0.006
17	1.392	0.0010	0.011	0.017	0.012	0.040	0.025	0.072	0.001

DISPLACEMENT THICKNESS = 0.744 CM.   MOMENTUM THICKNESS = 0.536 CM.   DELTA 99 = 4.536 CM.

MOMENTUM THICKNESS REYNOLDS NO. = 4983.   UTAU = 0.521 M/SEC   UPW = 15.03 M/SEC

OUTPUT NONDIMENSIONALIZED ON WALL VELOCITY

PT	Y/DEL	UV/UPWS	USQ/UPWS	VSQ/UPWS	WSQ/UPWS	QSQ/UPWS
1	0.046	0.00106	0.00321	0.00175	0.00246	0.00742
2	0.060	0.00097	0.00293	0.00159	0.00232	0.00684
3	0.074	0.00088	0.00277	0.00149	0.00217	0.00644
4	0.091	0.00079	0.00259	0.00137	0.00206	0.00602
5	0.112	0.00067	0.00240	0.00126	0.00192	0.00557
6	0.138	0.00054	0.00212	0.00116	0.00180	0.00508
7	0.171	0.00042	0.00198	0.00106	0.00167	0.00470
8	0.211	0.00029	0.00180	0.00102	0.00157	0.00439
9	0.260	0.00017	0.00169	0.00101	0.00150	0.00421
10	0.320	0.00003	0.00160	0.00101	0.00142	0.00403
11	0.395	0.00003	0.00152	0.00101	0.00135	0.00388
12	0.487	-0.00005	0.00137	0.00095	0.00123	0.00355
13	0.601	-0.00011	0.00118	0.00083	0.00099	0.00299
14	0.742	-0.00016	0.00085	0.00064	0.00068	0.00218
15	0.915	-0.00012	0.00034	0.00035	0.00008	0.00097
16	1.129	-0.00001	0.00005	0.00010	0.00003	0.00019
17	1.392	0.00000	0.00001	0.00002	0.00001	0.00005

SECOND EXPT., REYNOLDS STRESSES AT STN. 9, S = 41.48 CM. (52.82 DEG)

OUTPUT NONDIMENSIONALIZED ON FRICTION VELOCITY

PT	Y/DEL	UV/UTSQ	USQ/UTSQ	VSQ/UTSQ	WSQ/UTSQ	QSQ/UTSQ	A	SHEAR CORR	ANISOTROPY
1	0.044	0.9287	2.749	1.530	2.035	6.314	0.147	0.453	0.043
2	0.058	0.8488	2.558	1.372	1.923	5.853	0.145	0.453	0.042
3	0.071	0.7949	2.438	1.305	1.838	5.581	0.142	0.446	0.041
4	0.087	0.7248	2.308	1.184	1.749	5.241	0.138	0.439	0.038
5	0.108	0.6364	2.180	1.078	1.628	4.887	0.130	0.415	0.034
6	0.133	0.5425	1.952	0.943	1.498	4.393	0.123	0.400	0.030
7	0.165	0.4508	1.670	0.821	1.343	3.834	0.118	0.385	0.028
8	0.203	0.3559	1.415	0.707	1.207	3.329	0.107	0.356	0.023
9	0.251	0.2740	1.202	0.637	1.093	2.931	0.093	0.313	0.017
10	0.309	0.2136	1.033	0.603	0.994	2.631	0.081	0.271	0.013
11	0.381	0.1661	0.912	0.595	0.914	2.420	0.069	0.226	0.009
12	0.470	0.1143	0.802	0.609	0.838	2.249	0.051	0.164	0.005
13	0.580	0.0421	0.688	0.598	0.729	2.015	0.021	0.066	0.001
14	0.715	-0.0108	0.551	0.597	0.541	1.689	-0.006	-0.019	0.000
15	0.882	-0.0399	0.263	0.401	0.275	0.938	-0.043	-0.123	0.004
16	1.089	-0.0108	0.042	0.111	0.068	0.221	-0.049	-0.158	0.005
17	1.343	0.0000	0.014	0.025	0.016	0.055	0.000	0.000	0.000

DISPLACEMENT THICKNESS = 0.825 CM.   MOMENTUM THICKNESS = 0.577 CM.   DELTA 99 = 4.704 CM.

MOMENTUM THICKNESS REYNOLDS NO. = 5414.   UTAU = 0.500 M/SEC   UPW = 15.14 M/SEC

OUTPUT NONDIMENSIONALIZED ON WALL VELOCITY

PT	Y/DEL	UV/UPWS	USQ/UPWS	VSQ/UPWS	WSQ/UPWS	QSQ/UPWS
1	0.044	0.00101	0.00300	0.00167	0.00222	0.00688
2	0.058	0.00093	0.00279	0.00150	0.00210	0.00638
3	0.071	0.00087	0.00266	0.00142	0.00200	0.00608
4	0.087	0.00079	0.00252	0.00129	0.00191	0.00571
5	0.108	0.00069	0.00238	0.00118	0.00177	0.00533
6	0.133	0.00057	0.00213	0.00103	0.00163	0.00479
7	0.165	0.00049	0.00182	0.00090	0.00146	0.00418
8	0.203	0.00039	0.00154	0.00077	0.00132	0.00363
9	0.251	0.00030	0.00131	0.00069	0.00119	0.00320
10	0.309	0.00023	0.00113	0.00066	0.00108	0.00287
11	0.381	0.00018	0.00099	0.00065	0.00100	0.00264
12	0.470	0.00012	0.00087	0.00066	0.00091	0.00245
13	0.580	0.00005	0.00075	0.00065	0.00079	0.00220
14	0.715	-0.00001	0.00060	0.00065	0.00059	0.00184
15	0.882	-0.00004	0.00029	0.00044	0.00030	0.00102
16	1.089	-0.00001	0.00005	0.00012	0.00007	0.00024
17	1.343	0.00000	0.00002	0.00003	0.00002	0.00006

SECOND EXPT., REYNOLDS STRESSES AT STN. 10, S = 61.72 CM. (78.57 DEG)

OUTPUT NONDIMENSIONALIZED ON FRICTION VELOCITY

PT	Y/DEL	UV/UTSQ	USQ/UTSQ	VSQ/UTSQ	WSQ/UTSQ	QSQ/UTSQ	A	SHEAR CORR	ANISOTROPY
1	0.044	0.8349	2.377	1.386	1.876	5.639	0.148	0.460	0.044
2	0.057	0.7626	2.180	1.256	1.767	5.203	0.147	0.461	0.043
3	0.070	0.7342	2.074	1.200	1.689	4.962	0.148	0.466	0.044
4	0.086	0.6773	1.971	1.126	1.623	4.719	0.144	0.455	0.041
5	0.106	0.6215	1.860	1.059	1.531	4.450	0.140	0.443	0.039
6	0.131	0.5504	1.678	0.945	1.414	4.037	0.136	0.437	0.037
7	0.162	0.4497	1.472	0.814	1.251	3.537	0.127	0.411	0.032
8	0.200	0.3370	1.242	0.659	1.063	2.965	0.114	0.372	0.026
9	0.247	0.2243	0.980	0.525	0.874	2.378	0.094	0.313	0.018
10	0.304	0.1368	0.809	0.417	0.728	1.954	0.070	0.235	0.010
11	0.375	0.0919	0.703	0.370	0.651	1.724	0.053	0.180	0.006
12	0.462	0.0689	0.634	0.356	0.602	1.592	0.043	0.145	0.004
13	0.571	0.0427	0.548	0.359	0.535	1.442	0.030	0.096	0.002
14	0.704	0.0416	0.450	0.377	0.437	1.265	0.033	0.101	0.002
15	0.868	0.0142	0.224	0.312	0.226	0.762	0.019	0.054	0.001
16	1.071	-0.0066	0.042	0.110	0.065	0.218	-0.030	-0.096	0.002
17	1.321	0.0219	0.017	0.028	0.020	0.066	0.333	0.990	0.221

DISPLACEMENT THICKNESS = 0.861 CM.   MOMENTUM THICKNESS = 0.597 CM.   DELTA 99 = 4.780 CM.

MOMENTUM THICKNESS REYNOLDS NO. = 5637.   UTAU = 0.497 M/SEC   UPW = 15.26 M/SEC

OUTPUT NONDIMENSIONALIZED ON WALL VELOCITY

PT	Y/DEL	UV/UPWS	USQ/UPWS	VSQ/UPWS	WSQ/UPWS	QSQ/UPWS
1	0.044	0.00088	0.00252	0.00147	0.00199	0.00597
2	0.057	0.00081	0.00231	0.00133	0.00187	0.00551
3	0.070	0.00078	0.00220	0.00127	0.00179	0.00526
4	0.086	0.00072	0.00209	0.00119	0.00172	0.00500
5	0.106	0.00066	0.00197	0.00112	0.00162	0.00471
6	0.131	0.00058	0.00178	0.00100	0.00150	0.00428
7	0.162	0.00048	0.00156	0.00086	0.00132	0.00375
8	0.200	0.00036	0.00132	0.00070	0.00113	0.00314
9	0.247	0.00024	0.00104	0.00056	0.00093	0.00252
10	0.304	0.00014	0.00086	0.00044	0.00077	0.00207
11	0.375	0.00010	0.00074	0.00039	0.00069	0.00183
12	0.462	0.00007	0.00067	0.00038	0.00064	0.00169
13	0.571	0.00005	0.00058	0.00038	0.00057	0.00153
14	0.704	0.00004	0.00048	0.00040	0.00046	0.00134
15	0.868	0.00002	0.00024	0.00033	0.00024	0.00081
16	1.071	-0.00001	0.00004	0.00012	0.00007	0.00023
17	1.321	0.00002	0.00002	0.00003	0.00002	0.00007

SECOND EXPT., REYNOLDS STRESSES AT STN. 12, S = 88.47 CM.

OUTPUT NONDIMENSIONALIZED ON FRICTION VELOCITY

PT	Y/DEL	UV/UTSQ	USQ/UTSQ	VSQ/UTSQ	WSQ/UTSQ	QSQ/UTSQ	A	SHEAR CORR	ANISOTROPY
1	0.037	1.0901	3.651	1.811	2.703	8.165	0.134	0.424	0.036
2	0.044	1.0704	3.468	1.747	2.543	7.758	0.138	0.435	0.038
3	0.057	1.0844	3.312	1.723	2.436	7.470	0.145	0.454	0.042
4	0.070	1.1147	3.250	1.750	2.380	7.380	0.151	0.467	0.046
5	0.086	1.1237	3.194	1.752	2.335	7.281	0.154	0.475	0.048
6	0.107	1.1499	3.163	1.744	2.320	7.227	0.159	0.490	0.051
7	0.132	1.1458	3.103	1.692	2.278	7.073	0.162	0.500	0.052
8	0.163	1.0778	2.948	1.586	2.141	6.674	0.161	0.499	0.052
9	0.200	0.9508	2.582	1.372	1.915	5.869	0.162	0.505	0.052
10	0.247	0.7532	2.064	1.060	1.560	4.684	0.161	0.509	0.052
11	0.305	0.5229	1.442	0.771	1.154	3.367	0.155	0.496	0.048
12	0.376	0.3393	0.953	0.513	0.830	2.297	0.148	0.485	0.044
13	0.464	0.2352	0.695	0.387	0.654	1.736	0.135	0.454	0.037
14	0.572	0.1844	0.601	0.337	0.560	1.498	0.123	0.410	0.030
15	0.706	0.1615	0.509	0.325	0.462	1.295	0.125	0.397	0.031
16	0.871	0.1057	0.320	0.273	0.262	0.855	0.124	0.357	0.031
17	1.075	0.0000	0.056	0.112	0.063	0.231	0.000	0.000	0.000
18	1.326	-0.0008	0.026	0.041	0.030	0.098	-0.008	-0.025	0.000

DISPLACEMENT THICKNESS = 0.879 CM.   MOMENTUM THICKNESS = 0.597 CM.   DELTA 99 = 4.765 CM.

MOMENTUM THICKNESS REYNOLDS NO. = 5829.   UTAU = 0.487 M/SEC   UPW = 14.97 M/SEC

OUTPUT NONDIMENSIONALIZED ON WALL VELOCITY

PT	Y/DEL	UV/UPWS	USQ/UPWS	VSQ/UPWS	WSQ/UPWS	QSQ/UPWS
1	0.037	0.00116	0.00387	0.00192	0.00287	0.00866
2	0.044	0.00113	0.00369	0.00185	0.00270	0.00822
3	0.057	0.00115	0.00351	0.00183	0.00258	0.00792
4	0.070	0.00118	0.00345	0.00186	0.00252	0.00782
5	0.086	0.00119	0.00339	0.00186	0.00248	0.00772
6	0.107	0.00122	0.00335	0.00185	0.00246	0.00766
7	0.132	0.00121	0.00329	0.00179	0.00241	0.00750
8	0.163	0.00114	0.00312	0.00168	0.00227	0.00708
9	0.200	0.00101	0.00274	0.00145	0.00203	0.00622
10	0.247	0.00080	0.00219	0.00112	0.00165	0.00497
11	0.305	0.00055	0.00153	0.00082	0.00122	0.00357
12	0.376	0.00036	0.00101	0.00054	0.00088	0.00243
13	0.464	0.00025	0.00074	0.00041	0.00069	0.00184
14	0.572	0.00020	0.00064	0.00036	0.00059	0.00159
15	0.706	0.00017	0.00054	0.00034	0.00049	0.00137
16	0.871	0.00011	0.00034	0.00029	0.00028	0.00091
17	1.075	0.00000	0.00006	0.00012	0.00007	0.00024
18	1.326	-0.00000	0.00003	0.00004	0.00003	0.00010

SECOND EXPT., REYNOLDS STRESSES AT STN. 13, S = 103.71 CM.

OUTPUT NONDIMENSIONALIZED ON FRICTION VELOCITY

PT	Y/DEL	UV/UTSQ	USQ/UTSQ	VSQ/UTSQ	WSQ/UTSQ	QSQ/UTSQ	A	SHEAR CORR	ANISOTROPY
1	0.037	1.0791	4.112	1.793	2.801	8.706	0.124	0.397	0.031
2	0.043	1.0766	3.944	1.764	2.658	8.366	0.129	0.408	0.033
3	0.056	1.0694	3.759	1.730	2.516	8.005	0.134	0.419	0.036
4	0.069	1.0779	3.690	1.712	2.441	7.843	0.137	0.429	0.038
5	0.085	1.0899	3.589	1.716	2.405	7.709	0.141	0.439	0.040
6	0.105	1.0996	3.530	1.729	2.377	7.635	0.144	0.445	0.041
7	0.130	1.1032	3.430	1.725	2.351	7.506	0.147	0.454	0.043
8	0.160	1.1201	3.342	1.697	2.334	7.374	0.152	0.470	0.046
9	0.198	1.0766	3.268	1.620	2.222	7.109	0.151	0.468	0.046
10	0.244	0.9873	2.967	1.449	2.057	6.473	0.153	0.476	0.047
11	0.301	0.8220	2.482	1.194	1.716	5.392	0.152	0.477	0.046
12	0.371	0.5721	1.751	0.833	1.261	3.845	0.149	0.474	0.044
13	0.457	0.3693	1.113	0.528	0.866	2.507	0.147	0.482	0.043
14	0.564	0.2655	0.750	0.375	0.647	1.772	0.150	0.501	0.045
15	0.696	0.2136	0.614	0.320	0.501	1.435	0.149	0.482	0.044
16	0.859	0.1376	0.388	0.252	0.285	0.925	0.149	0.440	0.044
17	1.059	0.0169	0.094	0.129	0.088	0.311	0.054	0.154	0.006
18	1.307	-0.0024	0.031	0.051	0.034	0.116	-0.021	-0.061	0.001

DISPLACEMENT THICKNESS = 0.897 CM.   MOMENTUM THICKNESS = 0.612 CM.   DELTA 99 = 4.834 CM.

MOMENTUM THICKNESS REYNOLDS NO. = 5679.   UTAU = 0.492 M/SEC   UPW = 14.97 M/SEC

OUTPUT NONDIMENSIONALIZED ON WALL VELOCITY

PT	Y/DEL	UV/UPWS	USQ/UPWS	VSQ/UPWS	WSQ/UPWS	QSQ/UPWS
1	0.037	0.00117	0.00444	0.00194	0.00303	0.00940
2	0.043	0.00116	0.00426	0.00191	0.00287	0.00904
3	0.056	0.00115	0.00406	0.00187	0.00272	0.00865
4	0.069	0.00116	0.00399	0.00185	0.00264	0.00847
5	0.085	0.00118	0.00388	0.00185	0.00260	0.00833
6	0.105	0.00119	0.00381	0.00187	0.00257	0.00825
7	0.130	0.00119	0.00371	0.00186	0.00254	0.00811
8	0.160	0.00121	0.00361	0.00183	0.00252	0.00796
9	0.198	0.00116	0.00353	0.00175	0.00240	0.00768
10	0.244	0.00107	0.00320	0.00156	0.00222	0.00699
11	0.301	0.00089	0.00268	0.00129	0.00185	0.00582
12	0.371	0.00062	0.00189	0.00090	0.00136	0.00415
13	0.457	0.00040	0.00120	0.00057	0.00093	0.00271
14	0.564	0.00029	0.00081	0.00041	0.00070	0.00191
15	0.696	0.00023	0.00066	0.00035	0.00054	0.00155
16	0.859	0.00015	0.00042	0.00027	0.00031	0.00100
17	1.059	0.00002	0.00010	0.00014	0.00009	0.00034
18	1.307	-0.00000	0.00003	0.00006	0.00004	0.00013

SECOND EXPT., REYNOLDS STRESSES AT STN. 14, S = 118.95 CM.

OUTPUT NONDIMENSIONALIZED ON FRICTION VELOCITY

PT	Y/DEL	UV/UTSQ	USQ/UTSQ	VSQ/UTSQ	WSQ/UTSQ	QSQ/UTSQ	A	SHEAR CORR	ANISOTROPY
1	0.036	1.0180	4.069	1.706	2.702	8.478	0.120	0.386	0.029
2	0.042	1.0065	4.053	1.654	2.601	8.308	0.121	0.389	0.029
3	0.054	1.0168	3.777	1.608	2.449	7.834	0.130	0.413	0.034
4	0.067	1.0363	3.696	1.628	2.389	7.714	0.134	0.422	0.036
5	0.082	1.0443	3.660	1.657	2.343	7.660	0.136	0.424	0.037
6	0.102	1.0696	3.578	1.650	2.321	7.549	0.142	0.440	0.040
7	0.126	1.0742	3.536	1.679	2.300	7.516	0.143	0.441	0.041
8	0.155	1.0856	3.472	1.679	2.294	7.445	0.146	0.450	0.043
9	0.191	1.0707	3.313	1.657	2.258	7.228	0.148	0.457	0.044
10	0.236	1.0214	3.182	1.580	2.163	6.925	0.147	0.456	0.044
11	0.291	0.9435	2.986	1.402	1.972	6.360	0.148	0.461	0.044
12	0.359	0.7715	2.459	1.143	1.650	5.252	0.147	0.460	0.043
13	0.442	0.5468	1.734	0.794	1.206	3.734	0.146	0.466	0.043
14	0.546	0.3531	1.087	0.497	0.779	2.382	0.148	0.481	0.044
15	0.673	0.2522	0.745	0.340	0.563	1.648	0.153	0.501	0.047
16	0.830	0.1697	0.481	0.257	0.340	1.079	0.157	0.482	0.049
17	1.070	0.0344	0.120	0.122	0.101	0.342	0.101	0.285	0.020
18	1.264	-0.0138	0.030	0.050	0.030	0.109	-0.126	-0.359	0.032

DISPLACEMENT THICKNESS = 0.922 CM.   MOMENTUM THICKNESS = 0.638 CM.   DELTA 99 = 4.999 CM.

MOMENTUM THICKNESS REYNOLDS NO. = 5867.   UTAU = 0.505 M/SEC   UPW = 15.01 M/SEC

OUTPUT NONDIMENSIONALIZED ON WALL VELOCITY

PT	Y/DEL	UV/UPWS	USQ/UPWS	VSQ/UPWS	WSQ/UPWS	QSQ/UPWS
1	0.036	0.00115	0.00460	0.00193	0.00306	0.00958
2	0.042	0.00114	0.00458	0.00187	0.00294	0.00939
3	0.054	0.00115	0.00427	0.00182	0.00277	0.00886
4	0.067	0.00117	0.00418	0.00184	0.00270	0.00872
5	0.082	0.00118	0.00414	0.00187	0.00265	0.00866
6	0.102	0.00121	0.00404	0.00187	0.00262	0.00854
7	0.126	0.00121	0.00400	0.00190	0.00260	0.00850
8	0.155	0.00123	0.00393	0.00190	0.00259	0.00842
9	0.191	0.00121	0.00375	0.00187	0.00255	0.00817
10	0.236	0.00115	0.00360	0.00179	0.00245	0.00783
11	0.291	0.00107	0.00338	0.00159	0.00223	0.00719
12	0.359	0.00087	0.00278	0.00129	0.00187	0.00594
13	0.442	0.00062	0.00196	0.00090	0.00136	0.00422
14	0.546	0.00040	0.00123	0.00056	0.00090	0.00269
15	0.673	0.00029	0.00084	0.00038	0.00064	0.00186
16	0.830	0.00019	0.00054	0.00029	0.00038	0.00122
17	1.070	0.00004	0.00014	0.00014	0.00011	0.00039
18	1.264	-0.00002	0.00003	0.00006	0.00003	0.00012

SECOND EXPT., REYNOLDS STRESSES AT STN. 15, S = 124.79 CM.

OUTPUT NONDIMENSIONALIZED ON FRICTION VELOCITY

PT	Y/DEL	UV/UTSQ	USQ/UTSQ	VSQ/UTSQ	WSQ/UTSQ	QSQ/UTSQ	A	SHEAR CORR	ANISOTROPY
1	0.035	1.0409	4.587	1.817	3.124	9.528	0.109	0.361	0.024
2	0.041	1.0375	4.432	1.773	2.860	9.065	0.114	0.370	0.026
3	0.054	1.0307	4.178	1.666	2.632	8.476	0.122	0.391	0.030
4	0.066	1.0443	4.090	1.652	2.534	8.276	0.126	0.402	0.032
5	0.081	1.0443	4.010	1.682	2.431	8.123	0.129	0.402	0.033
6	0.100	1.0568	3.835	1.690	2.400	7.925	0.133	0.415	0.036
7	0.124	1.0749	3.819	1.704	2.390	7.914	0.136	0.421	0.037
8	0.153	1.0492	3.718	1.710	2.362	7.790	0.137	0.424	0.038
9	0.189	1.0817	3.662	1.731	2.319	7.713	0.140	0.430	0.039
10	0.233	1.0738	3.513	1.665	2.299	7.478	0.144	0.444	0.041
11	0.287	1.0149	3.306	1.577	2.216	7.099	0.143	0.445	0.041
12	0.355	0.8959	2.936	1.389	1.968	6.293	0.142	0.444	0.041
13	0.437	0.7306	2.422	1.110	1.604	5.137	0.142	0.445	0.040
14	0.539	0.5018	1.649	0.751	1.129	3.529	0.142	0.451	0.040
15	0.665	0.3069	0.998	0.444	0.709	2.152	0.143	0.461	0.041
16	0.821	0.1993	0.598	0.285	0.417	1.300	0.153	0.483	0.047
17	1.013	0.0702	0.233	0.161	0.158	0.552	0.127	0.363	0.032
18	1.249	-0.0170	0.038	0.063	0.029	0.130	-0.131	-0.350	0.034

DISPLACEMENT THICKNESS = 0.940 CM.   MOMENTUM THICKNESS = 0.650 CM.   DELTA 99 = 5.057 CM.

MOMENTUM THICKNESS REYNOLDS NO. = 5968.   UTAU = 0.508 M/SEC   UPW = 14.97 M/SEC

OUTPUT NONDIMENSIONALIZED ON WALL VELOCITY

PT	Y/DEL	UV/UPWS	USQ/UPWS	VSQ/UPWS	WSQ/UPWS	QSQ/UPWS
1	0.035	0.00120	0.00527	0.00209	0.00359	0.01096
2	0.041	0.00119	0.00510	0.00204	0.00329	0.01042
3	0.054	0.00119	0.00480	0.00192	0.00303	0.00975
4	0.066	0.00120	0.00470	0.00190	0.00291	0.00952
5	0.081	0.00120	0.00461	0.00193	0.00280	0.00934
6	0.100	0.00122	0.00441	0.00194	0.00276	0.00911
7	0.124	0.00124	0.00439	0.00196	0.00275	0.00910
8	0.153	0.00123	0.00428	0.00197	0.00272	0.00896
9	0.189	0.00124	0.00421	0.00199	0.00267	0.00837
10	0.233	0.00123	0.00404	0.00191	0.00264	0.00860
11	0.287	0.00117	0.00380	0.00181	0.00255	0.00816
12	0.355	0.00103	0.00338	0.00160	0.00226	0.00724
13	0.437	0.00084	0.00279	0.00128	0.00184	0.00591
14	0.539	0.00058	0.00190	0.00086	0.00130	0.00406
15	0.665	0.00035	0.00115	0.00051	0.00082	0.00247
16	0.821	0.00023	0.00069	0.00033	0.00048	0.00149
17	1.013	0.00008	0.00027	0.00018	0.00013	0.00063
18	1.249	-0.00000	0.00004	0.00007	0.00003	0.00015

SECOND EXPT., REYNOLDS STRESSES AT STN. 16, S = 149.43 CM.

OUTPUT NONDIMENSIONALIZED ON FRICTION VELOCITY

PT	Y/DEL	UV/UTSQ	USQ/UTSQ	VSQ/UTSQ	WSQ/UTSQ	QSQ/UTSQ	A	SHEAR CORR	ANISOTROPY
1	0.034	1.0715	4.813	1.838	3.158	9.809	0.109	0.360	0.024
2	0.040	1.0556	4.533	1.741	3.006	9.281	0.114	0.376	0.026
3	0.052	1.0511	4.497	1.704	2.709	8.910	0.118	0.380	0.028
4	0.064	1.0579	4.252	1.664	2.625	8.541	0.124	0.398	0.031
5	0.079	1.0726	4.170	1.686	2.542	8.398	0.128	0.405	0.033
6	0.098	1.1009	4.147	1.741	2.463	8.350	0.132	0.410	0.035
7	0.121	1.1281	4.081	1.737	2.480	8.298	0.136	0.424	0.037
8	0.149	1.1236	4.113	1.778	2.472	8.364	0.134	0.415	0.036
9	0.184	1.1530	3.985	1.833	2.455	8.273	0.139	0.427	0.039
10	0.226	1.1395	3.901	1.816	2.452	8.169	0.139	0.428	0.039
11	0.279	1.1168	3.707	1.769	2.432	7.909	0.141	0.436	0.040
12	0.345	1.0239	3.473	1.621	2.223	7.318	0.140	0.432	0.039
13	0.425	0.8959	2.946	1.351	1.915	6.213	0.144	0.449	0.042
14	0.524	0.6626	2.249	1.006	1.438	4.693	0.141	0.440	0.040
15	0.647	0.4349	1.387	0.621	0.939	2.947	0.148	0.469	0.044
16	0.797	0.2356	0.747	0.348	0.507	1.602	0.147	0.462	0.043
17	0.984	0.0917	0.303	0.174	0.195	0.673	0.136	0.399	0.037
18	1.214	-0.0125	0.048	0.072	0.043	0.163	-0.076	-0.211	0.012

DISPLACEMENT THICKNESS = 0.973 CM.   MOMENTUM THICKNESS = 0.673 CM.   DELTA 99 = 5.204 CM.

MOMENTUM THICKNESS REYNOLDS NO. = 6234.   UTAU = 0.508 M/SEC   UPW = 14.98 M/SEC

OUTPUT NONDIMENSIONALIZED ON WALL VELOCITY

PT	Y/DEL	UV/UPWS	USQ/UPWS	VSQ/UPWS	WSQ/UPWS	QSQ/UPWS
1	0.034	0.00123	0.00553	0.00211	0.00363	0.01127
2	0.040	0.00121	0.00522	0.00200	0.00346	0.01067
3	0.052	0.00121	0.00517	0.00196	0.00311	0.01024
4	0.064	0.00122	0.00489	0.00191	0.00302	0.00982
5	0.079	0.00123	0.00479	0.00194	0.00292	0.00965
6	0.098	0.00127	0.00477	0.00200	0.00283	0.00960
7	0.121	0.00130	0.00469	0.00200	0.00285	0.00954
8	0.149	0.00129	0.00473	0.00204	0.00284	0.00961
9	0.184	0.00133	0.00458	0.00211	0.00282	0.00951
10	0.226	0.00131	0.00448	0.00209	0.00282	0.00939
11	0.279	0.00128	0.00426	0.00203	0.00280	0.00909
12	0.345	0.00118	0.00399	0.00186	0.00256	0.00841
13	0.425	0.00103	0.00339	0.00155	0.00220	0.00714
14	0.524	0.00076	0.00258	0.00116	0.00165	0.00539
15	0.647	0.00050	0.00159	0.00071	0.00108	0.00339
16	0.797	0.00027	0.00086	0.00040	0.00058	0.00184
17	0.984	0.00011	0.00035	0.00020	0.00022	0.00077
18	1.214	-0.00001	0.00006	0.00008	0.00005	0.00019

SECOND EXPT., REYNOLDS STRESSES AT STN. 17, S = 164.67 CM.

OUTPUT NONDIMENSIONALIZED ON FRICTION VELOCITY

PT	Y/DEL	UV/UTSQ	USQ/UTSQ	VSQ/UTSQ	WSQ/UTSQ	QSQ/UTSQ	A	SHEAR CORR	ANISOTROPY
1	0.033	1.0267	4.689	1.721	2.919	9.329	0.110	0.361	0.024
2	0.039	1.0346	4.537	1.656	2.770	8.963	0.115	0.377	0.027
3	0.050	1.0357	4.479	1.636	2.687	8.803	0.118	0.383	0.028
4	0.062	1.0436	4.292	1.660	2.573	8.526	0.122	0.391	0.030
5	0.076	1.0537	4.332	1.674	2.534	8.540	0.123	0.391	0.030
6	0.094	1.0784	4.253	1.693	2.506	8.458	0.128	0.401	0.033
7	0.116	1.0897	4.274	1.729	2.496	8.498	0.128	0.401	0.033
8	0.143	1.1144	4.153	1.785	2.471	8.409	0.133	0.409	0.035
9	0.177	1.1313	4.099	1.791	2.472	8.362	0.135	0.418	0.037
10	0.218	1.1437	4.037	1.787	2.440	8.264	0.138	0.426	0.038
11	0.269	1.1335	3.944	1.776	2.417	8.137	0.139	0.428	0.039
12	0.332	1.0706	3.622	1.669	2.337	7.627	0.140	0.435	0.039
13	0.409	0.9674	3.283	1.487	2.091	6.861	0.141	0.439	0.040
14	0.505	0.7737	2.619	1.205	1.697	5.521	0.140	0.436	0.039
15	0.623	0.5218	1.777	0.780	1.160	3.717	0.140	0.443	0.039
16	0.768	0.2744	0.944	0.428	0.609	1.980	0.139	0.432	0.038
17	0.947	0.0978	0.374	0.195	0.222	0.790	0.124	0.363	0.031
18	1.169	-0.0180	0.060	0.085	0.044	0.189	-0.095	-0.251	0.018

DISPLACEMENT THICKNESS = 0.998 CM.   MOMENTUM THICKNESS = 0.696 CM.   DELTA 99 = 5.405 CM.

MOMENTUM THICKNESS REYNOLDS NO. = 6431.   UTAU = 0.510 M/SEC   UPW = 14.96 M/SEC

OUTPUT NONDIMENSIONALIZED ON WALL VELOCITY

PT	Y/DEL	UV/UPWS	USQ/UPWS	VSQ/UPWS	WSQ/UPWS	QSQ/UPWS
1	0.033	0.00119	0.00544	0.00200	0.00339	0.01082
2	0.039	0.00120	0.00526	0.00192	0.00321	0.01040
3	0.050	0.00120	0.00520	0.00190	0.00312	0.01021
4	0.052	0.00121	0.00498	0.00193	0.00298	0.00989
5	0.076	0.00122	0.00503	0.00194	0.00294	0.00991
6	0.094	0.00125	0.00493	0.00197	0.00291	0.00981
7	0.116	0.00126	0.00496	0.00201	0.00290	0.00986
8	0.143	0.00129	0.00482	0.00207	0.00287	0.00975
9	0.177	0.00131	0.00476	0.00208	0.00287	0.00970
10	0.218	0.00133	0.00468	0.00207	0.00283	0.00959
11	0.269	0.00131	0.00457	0.00206	0.00280	0.00944
12	0.332	0.00124	0.00420	0.00194	0.00271	0.00885
13	0.409	0.00112	0.00381	0.00173	0.00243	0.00796
14	0.505	0.00090	0.00304	0.00140	0.00197	0.00640
15	0.623	0.00061	0.00206	0.00090	0.00135	0.00431
16	0.768	0.00032	0.00109	0.00050	0.00071	0.00230
17	0.947	0.00011	0.00043	0.00023	0.00026	0.00092
18	1.169	-0.00002	0.00007	0.00010	0.00005	0.00022

ERROR END OF FILE ENCOUNTERED ON UNIT   5 (IBM CODE IHC217)

PROGRAM WAS EXECUTING LINE   8 IN ROUTINE M.PROG WHEN TERMINATION OCCURRED

STATEMENTS EXECUTED=   7620

CORE USAGE   OBJECT CODE=   5992 BYTES,ARRAY AREA=   2032 BYTES,TOTAL AREA AVAILABLE= 147456 BYTES

SECOND EXPT., STN. 5, S = -29.04 CM.

PT	Y/DEL	U/UPW	UCALC	VELGRAD
1	0.013	0.429	0.434	9.912
2	0.024	0.540	0.532	6.846
3	0.035	0.579	0.581	2.889
4	0.045	0.603	0.604	1.908
5	0.063	0.634	0.634	1.451
6	0.077	0.653	0.654	1.417
7	0.093	0.676	0.676	1.200
8	0.113	0.694	0.694	0.786
9	0.139	0.714	0.714	0.751
10	0.172	0.738	0.738	0.679
11	0.211	0.762	0.762	0.571
12	0.260	0.788	0.788	0.484
13	0.321	0.815	0.815	0.426
14	0.395	0.846	0.846	0.395
15	0.488	0.879	0.879	0.327
16	0.601	0.914	0.914	0.295
17	0.742	0.952	0.952	0.233
18	0.915	0.983	0.983	0.130
19	1.128	1.000	1.000	0.035
20	1.391	1.001	1.001	-0.008
21	1.716	1.000	1.000	0.000

PT	Y/DEL	UCAL/UP	VELGRAD	MIX LN/DEL	PROD	L/LO	RIC	BETA	ED.RE
1	0.091	0.673	1.272	0.0314	31.41	0.846	0.0000	0.0	89.74
2	0.112	0.693	0.789	0.0505	19.39	1.101	0.0000	0.0	143.73
3	0.138	0.713	0.751	0.0530	18.44	0.937	0.0000	0.0	150.89
4	0.170	0.737	0.687	0.0572	16.42	0.920	0.0000	0.0	160.60
5	0.210	0.761	0.572	0.0676	13.24	0.795	0.0000	0.0	186.82
6	0.259	0.788	0.486	0.0772	10.57	0.908	0.0000	0.0	206.80
7	0.320	0.815	0.426	0.0853	8.71	1.004	0.0000	0.0	221.73
8	0.395	0.846	0.395	0.0871	7.21	1.024	0.0000	0.0	213.85
9	0.487	0.879	0.327	0.0964	5.04	1.135	0.0000	0.0	217.55
10	0.600	0.914	0.295	0.0939	3.52	1.105	0.0000	0.0	186.40
11	0.741	0.952	0.234	0.0970	1.86	1.141	0.0000	0.0	157.18
12	0.914	0.983	0.130	0.1162	0.46	1.368	0.0000	0.0	126.02
13	1.128	1.000	0.035	0.2446	0.04	2.878	0.0000	0.0	148.39
14	1.391	1.001	-0.008	0.0000	0.00	0.000	0.0000	0.0	0.00

SECOND EXPT., STN. 6, S= 0.00 CM.

PT	Y/DEL	U/UPH	UCALC	VELGRAD
1	0.003	0.116	0.111	8.144
2	0.005	0.129	0.137	22.638
3	0.007	0.205	0.204	40.447
4	0.009	0.289	0.286	38.722
5	0.020	0.498	0.498	8.143
6	0.030	0.558	0.558	4.246
7	0.040	0.591	0.591	2.704
8	0.058	0.631	0.631	1.704
9	0.072	0.651	0.651	1.307
10	0.089	0.673	0.673	1.229
11	0.109	0.695	0.695	0.979
12	0.135	0.718	0.718	0.843
13	0.166	0.743	0.743	0.720
14	0.206	0.767	0.767	0.535
15	0.254	0.792	0.792	0.504
16	0.313	0.820	0.820	0.438
17	0.386	0.849	0.849	0.370
18	0.477	0.881	0.881	0.332
19	0.588	0.915	0.915	0.279
20	0.726	0.949	0.949	0.217
21	0.896	0.980	0.980	0.145
22	1.105	1.000	1.000	0.044
23	1.366	1.000	1.000	0.000

PT	Y/DEL	UCAL/UP	VELGRAD	MIX LN/DEL	PROD	L/LO	RIC	BETA	ED.RE
1	0.047	0.609	2.340	0.0126	75.49	0.705	0.0000	0.0	26.17
2	0.060	0.634	1.591	0.0195	51.14	0.780	0.0000	0.0	38.32
3	0.072	0.651	1.307	0.0229	43.19	0.789	0.0000	0.0	47.97
4	0.089	0.673	1.229	0.0043	40.39	0.670	0.0000	0.0	50.74
5	0.110	0.695	0.923	0.0309	31.38	0.667	0.0000	0.0	64.78
6	0.135	0.718	0.843	0.0355	27.90	0.642	0.0000	0.0	74.50
7	0.167	0.744	0.712	0.0409	22.06	0.598	0.0000	0.0	83.43
8	0.206	0.767	0.535	0.0539	16.39	0.613	0.0000	0.0	103.66
9	0.254	0.792	0.504	0.0555	14.55	0.653	0.0000	0.0	103.72
10	0.314	0.820	0.436	0.0621	11.02	0.730	0.0000	0.0	117.77
11	0.327	0.849	0.370	0.0688	8.82	0.810	0.0000	0.0	122.54
12	0.478	0.881	0.330	0.0713	6.06	0.839	0.0000	0.0	116.10
13	0.588	0.915	0.278	0.0170	4.73	0.906	0.0000	0.0	115.69
14	0.727	0.949	0.217	0.0642	2.65	0.990	0.0000	0.0	107.39
15	0.896	0.970	0.145	0.0035	0.89	1.041	0.0000	0.0	79.77
16	1.106	1.000	0.044	0.1510	0.07	1.776	0.0000	0.0	69.78
17	1.364	1.000	-0.022	-0.0334	0.00	*****	0.0000	0.0	-2.29

SECOND EXPT., STN. 7, S= 10.39 CM.

PT	Y/DEL	U/UPH	UCALC	VELGRAD
1	0.010	0.395	0.400	13.429
2	0.018	0.505	0.497	9.567
3	0.026	0.547	0.549	4.308
4	0.034	0.574	0.576	2.830
5	0.047	0.610	0.609	2.251
6	0.058	0.631	0.631	1.875
7	0.070	0.653	0.653	1.579
8	0.085	0.672	0.672	1.018
9	0.105	0.689	0.689	0.829
10	0.129	0.709	0.709	0.742
11	0.159	0.727	0.727	0.561
12	0.195	0.748	0.748	0.527
13	0.242	0.770	0.770	0.431
14	0.298	0.792	0.792	0.382
15	0.368	0.817	0.817	0.328
16	0.453	0.843	0.843	0.275
17	0.559	0.868	0.868	0.195
18	0.690	0.882	0.882	0.000
19	0.851	0.876	0.876	0.034
20	1.049	0.899	0.899	0.057
21	1.295	0.878	0.878	-0.129
22	1.598	0.852	0.652	0.000

PT	Y/DEL	UCAL/UP	VELGRAD	MIX LN/DEL	PROD	L/LO	RIC	BETA	ED.RE
1	0.036	0.531	2.792	0.0119	53.24	0.868	0.0448	2.9	36.83
2	0.043	0.600	2.497	0.0129	44.97	0.765	0.0514	4.6	38.77
3	0.056	0.628	1.887	0.0160	29.49	0.709	0.0708	4.1	44.97
4	0.069	0.651	1.627	0.0174	22.09	0.618	0.0949	4.5	45.67
5	0.084	0.671	1.044	0.0253	12.03	0.736	0.1344	2.0	62.07
6	0.104	0.683	0.824	0.0297	7.96	0.697	0.1731	1.8	67.55
7	0.129	0.709	0.742	0.0331	7.14	0.627	0.1966	1.5	75.72
8	0.159	0.727	0.561	0.0397	4.23	0.608	0.2621	1.5	81.94
9	0.195	0.748	0.527	0.0403	3.57	0.502	0.2849	1.7	79.56
10	0.242	0.770	0.431	0.0466	2.48	0.548	0.3520	1.3	85.25
11	0.298	0.792	0.382	0.0482	1.78	0.567	0.4030	1.1	82.50
12	0.368	0.817	0.328	0.0506	1.17	0.595	0.4738	0.9	77.93
13	0.453	0.843	0.275	0.0532	0.70	0.626	0.5668	0.7	72.34
14	0.559	0.868	0.195	0.0603	0.25	0.710	0.7707	0.4	66.06
15	0.690	0.882	0.000	31.4072	-0.09	*****	3.8245	-95.3	*******
16	0.851	0.876	0.034	0.0908	-0.01	0.951	2.2803	0.0	20.56
17	1.049	0.899	0.057	0.0000	0.00	0.000	1.8059	0.6	0.00

SECOND EXPT., STN. 8, S= 25.19 CM.

PT	Y/DEL	U/UPW	UCALC	VELGRAD
1	0.011	0.337	0.342	11.345
2	0.020	0.443	0.435	8.312
3	0.028	0.483	0.483	4.302
4	0.036	0.508	0.510	2.668
5	0.051	0.543	0.543	1.935
6	0.063	0.565	0.566	1.817
7	0.076	0.588	0.588	1.533
8	0.093	0.610	0.611	1.268
9	0.114	0.638	0.638	1.197
10	0.140	0.665	0.665	0.968
11	0.172	0.694	0.694	0.805
12	0.211	0.720	0.720	0.572
13	0.260	0.745	0.745	0.473
14	0.321	0.771	0.771	0.383
15	0.396	0.798	0.798	0.339
16	0.487	0.826	0.826	0.279
17	0.601	0.854	0.854	0.216
18	0.742	0.881	0.881	0.163
19	0.915	0.901	0.901	0.051
20	1.129	0.897	0.897	-0.062
21	1.392	0.877	0.877	-0.081
22	1.718	0.852	0.852	0.000

PT	Y/DEL	UCAL/UP	VELGRAD	MIX LN/DEL	PROD	L/LO	RIC	BETA	ED.RE
1	0.046	0.533	2.076	0.0157	51.78	0.885	0.0511	2.3	38.93
2	0.060	0.560	1.828	0.0170	41.19	0.709	0.0607	4.8	40.14
3	0.074	0.585	1.610	0.0184	32.81	0.613	0.0718	5.4	41.46
4	0.091	0.608	1.253	0.0224	22.63	0.603	0.0953	4.2	47.87
5	0.112	0.635	1.230	0.0211	18.83	0.459	0.1012	5.3	41.45
6	0.138	0.663	0.970	0.0240	11.80	0.425	0.1327	4.3	42.58
7	0.171	0.693	0.815	0.0251	7.51	0.358	0.1636	3.9	39.08
8	0.211	0.720	0.572	0.0300	3.55	0.353	0.2367	2.7	39.14
9	0.260	0.745	0.473	0.0278	1.66	0.327	0.2916	2.3	27.79
10	0.320	0.771	0.384	0.0251	0.69	0.296	0.3634	1.9	18.42
11	0.395	0.798	0.340	0.0154	0.17	0.181	0.4177	2.0	6.14
12	0.487	0.826	0.279	0.0250	-0.23	0.295	0.5110	1.4	13.31
13	0.601	0.854	0.216	0.0485	-0.34	0.570	0.6511	0.7	38.60
14	0.742	0.881	0.163	0.0779	-0.29	0.916	0.8336	0.1	75.31
15	0.915	0.901	0.051	0.2109	0.11	2.481	1.7784	-0.8	173.29
16	1.129	0.897	-0.062	-0.0526	0.04	*****	******	0.0	-13.13
17	1.392	0.877	-0.081	-0.0135	-0.00	*****	******	0.0	-1.13

SECOND EXPT., STN. 9, S= 41.48 CM.

PT	Y/DEL	U/UPW	UCALC	VELGRAD
1	0.010	0.312	0.317	11.292
2	0.019	0.417	0.409	8.097
3	0.027	0.454	0.455	4.009
4	0.035	0.478	0.480	2.413
5	0.049	0.507	0.508	1.868
6	0.060	0.529	0.529	1.828
7	0.073	0.551	0.551	1.532
8	0.089	0.573	0.573	1.336
9	0.110	0.601	0.601	1.313
10	0.135	0.632	0.632	1.182
11	0.166	0.665	0.665	0.919
12	0.204	0.694	0.694	0.684
13	0.251	0.725	0.725	0.577
14	0.309	0.753	0.753	0.431
15	0.382	0.783	0.783	0.366
16	0.470	0.810	0.810	0.289
17	0.580	0.841	0.841	0.254
18	0.715	0.870	0.870	0.190
19	0.882	0.895	0.895	0.091
20	1.088	0.897	0.847	-0.052
21	1.343	0.877	0.877	-0.087
22	1.657	0.852	0.852	0.000

PT	Y/DEL	UCAL/UP	VELGRAD	MIX LN/DEL	PROD	L/LO	RIC	BETA	ED.RE
1	0.044	0.499	1.907	0.0167	52.17	0.992	0.0539	0.2	40.46
2	0.058	0.525	1.856	0.0164	46.31	0.709	0.0582	5.0	37.98
3	0.071	0.547	1.588	0.0185	36.85	0 645	0.0707	5.0	41.58
4	0 087	0.570	1.531	0.0211	27.92	0.595	0.0874	4.6	45.22
5	0.108	0.598	1.325	0.0199	24.33	0.450	0.0921	6.0	39.90
6	0.133	0.630	1.190	0.0204	18.48	0.375	0.1074	5.8	37.85
7	0.165	0.664	0.932	0.0238	11.78	0.352	0.1433	4.5	40.17
8	0.203	0.694	0.684	0.0288	6.59	0.346	0.2006	3.3	43.23
9	0.251	0.725	0.577	0.0299	4.16	0.352	0.2451	2.6	39.42
10	0.309	0.753	0.431	0.0354	2.28	0.417	0.3324	1.8	41.17
11	0.381	0.782	0.368	0.0365	1.44	0.430	0.3965	1.4	37.45
12	0.470	0.810	0.289	0.0387	0.71	0.455	0.5067	1.1	32.91
13	0.580	0.841	0.254	0.0267	0.21	0.314	0.5833	1.2	13.77
14	0.715	0.870	0.190	0.0181	-0.03	0.213	0.7615	1.0	4.73
15	0.882	0.895	0.091	0.0728	0.00	0.856	1.3259	0.1	36.56
16	1.089	0.897	-0.053	-0.0652	0.05	*****	******	0.0	-17.05
17	1.343	0.877	-0.087	0.0000	0.00	0.000	******	0.0	0.00

263

SECOND EXPT., STN. 10, S = 61.72 CM.

PT	Y/DEL	U/UPW	UCALC	VELGRAD
1	0.010	0.309	0.314	10.544
2	0.019	0.409	0.401	7.890
3	0.027	0.448	0.448	4.244
4	0.035	0.472	0.474	2.586
5	0.048	0.501	0.502	1.786
6		0.520	0.520	1.505
7		0.538	0.538	1.299
8	.088	0.558	0.558	1.250
9	.108	0.583	0.583	1.251
10	0.133	0.613	0.613	1.172
11	0.163	0.647	0.647	1.017
12	0.201	0.680	0.680	0.796
13	0.247	0.714	0.714	0.673
14	0.304	0.748	0.748	0.496
15	0.376	0.777	0.777	0.349
16	0.463	0.805	0.805	0.305
17	0.571	0.835	0.835	0.247
18	0.704	0.864	0.864	0.200
19	0.868	0.892	0.892	0.109
20	1.074	0.897	0.897	-0.044
21	1.321	0.877	0.877	-0.092
22	1.631	0.851	0.851	0.000

PT	Y/DEL	UCAL/UP	VELGRAD	MIX LN/DEL	PROD	L/LO	RIC	BETA	ED.RE
1	0.044	0.494	1.946	0.0153	48.58	0.906	0.0532	1.8	35.21
2	0.057	0.517	1.548	0.0184	34.99	0.809	0.0696	2.7	40.44
3	0.070	0.535	1.323	0.0211	28.57	0.744	0.0840	3.0	45.55
4	0.086	0.555	1.242	0.0216	24.62	0.615	0.0927	4.2	44.77
5	0.106	0.581	1.260	0.0204	22.88	0.469	0.0954	5.6	40.49
6	0.131	0.611	1.175	0.0205	18.78	0.383	0.1073	5.8	38.45
7	0.162	0.646	1.026	0.0213	13.23	0.320	0.1291	5.3	35.98
8	0.200	0.680	0.799	0.0236	7.53	0.288	0.1724	4.1	34.62
9	0.247	0.714	0.673	0.0229	4.12	0.269	0.2127	3.4	27.36
10	0.304	0.748	0.496	0.0242	1.75	0.285	0.2949	2.4	22.62
11	0.375	0.777	0.350	0.0282	0.75	0.332	0.4195	1.6	21.59
12	0.462	0.805	0.306	0.0280	0.47	0.329	0.4872	1.4	18.51
13	0.571	0.835	0.247	0.0272	0.21	0.320	0.6030	1.1	14.18
14	0.704	0.864	0.200	0.0331	0.14	0.390	0.7372	0.8	17.05
15	0.868	0.892	0.109	0.0354	0.01	0.417	1.1857	0.5	10.65
16	1.071	0.897	-0.042	-0.0623	0.03	*****	******	0.1	-12.77
17	1.321	0.877	-0.092	-0.0523	-0.12	*****	******	0.0	-19.52

SECOND EXPT., STN. 12, S= 88.47 CM.

PT	Y/DEL	U/UPW	UCALC	VELGRAD
1	0.010	0.310	0.315	10.399
2	0.019	0.409	0.401	7.668
3	0.027	0.445	0.446	3.965
4	0.035	0.468	0.470	2.262
5	0.048	0.492	0.493	1.473
6	0.059	0.508	0.508	1.350
7	0.072	0.525	0.525	1.323
8	0.088	0.546	0.546	1.176
9	0.108	0.567	0.567	1.087
10	0.133	0.597	0.597	1.235
11	0.164	0.633	0.633	1.030
12	0.202	0.668	0.668	0.939
13	0.248	0.714	0.714	0.951
14	0.306	0.761	0.761	0.722
15	0.377	0.808	0.808	0.588
16	0.464	0.851	0.851	0.415
17	0.573	0.890	0.890	0.326
18	0.706	0.932	0.932	0.302
19	0.871	0.975	0.975	0.201
20	1.074	0.999	0.999	0.050
21	1.325	1.001	1.001	-0.009
22	1.636	1.000	1.000	0.000

PT	Y/DEL	UCAL/UP	VELGRAD	MIX LN/DEL	PROD	L/LO	RIC	BETA	ED.RE
1	0.037	0.474	2.063	0.0165	69.06	1.216	0.0000	0.0	41.69
2	0.044	0.486	1.588	0.0212	52.20	1.264	0.0000	0.0	53.17
3	0.057	0.505	1.367	0.0248	45.54	1.096	0.0000	0.0	62.56
4	0.070	0.523	1.318	0.0261	45.11	0.922	0.0000	0.0	66.72
5	0.086	0.543	1.216	0.0284	41.98	0.809	0.0000	0.0	72.87
6	0.107	0.566	1.075	0.0325	37.97	0.741	0.0000	0.0	84.37
7	0.132	0.596	1.236	0.0282	43.51	0.521	0.0000	0.0	73.09
8	0.163	0.632	1.042	0.0305	34.48	0.486	0.0000	0.0	81.62
9	0.200	0.666	0.926	0.0343	27.05	0.418	0.0000	0.0	80.97
10	0.247	0.713	0.958	0.0295	22.16	0.347	0.0000	0.0	62.03
11	0.305	0.760	0.723	0.0326	11.62	0.383	0.0000	0.0	57.02
12	0.376	0.807	0.590	0.0321	6.15	0.378	0.0000	0.0	45.33
13	0.464	0.851	0.415	0.0381	3.00	0.448	0.0000	0.0	44.74
14	0.572	0.890	0.327	0.0428	1.85	0.504	0.0000	0.0	44.54
15	0.706	0.932	0.302	0.0434	1.50	0.510	0.0000	0.0	42.24
16	0.871	0.975	0.201	0.0527	0.65	0.620	0.0000	0.0	41.53
17	1.075	0.999	0.049	0.0000	0.00	0.000	0.0000	0.0	0.00
18	1.326	1.001	-0.009	-0.0993	0.00	*****	0.0000	0.0	-6.80

SECOND EXPT., STN. 13, S= 103.47 CM.

PT	Y/DEL	U/UPW	UCALC	VELGRAD
1	0.010	0.319	0.324	12.114
2	0.018	0.420	0.412	8.608
3	0.026	0.457	0.458	3.638
4	0.034	0.477	0.479	2.059
5	0.048	0.505	0.505	1.644
6	0.058	0.520	0.520	1.362
7	0.071	0.536	0.536	1.156
8	0.087	0.554	0.554	1.112
9	0.107	0.576	0.576	1.058
10	0.131	0.600	0.600	0.962
11	0.161	0.628	0.628	0.900
12	0.199	0.661	0.661	0.850
13	0.245	0.700	0.700	0.852
14	0.301	0.747	0.747	0.802
15	0.372	0.798	0.798	0.628
16	0.458	0.844	0.844	0.465
17	0.565	0.888	0.888	0.362
18	0.697	0.930	0.930	0.288
19	0.859	0.971	0.971	0.206
20	1.060	0.998	0.998	0.065
21	1.307	1.001	1.001	-0.010
22	1.613	1.000	1.000	0.000
23	1.839	1.000	1.000	0.000

PT	Y/DEL	UCAL/UP	VELGRAD	MIX LN/DEL	FROD	L/LO	RIC	BETA	ED.RE
1	0.037	0.485	1.973	0.0173	64.76	1.269	0.0000	0.0	45.08
2	0.043	0.496	1.796	0.0190	58.81	1.158	0.0000	0.0	49.41
3	0.056	0.517	1.414	0.0240	46.01	1.080	0.0000	0.0	62.30
4	0.069	0.534	1.171	0.0291	38.40	1.045	0.0000	0.0	75.85
5	0.085	0.552	1.111	0.0309	36.84	0.891	0.0000	0.0	80.82
6	0.105	0.574	1.070	0.0322	35.79	0.749	0.0000	0.0	84.69
7	0.130	0.599	0.964	0.0358	32.36	0.672	0.0000	0.0	94.27
8	0.160	0.627	0.903	0.0385	30.76	0.597	0.0000	0.0	102.24
9	0.198	0.660	0.850	0.0401	27.84	0.494	0.0000	0.0	104.38
10	0.244	0.699	0.851	0.0384	25.57	0.451	0.0000	0.0	95.56
11	0.301	0.747	0.802	0.0371	20.06	0.437	0.0000	0.0	84.43
12	0.371	0.797	0.631	0.0394	10.98	0.464	0.0000	0.0	74.72
13	0.457	0.844	0.466	0.0429	5.24	0.504	0.0000	0.0	65.29
14	0.564	0.888	0.362	0.0467	2.93	0.550	0.0000	0 0	60.37
15	0.696	0.930	0.288	0.0528	1.87	0.621	0.0000	0.0	61.15
16	0.859	0.971	0.206	0.0592	0.86	0.696	0.0000	0.0	55.02
17	1.059	0.998	0.065	0.0654	.03	0.769	0.0000	0.0	21.30
18	1.307	1.001	-0.010	-0.1607	0.00	*****	0.0000	0.0	-19.73

SECOND EXPT., STN. 14, S = 118.95 CM.

PT	Y/DEL	U/UPW	UCALC	VELGRAD
1	0.010	0.333	0.338	11.868
2	0.018	0.433	0.425	8.696
3	0.025	0.469	0.469	4.331
4	0.033	0.491	0.493	2.173
5	0.046	0.516	0.516	1.589
6	0.056	0.532	0.532	1.406
7	0.069	0.548	0.548	1.213
8	0.084	0.566	0.566	1.076
9	0.103	0.584	0.584	0.926
10	0.127	0.607	0.607	0.949
11	0.156	0.633	0.633	0.836
12	0.192	0.661	0.661	0.747
13	0.237	0.695	0.695	0.778
14	0.291	0.737	0.737	0.732
15	0.359	0.782	0.782	0.636
16	0.443	0.834	0.834	0.563
17	0.546	0.882	0.882	0.389
18	0.673	0.924	0.924	0.286
19	0.830	0.963	0.963	0.213
20	1.024	0.994	0.994	0.094
21	1.264	1.001	1.001	-0.003
22	1.559	1.000	1.000	-0.004
23	1.778	0.999	0.999	0.000

PT	Y/DEL	UCAL/UP	VELGRAD	MIX LN/DEL	PROD	L/LO	RIC	BETA	ED.RE
1	0.036	0.499	1.945	0.0174	58.88	1.304	0.0000	0.0	47.97
2	0.042	0.510	1.657	0.0204	49.59	1.262	0.0000	0.0	55.69
3	0.054	0.529	1.465	0.0231	44.29	1.076	0.0000	0.0	63.62
4	0.067	0.546	1.213	0.0282	37.39	1.040	0.0000	0.0	78.29
5	0.082	0.564	1.115	0.0308	34.63	0.921	0.0000	0.0	85.85
6	0.102	0.583	0.922	0.0377	29.33	0.903	0.0000	0.0	106.32
7	0.126	0.606	0.952	0.0366	30.42	0.709	0.0000	0.0	103.40
8	0.155	0.632	0.841	0.0417	27.15	0.656	0.0000	0.0	118.31
9	0.191	0.660	0.747	0.0466	23.80	0.595	0.0000	0.0	131.32
10	0.236	0.694	0.777	0.0438	23.59	0.515	0.0000	0.0	120.53
11	0.291	0.737	0.732	0.0446	20.54	0.525	0.0000	0.0	118.15
12	0.359	0.782	0.635	0.0464	14.59	0.546	0.0000	0.0	111.19
13	0.442	0.833	0.565	0.0440	9.19	0.518	0.0000	0.0	88.67
14	0.546	0.882	0.389	0.0514	4.08	0.605	0.0000	0.0	83.25
15	0.673	0.924	0.286	0.0591	2.14	0.695	0.0000	0.0	80.89
16	0.830	0.963	0.213	0.0650	1.08	0.764	0.0000	0.0	72.95
17	1.070	0.998	0.060	0.1036	0.06	1.019	0.0000	0.0	52.36
18	1.264	1.001	-0.003	-1.2649	0.00	*****	0.0000	0.0	-405.03

SECOND EXPT., STN. 15, S= 124.79 CM.

PT	Y/DEL	U/UPW	UCALC	VELGRAD
1	0.010	0.335	0.340	12.173
2	0.018	0.437	0.429	8.835
3	0.025	0.473	0.473	4.308
4	0.033	0.495	0.497	2.148
5	0.046	0.520	0.520	1.600
6	0.056	0.536	0.536	1.470
7	0.068	0.552	0.552	1.192
8	0.083	0.568	0.568	1.034
9	0.102	0.588	0.588	1.050
10	0.125	0.611	0.611	0.905
11	0.154	0.634	0.634	0.742
12	0.190	0.661	0.661	0.762
13	0.234	0.694	0.694	0.705
14	0.288	0.729	0.729	0.628
15	0.355	0.772	0.772	0.647
16	0.437	0.823	0.823	0.574
17	0.540	0.874	0.874	0.428
18	0.666	0.920	0.920	0.309
19	0.821	0.960	0.960	0.217
20	1.013	0.992	0.992	0.105
21	1.249	1.002	1.002	0.005
22	1.542	1.001	1.001	-0.006
23	1.758	1.000	1.000	0.000

PT	Y/DEL	UCAL/UP	VELGRAD	MIX LN/DEL	PROD	L/LO	RIC	BETA	ED.RE
1	0.035	0.501	1.998	0.0173	61.34	1.334	0.0000	0.0	49.30
2	0.041	0.512	1.692	0.0204	51.76	1.298	0.0000	0.0	58.04
3	0.054	0.533	1.511	0.0228	45.93	1.057	0.0000	0.0	64.56
4	0.066	0.549	1.240	0.0279	38.19	1.045	0.0000	0.0	79.71
5	0.081	0.566	1.032	0.0336	31.78	1.015	0.0000	0.0	95.76
6	0.100	0.586	1.050	0.0332	32.77	0.810	0.0000	0.0	95.11
7	0.124	0.610	0.917	0.0384	29.05	0.755	0.0000	0.0	110.99
8	0.153	0.633	0.742	0.0473	23.39	0.754	0.0000	0.0	136.42
9	0.189	0.660	0.761	0.0464	24.27	0.593	0.0000	0.0	144.55
10	0.233	0.693	0.709	0.0496	22.44	0.583	0.0000	0.0	143.38
11	0.287	0.728	0.628	0.0544	18.79	0.640	0.0000	0.0	152.99
12	0.355	0.772	0.647	0.0496	17.10	0.583	0.0000	0.0	130.98
13	0.437	0.823	0.574	0.0505	12.36	0.594	0.0000	0.0	120.54
14	0.539	0.874	0.429	0.0560	6.34	0.659	0.0000	0.0	110.76
15	0.665	0.920	0.310	0.0606	2.80	0.713	0.0000	0.0	93.73
16	0.821	0.960	0.217	0.0693	1.27	0.822	0.0000	0.0	87.00
17	1.013	0.992	0.105	0.0852	0.22	1.002	0.0000	0.0	63.00
18	1.249	1.002	0.005	0.8692	-0.00	*****	0.0000	0.0	316.30

SECOND EXPT., STN. 16, S= 149.43 CM.

PT	Y/DEL	U/UPW	UCALC	VELGRAD
1	0.009	0.333	0.338	12.654
2	0.017	0.438	0.430	9.131
3	0.024	0.476	0.475	4.235
4	0.032	0.495	0.498	2.108
5	0.044	0.522	0.522	1.792
6	0.054	0.538	0.538	1.471
7	0.066	0.554	0.554	1.186
8	0.080	0.569	0.569	1.026
9	0.099	0.588	0.588	0.937
10	0.121	0.607	0.607	0.815
11	0.150	0.630	0.630	0.790
12	0.184	0.657	0.657	0.785
13	0.227	0.689	0.689	0.691
14	0.280	0.723	0.723	0.625
15	0.345	0.764	0.764	0.622
16	0.425	0.811	0.811	0.546
17	0.525	0.861	0.861	0.468
18	0.647	0.913	0.913	0.364
19	0.798	0.956	0.956	0.228
20	0.984	0.989	0.989	0.119
21	1.214	1.002	1.002	0.013
22	1.498	1.001	1.001	-0.008
23	1.708	1.000	1.000	0.000

PT	Y/DEL	UCAL/UP	VELGRAD	MIX LN/DEL	PROD	L/LO	RIC	BETA	ED.RE
1	0.034	0.502	2.075	0.0169	65.59	1.342	0.0000	0.0	50.27
2	0.040	0.514	1.930	0.0180	60.09	1.175	0.0000	0.0	53.26
3	0.052	0.535	1.525	0.0228	47.28	1.100	0.0000	0.0	67.12
4	0.064	0.552	1.230	0.0283	38.39	1.093	0.0000	0.0	83.73
5	0.079	0.568	1.028	0.0341	32.53	1.059	0.0000	0.0	101.59
6	0.098	0.587	0.945	0.0376	30.70	0.938	0.0000	0.0	113.41
7	0.121	0.607	0.815	0.0442	27.10	0.891	0.0000	0.0	134.86
8	0.149	0.629	0.789	0.0456	26.14	0.746	0.0000	0.0	138.70
9	0.184	0.657	0.785	0.0464	26.69	0.615	0.0000	0.0	143.07
10	0.226	0.688	0.694	0.0522	23.32	0.614	0.0000	0.0	159.95
11	0.279	0.722	0.625	0.0574	20.58	0.675	0.0000	0.0	174.11
12	0.345	0.764	0.622	0.0551	18.79	0.649	0.0000	0.0	160.27
13	0.425	0.811	0.546	0.0588	14.43	0.691	0.0000	0.0	159.76
14	0.524	0.861	0.468	0.0589	9.16	0.693	0.0000	0.0	137.74
15	0.647	0.913	0.364	0.0614	4.67	0.722	0.0000	0.0	116.30
16	0.797	0.956	0.228	0.0721	1.59	0.848	0.0000	0.0	100.49
17	0.984	0.989	0.119	0.0862	0.32	1.015	0.0000	0.0	75.01
18	1.214	1.002	0.013	0.2815	-0.00	3.312	0.0000	0.0	90.40

SECOND EXPT., STN. 17, 3= 164.67 CM.

PT	Y/DEL	U/UPW	UCALC	VELGRAD
1	0.009	0.343	0.348	14.436
2	0.016	0.446	0.438	9.691
3	0.024	0.481	0.484	3.378
4	0.031	0.503	0.503	2.322
5	0.043	0.527	0.527	1.818
6	0.052	0.543	0.543	1.533
7	0.063	0.557	0.557	1.168
8	0.077	0.573	0.573	1.139
9	0.095	0.593	0.593	1.006
10	0.117	0.612	0.612	0.793
11	0.144	0.633	0.633	0.755
12	0.177	0.657	0.657	0.707
13	0.219	0.686	0.686	0.676
14	0.269	0.719	0.719	0.645
15	0.332	0.758	0.758	0.586
16	0.409	0.801	0.801	0.552
17	0.505	0.853	0.853	0.503
18	0.623	0.904	0.904	0.372
19	0.768	0.950	0.950	0.268
20	0.947	0.937	0.987	0.136
21	1.169	1.001	1.001	0.016
22	1.442	1.001	1.001	-0.007
23	1.644	1.000	1.000	0.000

PT	Y/DEL	UCAL/UP	VELGPAD	MIX LN/DEL	PROD	L/LO	RIC	BETA	ED.RE
1	0.033	0.509	2.176	0.0159	65.60	1.293	0.0000	0.0	48.28
2	0.039	0.520	1.887	0.0184	57.31	1.222	0.0000	0.0	56.11
3	0.050	0.540	1.638	0.0212	49.82	1.061	0.0000	0.0	64.70
4	0.062	0.556	1.179	0.0295	36.11	1.175	0.0000	0.0	90.61
5	0.076	0.572	1.135	0.0308	35.13	0.992	0.0000	0.0	94.97
6	0.094	0.592	1.023	0.0346	32.40	0.898	0.0000	0.0	107.83
7	0.116	0.611	0.794	0.0448	25.42	0.941	0.0000	0.0	140.37
8	0.143	0.632	0.757	0.0475	24.76	0.810	0.0000	0.0	150.68
9	0.177	0.657	0.707	0.0513	23.47	0.706	0.0000	0.0	163.82
10	0.218	0.685	0.676	0.0539	22.71	0.634	0.0000	0.0	173.07
11	0.269	0.719	0.645	0.0562	21.46	0.662	0.0000	0.0	179.90
12	0.332	0.758	0.586	0.0601	18.43	0.707	0.0000	0.0	186.90
13	0.409	0.801	0.552	0.0608	15.71	0.715	0.0000	0.0	179.77
14	0.505	0.853	0.503	0.0595	11.43	0.700	0.0000	0.0	157.33
15	0.623	0.904	0.372	0.0661	5.70	0.778	0.0000	0.0	143.55
16	0.768	0.950	0.268	0.0665	2.16	0.782	0.0000	0.0	104.59
17	0.947	0.987	0.136	0.0783	0.39	0.922	0.0000	0.0	73.61
18	1.169	1.001	0.016	0.2831	-0.01	3.331	0.0000	0.0	114.14

Wall static pressure distribution -- THIRD EXPERIMENT

TAP	s, cm	C_p
0	-132.08	0.004
1	- 93.98	.000
2	- 63.50	.008
3	- 27.31	.000
4	- 15.24	.006
5	2.54	- .010
6	7.62	- .009
7	12.70	.010
8	17.78	.017
9	22.86	.015
10	27.94	.011
11	33.02	.005
12	38.10	.003
13	43.18	.000
14	48.26	.010
15	53.34	.011
16	58.42	.004
17	63.50	- .012
18	68.58	- .016
19	82.04	.017
20	92.20	- .004
21	98.63	- .008
22	129.03	- .009
23	159.51	- .003
24	189.99	- .003

$$C_p = \frac{P - P_{TAP_1}}{\frac{1}{2} \rho U_{pw}^2} \qquad s = 0 \text{ at start of curvature}$$

THIRD EXPT., STATION 3, S = -52.71 CM., UPW = 14.67 M/SEC

PT	Y/DEL	U/UP	DY PR	YPLUS	UPLUS	CF/2
1	0.034	0.522	0.351	20.	11.7	0.00181
2	0.063	0.614	0.485	37.	13.7	0.00196
3	0.089	0.656	0.554	53.	14.7	0.00198
4	0.116	0.682	0.599	69.	15.3	0.00197
5	0.163	0.717	0.663	97.	16.1	0.00196
6	0.199	0.743	0.711	118.	16.6	0.00198
7	0.242	0.767	0.759	144.	17.2	0.00200
8	0.295	0.793	0.810	175.	17.7	0.00201
9	0.362	0.824	0.876	216.	18.4	0.00205
10	0.445	0.858	0.950	265.	19.2	0.00210
11	0.548	0.896	1.036	326.	20.1	0.00217
12	0.674	0.935	1.130	401.	20.9	0.00223
13	0.831	0.969	1.214	494.	21.7	0.00228
14	1.023	0.993	1.275	609.	22.2	0.00227
15	1.262	1.000	1.295	751.	22.4	0.00221
16	1.555	1.000	1.295	925.	22.4	0.00212
17	1.919	1.000	1.295	1142.	22.4	0.00203

DISP. THICKNESS = 0.208 CM.   MOMT. THICKESS =0.158 CM.

SHAPE FACTOR = 1.320   DELTA 99 = 1.422 CM.

MOMENTUM THICKNESS REYNOLDS NO. = 1477.   CF/2 = 0.00200

THIRD EXPT., STATICN 5, S = -34.93 CM., UPW = 14.67 M/SEC

PT	Y/DEL	U/UP	DY PR	YPLUS	UPLUS	CF/2
1	0.028	0.498	0.320	20.	11.5	0.00168
2	0.051	0.596	0.457	36.	13.8	0.00187
3	0.072	0.636	0.521	51.	14.7	0.00188
4	0.094	0.658	0.559	67.	15.2	0.00186
5	0.131	0.693	0.620	93.	16.0	0.00186
6	0.160	0.713	0.655	114.	16.5	0.00185
7	0.196	0.737	0.701	139.	17.1	0.00186
8	0.238	0.761	0.747	170.	17.6	0.00185
9	0.292	0.787	0.800	208.	18.2	0.00190
10	0.360	0.818	0.864	256.	18.9	0.00193
11	0.443	0.853	0.940	316.	19.7	0.00199
12	0.545	0.890	1.024	388.	20.6	0.00204
13	0.672	0.930	1.118	479.	21.5	0.00211
14	0.827	0.968	1.212	589.	22.4	0.00217
15	1.020	0.993	1.275	727.	23.0	0.00218
16	1.257	0.999	1.293	895.	23.1	0.00211
17	1.551	1.000	1.295	1105.	23.1	0.00203
18	1.914	0.999	1.293	1363.	23.1	0.00194

DISP. THICKNESS = 0.266 CM.   MOMT. THICKESS = 0.201 CM.

SHAPE FACTOR = 1.325   DELTA 99 = 1.758 CM.

MOMENTUM THICKNESS REYNOLDS NO. = 1883.   CF/2 = 0.00187

273

THIRD EXPT., STATION 7, S = 10.39 CM., UPW = 14.63 M/SEC

PT	Y/DEL	U/UP	DY PR	YPLUS	UPLUS	CF/2
1	0.019	0.418	0.226	18.	10.7	0.00125
2	0.035	0.520	0.351	32.	13.3	0.00148
3	0.050	0.559	0.406	46.	14.3	0.00151
4	0.065	0.586	0.447	60.	15.0	0.00151
5	0.091	0.624	0.508	84.	15.9	0.00153
6	0.111	0.648	0.549	103.	16.5	0.00155
7	0.135	0.671	0.589	125.	17.1	0.00156
8	0.164	0.696	0.6.5	152.	17.7	0.00158
9	0.202	0.720	0.681	187.	18.3	0.00159
10	0.248	0.746	0.732	230.	18.9	0.00161
11	0.306	0.775	0.790	284.	19.6	0.00163
12	0.376	0.808	0.859	349.	20.3	0.00166
13	0.464	0.848	0.942	430.	21.2	0.00171
14	0.571	0.889	1.034	530.	22.1	0.00177
15	0.705	0.932	1.130	654.	23.0	0.00181
16	0.868	0.975	1.229	805.	23.9	0.00186
17	1.071	0.998	1.283	993.	24.2	0.00182
18	1.321	1.001	1.290	1225.	23	0.00171
19	1.629	1.000	1.288	1511.	23.5	0.00160

DISP. THICKNESS = 0.421 CM.   MOMT. THICKNESS = 0.306 CM.

SHAPE FACTOR = 1.376   DELTA 99 = 2.548 CM.

MOMENTUM THICKNESS REYNOLDS NO. = 2863.   CF/2 = 0.00152

THIRD EXPT., STATION 8, S = 25.20 CM., UPW = 14.51 M/SEC

PT	Y/DEL	U/UP	DY PR	YPLUS	UPLUS	CF/2
1	0.018	0.393	0.198	17.	10.7	0.00114
2	0.034	0.487	0.305	30.	13.2	0.00133
3	0.048	0.521	0.351	43.	14.2	0.00134
4	0.063	0.547	0.386	56.	14.8	0.00135
5	0.088	0.581	0.437	79.	15.7	0.00136
6	0.108	0.603	0.472	97.	16.3	0.00137
7	0.131	0.628	0.513	118.	17.0	0.00140
8	0.159	0.655	0.559	144.	17.7	0.00143
9	0.195	0.687	0.615	176.	18.5	0.00147
10	0.240	0.720	0.676	216.	19.3	0.00151
11	0.296	0.756	0.744	266.	20.2	0.00156
12	0.364	0.793	0.818	328.	21.1	0.00161
13	0.448	0.831	0.897	404.	22.0	0.00166
14	0.552	0.871	0.983	497.	23.0	0.00171
15	0.681	0.916	1.082	614.	24.0	0.00176
16	0.838	0.964	1.189	756.	25.0	0.00182
17	1.034	0.995	1.260	932.	25.6	0.00181
18	1.276	1.000	1.270	1150.	25.3	0.00171
19	1.573	1.000	1.270	1418.	24.9	0.00160
20	1.941	1.000	1.270	1750.	24.4	0.00148

DISP. THICKNESS = 0.475 CM.   MOMT. THICKESS = 0.336 CM.

SHAPE FACTOR = 1.416   DELTA 99 = 2.638 CM.

MOMENTUM THICKNESS REYNOLDS NO. = 3122.   CF/2 = 0.00135

THIRD EXPT., STATION 9, S = 41.48 CM., UPW = 14.73 M/SEC

PT	Y/DEL	U/UP	DY PR	YPLUS	UPLUS	CF/2
1	0.018	0.395	0.206	16.	11.0	0.00114
2	0.033	0.478	0.302	30.	13.3	0.00128
3	0.047	0.509	0.343	43.	14.1	0.00128
4	0.061	0.536	0.381	56.	14.9	0.00129
5	0.085	0.566	0.427	78.	15.7	0.00129
6	0.104	0.590	0.465	96.	16.3	0.00131
7	0.127	0.610	0.498	117.	16.9	0.00132
8	0.155	0.641	0.551	143.	17.7	0.00137
9	0.189	0.671	0.605	175.	18.5	0.00140
10	0.233	0.703	0.663	215.	19.3	0.00144
11	0.287	0.741	0.737	264.	20.3	0.00150
12	0.352	0.782	0.820	325.	21.4	0.00156
13	0.434	0.822	0.904	400.	22.3	0.00162
14	0.535	0.864	0.996	493.	23.3	0.00167
15	0.660	0.907	1.092	608.	24.3	0.00172
16	0.812	0.953	1.199	749.	25.3	0.00178
17	1.002	0.990	1.285	924.	26.0	0.00179
18	1.236	1.000	1.308	1140.	25.9	0.00171
19	1.525	1.000	1.308	1406.	25.5	0.00159
20	1.881	0.999	1.306	1734.	25.0	0.00147

DISP. THICKNESS = 0.506 CM.   MOMT. THICKESS =0.355 CM.

SHAPE FACTOR = 1.426   DELTA 99 = 2.722 CM.

MOMENTUM THICKNESS REYNOLDS NO. = 3347.   CF/2 = 0.00129

C-4

THIRD EXPT., STATION 10, S = 61.72 CM., UPW = 14.66 M/SEC

PT	Y/DEL	U/UP	DY PR	YPLUS	UPLUS	CF/2
1	0.016	0.333	0.147	15.	9.9	0.00086
2	0.030	0.431	0.246	28.	12.8	0.00107
3	0.043	0.468	0.292	41.	13.9	0.00111
4	0.056	0.493	0.325	53.	14.7	0.00112
5	0.079	0.524	0.368	74.	15.6	0.00113
6	0.096	0.545	0.399	90.	16.2	0.00114
7	0.118	0.566	0.432	110.	16.8	0.00116
8	0.143	0.592	0.472	134.	17.5	0.00119
9	0.176	0.620	0.521	165.	18.3	0.00122
10	0.216	0.656	0.582	202.	19.3	0.00127
11	0.266	0.695	0.653	249.	20.4	0.00134
12	0.327	0.740	0.739	306.	21.6	0.00142
13	0.403	0.788	0.836	377.	22.9	0.00150
14	0.496	0.839	0.942	464.	24.3	0.00159
15	0.611	0.889	1.052	573.	25.5	0.00166
16	0.753	0.937	1.161	705.	26.7	0.00172
17	0.929	0.985	1.270	870.	27.7	0.00177
18	1.146	1.001	1.308	1074.	27.8	0.00171
19	1.413	1.001	1.308	1324.	27.4	0.00159
20	1.743	1.001	1.308	1633.	26.8	0.00148

DISP. THICKNESS = 0.586 CM.   MOMT. THICKESS =0.391 CM.

SHAPE FACTOR = 1.498   DELTA 99 = 2.938 CM.

MOMENTUM THICKNESS REYNOLDS NO. = 3724.   CF/2 = 0.00112

THIRD EXPT., STATION 12, S = 88.47 CM., UPW = 14.62 M/SEC

PT	Y/DEL	U/UP	DY PR	YPLUS	UPLUS	CF/2
1	0.015	0.348	0.157	15.	10.4	0.00093
2	0.028	0.438	0.249	28.	13.1	0.00111
3	0.040	0.470	0.287	40.	14.0	0.00112
4	0.052	0.488	0.310	52.	14.6	0.00111
5	0.072	0.514	0.343	73.	15.3	0.00111
6	0.088	0.529	0.363	89.	15.8	0.00110
7	0.108	0.545	0.386	109.	16.3	0.00110
8	0.132	0.564	0.414	133.	16.9	0.00111
9	0.162	0.588	0.450	164.	17.6	0.00114
10	0.199	0.616	0.493	201.	18.4	0.00117
11	0.245	0.650	0.549	248.	19.4	0.00123
12	0.301	0.692	0.622	305.	20.7	0.00131
13	0.371	0.739	0.709	376.	22.1	0.00140
14	0.457	0.795	0.820	463.	23.7	0.00153
15	0.564	0.854	0.947	571.	25.5	0.00166
16	0.694	0.913	1.082	703.	27.3	0.00179
17	0.856	0.967	1.214	867.	28.9	0.00191
18	1.056	0.999	1.295	1069.	29.8	0.00194
19	1.302	1.000	1.298	1318.	29.9	0.00187
20	1.606	0.999	1.295	1627.	29.8	0.00179

DISP. THICKNESS = 0.680 CM.   MOMT. THICKESS =0.448 CM.

SHAPE FACTOR = 1.516   DELTA 99 = 3.188 CM.

MOMENTUM THICKNESS REYNOLDS NO. = 4253.   CF/2 = 0.00112

THIRD EXPT., STATION 13, S = 103.71 CM., UPW = 14.64 M/SEC

PT	Y/DEL	U/UP	DY PR	YPLUS	UPLUS	CF/2
1	0.015	0.348	0.157	15.	10.4	0.00093
2	0.027	0.440	0.251	28.	13.2	0.00112
3	0.038	0.472	0.290	40.	14.1	0.00113
4	0.050	0.493	0.315	52.	14.7	0.00113
5	0.069	0.512	0.340	73.	15.3	0.00110
6	0.085	0.529	0.363	89.	15.8	0.00110
7	0.104	0.545	0.386	109.	16.3	0.00110
8	0.126	0.563	0.411	133.	16.8	0.00111
9	0.155	0.585	0.444	163.	17.5	0.00112
10	0.191	0.609	0.483	201.	18.2	0.00115
11	0.235	0.638	0.528	248.	19.1	0.00118
12	0.289	0.672	0.587	305.	20.1	0.00124
13	0.357	0.714	0.663	375.	21.4	0.00132
14	0.439	0.762	0.754	462.	22.8	0.00141
15	0.542	0.821	0.876	570.	24.6	0.00155
16	0.667	0.887	1.024	702.	26.6	0.00170
17	0.823	0.950	1.173	866.	28.4	0.00184
18	1.015	0.993	1.283	1068.	29.7	0.00192
19	1.251	1.000	1.300	1317.	29.9	0.00187
20	1.543	1.000	1.300	1625.	29.9	0.00179
21	1.900	0.999	1.298	2001.	29.9	0.00172

DISP. THICKNESS = 0.741 CM.   MOMT. THICKESS =0.490 CM.

SHAPE FACTOR = 1.513   DELTA 99 = 3.318 CM.

MOMENTUM THICKNESS REYNOLDS NO. = 4652.   CF/2 = 0.00112

THIRD EXPT., STATION 14, S = 118.95 CM., UPW = 14.61 M/SEC

PT	Y/DEL	U/UP	DY PR	YPLUS	UPLUS	CF/2
1	0.013	0.361	0.168	15.	10.8	0.00098
2	0.025	0.438	0.246	28.	13.1	0.00110
3	0.035	0.475	0.290	40.	14.2	0.00113
4	0.046	0.495	0.315	52.	14.8	0.00113
5	0.064	0.516	0.343	73.	15.4	0.00111
6	0.078	0.530	0.361	89.	15.8	0.00110
7	0.096	0.548	0.386	109.	16.4	0.00110
8	0.117	0.565	0.411	133.	16.9	0.00111
9	0.143	0.587	0.444	163.	17.6	0.00113
10	0.176	0.610	0.480	201.	18.2	0.00115
11	0.217	0.634	0.518	247.	18.9	0.00117
12	0.267	0.666	9.572	304.	19.9	0.00122
13	0.330	0.701	0.635	375.	21.0	0.00127
14	0.406	0.743	0.714	462.	22.2	0.00135
15	0.501	0.781	0.787	570.	23.3	0.00141
16	0.617	0.860	0.955	702.	25.7	0.00161
17	0.761	0.928	1.113	866.	27.7	0.00176
18	0.938	0.986	1.257	1068.	29.5	0.00189
19	1.157	1.000	1.295	1317.	29.9	0.00187
20	1.427	1.000	1.295	1625.	29.9	0.00179
21	1.746	1.000	1.295	1987.	29.9	0.00173

DISP. THICKNESS = 0.795 CM.   MOMT. THICKESS = 0.529 CM.

SHAPE FACTOR = 1.503   DELTA 99 = 3.588 CM.

MOMENTUM THICKNESS REYNOLDS NO. = 5013.   CF/2 = 0.00112

THIRD EXPT., STATION 15, S = 134.19 CM., UPW = 14.59 M/SEC

PT	Y/DEL	U/UP	DY PR	YPLUS	UPLUS	CF/2
1	0.012	0.344	0.152	15.	10.4	0.00091
2	0.023	0.429	0.236	28.	12.9	0.00107
3	0.032	0.464	0.277	40.	14.0	0.00110
4	0.042	0.487	0.305	52.	14.7	0.00110
5	0.059	0.514	0.340	72.	15.5	0.00110
6	0.071	0.529	0.361	88.	16.0	0.00110
7	0.087	0.540	0.376	107.	16.3	0.00108
8	0.106	0.558	0.401	131.	16.8	0.00109
9	0.131	0.577	0.429	161.	17.4	0.00110
10	0.161	0.602	0.467	198.	18.1	0.00113
11	0.198	0.625	0.503	244.	18.8	0.00114
12	0.244	0.651	0.546	301.	19.6	0.00117
13	0.300	0.685	0.605	371.	20.6	0.00122
14	0.370	0.724	0.676	456.	21.8	0.00129
15	0.456	0.773	0.770	563.	23.3	0.00139
16	0.562	0.830	0.889	693.	25.0	0.00151
17	0.693	0.898	1.039	855.	27.0	0.00167
18	0.855	0.965	1.201	1055.	29.1	0.00182
19	1.054	0.999	1.288	1301.	30.1	0.00186
20	1.300	1.000	1.290	1604.	30.1	0.00179
21	1.594	0.999	1.288	1967.	30.1	0.00173

DISP. THICKNESS = 0.865 CM.   MOMT. THICKESS =0.576 CM.

SHAPE FACTOR = 1.502   DELTA 99 = 3.939 CM.

MOMENTUM THICKNESS REYNOLDS NO. = 5436.   CF/2 = 0.00110

THIRD EXPT., STATION 16, S = 149.43 CM., UPW = 14.54 M/SEC

PT	Y/DEL	U/UP	DY PR	YPLUS	UPLUS	CF/2
1	0.012	0.338	0.147	15.	10.3	0.00089
2	0.022	0.407	0.213	27.	12.5	0.00099
3	0.031	0.449	0.259	39.	13.7	0.00105
4	0.040	0.474	0.290	51.	14.5	0.00106
5	0.056	0.501	0.323	71.	15.3	0.00106
6	0.069	0.518	0.345	87.	15.9	0.00107
7	0.084	0.533	0.366	105.	16.3	0.00107
8	0.102	0.550	0.389	128.	16.8	0.00107
9	0.125	0.566	0.411	158.	17.3	0.00107
10	0.154	0.587	0.442	195.	17.9	0.00108
11	0.190	0.613	0.483	240.	18.8	0.00111
12	0.234	0.637	0.521	295.	19.5	0.00113
13	0.289	0.669	0.574	363.	20.5	0.00118
14	0.355	0.708	0.643	448.	21.7	0.00124
15	0.438	0.753	0.726	552.	23.0	0.00133
16	0.540	0.805	0.831	680.	24.6	0.00143
17	0.666	0.868	0.965	839.	26.5	0.00157
18	0.822	0.938	1.128	1035.	28.7	0.00174
19	1.013	0.994	1.265	1276.	30.4	0.00185
20	1.250	1.000	1.280	1574.	30.6	0.00180
21	1.541	1.000	1.280	1942.	30.6	0.00173

DISP. THICKNESS = 0.948 CM.   MOMT. THICKESS =0.628 CM.

SHAPE FACTOR = 1.510   DELTA 99 = 4.098 CM.

MOMENTUM THICKNESS REYNOLDS NO. = 5901.   CF/2 = 0.00107

THIRD EXPT., STATION 17, S = 164.67 CM., UPW = 14.54 M/SEC

PT	Y/DEL	U/UP	DY PR	YPLUS	UPLUS	CF/2
1	0.010	0.327	0.137	15.	10.0	0.00084
2	0.019	0.420	0.226	27.	12.8	0.00104
3	0.027	0.459	0.269	39.	14.0	0.00108
4	0.036	0.478	0.292	51.	14.6	0.00107
5	0.050	0.508	0.330	71.	15.5	0.00109
6	0.060	0.522	0.348	86.	15.9	0.00108
7	0.074	0.535	0.366	106.	16.3	0.00107
8	0.090	0.551	0.389	129.	16.8	0.00107
9	0.111	0.569	0.414	158.	17.3	0.00108
10	0.136	0.586	0.439	195.	17.9	0.00108
11	0.168	0.608	0.472	240.	18.5	0.00109
12	0.207	0.633	0.513	296.	19.3	0.00112
13	0.255	0.663	0.561	364.	20.2	0.00116
14	0.314	0.698	0.622	449.	21.3	0.00121
15	0.387	0.738	0.696	554.	22.5	0.00128
16	0.477	0.789	0.795	682.	24.0	0.00138
17	0.588	0.846	0.914	841.	25.8	0.00150
18	0.726	0.913	1.064	1038.	27.8	0.00165
19	0.894	0.979	1.224	1279.	29.8	0.00180
20	1.103	1.001	1.280	1578.	30.5	0.00180
21	1.357	1.001	1.280	1941.	30.5	0.00173

DISP. THICKNESS = 1.008 CM.   MOMT. THICKESS =0.673 CM.

SHAPE FACTOR = 1.498   LELTA 99 = 4.641 CM.

MOMENTUM THICKNESS REYNOLDS NO = 6317.   CF/2 = 0.00108

THIRD EXPT., RENOLDS' STRESSES AT STN. 5, S = -34.92 CM.

OUTPUT NONDIMENSIONALIZED ON FRICTION VELOCITY

PT	Y/DEL	UV/UTSQ	USQ/UTSQ	VSQ/UTSQ	WSQ/UTSQ	QSQ/UTSQ	A	SHEAR CORR	ANISOTROPY
1	0.114	1.0313	3.014	1.569	2.125	6.708	0.154	0.474	0.047
2	0.155	1.0125	2.822	1.494	1.977	6.293	0.161	0.493	0.052
3	0.191	0.9806	2.727	1.449	1.888	6.063	0.162	0.493	0.052
4	0.234	0.9487	2.672	1.420	1.826	5.918	0.160	0.487	0.051
5	0.289	0.9129	2.493	1.366	1.756	5.615	0.163	0.495	0.053
6	0.357	0.8542	2.330	1.263	1.630	5.223	0.164	0.498	0.053
7	0.441	0.7591	2.049	1.156	1.472	4.677	0.162	0.493	0.053
8	0.543	0.6293	1.751	0.977	1.236	3.964	0.159	0.481	0.050
9	0.671	0.4510	1.373	0.741	0.885	2.999	0.150	0.447	0.045
10	0.827	0.2397	0.773	0.450	0.484	1.708	0.140	0.406	0.039
11	1.020	0.0621	0.237	0.194	0.165	0.596	0.104	0.290	0.022
12	1.257	-0.0046	0.033	0.048	0.026	0.107	-0.043	-0.115	0.004
13	1.552	-0.0103	0.007	0.010	0.003	0.020	-0.502	-1.211	0.505

DISPLACEMENT THICKNESS = 0.267 CM.   MOMENTUM THICKNESS = 0.201 CM.   DELTA 99 = 1.758 CM.

MOMENTUM THICKNESS REYNOLDS NO. = 1883.   UTAU = 0.634 M/SEC   UPW = 14.67 M/SEC

OUTPUT NONDIMENSIONALIZED ON WALL VELOCITY

PT	Y/DEL	UV/UPWS	USQ/UPWS	VSQ/UPWS	WSQ/UPWS	QSQ/UPWS
1	0.114	0.00193	0.00563	0.00293	0.00397	0.01254
2	0.155	0.00189	0.00528	0.00279	0.00370	0.01176
3	0.191	0.00183	0.00510	0.00271	0.00353	0.01134
4	0.234	0.00177	0.00500	0.00265	0.00341	0.01106
5	0.289	0.00171	0.00466	0.00255	0.00328	0.01050
6	0.357	0.00160	0.00436	0.00236	0.00305	0.00976
7	0.441	0.00142	0.00383	0.00216	0.00275	0.00874
8	0.543	0.00118	0.00327	0.00183	0.00231	0.00741
9	0.671	0.00084	0.00257	0.00139	0.00165	0.00561
10	0.827	0.00045	0.00145	0.00084	0.00091	0.00319
11	1.020	0.00012	0.00044	0.00036	0.00031	0.00111
12	1.257	-0.00001	0.00006	0.00009	0.00005	0.00020
13	1.552	-0.00002	0.00001	0.00002	0.00001	0.00004

THIRD EXPT., RENOLDS' STRESSES AT STN. 7, S = 10.39 CM. (13.25 DEG)

OUTPUT NONDIMENSIONALIZED ON FRICTION VELOCITY

PT	Y/DEL	UV/UTSQ	USQ/UTSQ	VSQ/UTSQ	WSQ/UTSQ	QSQ/UTSQ	A	SHEAR CORR	ANISOTROPY
1	0.079	1.0143	3.336	1.751	2.333	7.421	0.137	0.420	0.037
2	0.107	0.8710	3.085	1.514	2.142	6.741	0.129	0.403	0.033
3	0.132	0.8190	3.026	1.476	2.106	6.607	0.124	0.388	0.031
4	0.162	0.7350	2.876	1.401	2.043	6.320	0.116	0.366	0.031
5	0.199	0.6658	2.742	1.360	1.970	6.072	0.110	0.345	0.027
6	0.246	0.6213	2.716	1.328	1.935	5.980	0.104	0.327	0.024
7	0.304	0.5718	2.549	1.304	1.865	5.718	0.100	0.314	0.022
8	0.375	0.5199	2.423	1.239	1.751	5.414	0.096	0.300	0.020
9	0.463	0.4458	2.179	1.125	1.622	5.414	0.090	0.285	0.018
10	0.570	0.3411	1.837	0.948	1.340	4.926	0.083	0.259	0.016
11	0.704	0.2200	1.410	0.734	0.989	4.125	0.070	0.216	0.014
12	0.867	0.0915	0.745	0.450	0.487	3.133	0.054	0.158	0.010
13	1.071	0.0115	0.164	0.175	0.137	1.683	0.024	0.068	0.006
14	1.321	-0.0041	0.033	0.049	0.034	0.476	-0.035	-0.102	0.001
15	1.629	-0.0049	0.026	0.029	0.028	0.116	-0.060	-0.179	0.003
						0.083			0.007

DISPLACEMENT THICKNESS = 0.422 CM.   MOMENTUM THICKNESS = 0.307 CM.   DELTA 99 = 2.548 CM.

MOMENTUM THICKNESS REYNOLDS NO. = 2863.   UTAU = 0.527 M/SEC   UPW = 14.73 M/SEC

OUTPUT NONDIMENSIONALIZED ON WALL VELOCITY

PT	Y/DEL	UV/UPWS	USQ/UPWS	VSQ/UPWS	WSQ/UPWS	QSQ/UPWS
1	0.079	0.00130	0.00428	0.00225	0.00299	0.00951
2	0.107	0.00112	0.00395	0.00194	0.00275	0.00864
3	0.132	0.00105	0.00388	0.00189	0.00270	0.00847
4	0.162	0.00094	0.00369	0.00180	0.00262	0.00810
5	0.199	0.00085	0.00351	0.00174	0.00253	0.00778
6	0.246	0.00080	0.00348	0.00170	0.00248	0.00767
7	0.304	0.00073	0.00327	0.00167	0.00239	0.00733
8	0.375	0.00067	0.00311	0.00159	0.00225	0.00694
9	0.463	0.00057	0.00279	0.00144	0.00208	0.00631
10	0.570	0.00044	0.00235	0.00122	0.00172	0.00529
11	0.704	0.00028	0.00181	0.00094	0.00127	0.00402
12	0.867	0.00012	0.00096	0.00058	0.00062	0.00216
13	1.071	0.00001	0.00021	0.00022	0.00018	0.00061
14	1.321	-0.00001	0.00004	0.00006	0.00004	0.00015
15	1.629	-0.00001	0.00003	0.00004	0.00004	0.00011

THIRD EXPT., RENOLDS' STRESSES AT STN. 9, S = 41.48 CM. (52.82)

OUTPUT NONDIMENSIONALIZED ON FRICTION VELOCITY

PT	Y/DEL	UV/UTSQ	USQ/UTSQ	VSQ/UTSQ	WSQ/UTSQ	QSQ/UTSQ	A	SHEAR CORR	ANISOTROPY
1	0.074	0.9233	2.619	1.683	2.123	6.424	0.144	0.440	0.041
2	0.100	0.8274	2.351	1.416	1.843	5.611	0.147	0.453	0.043
3	0.123	0.7914	2.254	1.326	1.756	5.335	0.148	0.458	0.044
4	0.151	0.7349	2.120	1.231	1.694	5.046	0.146	0.455	0.042
5	0.187	0.6554	1.966	1.137	1.580	4.683	0.140	0.438	0.039
6	0.231	0.5710	1.806	1.012	1.482	4.300	0.133	0.422	0.035
7	0.285	0.4678	1.565	0.875	1.313	3.753	0.125	0.400	0.031
8	0.351	0.3539	0.555	0.729	0.230	1.514	0.234	0.556	0.109
9	0.433	0.2581	1.059	0.595	0.938	2.592	0.100	0.325	0.020
10	0.534	0.1843	0.839	0.490	0.780	2.109	0.087	0.287	0.015
11	0.659	0.1237	0.661	0.410	0.621	1.692	0.073	0.238	0.011
12	0.812	0.0573	0.473	0.337	0.404	1.214	0.047	0.144	0.004
13	1.003	-0.0107	0.142	0.195	0.139	0.477	-0.022	-0.064	0.001
14	1.237	-0.0270	0.026	0.050	0.028	0.104	-0.260	-0.756	0.136
15	1.526	-0.0246	0.011	0.017	0.014	0.042	-0.580	-1.777	0.672

DISPLACEMENT THICKNESS = 0.505 CM.   MOMENTUM THICKNESS = 0.356 CM.   DELTA 99 = 2.720 CM.

MOMENTUM THICKNESS REYNOLDS NO. = 3347.   UTAU = 0.529 M/SEC   UPW = 14.73 M/SEC

OUTPUT NONDIMENSIONALIZED ON WALL VELOCITY

PT	Y/DEL	UV/UPWS	USQ/UPWS	VSQ/UPWS	WSQ/UPWS	QSQ/UPWS
1	0.074	0.00119	0.00338	0.00217	0.00274	0.00828
2	0.100	0.00107	0.00303	0.00183	0.00238	0.00723
3	0.123	0.00102	0.00291	0.00171	0.00226	0.00688
4	0.151	0.00095	0.00273	0.00159	0.00218	0.00651
5	0.187	0.00084	0.00253	0.00147	0.00204	0.00604
6	0.231	0.00074	0.00233	0.00130	0.00191	0.00554
7	0.285	0.00060	0.00202	0.00113	0.00169	0.00484
8	0.351	0.00046	0.00072	0.00094	0.00030	0.00195
9	0.433	0.00033	0.00137	0.00077	0.00121	0.00334
10	0.534	0.00024	0.00108	0.00063	0.00101	0.00272
11	0.659	0.00016	0.00085	0.00053	0.00080	0.00218
12	0.812	0.00007	0.00061	0.00043	0.00052	0.00156
13	1.003	-0.00001	0.00018	0.00025	0.00018	0.00061
14	1.237	-0.00003	0.00003	0.00006	0.00004	0.00013
15	1.526	-0.00003	0.00001	0.00002	0.00002	0.00005

THIRD EXPT., RENOLDS' STRESSES AT STN. 12, S = 88.47 CM.

OUTPUT NONDIMENSIONALIZED ON FRICTION VELOCITY

PT	Y/DEL	UV/UTSQ	USQ/UTSQ	VSQ/UTSQ	WSQ/UTSQ	QSQ/UTSQ	A	SHEAR CORR	ANISOTROPY
1	0.063	1.0866	3.172	1.750	2.424	7.346	0.148	0.461	0.044
2	0.085	1.0894	3.022	1.712	2.342	7.076	0.154	0.479	0.047
3	0.105	1.1229	2.984	1.762	2.345	7.091	0.158	0.490	0.050
4	0.129	1.1526	2.982	1.813	2.349	7.143	0.161	0.496	0.052
5	0.159	1.2015	3.015	1.838	2.381	7.234	0.166	0.510	0.055
6	0.197	1.2149	3.028	1.864	2.398	7.290	0.167	0.511	0.056
7	0.243	1.1919	2.962	1.799	2.384	7.146	0.167	0.516	0.056
8	0.300	1.1344	2.793	1.680	2.245	6.719	0.169	0.524	0.057
9	0.370	0.9746	2.388	1.422	1.962	5.772	0.169	0.529	0.057
10	0.456	0.7324	1.838	1.078	1.509	4.425	0.166	0.520	0.055
11	0.563	0.4729	1.197	0.694	1.010	2.900	0.163	0.519	0.053
12	0.693	0.2326	0.646	0.399	0.580	1.625	0.143	0.458	0.041
13	0.856	0.0766	0.308	0.226	0.251	0.785	0.098	0.290	0.019
14	1.056	-0.0019	0.043	0.082	0.047	0.172	-0.011	-0.032	0.000
15	1.302	-0.0316	0.019	0.025	0.019	0.062	-0.509	-1.470	0.517
16	1.554	-0.0335	0.015	0.019	0.019	0.052	-0.640	-2.001	0.819

DISPLACEMENT THICKNESS = 0.681 CM.   MOMENTUM THICKNESS = 0.447 CM.   DELTA 99 = 3.188 CM.

MOMENTUM THICKNESS REYNOLDS NO. = 4253.   UTAU = 0.489 M/SEC   UPW = 14.62 M/SEC

OUTPUT NONDIMENSIONALIZED ON WALL VELOCITY

PT	Y/DEL	UV/UPWS	USQ/UPWS	VSQ/UPWS	WSQ/UPWS	QSQ/UPWS
1	0.063	0.00122	0.00355	0.00196	0.00271	0.00822
2	0.085	0.00122	0.00338	0.00192	0.00262	0.00792
3	0.105	0.00126	0.00334	0.00197	0.00263	0.00794
4	0.129	0.00129	0.00334	0.00203	0.00263	0.00800
5	0.159	0.00134	0.00338	0.00206	0.00267	0.00810
6	0.197	0.00136	0.00339	0.00209	0.00268	0.00816
7	0.243	0.00133	0.00332	0.00201	0.00267	0.00800
8	0.300	0.00127	0.00313	0.00188	0.00251	0.00752
9	0.370	0.00109	0.00267	0.00159	0.00220	0.00646
10	0.456	0.00082	0.00206	0.00121	0.00169	0.00495
11	0.563	0.00053	0.00134	0.00078	0.00113	0.00325
12	0.693	0.00026	0.00072	0.00045	0.00065	0.00182
13	0.856	0.00009	0.00035	0.00025	0.00028	0.00088
14	1.056	-0.00000	0.00005	0.00009	0.00005	0.00019
15	1.302	-0.00004	0.00002	0.00003	0.00002	0.00007
16	1.554	-0.00004	0.00002	0.00002	0.00002	0.00006

THIRD EXPT., RENOLDS' STRESSES AT STN. 14, S = 118.95 CM.

OUTPUT NONDIMENSIONALIZED ON FRICTION VELOCITY

PT	Y/DEL	UV/UTSQ	USQ/UTSQ	VSQ/UTSQ	WSQ/UTSQ	QSQ/UTSQ	A	SHEAR CORR	ANISOTROPY
1	0.053	1.0342	3.636	1.730	2.520	7.887	0.131	0.412	0.034
2	0.071	1.0630	3.527	1.735	2.468	7.730	0.138	0.430	0.038
3	0.088	1.0716	3.407	1.748	2.456	7.611	0.141	0.439	0.040
4	0.108	1.0889	3.375	1.789	2.464	7.629	0.143	0.443	0.041
5	0.133	1.1157	3.383	1.840	2.433	7.656	0.146	0.447	0.042
6	0.164	1.1291	3.327	1.855	2.490	7.671	0.147	0.455	0.043
7	0.203	1.1368	3.345	1.885	2.512	7.741	0.147	0.453	0.043
8	0.250	1.1502	3.360	1.900	2.544	7.804	0.147	0.455	0.043
9	0.309	1.1368	3.221	1.894	2.544	7.659	0.148	0.460	0.044
10	0.381	1.1119	3.100	1.799	2.462	7.361	0.151	0.471	0.046
11	0.470	1.0026	2.753	1.601	2.178	6.532	0.153	0.477	0.047
12	0.579	0.7668	2.162	1.212	1.637	5.011	0.153	0.474	0.047
13	0.715	0.4055	1.183	0.644	0.838	2.665	0.152	0.465	0.046
14	0.882	0.0776	0.235	0.201	0.179	0.615	0.126	0.357	0.032
15	1.087	0.0077	0.028	0.044	0.029	0.101	0.076	0.218	0.012

DISPLACEMENT THICKNESS = 0.795 CM.   MOMENTUM THICKNESS = 0.528 CM.   DELTA 99 = 3.818 CM.

MOMENTUM THICKNESS REYNOLDS NO. = 5013.   UTAU = 0.489 M/SEC   UPW = 14.61 M/SEC

OUTPUT NONDIMENSIONALIZED ON WALL VELOCITY

PT	Y/DEL	UV/UPWS	USQ/UPWS	VSQ/UPWS	WSQ/UPWS	QSQ/UPWS
1	0.053	0.00116	0.00407	0.00194	0.00282	0.00884
2	0.071	0.00119	0.00395	0.00194	0.00277	0.00866
3	0.088	0.00120	0.00382	0.00196	0.00275	0.00853
4	0.108	0.00122	0.00378	0.00200	0.00276	0.00855
5	0.133	0.00125	0.00379	0.00206	0.00273	0.00858
6	0.164	0.00127	0.00373	0.00208	0.00279	0.00860
7	0.203	0.00127	0.00375	0.00211	0.00281	0.00867
8	0.250	0.00129	0.00376	0.00213	0.00285	0.00874
9	0.309	0.00127	0.00361	0.00212	0.00285	0.00858
10	0.381	0.00125	0.00347	0.00202	0.00276	0.00825
11	0.470	0.00112	0.00309	0.00179	0.00244	0.00732
12	0.579	0.00086	0.00242	0.00136	0.00183	0.00561
13	0.715	0.00045	0.00133	0.00072	0.00094	0.00299
14	0.882	0.00009	0.00026	0.00023	0.00020	0.00069
15	1.087	0.00001	0.00003	0.00005	0.00003	0.00011

THIRD EXPT., RENOLDS' STRESSES AT STN. 17, S = 164.67 CM.

OUTPUT NONDIMENSIONALIZED ON FRICTION VELOCITY

PT	Y/DEL	UV/UTSQ	USQ/UTSQ	VSQ/UTSQ	WSQ/UTSQ	QSQ/UTSQ	A	SHEAR CORR	ANISOTROPY
1	0.047	1.1092	4.332	1.878	2.959	9.169	0.121	0.389	0.029
2	0.071	1.1062	4.057	1.743	2.722	8.523	0.130	0.416	0.034
3	0.088	1.1072	3.922	1.752	2.661	8.335	0.133	0.422	0.035
4	0.108	1.1213	3.913	1.783	2.611	8.307	0.135	0.424	0.036
5	0.134	1.1544	3.889	1.842	2.583	8.315	0.139	0.431	0.039
6	0.165	1.1685	3.804	1.913	2.617	8.334	0.140	0.433	0.039
7	0.204	1.1967	3.787	1.970	2.668	8.425	0.142	0.438	0.040
8	0.251	1.2178	3.773	2.009	2.678	8.460	0.144	0.442	0.041
9	0.310	1.2329	3.696	2.044	2.757	8.497	0.145	0.449	0.042
10	0.382	1.2309	3.726	2.085	2.774	8.585	0.143	0.442	0.041
11	0.471	1.2258	3.576	2.051	2.732	8.359	0.147	0.453	0.043
12	0.581	1.1735	3.325	1.925	2.582	7.832	0.150	0.464	0.045
13	0.717	1.0187	2.902	1.672	2.244	6.818	0.149	0.462	0.045
14	0.885	0.6758	1.988	1.137	1.423	4.548	0.149	0.449	0.044
15	1.091	0.1870	0.551	0.441	0.378	1.371	0.136	0.379	0.037
16	1.346	0.0080	0.039	0.062	0.040	0.141	0.057	0.164	0.006

DISPLACEMENT THICKNESS = 1.008 CM.   MOMENTUM THICKNESS = 0.673 CM.   DELTA 99 = 3.805 CM.

MOMENTUM THICKNESS REYNOLDS NO. = 6317.   UTAU = 0.477 M/SEC   UPW = 14.54 M/SEC

OUTPUT NONDIMENSIONALIZED ON WALL VELOCITY

PT	Y/DEL	UV/UPWS	USQ/UPWS	VSQ/UPWS	WSQ/UPWS	QSQ/UPWS
1	0.047	0.00120	0.00467	0.00203	0.00319	0.00989
2	0.071	0.00119	0.00437	0.00188	0.00294	0.00919
3	0.088	0.00119	0.00423	0.00189	0.00287	0.00899
4	0.108	0.00121	0.00422	0.00192	0.00282	0.00896
5	0.134	0.00124	0.00419	0.00199	0.00279	0.00897
6	0.165	0.00126	0.00410	0.00206	0.00282	0.00899
7	0.204	0.00129	0.00408	0.00212	0.00288	0.00908
8	0.251	0.00131	0.00407	0.00217	0.00289	0.00912
9	0.310	0.00133	0.00399	0.00220	0.00297	0.00916
10	0.382	0.00133	0.00402	0.00225	0.00299	0.00926
11	0.471	0.00132	0.00386	0.00221	0.00295	0.00901
12	0.581	0.00127	0.00359	0.00208	0.00278	0.00844
13	0.717	0.00110	0.00313	0.00180	0.00242	0.00735
14	0.885	0.00073	0.00214	0.00123	0.00153	0.00490
15	1.091	0.00020	0.00059	0.00048	0.00041	0.00148
16	1.346	0.00001	0.00004	0.00007	0.00004	0.00015

THIRD EXPT., STN. 5, S = -34.92 CM.

PT	Y/DEL	U/UPW	UCALC	VELGRAD
1	0.028	0.498	0.503	4.019
2	0.051	0.596	0.588	3.026
3	0.072	0.636	0.635	1.574
4	0.094	0.658	0.661	0.948
5	0.131	0.693	0.693	0.761
6	0.160	0.713	0.713	0.678
7	0.196	0.737	0.737	0.623
8	0.238	0.761	0.761	0.524
9	0.292	0.787	0.787	0.462
10	0.360	0.818	0.818	0.444
11	0.443	0.853	0.853	0.394
12	0.545	0.890	0.890	0.339
13	0.672	0.930	0.930	0.288
14	0.827	0.968	0.968	0.195
15	1.020	0.993	0.993	0.070
16	1.257	0.999	0.999	0.004
17	1.551	1.000	1.000	0.001
18	1.914	0.999	0.999	0.000

PT	Y/DEL	UCAL/UP	VELGRAD	MIX LN/DEL	PROD	L/LO	RIC	BETA	ED.RE
1	0.114	0.679	0.849	0.0517	20.24	1.149	0.0000	0.0	79.54
2	0.155	0.710	0.683	0.0637	15.99	1.014	0.0000	0.0	97.06
3	0.191	0.734	0.634	0.0675	14.39	0.665	0.0000	0.0	101.17
4	0.234	0.759	0.533	0.0790	11.69	0.930	0.0000	0.0	116.49
5	0.289	0.786	0.462	0.0893	9.76	1.051	0.0000	0.0	129.19
6	0.357	0.817	0.445	0.0897	8.80	1.056	0.0000	0.0	125.52
7	0.441	0.852	0.396	0.0951	6.95	1.119	0.0000	0.0	125.44
8	0.543	0.889	0.339	0.1011	4.94	1.189	0.0000	0.0	121.33
9	0.671	0.930	0.289	0.1006	3.01	1.183	0.0000	0.0	102.24
10	0.827	0.968	0.195	0.1085	1.0.	1.277	0.0000	0.0	80.41
11	1.020	0.993	0.070	0.1549	0.10	1.823	0.0000	0.0	58.44
12	1.257	0.999	0.004	0.7600	-0.00	8.941	0.0000	0.0	78.01
13	1.552	1.000	0.001	4.9301	-0.00	*****	0.0000	0.0	757.29

THIRD EXPT., STN. 7, S = 18.39 CM.

PT	Y/DEL	U/UPW	UCALC	VELGRAD
1	0.019	0.418	0.423	6.039
2	0.035	0.519	0.511	4.422
3	0.050	0.557	0.559	2.265
4	0.065	0.584	0.586	1.516
5	0.091	0.621	0.621	1.228
6	0.111	0.644	0.644	1.035
7	0.135	0.666	0.666	0.869
8	0.164	0.690	0.689	0.706
9	0.202	0.712	0.712	0.533
10	0.248	0.736	0.736	0.487
11	0.306	0.762	0.762	0.428
12	0.376	0.791	0.791	0.414
13	0.464	0.826	0.826	0.370
14	0.571	0.861	0.861	0.290
15	0.705	0.896	0.896	0.241
16	0.868	0.929	0.929	0.141
17	1.071	0.941	0.941	-0.005
18	1.321	0.931	0.931	-0.053
19	1.629	0.916	0.916	0.000

PT	Y/DEL	UCAL/UP	VELGRAD	MIX LN/DEL	PROD	L/LO	RIC	BETA	ED.RE
1	0.079	0.606	1.340	0.0269	36.98	0.887	0.0499	2.3	41.10
2	0.107	0.639	1.080	0.0309	25.39	0.722	0.0649	4.3	43.79
3	0.132	0.664	0.878	0.0369	19.22	0.689	0.0821	3.8	50.65
4	0.162	0.688	0.723	0.0424	14.04	0.641	0.1022	3.5	55.18
5	0.199	0.710	0.535	0.0546	9.21	0.669	0.1398	2.4	67.51
6	0.246	0.735	0.490	0.0576	7.78	0.678	0.1565	2.1	68.83
7	0.304	0.761	0.429	0.0631	6.16	0.743	0.1826	1.4	72.38
8	0.375	0.791	0.414	0.0623	5.37	0.733	0.1950	1.4	68.09
9	0.463	0.826	0.371	0.0644	4.04	0.758	0.2239	1.1	65.21
10	0.570	0.861	0.290	0.0721	2.30	0.848	0.2877	0.5	63.81
11	0.704	0.896	0.242	0.0695	1.17	0.817	0.3471	0.5	49.41
12	0.867	0.929	0.142	0.0760	0.23	0.894	0.5398	0.2	34.87
13	1.071	0.941	-0.005	-0.7034	-0.02	*****	2.2358	4.1	-114.36
14	1.321	0.931	-0.053	-0.0429	0.01	*****	******	0.0	-4.16
15	1.629	0.916	-0.050	-0.0500	0.01	*****	******	0.0	-5.31

291

THIRD EXPT., STN. 9, S = 41.48 CM.

PT	Y/DEL	U/UPW	UCALC	VELGRAD
1	0.018	0.395	0.400	5.019
2	0.033	0.477	0.469	3.309
3	0.047	0.508	0.509	2.196
4	0.061	0.534	0.535	1.485
5	0.085	0.563	0.564	1.135
6	0.104	0.586	0.585	1.002
7	0.127	0.605	0.606	0.943
8	0.155	0.635	0.635	0.980
9	0.189	0.663	0.663	0.742
10	0.233	0.693	0.693	0.652
11	0.287	0.728	0.728	0.630
12	0.352	0.766	0.766	0.505
13	0.434	0.801	0.801	0.384
14	0.535	0.837	0.837	0.320
15	0.660	0.872	0.872	0.260
16	0.812	0.908	0.908	0.202
17	1.002	0.933	0.933	0.056
18	1.236	0.930	0.930	-0.049
19	1.525	0.916	0.916	-0.053
20	1.881	0.897	0.897	0.000

PT	Y/DEL	UCAL/UP	VELGRAD	MIX LN/DEL	PROD	L/LO	RIC	BETA	ED.RE
1	0.074	0.552	1.189	0.0290	29.73	1.019	0.0546	-0.4	45.38
2	0.100	0.581	1.062	0.0308	23.66	0.768	0.0642	3.6	45.55
3	0.123	0.603	0.906	0.0353	19.16	0.706	0.0775	3.8	51.04
4	0.151	0.631	1.011	0.0304	19.91	0.494	0.0728	7.0	42.50
5	0.187	0.662	0.752	0.0387	12.99	0.505	0.1014	4.9	50.96
6	0.231	0.692	0.652	0.0416	9.70	0.490	0.1211	4.2	51.23
7	0.285	0.727	0.632	0.0388	7.67	0.457	0.1305	4.2	43.25
8	0.351	0.765	0.508	0.0420	4.55	0.495	0.1678	3.0	40.73
9	0.433	0.801	0.385	0.0474	2.42	0.558	0.2250	2.0	39.20
10	0.534	0.837	0.321	0.0481	1.39	0.566	0.2749	1.6	33.60
11	0.659	0.872	0.260	0.0485	0.72	0.571	0.3405	1.3	27.78
12	0.812	0.908	0.202	0.0706	0.64	0.831	0.4342	0.4	45.60
13	1.003	0.934	0.055	0.0675	0.00	0.794	1.0480	0.2	11.37
14	1.237	0.930	-0.049	-0.1209	0.08	*****	******	0.1	-32.35
15	1.526	0.916	-0.053	-0.1070	0.07	*****	******	0.0	-27.33

THIRD EXPT., STN. 12, S = 88.47 CM.

PT	Y/DEL	U/UPW	UCALC	VELGRAD
1	0.015	0.348	0.353	6.478
2	0.028	0.438	0.430	4.721
3	0.040	0.470	0.470	2.272
4	0.052	0.498	0.490	1.338
5	0.072	0.514	0.514	1.028
6	0.088	0.529	0.529	0.859
7	0.108	0.545	0.545	0.782
8	0.132	0.564	0.564	0.798
9	0.162	0.588	0.588	0.784
10	0.199	0.616	0.616	0.740
11	0.245	0.650	0.650	0.751
12	0.301	0.692	0.692	0.718
13	0.371	0.739	0.739	0.658
14	0.457	0.795	0.795	0.616
15	0.564	0.854	0.854	0.501
16	0.694	0.913	0.913	0.404
17	0.856	0.967	0.967	0.257
18	1.056	0.999	0.999	0.069
19	1.302	1.000	1.000	-0.019
20	1.606	0.999	0.999	0.000

PT	Y/DEL	UCAL/UP	VELGRAD	MIX LN/DEL	PROD	L/LO	RIC	BETA	ED.RE
1	0.063	0.504	1.155	0.0302	37.53	1.266	0.0000	0.0	51.37
2	0.085	0.526	0.885	0.0395	28.80	1.170	0.0000	0.0	67.28
3	0.105	0.543	0.783	0.0453	26.27	1.067	0.0000	0.0	78.37
4	0.129	0.562	0.795	0.0452	27.39	0.859	0.0000	0.0	79.20
5	0.159	0.586	0.789	0.0465	28.34	0.714	0.0000	0.0	83.18
6	0.197	0.615	0.741	0.0498	26.90	0.616	0.0000	0.0	89.58
7	0.243	0.649	0.749	0.0488	26.68	0.574	0.0000	0.0	86.93
8	0.330	0.691	0.720	0.0495	24.40	0.583	0.0000	0.0	86.11
9	0.370	0.738	0.657	0.0502	19.15	0.591	0.0000	0.0	81.00
10	0.456	0.794	0.617	0.0464	13.51	0.546	0.0000	0.0	64.81
11	0.563	0.854	0.502	0.0459	7.09	0.540	0.0000	0.0	51.50
12	0.693	0.913	0.405	0.0398	2.82	0.469	0.0000	0.0	31.38
13	0.856	0.967	0.257	0.0361	0.59	0.424	0.0000	0.0	16.30
14	1.056	0.999	0.069	0.0213	-0.00	0.250	0.0000	0.0	1.51
15	1.302	1.000	-0.019	-0.3169	0.02	*****	0.0000	0.0	-91.97
16	1.554	0.999	0.004	1.6266	-0.00	*****	0.0000	0.0	486.10

THIRD EXPT., STN. 14, S = 118.95 CM.

PT	Y/DEL	U/UPN	UCALC	VELGRAD
1	0.013	0.361	0.367	5.700
2	0.025	0.438	0.432	4.732
3	0.035	0.475	0.471	3.084
4	0.046	0.495	0.497	1.698
5	0.069	0.516	0.518	0.915
6	0.078	0.530	0.531	0.928
7	0.096	0.548	0.547	0.902
8	0.117	0.565	0.565	0.837
9	0.143	0.587	0.587	0.785
10	0.176	0.610	0.610	0.624
11	0.217	0.634	0.634	0.608
12	0.267	0.666	0.666	0.608
13	0.330	0.701	0.701	0.563
14	0.406	0.743	0.743	0.455
15	0.501	0.781	0.781	0.519
16	0.617	0.860	0.860	0.652
17	0.761	0.928	0.928	0.385
18	0.938	0.986	0.986	0.209
19	1.157	1.000	1.000	-0.005
20	1.427	1.000	1.000	0.002
21	1.746	1.000	1.000	0.000

PT	Y/DEL	UCAL/UP	VELGRAD	MIX LN/DEL	PROD	L/LO	RIC	BETA	ED.RE
1	0.053	0.507	1.221	0.0279	37.73	1.388	0.0000	0.0	55.36
2	0.071	0.524	0.907	0.0380	28.81	1.349	0.0000	0.0	76.59
3	0.088	0.540	0.942	0.0368	30.17	1.033	0.0000	0.0	74.33
4	0.105	0.558	0.840	0.0416	27.33	0.944	0.0000	0.0	84.72
5	0.133	0.579	0.827	0.0427	27.58	0.785	0.0000	0.0	88.16
6	0.164	0.602	0.676	0.0526	22.81	0.783	0.0000	0.0	109.16
7	0.203	0.626	0.579	0.0616	19.67	0.740	0.0000	0.0	128.32
8	0.250	0.655	0.645	0.0557	22.15	0.655	0.0000	0.0	116.66
9	0.309	0.690	0.542	0.0659	18.41	0.775	0.0000	0.0	137.12
10	0.381	0.730	0.545	0.0647	18.11	0.761	0.0000	0.0	133.29
11	0.470	0.767	0.386	0.0868	11.56	1.022	0.0000	0.0	169.80
12	0.579	0.833	0.733	0.0400	16.79	0.470	0.0000	0.0	68.38
13	0.715	0.910	0.411	0.0519	4.98	0.611	0.0000	0.0	64.54
14	0.882	0.971	0.304	0.0306	0.71	0.360	0.0000	0.0	16.67
15	1.087	1.000	0.014	0.2146	0.00	2.525	0.0000	0.0	36.78

THIRD EXPT., STN. 17, S = 164.67 CM.

PT	Y/DEL	U/UPW	UCALC	VELGRAD
1	0.010	0.327	0.332	9.689
2	0.019	0.420	0.413	7.391
3	0.027	0.459	0.457	3.880
4	0.036	0.478	0.482	2.102
5	0.050	0.508	0.508	1.595
6	0.060	0.522	0.522	1.162
7	0.074	0.535	0.535	0.933
8	0.090	0.551	0.551	0.949
9	0.111	0.569	0.569	0.759
10	0.136	0.586	0.586	0.667
11	0.168	0.608	0.608	0.674
12	0.207	0.633	0.633	0.627
13	0.255	0.663	0.663	0.616
14	0.314	0.698	0.698	0.565
15	0.387	0.738	0.738	0.555
16	0.477	0.789	0.789	0.550
17	0.588	0.846	0.846	0.494
18	0.726	0.913	0.913	0.471
19	0.894	0.979	0.979	0.263
20	1.103	1.001	1.001	0.016
21	1.357	1.001	1.001	0.000

PT	Y/DEL	UCAL/UP	VELGRAD	MIX LN/DEL	PROD	L/LO	RIC	BETA	ED.RE
1	0.047	0.503	1.722	0.0201	58.18	1.168	0.0000	0.0	39.23
2	0.071	0.533	0.921	0.0375	31.01	1.335	0.0000	0.0	73.20
3	0.088	0.549	0.963	0.0359	32.47	1.010	0.0000	0.0	70.06
4	0.108	0.567	0.789	0.0440	26.96	1.001	0.0000	0.0	86.55
5	0.134	0.585	0.662	0.0533	23.27	0.972	0.0000	0.0	106.26
6	0.165	0.606	0.680	0.0522	24.21	0.772	0.0000	0.0	104.64
7	0.204	0.631	0.627	0.0573	22.86	0.685	0.0000	0.0	116.24
8	0.251	0.661	0.619	0.0586	22.94	0.689	0.0000	0.0	119.95
9	0.310	0.696	0.569	0.0640	21.38	0.753	0.0000	0.0	131.91
10	0.382	0.735	0.551	0.0661	20.67	0.777	0.0000	0.0	136.02
11	0.471	0.786	0.556	0.0654	20.75	0.770	0.0000	0.0	134.38
12	0.581	0.843	0.495	0.0719	17.68	0.846	0.0000	0.0	144.54
13	0.717	0.909	0.473	0.0700	14.68	0.824	0.0000	0.0	131.13
14	0.885	0.977	0.282	0.0957	5.80	1.126	0.0000	0.0	146.00
15	1.091	1.001	0.019	0.7339	0.11	8.634	0.0000	0.0	588.82
16	1.346	1.001	-0.008	-0.3611	-0.00	*****	0.0000	0.0	-59.92